Transcriptome analysis reveals changes in whole gene expression, biological processes and molecular functions induced by nickel and copper ions in Jack Pine (*Pinus banksiana*)

By

Alistar Moy

Thesis submitted in partial fulfillment of requirements for the degree of Master of Science (MSc) in Biology

Faculty of Graduate Studies

Laurentian University

Sudbury, Ontario, Canada

THESIS DEFENCE COMMITTEE/COMITÉ DE SOUTENANCE DE THÈSE
Laurentian Université/Université Laurentienne
Office of Graduate Studies/Bureau des études supérieures

Title of Thesis
Titre de la thèse: Transcriptome analysis reveals changes in whole gene expression, biological processes and molecular functions induced by nickel and copper ions in Jack Pine (Pinus banksiana)

Name of Candidate
Nom du candidat: Moy, Alistar

Degree

Diplôme: Master of Science

Department/Program
Département/Programme: Biology

Date of Defence
Date de la soutenance: May 15, 2023

APPROVED/APPROUVÉ

Thesis Examiners/Examinateurs de thèse:

Dr. Kabwe Nkongolo
(Supervisor/Directeur(trice) de thèse)

Dr. Aseem Kumar
(Committee member/Membre du comité)

Dr. Frank Mallory
(Committee member/Membre du comité)

Dr. M. Mbikay
(External Examiner/Examinateur externe)

Approved for the Office of Graduate Studies
Approuvé pour le Bureau des études supérieures
Tammy Eger, PhD
Vice-President Research (Office of Graduate Studies)
Vice-rectrice à la recherche (Bureau des études supérieures)
Laurentian University / Université Laurentienne

ACCESSIBILITY CLAUSE AND PERMISSION TO USE

I, **Alistar Moy**, hereby grant to Laurentian University and/or its agents the non-exclusive license to archive and make accessible my thesis, dissertation, or project report in whole or in part in all forms of media, now or for the duration of my copyright ownership. I retain all other ownership rights to the copyright of the thesis, dissertation or project report. I also reserve the right to use in future works (such as articles or books) all or part of this thesis, dissertation, or project report. I further agree that permission for copying of this thesis in any manner, in whole or in part, for scholarly purposes may be granted by the professor or professors who supervised my thesis work or, in their absence, by the Head of the Department in which my thesis work was done. It is understood that any copying or publication or use of this thesis or parts thereof for financial gain shall not be allowed without my written permission. It is also understood that this copy is being made available in this form by the authority of the copyright owner solely for the purpose of private study and research and may not be copied or reproduced except as permitted by the copyright laws without written authority from the copyright owner.

Abstract

Understanding the genetic response of plants to nickel and copper stress is a necessary step to improving the utility of plants for environmental remediation and restoration. The objectives of this study were to: 1) Characterize the transcriptome of Jack Pine (*Pinus banksiana*) and 2) Analyze the gene expression profiles of genotypes exposed to nickel and copper ion toxicity. *Pinus banksiana* seedlings were treated with 1,600 mg/kg of nickel sulfate or 1,300 mg of copper sulfate and screened in a growth chamber. Overall, 25,552 transcripts were assigned gene ontology. Nickel resistant and water control genotypes were compared based on the gene expression of various gene ontology categories. The response to stress and to chemical terms comprised the highest proportion of upregulated gene expression whereas the biosynthetic process and carbohydrate metabolic process terms had the highest proportion of downregulated gene expression. The majority of upregulated genes were expressed in the extracellular region and the nucleus whereas most downregulated genes were expressed in the plasma membrane and extracellular region. For copper, there were 6,213 upregulated genes and 29038 downregulated genes expressed in the copper resistant genotype compared to the susceptible genotype at a high stringency. Among the top upregulated genes, the response to stress, the biosynthetic process and the response to chemical stimuli terms represented the highest proportion of gene expression for the biological processes. For the molecular function category, the majority of expressed genes were associated with nucleotide binding followed by transporter activity and kinase activity. For the cellular component category, the majority of upregulated genes were located in the plasma membrane. Half of the total downregulated genes were associated with the extracellular region. Two candidate genes associated with copper resistance were identified including genes encoding for heavy metal-associated isoprenylated plant proteins (AtHIP20 and AtHIP26) and a gene

encoding the pleiotropic drug resistance protein 1 (NtPDR1). This study represents the first report of transcriptomic response of a conifer species to nickel and copper ions.

Key Words: Jack Pine (Pinus banksiana); Nickel; Copper; Transcriptome analysis; Differential gene expression; Illumina sequencing; Gene ontologies; Biological process, Molecular function; cellular compartment.

Acknowledgements

I would like to express my sincere appreciation to Dr. Nkongolo for his thorough support and guidance throughout my master's studies. I would like to thank my committee members Dr. Kumar and Dr. Mallory for reviewing and evaluating my thesis. Additionally, I would like to extend my appreciation to Dr. Michael, Dr. Czajka and Abagail Warren for their valuable guidance and input on certain concepts and experimental procedures. Thank you Dr. Ryser and Dr. Mehes-Smith for the additional support. Finally, I would like to thank my friends and family for the unwavering support and words of encouragement you have given me.

Table of Contents

Abstract ..... **iii**
Acknowledgements ..... **v**
Table of Contents ..... **vi**
List of figures ..... **ix**
List of tables ..... **xii**
List of appendices ..... **xiii**
Chapter 1: Literature Review **14**
1.1 Anthropological sources of heavy metals and its current impact on the local environment 14
1.2 History of heavy metal pollution in Sudbury 15
1.3 Attempted environmental restoration in Sudbury 15
1.4 Genetic responses of plants to heavy metal toxicity 16
1.5 Classification of plant strategies used to counteract heavy metal toxicity 19
1.5.1 Heavy metal tolerance strategies 19
1.5.2 Heavy metal avoidance strategy 22
1.6 Physiological and genetic response to copper 24
1.6.1 Properties of copper in the soil 24
1.6.2 Copper uptake and transportation 24
1.6.3 Utilization of copper in plants 27
1.6.4 Copper deficiency in plants 28
1.6.5 Copper toxicity in plants 29
1.6.6 Genetic response of plants to excess copper 30
1.7 Physiological and genetic response to nickel 33
1.7.1 Properties of nickel in the soil 33
1.7.2 Nickel uptake and transportation 33
1.7.3 Utilization of nickel in plants 35
1.7.4 Nickel deficiency in plants 36
1.7.5 Nickel toxicity in plants 36
1.7.6 Genetic responses of plants to excess nickel 38
1.7.7 Transcriptome analysis of other plants in response to excess nickel 39
1.8 Description and physical appearance of the subject: *Pinus banksiana* 40

1.9 Thesis rationale and objectives 42

Chapter 2: Transcriptome Analysis of Nickel Resistant and Susceptible Jack Pine (*Pinus banksiana*) 44

2.1 Introduction 44

2.2 Materials and methods 46

2.2.1 Plant treatment, incubation and harvesting 46

2.2.2 RNA Extraction 48

2.2.3 RNA sequencing and De Novo Transcriptome Assembly 49

2.2.4 BLAT matching and annotation of *Pinus banksiana* genes 49

2.2.5 Quantification of gene expression and quality control (QC) analysis 50

2.2.6 Differential gene expression (DGE) analysis of pairwise comparisons 51

2.2.7 Analysis of top differentially regulated genes 52

2.3 Results 53

2.3.1 Transcript assembly and sequence data QC 53

2.3.2 Differential gene expression (DGE) analysis 53

2.3.3 Gene ontology classification of differentially expressed genes in *Pinus banksiana* 58

2.3.4 Gene ontology of the top 100 differentially expressed genes in *Pinus banksiana* 62

2.4 Discussion 82

2.4.1 Effects of excess nickel on *Pinus banksiana* seedlings 82

2.4.2 Differential Gene Expression (DEG) Analysis 82

2.4.3 Gene Ontology of the top 100 DEGs in response to excess nickel 84

2.4.3 Annotation of the top 100 upregulated genes between the resistant genotype and the control 87

2.4.4 Annotation of the top 100 downregulated genes between the resistant genotype and the control 89

2.4.5 Annotation of the top 100 upregulated genes between the susceptible genotype and the control 92

2.4.6 Annotation of the top 100 downregulated genes between the susceptible genotype and the control 93

2.5 Conclusion 95

Chapter 3: Transcriptome analysis of copper resistant and copper susceptible Jack Pine (*Pinus banksiana*) 97

3.1 Introduction 97

3.2 Materials and methods 99

3.2.1 Plant treatment, damage rating and collection 99
3.2.2 Transcriptome analysis of *Pinus banksiana* 100
3.3 Results 101
3.3.1 Transcript assembly and QC analysis of sequences 101
3.3.2 Differential gene expression (DGE) analysis between genotypes 101
3.3.4 Gene ontology of the top 100 differential expressed genes for *Pinus banksiana* 106
3.3.5 Top 25 differentially expressed genes between pairwise comparisons 116
3.4 Discussion 126
3.4.1 Effects of excess Copper on *Pinus banksiana* seedlings 126
3.4.2 DGE analysis of copper genotypes 126
3.4.3 Identification of candidate genes associated with copper resistance in *Pinus banksiana* 127
3.4.4 GO Annotation of the top 25 upregulated genes between the resistant genotype and the susceptible genotype 129
3.4.5 GO annotation of the top 25 downregulated genes between the resistant genotype and the susceptible genotype 131
3.4.6 GO annotation of the top 25 upregulated genes between the susceptible genotype and the control 132
3.4.7 GO annotation of the top 25 downregulated genes between the susceptible genotype and the control 133
3.5 Conclusion 134
Chapter 4: General conclusions 135
References 138
Appendices 187

List of figures

Figure 1. Damage rating of *Pinus banksiana* seedlings after treatment with 1600 mg/kg of nickel. Selected seedlings underwent treatment and were assigned damage ratings based on various attributes..... 48
Figure 2a. Heatmap of differentially expressed genes from the nickel resistant genotype compared to the nickel susceptible genotype in *Pinus banksiana*..... 55
Figure 2b. Volcano plot of differentially expressed genes from the nickel resistant genotype compared to the nickel susceptible genotype in *Pinus banksiana*..... 55
Figure 3a. Heatmap of differentially expressed genes from the nickel resistant genotype compared to the controls in *Pinus banksiana*..... 56
Figure 3b. Volcano plot of differentially expressed genes from the nickel resistant genotype compared to the controls in *Pinus banksiana*..... 57
Figure 4. Volcano plot of differentially expressed genes from the nickel susceptible genotype compared to the control in *Pinus banksiana*..... 58
Figure 5a. Percentage of annotated transcripts in *Pinus banksiana* control samples categorized by Biological Processes..... 59
Figure 5b. Percentage of annotated transcripts in *Pinus banksiana* control samples categorized by Molecular Function..... 60
Figure 5c. Percentage of annotated transcripts in *Pinus banksiana* control samples categorized by Cellular Component..... 61
Figure 6a. Percentage of the top 100 upregulated transcripts in *Pinus banksiana* resistant samples compared to the controls categorized by Biological Processes..... 62
Figure 6b. Percentage of the top 100 upregulated transcripts in *Pinus banksiana* resistant samples compared to the controls categorized by Molecular Function..... 63
Figure 6c. Percentage of the top 100 upregulated transcripts in *Pinus banksiana* resistant samples compared to the controls categorized by Cellular Component..... 64
Figure 7a. Percentage of the top 100 downregulated transcripts in *Pinus banksiana* resistant samples compared to water controls categorized by Biological Processes..... 65
Figure 7b. Percentage of the top 100 downregulated transcripts in *Pinus banksiana* resistant samples compared to water controls categorized by Molecular Function..... 66
Figure 7c. Percentage of the top 100 downregulated transcripts in *Pinus banksiana* resistant samples compared to water controls categorized by Cellular Component..... 67
Figure 8a. Percentage of the top 100 upregulated transcripts in *Pinus banksiana* susceptible samples compared to the controls categorized by Biological Processes..... 68
Figure 8b: Percentage of the top 100 upregulated transcripts in *Pinus banksiana* susceptible samples compared to the controls categorized by Molecular Function..... 69
Figure 8c. Percentage of the top 100 upregulated transcripts in *Pinus banksiana* susceptible samples compared to the controls categorized by Cellular Component..... 70
Figure 9a. Percentage of the top 100 downregulated transcripts in *Pinus banksiana* susceptible samples compared to water controls categorized by Biological Processes..... 71

Figure 9b. Percentage of the top 100 downregulated transcripts in *Pinus banksiana* susceptible samples compared to controls categorized by Molecular Function 72
Figure 9c. Percentage of the top 100 downregulated transcripts in *Pinus banksiana* susceptible samples compared to the controls categorized by terms in Cellular Component..... 73
Figure 10. Damage rating of *Pinus banksiana* seedlings after treatment with 1300 mg/kg of copper 100
Figure 11a. Heatmap of differentially expressed genes from the copper resistant genotype compared to the copper susceptible genotype in *Pinus banksiana* 102
Figure 11b. Volcano plot of differentially expressed genes from the copper resistant genotype compared to the copper susceptible genotype in *Pinus banksiana* 103
Figure 12a. Heatmap of differentially expressed genes from the copper resistant genotype compared to water controls in *Pinus banksiana*..... 104
Figure 12b. Volcano plot of differentially expressed genes from the copper resistant genotype compared to the controls in *Pinus banksiana*..... 104
Figure 13a. Heatmap of differentially expressed genes from the copper susceptible genotype compared to water controls in *Pinus banksiana*..... 105
Figure 13b. Volcano plot of differentially expressed genes from the copper susceptible genotype compared to water controls in *Pinus banksiana*..... 106
Figure 14a. Percentage of the top 100 Upregulated transcripts in *Pinus banksiana* resistant samples compared to susceptible samples categorized by Biological Processes 108
Figure 14b. Percentage of the top 100 Upregulated transcripts in *Pinus banksiana* resistant samples compared to susceptible samples categorized by Molecular Function..... 109
Figure 14c. Percentage of the top 100 Upregulated transcripts in *Pinus banksiana* resistant samples compared to susceptible samples categorized by Cellular Component..... 109
Figure 15a. Percentage of the top 100 downregulated transcripts in *Pinus banksiana* resistant samples compared to susceptible samples categorized by Biological Processes 110
Figure 15b. Percentage of the top 100 downregulated transcripts in *Pinus banksiana* resistant samples compared to susceptible samples categorized by Molecular Function..... 110
Figure 15c. Percentage of the top 100 downregulated transcripts in *Pinus banksiana* resistant samples compared to susceptible samples categorized by Cellular Component..... 111
Figure 16a. Percentage of the top 100 upregulated transcripts in *Pinus banksiana* susceptible samples compared to water controls categorized by Biological Processes 113
Figure 16b. Percentage of the top 100 upregulated transcripts in *Pinus banksiana* susceptible samples compared to water controls categorized by Molecular Function..... 114
Figure 16c. Percentage of the top 100 upregulated transcripts in *Pinus banksiana* susceptible samples compared to water controls categorized by Cellular Component..... 114
Figure 17a. Percentage of the top 100 downregulated transcripts in *Pinus banksiana* susceptible samples compared to water controls categorized by Biological Processes 115
Figure 17b. Percentage of the top 100 downregulated transcripts in *Pinus banksiana* susceptible samples compared to water controls categorized by Molecular Function..... 115

Figure 17c. Percentage of the top 100 downregulated transcripts in *Pinus banksiana* susceptible samples compared to water controls categorized by Cellular Component..... 116

List of tables

Table 1. Summary of copper utilizing enzymes involved in crucial plant processes 27
Table 2. Damage ratings based on the comparison of pre treatment and post treatment appearance 47
Table 3. Differentially expressed genes from the nickel resistant genotype compared to the nickel susceptible genotype in *Pinus banksiana* 54
Table 4. Differentially Expressed Genes from the nickel resistant genotype compared to the control in *Pinus banksiana* 55
Table 5. Differentially Expressed Genes from the nickel susceptible genotype compared to the water control in *Pinus banksiana* 57
Table 6a. Top 25 upregulated genes from nickel resistant samples compared to the controls in *Pinus banksiana*..... 74
Table 6b. Top 25 downregulated genes from nickel resistant samples compared to the control in *Pinus banksiana*..... 76
Table 7a. Top 25 upregulated genes from nickel susceptible samples compared to the controls in *Pinus banksiana*..... 78
Table 7b. Top 25 downregulated genes from nickel susceptible samples compared to the control in *Pinus banksiana*..... 80
Table 8. Differentially expressed genes from the copper resistant genotype compared to the copper susceptible genotype in *Pinus banksiana* 102
Table 9. Differentially expressed genes from the copper resistant genotype compared to the water controls in *Pinus banksiana*..... 103
Table 10. Differentially expressed genes from the copper susceptible genotype compared to the water controls in *Pinus banksiana*..... 105
Table 11: Identified candidate genes from the top upregulated genes in copper resistant vs copper susceptible *Pinus banksiana* 117
Table 12a. Top 25 upregulated genes from copper resistant samples compared to copper susceptible samples in *Pinus banksiana*..... 118
Table 12b. Top 25 downregulated genes from copper resistant samples compared to copper susceptible samples in *Pinus banksiana*..... 120
Table 13a. Top 25 upregulated genes from copper susceptible samples compared to water controls in *Pinus banksiana*..... 122
Table 13b. Top 25 downregulated genes from copper susceptible samples compared to water controls in *Pinus banksiana*..... 124

List of appendices

Sfigure 1. *Pinus banksiana* seedlings in a growth chamber prior to heavy metal treatment 188
Sfigure 2a. Sample clusters assessed via a multidimensional scale (MDS) plot 189
Sfigure 2b. Heatmap of 5000 genes between the samples 189
STable 1. Sequence Data QC verified by FastQC 190
STable 6a. Top 100 upregulated genes from nickel resistant samples compared to the water controls in *Pinus banksiana* 191
STable 6b. Top 100 downregulated genes from nickel resistant samples compared to the control in *Pinus banksiana* 196
STable 7a. Top 100 upregulated genes from nickel susceptible samples compared to the controls in *Pinus banksiana* 200
STable 7b. Top 100 downregulated genes from nickel susceptible samples compared to the control in *Pinus banksiana* 205
STable 12a. Top 50 upregulated genes from copper resistant samples compared to copper susceptible samples in *Pinus banksiana* 210
STable 12b. Top 50 downregulated genes from copper resistant samples compared to copper susceptible samples in *Pinus banksiana* 212
STable 13a. Top 25 upregulated genes from copper susceptible samples compared to water controls in *Pinus banksiana* 214

Chapter 1: Literature Review

1.1 Anthropological sources of heavy metals and its current impact on the local environment

Heavy metals come from a variety of sources which include mining facilities, metal processing facilities, agricultural areas, wood processing plants, technology plants, energy plants and fossil fuel related institutions (DeVolder et al., 2003; Gimeno-García et al., 1996; Atafar et al., 2008; Pazalja et al., 2021; Muniz et al., 2004). In its elemental form, heavy metals cannot be broken down by naturally occurring biological agents and therefore reside in the environment for an indefinite amount of time (Tchounwou et al., 2012; DeForest et al., 2007; Jara-Marini et al., 2009). Its presence leads to soil leaching into the environment, significant plant damage and bioaccumulation into various animal communities, inevitably causing disease in humans. Today, anthropological output of heavy metals continues to contribute to a considerable proportion of heavy metal accumulation in the environment and in plant biota (S. Chen et al., 2021). In Sudbury, wildlife and vegetation continue to be severely affected by heavy metals several decades after the decommissioning of open roast yards and smelters. Soils around decommissioned roast beds still have a very low pH, leading to deleterious effects to local biota (K. K. Nkongolo et al., 2013). Microbial decomposition is severely inhibited in the soil and for a long period of time, areas near smelters were only able to grow lichens (Hutchinson & Symington, 1997). Plant diversity, plant abundance, insect diversity and insect abundance decrease toward contaminated areas over a large area (Hutchinson & Symington, 1997; Babin-Fenske & Anand, 2011). Heavy metal contamination acidifies lakes and causes leaching, creating an environment inhospitable to fish and zooplankton (Hutchinson & Gunderman, 1998; Rutherford & Mellow, 1994). In some cases, a divide in niche habitation occurs with only acid tolerant species being able to survive downstream of contaminated

sites whereas other species are isolated to upstream areas (Rutherford & Mellow, 1994). Elevated levels of cadmium and nickel were also found in the liver and kidney tissue of *Ondatra zibethicus* near closed smelters, demonstrating significant bioaccumulation (Parker, 2004).

1.2 History of heavy metal pollution in Sudbury

Sudbury and the Greater Sudbury Area is a region in Ontario, Canada that is economically dependent on the mining industry and possesses a considerable amount of mining, ore smelting and metal processing facilities (Kramer et al., 2017). The city and surrounding area are situated within a crater formed by a meteorite impact 1.849 billion years ago, providing access to large quantities of mineral deposits and other rock formations (Rousell et al., 2003). Forestry, logging, and clear cutting were primary industries prevalent in the area (Davidson & Gunn, 2012). In the 1880s, large scale industrial mining operations began with the establishment of open bed roast yards and smelters (Schindler, 2014). From 1888 to 1923, thirteen open air roast yards processing sulfide ores were used and from 1928 to 1972, three smelters were used (Schindler, 2014; McCall et al., 1995). As nickel and copper became predominant exports, large amounts of sulfur dioxide and heavy metals were released into the atmosphere and soil (Jewiss, 2013; Hutchinson & Gunderman, 1998). Eventually, an area of 1000 km^2 became barren or semi-barren with 7000 acidified lakes, little vegetation, and eroded soil (Keller et al., 2007).

1.3 Attempted environmental restoration in Sudbury

Considerable efforts were made by the community, local governments, environmental institutions, mining institutions and Laurentian University to reduce the environmental impact caused by historical heavy metal pollution. The construction of a smokestack and other pollutant capture technology reduced the sulfur dioxide pollution by 90% over a period of several decades (Beckett

& Spiers, n.d.). Since 1978, regreening programs planted 10 million trees, mostly consisting of *Pinus banksia, Pinus resinosa, Picea glauca* and *Pinus strobus.* Additionally, large amounts of soil were limed, fertilized, and sowed with legumes to improve regreening efforts (Pabian et al., 2012; Schreffler & Sharpe, 2003; Rumney et al., 2021). Despite these efforts, copper and nickel exports remained the same or increased, leading to copper and nickel remaining as the highest pollutants of top soil in the area (Narendrula et al., 2011). Pre-deforestation old growth combined with recent reforestation efforts lead to a mixed forest biome ecosystem classification; a transition zone between deciduous forests and coniferous boreal forests (Hart & Chen, 2008). The vegetation in the area is currently dominated by trees used in the regreening program: *Pinus banksiana, Picea glauca, Picea rubens, Betula papyrifera* and *Populus tremuloides* (Lu et al., 2014; K. K. Nkongolo et al., 2013).

1.4 Genetic responses of plants to heavy metal toxicity

The various physiological responses that a plant may employ in response to excess heavy metals are driven by transcript expression at the genetic level (Shukla et al., 2018; Kintlová et al., 2017; Y. Wang et al., 2013; X.-Z. Yu et al., 2018). The genetic response of plants prioritizes the detoxification of heavy metals, the mitigation of metal induced tissue damage and the enhancement of growth and repair mechanisms (Yao et al., 2018; Shukla et al., 2018; Y.-F. Lin et al., 2014). Protein expression specific to heavy metal toxicity therefore represents and embodies these facets. A large portion of the genetic response that can be regulated are associated with the production of chelators and transporters.

Chelator proteins are ligands that bind to heavy metals, forming inert complexes that effectively reduce the viability of heavy metals (W. Zhang et al., 2010). Chelators bind to heavy metals by forming rings via a sulfur, oxygen, or nitrogen binding motif (Nag & Joardar, 1976; Fackler et al.,

1972). The binding and complexing of heavy metals reduces the number of reactions that would have otherwise occurred with free ions (Viarengo et al., 1997). Once the inactive complex is formed, mechanisms of detoxification can occur (Hall, 2002). The complex may be transported to different areas of the plant or to different organelles using transporters, which can transport the inactive complex with ease compared to the more reactive free ions (Irtelli et al., 2008). Chelated heavy metals may be delivered to or acted upon by enzymes, further complexing the heavy metal or altering the compound for a variety of other functions (Zaharieva & Abadía, 2003). Chelators may also bind to and inactivate reactive oxygen species (ROS) that form as a result of abundant redox reactions caused by excess heavy metals (G. Kumar et al., 2012; Z. Yang et al., 2009). Coordination with transporters, other enzymes and detoxification mechanisms therefore contribute immensely to heavy metal resistance. Chelators may be organic, inorganic and vary in molecular size (Rastogi et al., 2009; Irtelli et al., 2008). Common chelators include nicotianamine, amino acids such as histidine, arginine, glutamate, cysteine and organic acids such as malate, citrate and oxalate (Irtelli et al., 2008; Y. Zhang et al., 2017; D. Chen et al., 2020; Harada et al., 2002; Delhaize et al., 1993; Wasay et al., 1998). Two classifications of chelators have been demonstrated as being instrumental in heavy metal resistance in plants: Metallothionein (MT) and phytochelatin (PT).

Metallothionein (MT) are cystine rich polypeptides that are directly transcribed by genes (Zhou & Goldsbrough, 1995). MTs have beta and alpha domains containing thiol groups that coordinate binding with heavy metals via a sulfur binding motif (Ngu et al., 2010). In *Arabidopsis thaliana*, MT1 is highly expressed in roots and expressed in shoots (Zhou & Goldsbrough, 1995). MT2a and MT2b genes are highly expressed in the phloem of leaves, flowers, and roots whereas MT3 is highly expressed in seeds only (W.-J. Guo et al., 2003). Chelation and expression of MTs are involved in the maintenance of homeostasis for zinc, copper, lead, cadmium, and nickel (W.-J.

Guo et al., 2003; Kohler et al., 2004; R. Benatti et al., 2014; J. Guo et al., 2013; Auguy et al., 2013; Adhikari & Kumar, 2012). However, its role is species specific and requires further research to characterize function (Kohler et al., 2004).

Phytochelatin (PC) or Class III MTs are cystine rich polypeptides that require enzyme synthesis governed by Phytochelatin synthase (X. Zhang et al., 2012). PCs generally have a larger molecular weight and use glutathione as the base substrate, with every additional unit classifying a different phytochelatin. Increased phytochelatin accumulation is associated with excess copper, cadmium, lead, chromium, and nickel in multiple different species (Bačkor et al., 2007; Ramos et al., 2008; Mukta et al., 2019; Helaoui et al., 2022). However, transgenic expression of phytochelatin synthase conferred metal tolerance in some plants but not others, indicating that the efficacy had a strong dependency on other factors such as avoidance/tolerance strategy and transporter interaction (Bhuiyan et al., 2011; S. Lee & Kang, 2005; Pawlik-Skowronska et al., 2002; Picault et al., 2006).

Transporter proteins facilitate the mobilization of heavy metals between organs, subcellular compartments, receptors, enzymes, chaperones, and other transporters (Morel et al., 2008; Q. Yang et al., 2018; Hoppen et al., 2019; Shikanai et al., 2003; Jung et al., 2012). In regard to heavy metals, transporters function in moving free ions or chelated complexes through each step of transport. This includes initial uptake, intracellular root transport, xylem loading, root to shoot translocation, intracellular shoot transport, phloem loading, phloem translocation, and redistribution of metals into reproductive organs (Sancenón et al., 2004; Hoppen et al., 2019; F. Deng et al., 2013; Sautron et al., 2015; L. Zheng et al., 2012; S. Lee et al., 2007). Transporters belonging to the same family have similar or conserved protein regions, protein content and functional motifs (VATANSEVER et al., 2016). The metal specificity, tissue preference, function

and organelle specificity of transporters may differ between different species (Jogawat et al., 2021). In most cases, the types of transporters and genes that are expressed are a result of the classification strategy the plant species employs (Corso et al., 2018). Common transporter families include P_{1b} ATPase transporters (HMA), copper transporters (COPT), Zinc regulated transporters and Iron regulated transporters (ZIP/IRT), ATP-binding cassette (ABC) transporters, Yellow stripe like (YSL) transporters, Natural resistance associated macrophage protein (NRAMP), Iron regulated (IREG) transporters and Cation diffusion facilitator (CDF) transporters (Jain et al., 2018). Many of these transporters were found to be highly expressed in hyperaccumulators in conditions of heavy metal excess, demonstrating a coordinated response to heavy metal stress (Becher et al., 2004; P. Tan et al., 2021; Gendre et al., 2006; Fasani et al., 2021; Merlot et al., 2014; Chiang et al., 2006).

1.5 Classification of plant strategies used to counteract heavy metal toxicity

The response of plants to heavy metal stress varies greatly between different species and cultivated variants (Seregin et al., 2015; FAN & ZHOU, 2009). The responses and mechanisms of the plant species to toxicity can be collected and classified as a singular defense strategy toward a specific metal. Plants can be classified as using tolerance or avoidance strategies in response to heavy metal toxicity (Baker, 1981).

1.5.1 Heavy metal tolerance strategies

Plants that use the tolerance strategy in response to heavy metals can be subdivided into 3 classes: excluders, accumulators and bioindicators (Baker, 1981). This classification denotes plants based on the quantifiable distribution of metals throughout the plant and based on the organs in which it gathers. Tolerance strategies may target crucial points of vascular transportation as a means to

regulate storage. Crucial points of regulation include root tip cells, xylem loading, root to shoot translocation, phloem loading, phloem redistribution, intracellular transport in root cells, and intracellular transport in the cells of aerial organs (PAGE & FELLER, 2005; Yan et al., 2020; Ueno et al., 2011). The expression of different transporters or chelators can be used to modulate these points of regulation in vascular transport and heavy metal storage. This classification is also not relegated to a single metal, as a plant may be an excluder for one metal and an accumulator for another (Khawla et al., 2019).

Excluders

The majority of metal resistant plants are excluders. Excluders externally block the uptake of metals through the root system and actively inhibit xylem translocation (Baker, 1981). Sequestration to the root is necessary because in most cases, distribution to the aerial parts of the plant induces toxicity and tissue damage (Cox et al., 2018; Zemiani et al., 2021; Q. Yang et al., 2018). Storing and isolating metals to the roots and preventing root to shoot translocation are common methods of metal exclusion (Rosatto et al., 2021; J. Yoon et al., 2006). Other common means of regulation include intracellular sequestration, inhibition of xylem loading, inhibition of phloem loading and inhibition of phloem redistribution (Delhaize et al., 1993; Nguyen et al., 2016, p. 20; Kozhevnikova et al., 2020; Nishida et al., 2020; Herren & Feller, 1997; Ducic et al., 2006; W.-Y. Song et al., 2014). Aluminum resistant *Triticum aestivum* encourages the production of malate chelators in root cells, temporarily binding the metals to the root area until further action (Delhaize et al., 1993). The mobilization and increase of malate in the root tip cells is likely a factor that is associated with a higher level of metal tolerance in *Triticum aestivum* compared to individuals that lack chelator production. *Oryza sativa* highly expresses the transporter HMA3, sequestering cadmium to the vacuoles of root cells and inhibiting root to shoot translocation

(Wiggenhauser et al., 2021). The sequestration of nickel to the vacuoles of root cells is likely a factor that gives it higher nickel tolerance compared to other excluder individuals demonstrating a higher root to shoot translocation (H.-Q. Wang et al., 2020). Other physiological means of blocking metals include closing of the stomata, increasing the size of guard cells and increasing the wax content on the epicuticle (Zarinkamar et al., 2013). Stomata have also been observed to increase in size and reduce in number or decrease in size and increase in number to enhance the exclusion of heavy metals (Stolarska et al., 2007; Weryszko-Chmielewska & Chwil, 2005).

Hyperaccumulators

Hyperaccumulators distribute a larger proportion of metals to aerial organs and accumulate metals in plant tissue above a soil to plant ratio of 1 (Baker, 1981). The accumulation of large concentrations of metals allows hyperaccumulators to occupy metal contaminated soil with minimal side effects and to a greater extent than excluders and indicators (S. L. Brown et al., 1995; Seregin et al., 2014). Oftentimes the accumulation of metals to the shoots are not due to the risk of toxicity to the roots but because the aerial organs are better adapted to sequestering and dealing with heavy metals, garnering a pivotal advantage (Krämer et al., 2000). Hyperaccumulators can be further classified based on the proportion of the population that are hyperaccumulators (Pollard et al., 2014). Obligate hyperaccumulators consistently demonstrate a high rate of heavy metal uptake regardless of the heavy metal content in a given area (Kozhevnikova et al., 2021). Facultative hyperaccumulators do not demonstrate a consistently high rate of heavy metal uptake in areas without metals (Teptina & Paukov, 2015). Populations of facultative hyperaccumulators may also contain individuals that do not accumulate heavy metals. Transporter behaviour and crucial points of vascular transportation may be regulated to increase intracellular sequestration, encourage xylem loading, increase root to shoot xylem translocation, increase phloem loading and

increase phloem redistribution (S. Huang et al., 2022; Yamaji et al., 2008; van de Mortel et al., 2006; Uraguchi et al., 2011; T.-H.-B. Deng et al., 2021). For example, high expression of the HMA3 transporter in the hyperaccumulator *Thlaspi caerulescens* conferred cadmium resistance by increasing the sequestration of cadmium into the vacuoles of leaves (Ueno et al., 2011). Ecotype plants that under expressed HMA3 were unable to accumulate cadmium in the vacuole of the leaves and were therefore susceptible to cadmium toxicity. The hyperaccumulator *Arabidopsis helleri* overexpresses HMA4- a transporter involved in the root to shoot translocation of zinc. Plants with a lower expression of HMA4 demonstrated lower zinc accumulation in the shoots and lower tolerance (Nouet et al., 2015).

Bioindicators

Bioindicators accumulate heavy metals in the biomass of aerial organs such that it is responsive or representative of the metal content of the surrounding area (Baker, 1981). An indicator can be identified on the basis of whether the metal content in tissues represents or is proportional to the metal content of the soil in the surrounding environment (Salinitro et al., 2022). Bioindicator plants are able to transport and store heavy metals in the aerial organs to a higher extent than excluders but less than hyperaccumulators (El-Khatib et al., 2020). For example, the needles of *Pinus eldarica* and *Pinus mariana* are bioindicators for aluminum near an urban area and a refinery, respectively (Miri et al., 2016; Dion et al., 1993).

1.5.2 Heavy metal avoidance strategy

Plants that use an avoidance strategy will actively exclude or prevent the transportation of metals into the root area of the plant. The mechanisms used by the plant may also diminish the presence of heavy metals in the surrounding environment (Khare et al., 2016; Jutsz & Gnida, 2015). One

mechanism involves the alteration of the morphological structure and growth patterns to avoid heavy metal accumulation (Khare et al., 2016). In response to excess cadmium, *Arabidopsis thaliana* restructures the root network such that the growth of the roots with higher exposure are suppressed and the roots with less exposure are increased. In response to cadmium, *Triticum turgidum* increases the length of roots and number of root tips to decrease the ease at which cadmium translocation occurs through the root to xylem vasculature (Sabella et al., 2022). Another mechanism involves the formation of a mycorrhizal sheath complex with Ectomycorrhiza or Arbuscular fungi (Jourand et al., 2010; Hashem et al., 2016). The mycorrhizal sheath complex acts as a protective extension of the roots and an extra barrier the metals must cross before entering the roots (Jourand et al., 2010; T. Guo et al., 2006). For example, in response to excess nickel, *Ecualyptus globulus* formed an Ectomycorrhizal sheath complex with *Pisolithus albus*, reducing the effects of toxicity and growing at least 20 fold higher than plants without the sheath complex (Jourand et al., 2010). The mycorrhizal sheath also reduced heavy metal uptake for the plant, implying a symbiotic relationship that involves heavy metal distribution through the mycorrhizal sheath complex itself. Another defense mechanism that avoiders may employ is the release of root exudates into the surrounding external environment of the cells (Marastoni et al., 2020). Root exudates primarily function to bind and chelate heavy metals, detoxifying heavy metals and preventing its mobilization into the plant. Root exudates consist of chelators, proteins, organic acids, amino acids, carbohydrates, enzymes, and secondary metabolites (X. Zhang et al., 2019; Montiel-Rozas et al., 2016). Once metals enter the root tip, chelators and other organic acids are immediately mobilized to the root area to chelate and bind to the metals, forming inactive compounds (Morita et al., 2008). Chelators and other ligands may also bind foreign metals to the cell wall or transferred to vesicles for export out of the root cell (J. Song et al., 2013; Sabella et

al., 2022). At each stage of protection, whether it is the mycorrhizal sheath, the root exudate, the cell wall interior or the cytosol of the root cells, chelators, ligands and organic acids are actively mobilized to bind and inactivate heavy metals (Jourand et al., 2010).

1.6 Physiological and genetic response to copper

1.6.1 Properties of copper in the soil

Global samples of mean background copper content have been measured in the range of 15-50 mg/kg, whereas in industrial areas related to copper, the range increases significantly (Ballabio et al., 2018; Oorts, 2013). In Sudbury, the concentrations of copper near smelters ranged from 52.3 to 1330.3 mg/kg, with the majority of samples exceeding provincial guidelines (Narendrula et al., 2011). In comparison to other heavy metals, copper is among the lesser bioavailable ions due to its adsorption and complexing with organic matter, substrates, and inorganic compounds (Intawongse & Dean, 2006; Dudal et al., 2005; Di Palma et al., 2007). Commonly formed complexes involve copper binding to clays, acetate, silicates, sulphates, manganese, and phosphates (Siriwong et al., 2020; M. A. R. Khan et al., 2005; Tiberg et al., 2013). The bioavailability of copper ions in the soil increases with lower pH due to weaker adsorption to entities (K. Yang et al., 2015). From the bioavailable pool of copper, the ions may be found in the Cu^{2+} or divalent or monovalent form, with the divalent form being more prevalent (Sauvé et al., 1997).

1.6.2 Copper uptake and transportation

Using a variety of genomic studies and functional protein studies, the cumulative work of researchers is able to partially elucidate the uptake and transportation of copper through the plant vasculature and organs. Before the initial uptake of ions into the root cells, reductase enzymes

such as FRO4 and FRO5 in the plasma membrane may reduce Cu^{2+} to Cu^{+} in *Arabidopsis thaliana* (Jouvin et al., 2012; Bernal et al., 2012). Copper is transported into the cytosol of the root cells via COPT family transporter proteins that are strongly specific to copper (Sancenón et al., 2004; Romero et al., 2021); Romero *et al.*, 2021). In several plants, COPT1 and COPT2 are localized to the plasma membrane or endoplasmic reticulum at the root tip, although COPT1 is predominantly responsible for initial uptake. ZIP family proteins have also been found to transport copper into the root cells of *Arabidopsis thaliana*, albeit in a nonspecific fashion (Antala & Dempski, 2012; Milner et al., 2012). Once inside the root cells, transporters may store copper into intracellular organelles, transport copper to the xylem or continually chelate copper in the cytosol. Some transporters responsible for intracellular transport in root cells have been identified. In *Oryza sativa*, HMA4 is located on the vacuole membrane of root cells and is involved in the sequestration of copper into the vacuole (Huang *et al.*, 2016). This function is supported by a loss of function HMA4 gene causing increased root to shoot translocation and accumulation in the shoots. HMA7/Ran1 in *Silene vulgaris* and *Arabidopsis thaliana* transport copper from the ATX1 chaperone to the Golgi apparatus and endoplasmic reticulum, where it may interact with ethylene receptors to modulate growth signalling (Baloun et al., 2014; Hoppen et al., 2019). COPT5 is located on the tonoplast membrane of root cells and is involved in exporting copper from the vacuole to the cytosol (Klaumann et al., 2011). HMA5 is expressed in the plasma membrane of root cells and receives copper from ATX1 and CCH (Andrés-Colás et al., 2006). Knockout mutants expressing increased root growth and decreased tolerance suggest that HMA5 functions in exporting copper out of the root cells and may therefore be responsible for the mobilization of copper and preparation for xylem loading. In *Oryza sativa*, xylem loading is mediated by HMA5 located on the plasma membrane of various organs, especially the roots and xylem (F. Deng et al.,

2013). HMA5 also confers increased root to shoot translocation of copper, further supporting the xylem loading function. In the xylem sap of the Hyperaccumulator *Brassica carinata,* Nicotianamine, histidine and proline were found to be the most abundant chelators, with expression increasing in response to higher levels of copper (Irtelli et al., 2008). Once in the leaves, transporters may facilitate the storage of copper into the subcellular compartments of leaf cells or mediate phloem loading. In *Arabidopsis thaliana,* HMA1 and HMA6/PAA1 are both located on the chloroplast membrane and transport copper from the cytosol to the stroma of the chloroplast (Seigneurin-Berny et al., 2006; Boutigny et al., 2014; Sautron et al., 2015; Shikanai et al., 2003). HMA8 is located in the inner membrane of the thylakoid and is involved in transporting copper from the stroma of the chloroplast to the thylakoid lumen (Mayerhofer et al., 2016; Tapken et al., 2014). Some transporters are involved in phloem loading and phloem redistribution. Expression of COPT6 in *Arabidopsis Thaliana* in leaves, seeds, xylem and phloem suggest that it is involved in copper redistribution from the leaves to reproductive organs (Jung et al., 2012; Garcia-Molina et al., 2013). In addition to root expression, HMA7/Ran1 is also expressed in leaves and seeds, transporting copper to the Golgi apparatus and endoplasmic reticulum for ethylene signalling and growth (Baloun et al., 2014). In *Oryza sativa,* YSL16 is highly expressed in the vascular bundles of phloem compared to the roots and shoots (L. Zheng et al., 2012). YSL16 has been found to transport copper complexed to nicotinamide to seeds, newer leaves, flowers and other reproductive organs, implying a role in phloem redistribution (L. Zheng et al., 2012; C. Zhang et al., 2018). This is especially the case for flowers, which are provided with prioritized copper transport in comparison to the shoots and roots (C. Zhang et al., 2018). HMA9 is highly expressed on the plasma membrane of xylem, phloem, and anthers (S. Lee et al., 2007). The

strong, specific expression in the xylem and phloem indicates considerable involvement in phloem distribution, xylem unloading, and phloem unloading.

1.6.3 Utilization of copper in plants

Copper is an essential micronutrient and like other metals, it can become toxic at high concentrations (Dey et al., 2015; Demirevska-Kepova et al., 2004). The redox ability of copper makes it an important cofactor in enzymes involved in oxidation reduction reactions. The role of copper in plants are very broad and include structural fortification, photosynthesis, cellular respiration and antioxidative functions (Ghuge et al., 2015; Shahbaz et al., 2015; Garcia-Molina et al., 2011; Chamseddine et al., 2008). Additionally, copper is involved in many proteins involved in electron transfer reactions (Höhner et al., 2020; Mansilla et al., 2019). For many oxidases, copper is able to easily bind and reduce O_2 (Bhagi-Damodaran et al., 2016). The following table summarizes examples of crucial enzymes involved in normal plant function requiring copper.

Table 1. Summary of copper utilizing enzymes involved in crucial plant processes

Enzyme name	Location	Function	Citation
Plastocyanin	Thylakoid Lumen	Photosynthesis: Electron carrier from cytochrome B6F complex of Photosystem II to P700 complex of photosystem I	(Höhner et al., 2020)
Cytochrome oxidase	Electron transport chain in the Mitochondria	Cellular respiration: Reduces O_2 to H_2O	(Mansilla et al., 2019)
Superoxide Dismutase	Multiple organelles	Antioxidative function: Metabolize radical oxygen species	(Chamseddine et al., 2008)
Ethylene receptors	Endoplasmic reticulum	Modulation and signalling of ethylene for plant growth and development	(Hoppen et al., 2019; F. Zheng et al., 2017; Binder et al., 2004)

Phytocyanin	Chloroplast	Electron transport: Overall function unknown	(J. Cao et al., 2015)
Laccases	Apoplast	Lignification, immune response, seed growth	(Zhu et al., 2021; H.-Q. Wang et al., 2020)
Amine oxidase	Cell wall	Lignification leading to cell wall fortification, programmed cell death: Oxidizes putrescine to H_2O_2	(Ghuge et al., 2015; Tavladoraki et al., 2016)
Ascorbate oxidase	Apoplast space	Growth and development: Oxidizes ascorbic acid to dehydroascorbic acid	(Chatzopoulou et al., 2020)
Polyphenol oxidase	Thylakoid	Lignification, defense function: Hydroxylates monophenols to o-diphenols. Oxidizes aromatic compounds.	(Constabel et al., 1995; D. Chen et al., 2019)

1.6.4 Copper deficiency in plants

Copper deficiencies severely impair the ability of plants to grow properly. Malformation, curling of the leaves, chlorosis and necrosis are common symptoms of copper deficiency (Alloway & Tills, 1984). Copper deficiency negatively impacts enzymes involved in lignification, resulting in weaker cell walls and lower wood tissue production (Robson et al., 1981). Decreased lignin and downregulation of the floral activator FT results in diminished anthers, stigmas, and a decrease in overall reproductive organ development, which may subsequently decrease seed yield (Rahmati Ishka & Vatamaniuk, 2020). Copper deficiency may cause a decrease in plastocyanin and cytochrome c oxidase activity, although cytochrome c oxidase function may be prioritized over plastocyanin under more manageable conditions (Rahmati Ishka & Vatamaniuk, 2020; Scheiber et al., 2019). Nevertheless, inhibition of plastocyanin and cytochrome C oxidase diminishes photosynthesis and cellular respiration respectively, leading to chlorosis and necrosis on the outer edges of the leaves (Kaur & Manchanda, 2019; Tewari et al., 2006). Copper deficiency may also

result in the accumulation of ROS in the pollen, which have negative downstream effects on plant tissue and organelles (Rahmati Ishka & Vatamaniuk, 2020). The immune system of the plant may also be compromised under copper deficiency, hindering the ability of the plant to defend itself against pathogens and other foreign entities. Decreased expression of Cu/Zn superoxide dismutase occurs in plants with a copper deficiency, although restoration of function may be attempted by upregulating Fe SOD in chloroplasts (Yamasaki et al., 2007). An absence or decrease in polyphenol oxidase activity may also occur, which may cause the reduction of phenolic compound oxidation or cell wall lignification (Marziah & Lam, 1987; Seliga, 1999).

1.6.5 Copper toxicity in plants

Excess copper causes a disturbance in the homeostasis of metal ions to the point of deficiency. At high levels, copper can bind to the surface of roots and become readily absorbed, resulting in a lack of absorption of other essential ions such as iron, manganese, and zinc (S.-L. Lin & Wu, 1994; Ivanov et al., 2016; Martins & Mourato, 2006). Increased nitric oxide production was observed in plants, leading to a decrease in auxin production, cytokinin and mitotic activity in the root tips (Pető et al., 2011). The diminishment of these growth-related parameters may manifest as symptoms of decreased root meristem growth and overall decreased root growth (Yuan & Huang, 2016; Lequeux et al., 2010). Excess copper can outcompete other ions for enzyme binding sites leading to dysregulated enzyme activity (Pätsikkä et al., 2002; Letelier et al., 2005; Van Assche & Clijsters, 1990). In excess conditions, copper outcompetes iron for a binding site on plastoquinone QA of Photosystem II, resulting in reduced electron transfer and photosynthesis (Jegerschoeld et al., 1995). Copper causes a decrease in chlorophyl concentration and thylakoid membranes which may also lead to decreased photosynthesis and chlorosis (Pätsikkä et al., 2002). The addition of iron and excess copper recovers the function of photosystem II, suggesting that photosystem II

inhibition is caused by an iron deficiency induced by copper. Excess copper may also dysregulate stomata morphology, stomata number and gas exchange of CO_2 and O_2 (Panou-Filotheou, 2001; Możdżeń et al., 2017; Ouzounidou et al., 2008). The stomata misfunction may or may not contribute to photosynthesis inhibition, which likely depends on other variables (X. Li et al., 2021). Decreased photosynthesis, cellular respiration and altered stomata conductance may be implicated in decreased root length, shoot length and lower biomass overall (Kulikova et al., 2011). Despite other heavy metals such as cadmium and lead being more toxic to plants overall, copper has been found to reduce the root length and primary needle length the most (Ćurguz et al., 2012).

A common symptom of excess copper is the increased production of ROS (Thounaojam et al., 2012). Copper is directly involved in a large amount of redox reactions as it can exist as two oxidation states (Andreazza et al., 2013). Though the Haber-Weiss reaction, superoxide radicals, hydroxyl radicals and hydrogen peroxide are generated in excess (Opdenakker et al., 2012; L. Wang et al., 2010). In response to the copper induced ROS generation, the activity of SOD, catalase, guaiacol peroxidase, ascorbate peroxidase, glutathione reductase also increases (Thounaojam et al., 2012; Martins & Mourato, 2006). An overabundance of ROS and its generation outpaces the counteractive measures and controls imposed by antioxidation mechanisms, resulting in oxidative stress, lipid peroxidation, breakdown of plant tissue and the destruction of organelles (X. Wang et al., 2018; R. Sharma et al., 2019; Nair et al., 2014).

1.6.6 Genetic response of plants to excess copper

Plants regulate the expression of many transporters and chelators in response to excess copper. In *Arabidopsis thaliana,* genes encoding COPT1, COPT2, ZIP2 and ZIP4 were downregulated, indicating a decrease in initial copper uptake into the root cells (Sancenón et al., 2004; del Pozo et

al., 2010; Wintz et al., 2003). COPT4 is downregulated, although its function remains elusive (del Pozo et al., 2010). Differential transcription of COPT genes in *Solanum lycopersicum* demonstrates that in response to copper stress, COPT transporters coordinate to decrease initial uptake in the roots while increasing translocation to shoots (Romero et al., 2021). In *Arabidopsis Thalianais,* the upregulation of HMA5 occurs in the roots and leaves but more in the former (Andrés-Colás et al., 2006, p. 5; del Pozo et al., 2010). The upregulation of HMA5 may suggest mobilization from the roots and increased root to shoot translocation. OsHMA5 encoding HMA5 is also upregulated in the leaves of *Oryza sativa*, promoting xylem translocation (F. Deng et al., 2013). Genes encoding CCH is downregulated in the vascular bundles of older leaves and petioles in *Arabidopsis thaliana*, resulting in decreased copper transportation to the secretory pathway and decreased delivery of copper to HMA5 (del Pozo et al., 2010; Mira et al., 2001; Andrés-Colás et al., 2006). The downregulation of CCH genes suggests decreased mobilization and decreased transportation from older leaves to younger leaves (Mira et al., 2001). MT2a and MT2b encoding MT was found to be upregulated in root tips and shoots, implying an increase in MT production and chelation in those respective areas (Zhou & Goldsbrough, 1995; W.-J. Guo et al., 2003). Genes encoding HMA1 and HMA6/PAA1 were upregulated, increasing root to shoot translocation and increased copper transportation to the chloroplasts of leaves (del Pozo et al., 2010; Boutigny et al., 2014; S. Lee et al., 2007). HMA8 encoding HMA8/PAA2 is upregulated, demonstrating increased copper transport from the cytosol to the thylakoid lumen and to plastocyanin (del Pozo et al., 2010; Mayerhofer et al., 2016; Tapken et al., 2012). An increase in copper delivery to the chloroplast stroma, thylakoid lumen and to plastocyanin suggests increased photosynthesis in response to excess copper (Tapken et al., 2012, 2015). COPT6 is upregulated, demonstrating copper redistribution and transport between leaves and reproductive organs (Garcia-Molina et al., 2013).

The gene encoding ATX1 in *Arabidopsis Thaliana* and *Oryza sativa* is upregulated, increasing the delivery of copper to HMA5 and HMA7/Ran1 (Andrés-Colás et al., 2006; W. Li et al., 2017). ATX1 thus contributes to root to shoot translocation and the transport of copper to the ER Golgi complex for growth modulation (Y. Zhang et al., 2018; Shin et al., 2012). Coordinating with the upregulation of ATX1 is the increased expression of AtHMA7 encoding for HMA7/Ran1 (del Pozo et al., 2010; W. Li et al., 2017). The upregulation of AtHMA7 encourages increased copper transport from ATX1 to the Golgi apparatus, endoplasmic reticulum, and ethylene receptors located in the endoplasmic reticulum. Increased ethylene signalling in roots, leaves and reproductive organs induces growth and development, which is a strategy the plant may implement to counteract copper toxicity (B. Zhang et al., 2014). OsHMA9 encoding HMA9 is upregulated in *Oryza sativa* in the xylem and phloem, suggesting an increase in xylem and phloem loading (S. Lee et al., 2007). OsHMA9 may also be upregulated in roots, especially at earlier stages of growth. Genes encoding MT1a and MT2b were found to be upregulated in the phloem, indicating an increase of MT production and chelation in the phloem area (W.-J. Guo et al., 2003). Upregulation of MT4 genes in the seeds indicates increased metallothionein production and chelation in the seed area. Genes encoding CCS are upregulated, demonstrating increased copper delivery to Superoxide Dismutase (SODs), which subsequently drives the breakdown of superoxide radicals to oxygen and hydrogen peroxide (del Pozo et al., 2010; Cohu et al., 2009; Chu et al., 2005; McCord & Fridovich, 1969). COX17 is upregulated in roots and shoots, increasing Cytochrome C Oxidase activity which increases cellular respiration (del Pozo et al., 2010; Garcia et al., 2015). COX17 is located in the intermembrane space of the mitochondria and delivers copper to enzymes responsible for Cytochrome C Oxidase synthesis (Garcia et al., 2015, p. 201).

1.7 Physiological and genetic response to nickel

1.7.1 Properties of nickel in the soil

Nickel concentration in the soil is usually at low levels but can drastically increase near areas with high industrial output. Some studies found low nickel content samples to be in the range of 20-50 mg/kg, whereas samples in areas with heavy anthropological contamination or ultramafic rocks may approximate 10000 mg/kg (Echevarria et al., 2006). In Sudbury, nickel content near smelter sites ranges from 30.9 to 1600 mg/kg (Narendrula et al., 2011). Nickel is commonly available in its divalent cationic form or complexed with 6 hydrated ions, with the latter form being more prevalent in more acidic soils (Dunemann et al., 1991; Soares et al., 2011). Nickel can also be adsorbed to cation surfaces or chelated to other metal complexes in soil (Ashworth & Alloway, 2008; Sastre et al., 2001). At lower pH, nickel solubility increases leading to higher mobility within the soil and uptake within plants. pH seems to be the main factor that affects the amount of exchangeable nickel in the soil (Echevarria et al., 2006). The presence of non crystalline organic matter or silicates may also increase the bioavailability of nickel.

1.7.2 Nickel uptake and transportation

Nickel uptake and transportation is understudied, with large gaps of knowledge at multiple control points within the vascular system. The majority of initial nickel uptake occurs through the roots likely by nonspecific active diffusion (Cataldo et al., 1978). Unlike other heavy metals, there are few identified transporters or chelators in the root area that are specific or catered to the initial uptake of nickel. Transporters with broad metal specificity have been found to uptake nickel (Nishida et al., 2015, 2011). IRT1 in *Arabidopsis thaliana* is an iron transporter located in the roots that uptakes nickel under conditions of excess nickel (Nishida et al., 2011). Other divalent

metals can easily alter and interfere with initial uptake (Ghasemi et al., 2009). Iron deficiency increases nickel uptake whereas copper outcompetes and diminishes nickel uptake in *Alyssum inflatum*. In *Arabidopsis thaliana,* zinc deficiency induces the increased uptake of nickel (Nishida et al., 2015). IREG2 was found to induce the sequestration of nickel to the vacuole of root cells while diminishing root to shoot translocation in *Noccaea japonica* but not in other species such as *Noccaea caerulescens* (Nishida et al., 2020; Schaaf et al., 2006). Some nickel accumulators have increased transporter and chelator expression not found in other species that are instrumental in accumulation (Mari et al., 2006a). Chelators thus contribute more to xylem transportation and the relocation of nickel throughout the vasculature in comparison to other metals (Mnasri et al., 2015). Nicotianamine, histidine, and citric acid are highly expressed in the roots of hyperaccumulators and have been implicated in vacuole sequestration (Pianelli et al., 2005; Krämer et al., 1996; Amari et al., 2016). To date, there has yet to be an identified transporter responsible for the xylem loading of nickel. In the xylem sap, nickel is translocated as free ions or within a nicotianamine based complex, with the latter having been only identified in hyperaccumulator species (Mari et al., 2006a). Once in the xylem, nickel is transported and distributed through the shoots (da Silva et al., 2016). YSL3 in *Arabidopsis thaliana* transports nickel complexed with nicotianamine (Gendre et al., 2006). The high expression of YSL3 in the central cylinder of young root, phloem of old roots and xylem suggests that it is involved in root to shoot translocation and xylem unloading. Transporters responsible for shoot distribution requires further characterization, although multiple candidate genes including ZIP genes such as ZNT1 and ZNT2 have been identified (Visioli et al., 2014). Many hyperaccumulators store excess nickel in the vacuoles of the leaf epidermis, possibly to prevent damage to the photosynthetic machinery in the mesophyll cells (Sánchez-Mata et al., 2013; Küpper et al., 2001; Baklanov, 2011). Phloem loading and redistribution also require further

characterization, although it has been observed that nickel distributes to newer, growing shoots and reproductive organs at a much faster rate than zinc, manganese, cobalt, and cadmium (PAGE & FELLER, 2005; Riesen & Feller, 2005). The fast transportation of nickel to these areas and the large proportion of nickel mobilized implies highly efficient phloem loading and redistribution.

1.7.3 Utilization of nickel in plants

Nickel is an essential micronutrient that is involved in many aspects of plant health. Nickel can readily bind to the S-ligands and cysteine residues of enzymes and functional groups (Szunyog et al., 2019; Wuerges et al., 2004). Nickel is a cofactor for urease, an enzyme integral to nitrogen recycling and the ornithine-urea cycle (Barcelos et al., 2018; Urra et al., 2022). Urease hydrolyzes urea to usable ammonia and carbon dioxide, which are subsequently converted to nitrogen-based intermediates such as ornithine, citrulline, glutamine, aspartate, arginine, etc. Nitrogen wastes and by-products are thus repurposed into polyamines and amino acids required for other functions such as cellular respiration or cell wall restoration (Urra et al., 2022). Nickel is a cofactor for hydrogenase which is an enzyme required for nitrogen fixation in legumes and symbiotic bacteria (Baginsky et al., 2005). In the root nodules of the symbiotic complex, hydrogenase catalyzes the oxidation of H_2 and the reduction of acetylene, increasing the efficiency of nitrogenase. Nickel is also involved in a lesser extent in other plant functions associated with immune and defense mechanisms. Nickel superoxide dismutase operates in some plant species, metabolizing ROS and in some cases protecting other enzymes that are susceptible to ROS damage (C. Chen et al., 2022). In dealing with external stresses, nickel is a cofactor for glyoxalase I, an enzyme that converts methylglyoxal and other aldehydes to d-lactate (Turra et al., 2015). Methylglyoxal is a toxic by-product of glycolysis produced by the degradation of dihydroxyacetone phosphate and glyceraldehyde-3-phosphate (Yadav et al., 2005).

1.7.4 Nickel deficiency in plants

In comparison to other metals and essential micronutrients, nickel is not required in large concentrations (P. H. Brown et al., 1987). However, nickel deficiencies in plants often go undetected as many plants are unable to attain its highest growth potential (Siqueira Freitas et al., 2018). Due to its integral role in nitrogen recycling and urea detoxification, an absence of nickel may considerably hinder the cycling of nitrogen (C. Bai et al., 2006). Decreased urease activity causes the buildup of urea in above ground tissues, leading to phytotoxic effects which include browning of the leaf edges and decreased growth (X. W. Tan et al., 2000). Deregulation of the ornithine-urea cycle may also cause a buildup of ammonium, causing the necrosis of leaf tips, chlorosis of leaf edges, and hindered overall leaf growth. Nickel deficiency may cause the disruption of the TCA cycle leading to an increase in lactic acid, an increase in oxalic acid and a decrease of citric acid (C. Bai et al., 2006). The dysregulation of the TCA cycle indirectly causes lower cellular respiration, lower ATP production and the accumulation of intermediates such has oxalic acid and lactic acid. The toxic accumulation of these intermediates contributes to the appearance of "mouse ear", which is characterized by smaller leaves with necrosis on the rounded edges (C. Bai et al., 2006).

1.7.5 Nickel toxicity in plants

Nickel has a low requirement threshold, a large prevalence in soils and less identified functions compared to other micronutrients, thus nickel toxicity is more common than nickel deficiency (Yusuf et al., 2011). Excess nickel causes a severe dysfunction in the homeostasis of many metals including copper, iron, manganese, and zinc resulting in a variety of physiological problems corresponding to those metals (Ghasemi et al., 2009; Rubio et al., 1994; X. Yang et al., 1996). Nickel competitively binds to the binding sites of enzymes that would be otherwise functional with

its constituent ion (Wildner & Henkel, 1979). For example, nickel outcompetes iron for enzymes involved in photosystem II and diminishes chlorophyll production, resulting in decreased photosynthesis and chlorosis (El-Sheekh, 1993; Mohanty et al., 1989; Ghasemi et al., 2009). Excess nickel competitively replaces calcium in the oxygen evolving complex and causes conformational changes within the structure, rendering the structure and electron transport chain diminished in photosystem II (Boisvert et al., 2007). Excess nickel also competitively replaces magnesium in chlorophyll, decreasing chlorophyll content and function by inhibiting the transfer of energy to the reaction center (Küpper et al., 1996; Batool, 2018; Baran & Ekmekçi, 2021). The decreased chlorophyll function and concentration leads to diminished photosynthesis, which may physically manifest itself as leaf necrosis and chlorosis. Excess nickel may interfere with the transportation of other metals (Ghasemi et al., 2009; Rahman et al., 2005). Nickel blocks the root to shoot translocation of iron, diminishing its availability to enzymes located in the shoots and causing hindered shoot growth. Depending on the plant species, excess nickel may also affect the initial uptake and root to shoot translocation of zinc, copper, calcium, manganese, and magnesium (X. Yang et al., 1996). The faster delivery of nickels to newer, growing organs compared to other metals may severely impact early development sooner as demonstrated by decreased seed germination, meristem growth and seedling growth (PAGE & FELLER, 2005; Yadav et al., 2005; Pavlova, 2017). Decreased growth and development is further inhibited by the decreased distribution of auxin through the shoots as demonstrated by gravitropic defects (Lešková et al., 2020).

Nickel is a transition metal that can exist in two oxidation states and can indirectly cause the overproduction of ROS when in excess, causing tissue and organ damage (Schützendübel & Polle, 2002). Excess nickel may cause a decrease or increase of antioxidative enzyme activity which

include SOD, CAT, APX, POD and GSH-Px (Gajewska & Skłodowska, 2006; Baccouch et al., 2001). Some antioxidative enzymes may also increase at lower concentrations of nickel and decrease at higher concentrations (Gajewska & Skłodowska, 2006; Natasha et al., 2020; Demirezen Yilmaz & Uruç Parlak, 2011; Rizwan et al., 2017; Thakur & Sharma, 2015).

1.7.6 Genetic responses of plants to excess nickel

The regulation of some transporters and chelator genes have been observed in response to excess nickel. In comparison to other metals, excess nickel tends to elicit fewer genetic responses and genetic regulation. Genes encoding IREG2 in hyperaccumulators *Psychotria gabriellae* and *Noccaea japonica* were upregulated with some genes being solely expressed in root cells (Merlot et al., 2014; Nishida et al., 2020). The upregulation of IREG2 implies increased nickel sequestration into the vacuoles of root cells, decreasing root to shoot translocation (Nishida et al., 2020). NRAMP was found to be upregulated in *Picea glauca* in response to nickel stress, indicating a possible increase in nickel chelation and transport (Boyd & Nkongolo, 2020; Milner et al., 2014). Genes encoding chelators in multiple areas of the plant have been found to be highly expressed (S. Kim et al., 2005; Persans et al., 2001). TcNAS encoding nicotianamine was found to be upregulated in the shoots of the hyperaccumulator *Thlaspi caeulescens*, leading to increased nickel chelation in the shoots (Mari et al., 2006a). The function of shoot chelation in this context requires characterization, despite upregulation of TcNAS being associated with conferred nickel tolerance. Furthermore, transgenic plants overexpressing NAS genes were able to hyperaccumulate nickel with considerable tolerance to toxicity (S. Kim et al., 2005; Pianelli et al., 2005). Genes involved with the synthesis of histidine, ie. ATP-phosphoribosyltransferase (ATP-PRT), were highly expressed in the hyperaccumulator *Alyssum lesbiacum* compared to non hyperaccumulators (Ingle et al., 2005). The larger amount of free histidine in the xylem sap is

associated with a more efficient root to shoot translocation in addition to increase chelation of nickel (Ingle et al., 2005). Other candidate genes involved with nickel resistance include genes encoding glutathione-S-transferase, NRAMP transporters and thioredoxin family protein in *Betula papyrifa* (Theriault et al., 2016).

1.7.7 Transcriptome analysis of other plants in response to excess nickel

Transcriptome analysis of plants responding to excess nickel characterizes various attributes of gene expression and reveal mechanisms associated with nickel resistance. *Populus tremuloides* and *Betula papyrifera* are nickel accumulators that express differential gene expression between resistant and susceptible genotypes (Czajka & Nkongolo, 2022; Theriault et al., 2016). In contrast, *Acer rubrum* is a nickel avoider that does not exhibit differential gene expression between resistant and susceptible genotypes (K. Nkongolo et al., 2018). Resistant genotypes compared to water had more upregulated than downregulated genes in *Betula papyrifera*, *Acer rubrum* and *Populus tremuloides* (Czajka & Nkongolo, 2022; Theriault et al., 2016; K. Nkongolo et al., 2018). Susceptible gentoypes compared to water had more upregulated than downregulated genes in only *Betula papyrifera* and *Acer rubrum*. However, the number of differentially expressed genes in the susceptible genotype of both species was considerably lower than the resistant genotype, indicating lower gene expression associated with the susceptibility. In *Populus tremuloides*, *Betula papyrifera* and *Acer rubrum*, the largest proportion of genes in the biological processes functional category was associated with transport, cellular component organization and carbohydrate metabolic process (Czajka & Nkongolo, 2022; Theriault et al., 2016; K. Nkongolo et al., 2018). For metabolic processes, the largest percentage of expressed genes were associated with nucleotide binding, kinase activity and DNA binding. In regard to cellular compartment, the majority of expressed genes were localized to the ribosome, chloroplast and plasma membrane for *Populus*

tremuloides. In *Betula papyrifera,* the largest proportion of genes for cellular compartment was associated with the ribosome, cytosol and plasma membrane (Theriault et al., 2016). In *Acer rubrum*, the categories with the most expressed genes were the cytosol, ribosome and mitochondrion (K. Nkongolo et al., 2018). Identified candidate genes for *Betula papyrifera* include genes encoding Glutathione S-transferase, NRAMP transporters and thioredoxin family proteins (Theriault et al., 2016). ATOX1-related copper transport protein was the only candidate gene identified for *Populus tremuloides* (Czajka & Nkongolo, 2022).

1.8 Description and physical appearance of the subject: *Pinus banksiana*

Pinus Banksiana is a species of pine native to North America, ranging from the Northwest Territories in Canada to Minnesota, Michigan and smaller regions in Northeastern United states (McLeod & MacDonald, 1997; Rudolph & Laidly, 1990; Kashian et al., 2003; Tweiten, 2016). It is part of the *Pinus* genus comprised of 110 pine species and its closest relative is *Pinus contorta.* It is the most widely distributed pine in Canada, being able to grow on rocks, sands, frost, areas with poor soil quality and areas with a cold climate (Rudolph & Laidly, 1990; Pisaric et al., 2009; Greenwood et al., 2002; M. Huang et al., 2013; Coursolle et al., 2002). *Pinus banksiana* can grow around 150 years with a height range of 15-25 m and a diameter of 20-30 cm (Barton & Grenier, 2008; Kenkel et al., 1997). The taproot root system distributes widely and has an intermediate depth (Plourde *et al.*, 2009). Each fascicle consists of 2 stiff, short needles that are yellow to green, pointy and spaced far enough from each other, forming a distinctive V shape (Barton & Grenier, 2008). Each needle ranges from 2-4 cm in length and can be slightly curved or relatively straight. The twigs are thin and dark brown or grey. The cones are tightly closed, consist of approximately 80 scales and are attached to the branch by a very short stem, giving the appearance of growing from the branch (Rudolph & Laidly, 1990). The cones are also yellow to brown, conical,

asymmetrical and are in 2-3 clusters at the nodes of each branch. Hot temperatures or the presence of a fire will open the cones, releasing seeds to allow for fast seeding reproduction (Alexander & Cruz, 2012; Sharpe et al., 2017). Open cones have a flared, curved appearance. The bark is dark brown or grey, fragile, and susceptible to damage in seedlings and may grow into randomly layered plates with maturity (Zakrzewski & Duchesne, 2012). Jack pine is a softwood pine with intermediate hardness and intermediate mass compared to other pine trees (C. Huang et al., 2020).

Being widely distributed in Canada, *Pinus banksiana* is a very hardy, resilient tree. A pH range of 5-9 did not significantly affect photosynthesis or transpiration in *Pinus banksiana* (F. Xu et al., 2020). However, chlorophyl content decreased in seedlings and dry weight decreased at higher pH. Furthermore, high pH decreased phosphorous, calcium, manganese, magnesium, zinc, and iron content. In comparison to other pine species, *Pinus banksiana* is least affected by excess salinity and its physiology may be stimulated at lower concentrations (Croser et al., 2001; Franklin et al., 2002). Like other evergreen boreal pines, needle longevity and low nitrogen concentration is correlated with lower temperatures, likely as an adaptive trait to colder climates (Reich et al., 2014).

In Sudbury, a moderate genetic diversity for *Pinus banksiana* with low gene flow was observed in metal contaminated sites (Vandeligt et al., 2011). This is in contrast to other pine species such as *Pinus Resinosa* which demonstrated significantly lower genetic diversity and higher rates of inbreeding (Vandeligt et al., 2011; Ranger et al., 2008). *Pinus banksiana* populations were found to have no correlation between genetic diversity and metal accumulation. Populations in contaminated and uncontaminated areas were also found to be genetically close to each other, although newer trees involved in the regreening program had a significantly higher genetic diversity.

1.9 Thesis rationale and objectives

Policy makers and institutions are increasingly focusing on environmental restoration, encouraging the production and use of "eco friendly" or "environmentally sustainable" technology. However, technologies such as electric vehicles and smartphones require a large amount of nickel and copper alloys which involves a large amount of heavy metal processing and mining. As demand for these products and applications soar, demand for heavy metals such as copper and nickel also increase. At high levels, copper and nickel contamination cause considerable damage to plant biota, animal communities and ecosystems (J. Xu et al., 2006; Baccouch et al., 2001). It is therefore imperative to confront heavy metal toxicity and its impact on the environment, especially in areas with a high industrial output such as Sudbury. Current approaches to environmental remediation are unable to cater to northern environments due to its colder, subarctic climates. Currently, the majority of biomolecular and phytoextraction research has been focused to angiosperms and smaller plants, which can only operate optimally in warmer, moist climates (Pollard et al., 2014). Currently used hyperaccumulators have a small biomass, are difficult to grow in colder environments, and may pose a threat to the biodiversity and stability of the ecosystem. In contrast, conifers such as *Pinus banksiana* already grow in the general area and have been used extensively in successful regreening programs (Beckett & Spiers, n.d.). Conifers are better acclimated to colder climates, grow year-round, and are robust and hardy. Working with previously adapted and integrated conifers is ideal, less time consuming, and cost effective compared to other hyperaccumulators which require cautious attention to various different parameters.

Currently, there are large gaps of knowledge in regard to the genetic structure of conifer species. To improve the utility of *Pinus banksiana* as a remediation tool, the protein coding genes and

genetic response to copper and nickel must be further researched. A transcriptome profile of *Pinus banksiana* and other *Pinus* species has yet to be done. Additionally, genetic studies of conifer species in response to heavy metals are needed for a subject that has been overwhelmingly focused on angiosperms and other smaller plants. Transcriptional analysis is valuable in this regard as it will show similarities and differences between the genetic responses from both classifications of plants. *Pinus banksiana* is therefore a potential candidate for transcriptome analysis.

Objectives

Performing a transcriptome analysis on *Pinus banksiana* will provide an essential resource for understanding the genetic response of *Pinus banksiana* to heavy metals. For any given pine seedling treatment, the entire transcriptome will be revealed for that given state at the time of harvest. A transcriptional analysis of copper and nickel treated seedlings will fulfill the following objectives: 1) Comprehensively map and characterize the transcriptome of Jack Pine (*Pinus banksiana*), 2) Assess the gene expression of distinct genotypes exposed to nickel ion toxicity, 3) Assess the gene expression of distinct genotype exposed to copper ion toxicity, 4) Evaluate variations in gene expression between genotypes responding to nickel toxicity or copper toxicity.

Chapter 2: Transcriptome Analysis of Nickel Resistant and Susceptible Jack Pine (*Pinus banksiana*)

2.1 Introduction

Sudbury, Ontario is a region that has been afflicted by over 130 years of Nickel mining and processing (Schindler, 2014; Jewiss, 2013; Keller et al., 2007). Despite the large environmental risks, the region is poised to increase nickel production to keep up with rising global demand. Nickel contamination causes considerable damage to plant biota, animal communities and ecosystems (J. Xu et al., 2006; Baccouch et al., 2001). In plants, nickel is an essential micronutrient at low levels (Yusuf et al., 2011). At higher levels, nickel has been found to diminish photosynthesis by decreasing the functionality of photosystem II and inhibiting chlorophyl function and production (Boisvert et al., 2007; Küpper et al., 1996; Batool, 2018; Baran & Ekmekçi, 2021). Excess nickel causes a severe dysfunction of homeostasis for many metals including copper, iron, manganese, and zinc resulting in a variety of physiological problems corresponding to those metals (Ghasemi et al., 2009; Rubio et al., 1994; X. Yang et al., 1996). Unlike other heavy metals, nickel indirectly causes the overproduction of Reactive Oxygen Species (ROS) by increasing or decreasing the activity of antioxidative enzymes such as superoxide dismutase (SOD) and catalase (CAT) (Gajewska & Skłodowska, 2006; Baccouch et al., 2001). The inhibition of these physiological functions and mechanisms hinders the overall growth and development of the plant (Baran & Ekmekçi, 2021; Pavlova, 2017; Yadav, 2022). Jack Pine (*Pinus banksiana*) has been proposed as a potential candidate for genetic research to improve regreening and remediation efforts due to its acclimation to the cold, challenging climate. Additionally, Jack Pine has been successfully used in a regreening project in the Sudbury region (Beckett & Spiers, n.d.).

Mechanisms involved in nickel resistance and detoxification remain poorly elucidated in comparison to other heavy metals such as copper. In response to excess heavy metals, plants may modulate the production of chelators, metallothionein and transporter proteins in different areas of the plant. Plants may also regulate antioxidative enzyme activity in response to ROS produced as a by-product of heavy metal toxicity. In response to excess nickel, genes encoding the chelators nicotianamine and histidine were found to be upregulated in the hyperaccumulators *Thlaspi caeulescens* and *Alyssum lesbiacum*, respectively (Mari et al., 2006b; Ingle et al., 2005). The IREG2 transporter gene has been found to be upregulated in the hyperaccumulators *Psychotria gabriellae* and *Noccaea japonica*, suggesting nickel sequestration into the vacuoles of root cells during the initial uptake of nickel into the roots (Merlot et al., 2014; Nishida et al., 2020). In *Pinus banksiana* and *Pinus strobus*, excess nickel prompted a downregulation of the gene encoding the natural resistance associated macrophage protein (NRAMP3) (Moarefi & Nkongolo, 2022). In contrast, this gene was upregulated in *Picea glauca* under conditions of excess nickel (Boyd & Nkongolo, 2020). In some species, NRAMP3 is localized to the vacuole membrane, implying a possible role in nickel sequestration into the vacuole (Wei et al., 2009; Bastow et al., 2018). Although the expression of particular genes such as NRAMP3 have been studied in conifers, the extent to which the genes are expressed or regulated relative to other genes remain elusive. This study will be the first to map and describe the transcriptome in a nickel treated coniferous tree, providing an indispensable asset to other researchers for understanding conifer genetics and responses to nickel stress.

The objectives of this study were to: 1) Characterize the transcriptome of Jack Pine (*Pinus banksiana*). 2) Use transcriptome analysis and gene ontology to characterize the genes in response

to Nickel stress. 3) Evaluate differences in gene expression between different groups of nickel treated plants.

2.2 Materials and methods

2.2.1 Plant treatment

Pinus banksiana seedings were provided by College Boreal Plant Center located in Sudbury Ontario. The continued growth of the 6 month old seedlings at Laurentian University was conducted according to the methodology outlined in Moarefi and Nkongolo (2022) (Moarefi & Nkongolo, 2022). *Pinus Banksiana* was transplanted into planter pots containing a 1:1 mixture of sand and soil. The seedlings were incubated in a growth chamber for one month. The seedlings were also fertilized with a 1:1:1 mixture of nitrogen, phosphorous and potassium fertilizer when required. After one month, the seedlings were given treatments in a completely randomized block design. Fifteen seedlings were treated with 1600 mg of nickel sulphate per 1 kg of soil. This treatment represented the in field concentration of Ni from a survey on metal contaminated sites in the Greater Sudbury Region (Nkongolo et al., 2013). Fifteen seedlings were treated with 3200 mg of nickel sulphate per 1 kg of soil representing double concentration. Ten seedlings were given deionized water which represented the negative control. Selected plants were treated with potassium sulphate as a salt control to account for the effect of sulphate ions on the treatment regimen. 5 seedlings were treated with 1600 mg/kg of potassium sulphate corresponding to the 1600 mg/kg concentration of nickel sulphate. An additional 5 seedlings were treated with 3200 mg/kg of potassium sulphate corresponding to the 3200 mg/kg concentration of nickel sulphate. The seedlings underwent a 2 week incubation period. After the incubation period, a damage rating system was used to identify resistant and susceptible plants in

the nickel treatment group 1 day prior to harvest. Plants were rated based on overall changes in appearance between pre treatment and post treatment images. Needles from the selected seedlings were harvested and wrapped in individual aluminum foils. For longer term storage, the needles were flash frozen using liquid nitrogen and stored in a freezer at -4 ^{O}C.

Table 2. Damage ratings based on the comparison of pre treatment and post treatment appearance

Damage Rating	Evaluation	Description
1-3	Not affected by treatment	Underwent little to no change. Growth and appearance were similar to controls.
4-6	Some damage	Intermediate level of damage. Some green needles and growth but with variable discoloration, browning or weaker needles present.
7-10	Severe damage	Little to no growth. Brown or weakened needles with considerable amounts of discoloration.

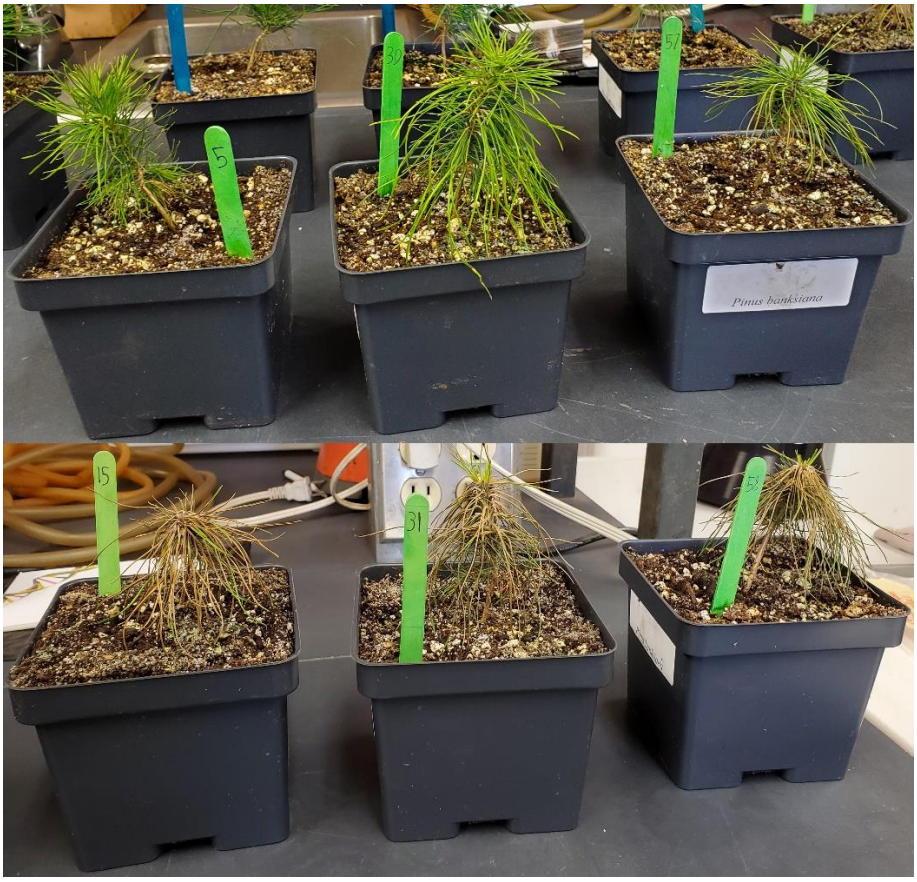

Figure 1. Damage rating of Pinus banksiana seedlings after treatment with 1600 mg/kg of nickel. Selected seedlings underwent treatment and were assigned damage ratings based on various attributes. The top image depicts seedlings from the resistant group and the lower image represents seedlings from the susceptible group.

2.2.2 RNA Extraction

RNA extraction was performed on the needles of the seedlings following the protocol from the NORGEN BIOTEK Plant/fungi total RNA purification Kit which can be found here: https://norgenbiotek.com/product/plantfungi-total-rna-purification-kit. Agarose gel electrophoresis was performed on the extracted RNA to assess RNA quality. The quantity of RNA for each sample was determined using the Qubit™ RNA BR assay kit. The extracted RNA samples were stored in a freezer at -80 ^{O}C.

2.2.3 RNA sequencing and De Novo Transcriptome Assembly

Messenger RNA (mRNA) was isolated from total RNA. Chemical RNA fragmentation was done to account for the size limitation of the sequencing platform. mRNA was reverse transcribed to cDNA using reverse transcriptase and RNAse was added to prevent unnecessary ligation between different nucleotide strands. Second strand synthesis was performed followed by 3' end ligation with adaptors and adenosine caps. The cDNA was amplified to generate cDNA libraries. Illumina sequencing (performed at Seqmatic in San Francisco, California, USA) was used to sequence the cDNA libraries. FASTQC files for each sample were generated corresponding to each cDNA library. The FASTQC program verified the quality of raw data from the files and provided attributes for each sequence which included average sequence length, %GC content, total deduplicated percentage and sequences flagged as poor quality. The Cutadapt program was used to remove adaptor sequences and low-quality bases from the raw read data. The Bowtie2 algorithm in Trinity was used to map RNA sequence raw reads to the trinity transcript assembly, generating sequence alignment map (SAM) files which were then converted to BAM (binary form of SAM) files. Transcript assembly was performed by inputting RNA sequence data from all samples into the TRINITY program, which quantified the number of genes based on the number of detected isoforms.

2.2.4 BLAT matching and annotation of *Pinus banksiana* genes

Transcripts were characterized by performing a 2 way BLAST-like alignment tool (BLAT) matching with the *Pinus taeda* genome as a reference. Attributes such as Transcript ID, Gene ID, and corresponding log (E-value) for sequence similarity with the reference genome was characterized. Other identified characteristics identified by BLAT matching include query sequence size, transcript sequence size, and the percentage of net match for each characteristic.

Every transcript was mapped to protein sequences in the UniProt database, generating corresponding UniProt IDs. Protein matches with the highest degree of similarity were used to annotate genes and assign gene ontology information such as gene description.

2.2.5 Quantification of gene expression and quality control (QC) analysis

The RNA-Seq by Expectation-Maximization (RSEM) abundance estimation method was used to quantify the expression level of each gene/transcript and related isoforms. Quality control for read count was performed to critically assess the number of counts from each gene. Raw reads were filtered and selected for counts of at least 1,2, 10, 50 or 100. Genes with 1 read were considered noise. Genes with 2 or more counts were used as an estimate for the number of genes expressed. Genes with 10 or more counts were considered an adequate indication of the number of genes that had enough reads for downstream statistical analysis. For each treatment group, genes with a counts per million (CPM) value of 1 or higher in at least 2 samples were included in downstream analysis. Genes with a CPM value of less than 1 in at least 2 samples were unexpressed and removed. Normalization factors for raw counts were generated using a trimmed mean of M-values (TMM) from edge R to remove variations from samples and normalize the samples.

The normalized read counts were log-scale transformed using the voom method (log2 scale) from the R limma package. Boxplots of the transformed expression values were generated to show the mean distribution of every sample. Deviation from the mean distribution in a particular sample may indicate variations among experimental conditions, sample contamination or batch effect. Samples that deviated significantly from the mean distribution within the same objective group were excluded.

Multidimensional scaling plots were generated to display the clustering of sample groups based on the leading logFC of normalized data. Groups of samples that deviated significantly from other groups of samples were considered differentially regulated. Samples that deviated significantly from the other samples within the same group were considered outliers and not included in downstream analysis.

A heatmap was generated from the logFC of 5000 genes to show the visual relationship of gene expression between the samples. Samples that did not have a similar logFC pattern of gene expression from other samples within the same group were considered outliers and were not included in downstream analysis. The proportion of raw reads expressed by the top 100 upregulated and downregulated genes were also assessed in every sample to identify potential bottlenecking issues.

2.2.6 Differential gene expression (DGE) analysis of pairwise comparisons

The cutoff for pairwise comparisons was calculated to be equivalent to 10 raw counts. From the average of total counts in all samples, a CPM of 0.361 was calculated as the minimum threshold required to be included in pairwise comparisons. Genes that had a CPM higher than the cutoff in at least 2 samples were included in downstream analysis whereas genes that did not fulfill these parameters were excluded. The pairwise comparisons of transcripts were performed between RG and the control, SG and the control, and RG and SG. Differential gene expression expressed as logFC values were evaluated using the R limma package. To assess the interference of sulphate ions on the treatment regimen, pairwise comparisons of expressed genes were also conducted between RG and the potassium control, SG and the potassium control, and water and the potassium control. The entire set of genes for each pairwise comparison was annotated using Trinotate and

Trinity. Gene ontology was performed by assigning GO terms and gene IDs from available databases to the set of genes for a particular pairwise comparison. Genes that could not be annotated were filtered out of the set of annotated genes. Each gene set was run through a plant slim function using the Omicsbox program. Gene ontology charts functionally categorizing biological process, metabolic function and cellular component were generated. For each functional category, sequences were distributed using the NodeScore of each assigned GO term.

2.2.7 Analysis of top differentially regulated genes

The top 100 upregulated genes and downregulated genes were ranked for the following pairwise comparisons: RG and the control, and SG and the control. Genes were ranked based on LogFC and fulfillment of high stringency parameters. UniProt annotation and review of the current literature was done to characterize genes associated with copper detoxification or tolerance mechanisms. Genes associated with nickel resistance were considered candidate genes. Gene ontology charts functionally categorizing biological process, metabolic function and cellular component were generated for the top 100 regulated genes using the aforementioned process in DGE analysis. Charts comprised of the top 25 genes were provided for each pairwise comparison.

2.3 Results

2.3.1 Transcript assembly and sequence data QC

The FastQC program characterizes the raw reads from Illumina sequencing and verifies the quality of the data. None of the sequences were flagged as poor quality. Nickel resistant plants had 35-51 million total sequences whereas nickel susceptible plants had 24-28 million total sequences. Both treatment groups had an average sequence length of 51 bases. Nickel resistance samples had a total deduplicated percentage of 24-41%, indicating that a significant portion of gene expression was from duplicated gene expression. Nickel susceptible samples had a total deduplicated percentage of 38-52%, indicating that a slightly smaller portion of gene expression was from duplicated gene expression. Transcript assembly using the Trinity program produced a total of 581037 transcripts with 435293 genes. Out of 435293 genes, 261199 genes fulfilled the CPM parameters and were thus used for differential gene expression analysis.

2.3.2 Differential gene expression (DGE) analysis

This transcriptome shotgun assembly project has been deposited in the DDBJ/EMBL/GenBank under the BioProject accession number PRJNA962116. A multidimensional scale plot and hierarchical cluster map assessed the clustering between samples. The water and potassium controls clustered close to each other, indicating that gene expression was similar between the treatment groups and sulphate had a negligible effect on the treatment regimen. The clustering of the resistant genotype (RG) and the susceptible genotype (SG) demonstrated that treated samples were similar in regard to gene expression, albeit to a lesser extant compared to the controls. Clustering between individuals did not indicate the presence of potential outliers. Expression of treated samples were significantly different from the water and potassium controls. There were

no DEGs between RG and SG. DEGs only from the high stringency cut off (two fold and FDR 0.05) were considered due to strict confidence levels associated with the false discovery rate (FDR). Although the low stringency is held to a high scrutiny with a p value of 0.01, the higher false discovery rate indicates that the expression of any particular gene may be a false positive and will therefore have a lower statistical confidence. Hierarchical clustering in all samples indicated that the samples within each treatment group were more similar to each other than to samples in other treatment groups. The high stringency cutoff was used for all heatmaps depicting pairwise comparisons excluding RG vs SG, which used the low stringency cutoff.

Table 3. Differentially expressed genes from the nickel resistant genotype compared to the nickel susceptible genotype in *Pinus banksiana*

Cutoff	**Standard (two fold and FDR 0.05)**	**Low Stringency (two fold and pvalue 0.01)**
Up-regulated genes	0	4812
Down-regulated genes	0	2956
Total genes	0	7768

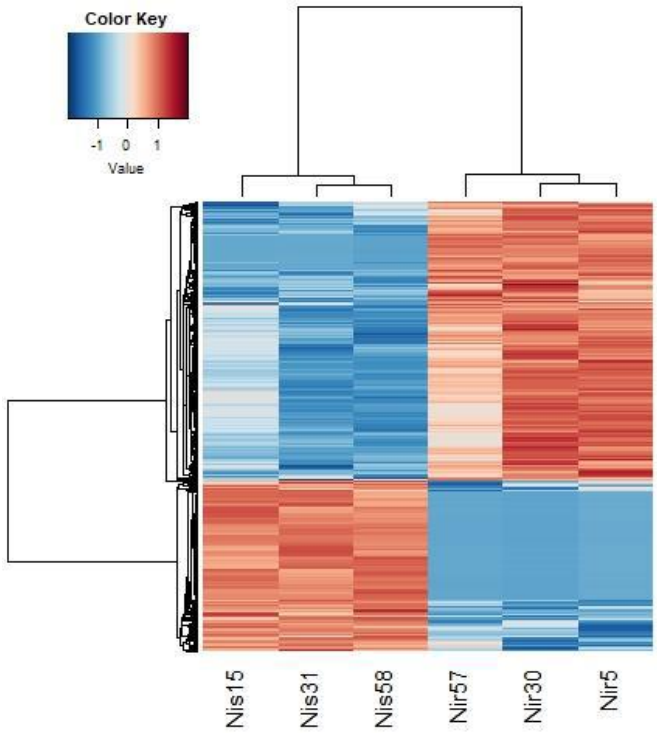

Figure 2a. Heatmap of differentially expressed genes from the nickel resistant genotype compared to the nickel susceptible genotype in Pinus banksiana. Nickel resistant genotypes are labelled as Nir57, Nir30 and Nir5. Nickel susceptible genotypes are indicated as Nis15, Nis31 and Nis58. Red cells represent upregulation whereas blue cells represent downregulation based on Log2 normalized fold change.

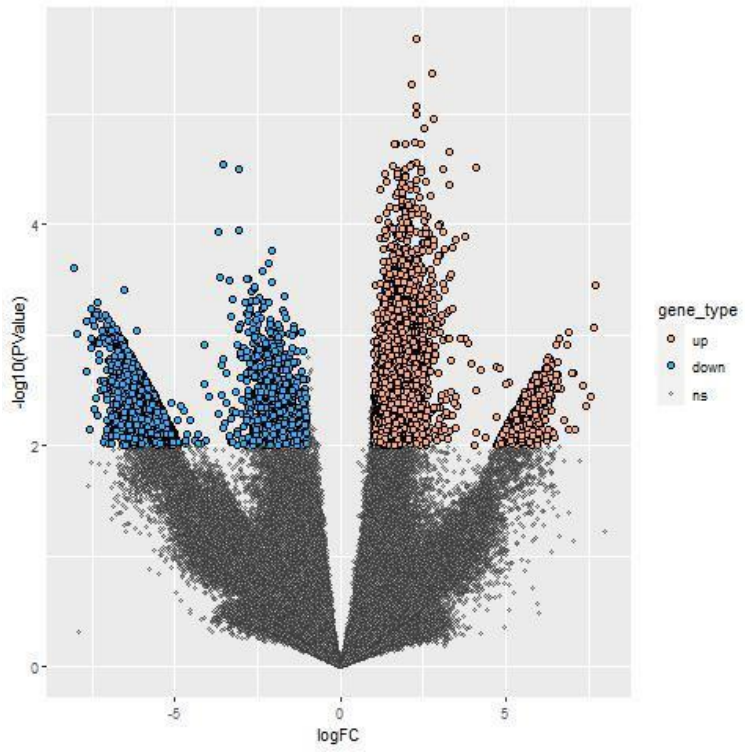

Figure 2b. Volcano plot of differentially expressed genes from the nickel resistant genotype compared to the nickel susceptible genotype in Pinus banksiana. Brown points represents upregulated gene expression whereas blue points represent downregulated gene expression using the susceptible genotype as a reference. Grey points represent genes with no significantly different expression from the susceptible genotype. Log10(FDR) is the log10 of the false discovery rate. The border between the nonsignificant points and the differentially regulated genes represents a false discovery rate of 0.05 (two fold).

Table 4. Differentially Expressed Genes from the nickel resistant genotype compared to the control in *Pinus banksiana*

Cutoff	**Standard (two fold and FDR 0.05)**	**Low Stringency (two fold and pvalue 0.01)**
Up-regulated genes	**4128**	11903
Down-regulated genes	**3754**	6332
Total genes	**7882**	18235

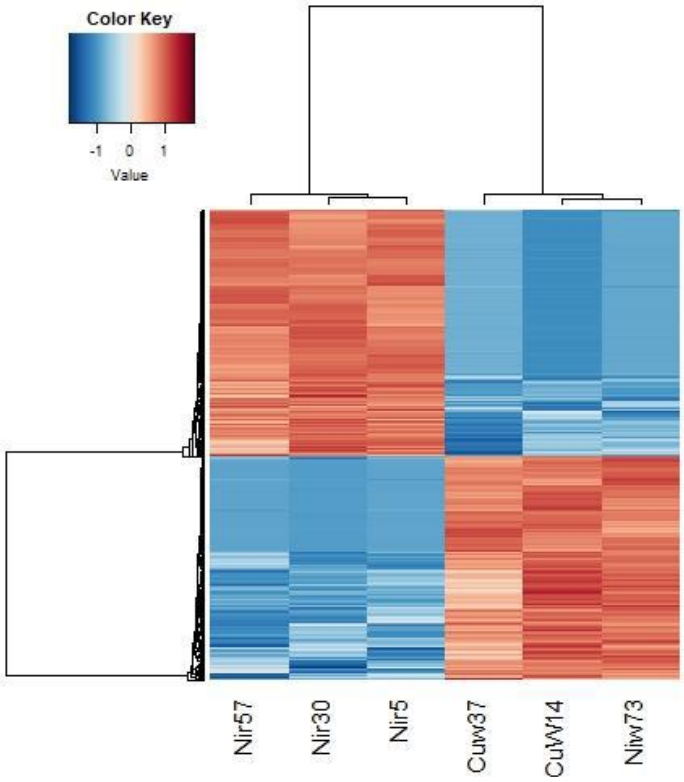

Figure 3a. Heatmap of differentially expressed genes from the nickel resistant genotype compared to the controls in Pinus banksiana. Differentially expressed gene values are based on the Log2 normalized FC, with red cells representing upregulation and blue cells representing downregulation. Nickel resistant genotypes are labelled Nir57, Nir30 and Nir5. Water controls are labelled Cuw37, Cuw14 and Niw73.

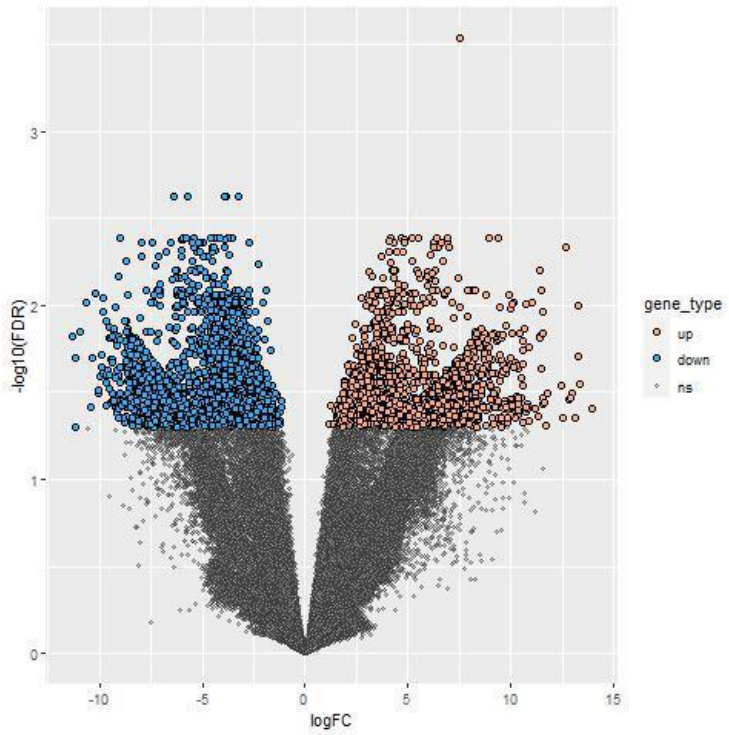

Figure 3b. Volcano plot of differentially expressed genes from the nickel resistant genotype compared to the controls in Pinus banksiana. Brown points represent upregulated gene expression whereas blue points represent downregulated gene expression when compared to the susceptible genotype. Grey points represent genes with no significantly different expression from the water control. Log10(FDR) is the log10 of the false discovery rate. The border between the nonsignificant points and the differentially regulated genes represents a false discovery rate of 0.05 (two fold).

Table 5. Differentially Expressed Genes from the nickel susceptible genotype compared to the water control in *Pinus banksiana*

Cutoff	**Standard (two fold and FDR 0.05)**	**Low Stringency (two fold and pvalue 0.01)**
Up-regulated genes	**37116**	35167
Down-regulated genes	**12053**	11224
Total genes	**49169**	46391

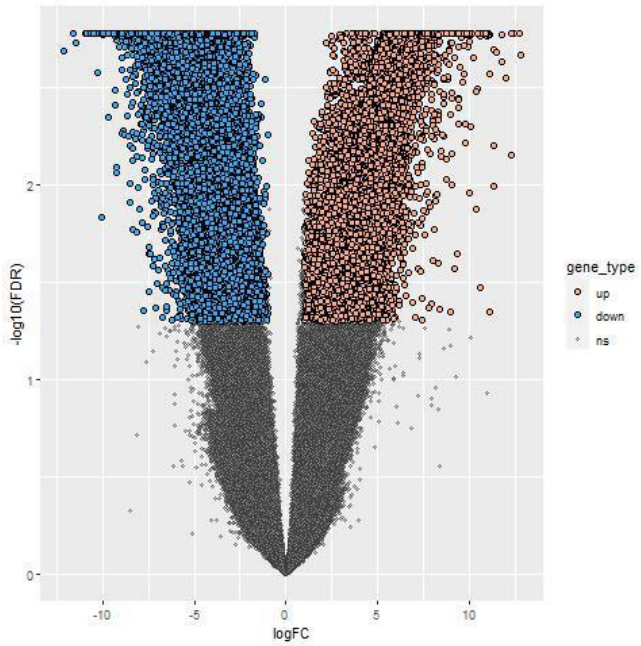

Figure 4. Volcano plot of differentially expressed genes from the nickel susceptible genotype compared to the control in Pinus banksiana. Brown points represent upregulated gene expression whereas blue points represent downregulated gene expression when compared to the water control. Grey points represent genes with no significant difference in expression. The border between the nonsignificant points and the differentially regulated genes represents the false discovery rate of 0.05 (two fold).

2.3.3 Gene ontology classification of differentially expressed genes in *Pinus banksiana*

Gene ontology graphs show the distribution of annotated genes to different terms within the categories biological processes, metabolic function, and cellular compartment (fig 5a-5c). The proportion of genes allocated to each term was similar among the water control, the resistant genotype, and the susceptible genotype.

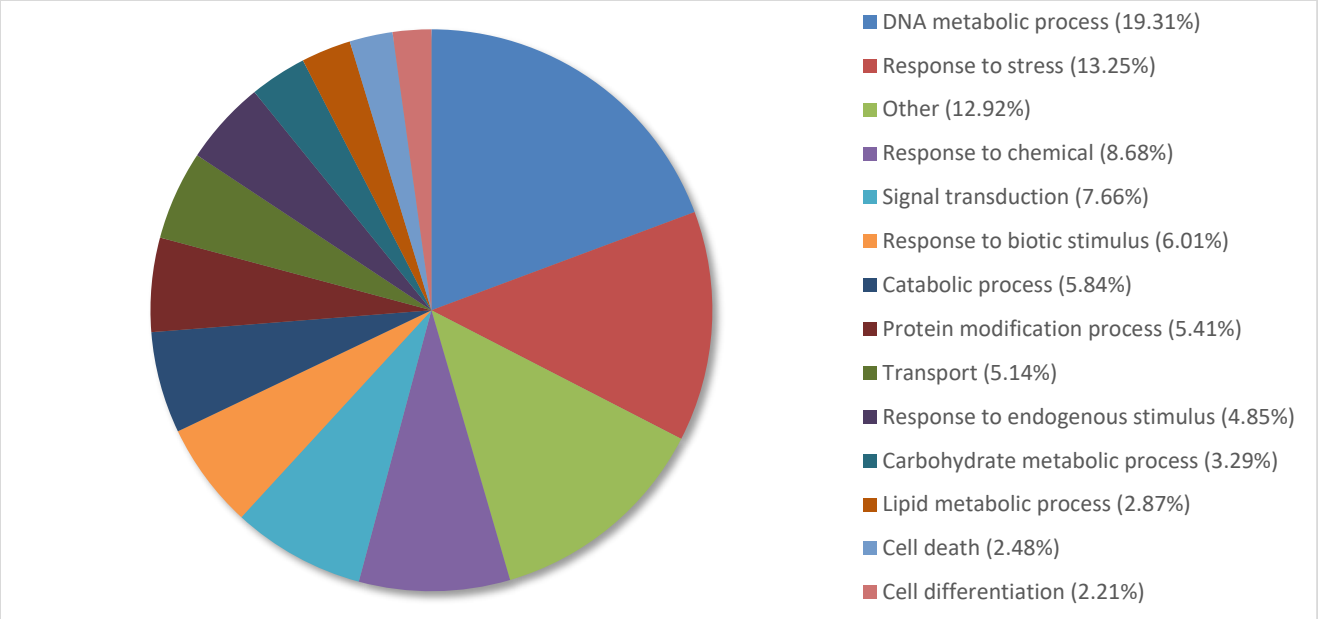

Figure 5a. Percentage of annotated transcripts in *Pinus banksiana* control samples categorized by Biological Processes. A total of 5112 transcripts from the water controls were grouped by Gene Ontology terms within the Biological Processes category using Omicsbox (BLAST2GO). Terms with lower than 2% of total gene expression were combined and assigned the label "other".

Overall, 5112 transcripts were annotated and categorized in biological processes. Detailled transcriptome analysis showed that 54.91% of transcripts were categorized under the following terms: DNA metabolic process (19.31%), response to stress (13.25%), response to chemical (8.68%), signal transduction (7.66%) and response to biotic stimulus (6.01). Response to stress, response to chemicals, and response to biotic stimulus were among the top 5 terms with the most expression that fell under the parent category of response to stimulus. Eighteen (18) terms had less than 2% of the distribution of genes collectively assigned in the category "other".

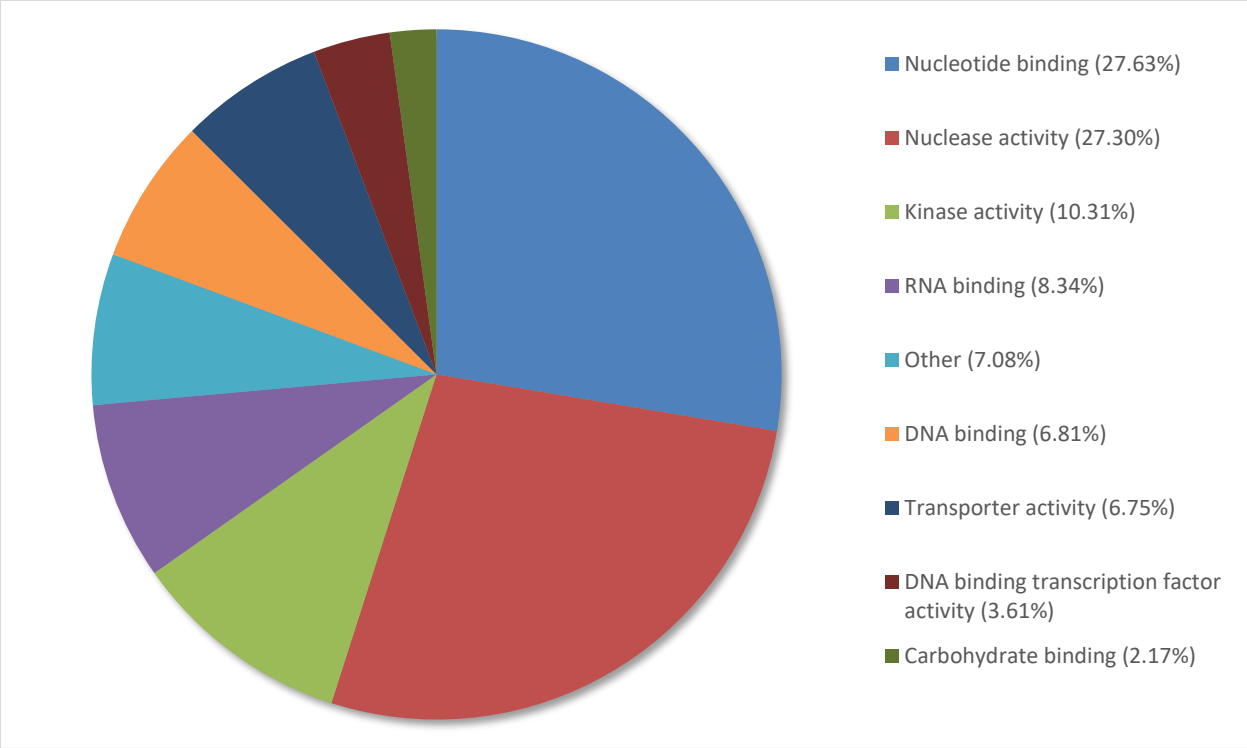

Figure 5b. Percentage of annotated transcripts in *Pinus banksiana* control samples categorized by Molecular Function. A total of 3755 transcripts from the water controls grouped by Gene Ontology terms within the molecular function category using Omicsbox (BLAST2GO). Terms with lower than 2% of total gene expression were combined and assigned the label "other".

Overall, 3755 transcripts were annotated and categorized by molecular function. Out of these transcripts, 65.24% of were allocated to the following terms: Nucleotide binding (27.63%), nuclease activity (27.30%) and kinase activity (10.31). Five (5) out of eight categories were related to nucleotide function and genetic regulation. Nucleotide binding, nuclease activity, RNA binding and DNA binding represented four of the top five categories, indicating the prominence of nucleotide function and genetic regulation in top regulated genes. Additionally, Nucleotide binding, RNA binding and DNA binding fell under the parent category nucleic acid binding. Nine terms had less than 2% of total gene expression and collectively assigned to the category "other".

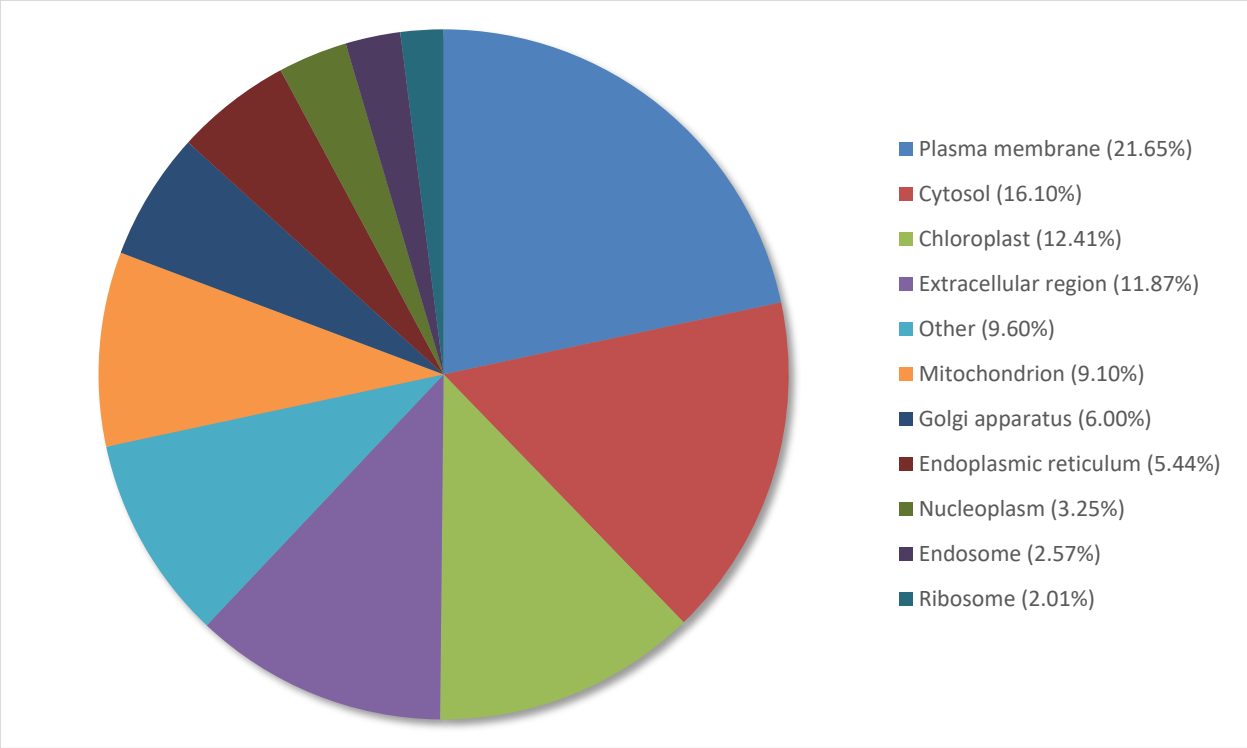

Figure 5c. Percentage of annotated transcripts in *Pinus banksiana* control samples categorized by Cellular Component. A total of 3385 transcripts from the water controls grouped by Gene Ontology terms within the cellular component using Omicsbox (BLAST2GO). Terms with lower than 2% of total gene expression were combined and assigned the label "other".

Over all, 3385 transcripts were annotated and categorized based on cellular compartment location. Of these transcripts, 62.03% of genes were categorized under the following terms: plasma membrane (21.65%), cytosol (16.10%), chloroplast (12.41%), extracellular region (11.87%). Plasma membrane, cytosol and the extracellular region represented three of the top five categories, which were relegated to compartments encompassing or adjacent to the plasma membrane. 7 categories had less than 2% of the distribution of genes collectively assigned to the category "other".

2.3.4 Gene ontology of the top 100 differentially expressed genes in *Pinus banksiana*

Gene ontology graphs show the distribution of the top 100 genes allocated to different terms within the categories biological processes, metabolic function, and cellular compartment (fig 6a-9c). The top 100 genes for each pairwise comparison was obtained from the set of differentially expressed genes and categorized into upregulated and downregulated values.

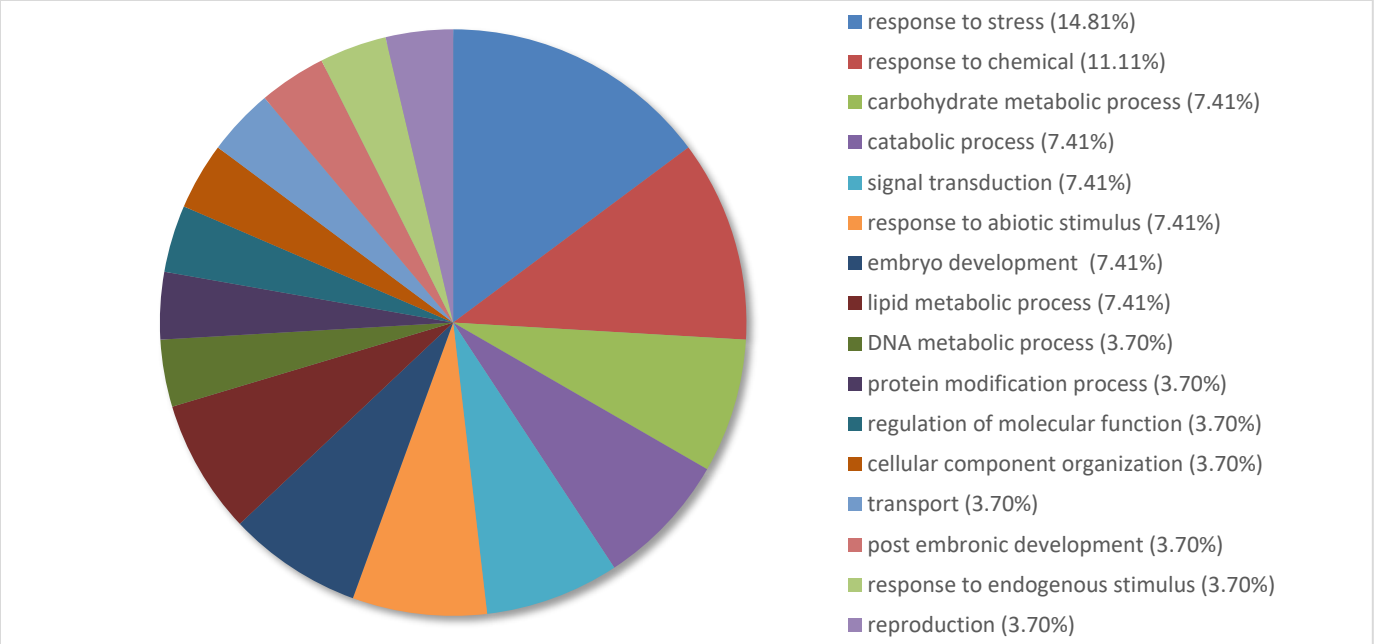

Figure 6a. Percentage of the top 100 upregulated transcripts in *Pinus banksiana* resistant samples compared to the controls categorized by Biological Processes. A total of 100 transcripts from the resistant samples compared to water controls were grouped by Gene Ontology terms within the Biological Processes category using Omicsbox (BLAST2GO). Terms with lower than 2% of total gene expression were combined and assigned the label "other".

The 100 most upregulated genes in RG compared to water were annotated and categorized based on biological processes. Overall, 70.38% of genes were distributed under the following processes: Response to stress (14.81%), response to chemical (11.11%), carbohydrate metabolic process (7.41%), catabolic process (7.41%), signal transduction (7.41%), response to abiotic stimulus (7.41%), embryo development (7.41%), lipid metabolic process (7.41%). Response to stress, response to chemicals and response to abiotic stimulus fell under the same parent category response to stimulus. Compared to the entire transcriptome, DNA metabolic process had a smaller

percentage of expressed genes. In contrast, carbohydrate metabolic process and lipid metabolic process had a high proportion of expressed genes but were underrepresented in the entire transcriptome. Embryo development, post embryonic development and reproduction were also represented in this instance but had less than 2% of expressed genes in the entire transcriptome (Fig 6a, fig 5a).

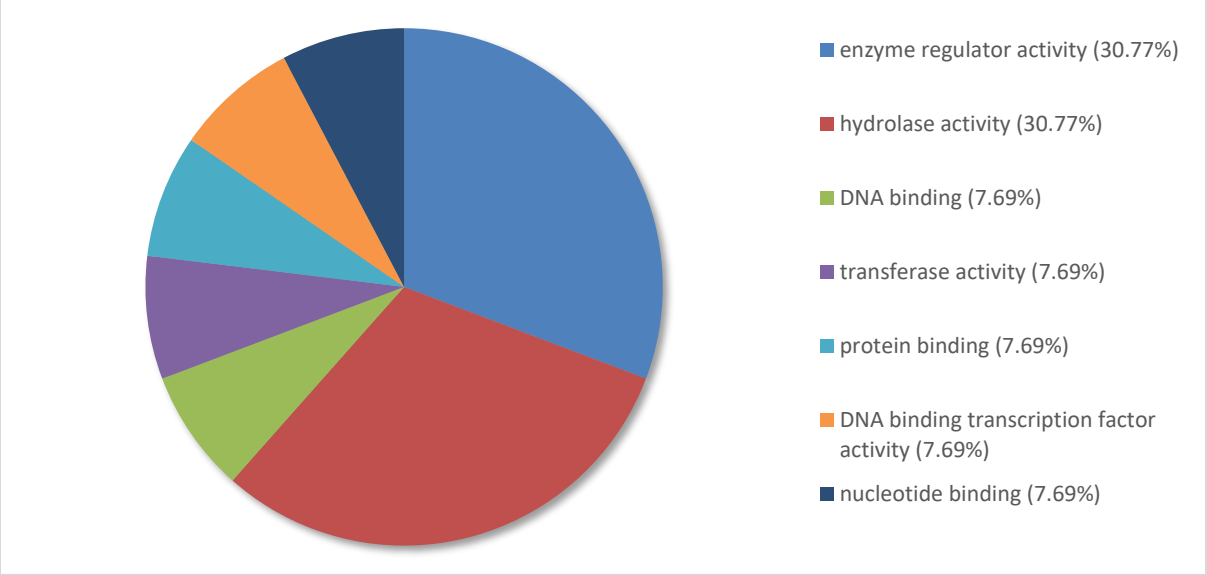

Figure 6b. Percentage of the top 100 upregulated transcripts in *Pinus banksiana* resistant samples compared to the controls categorized by Molecular Function. A total of 100 transcripts from the resistant samples compared to the water controls were grouped by Gene Ontology terms within the Molecular Function category using Omicsbox (BLAST2GO). Terms with lower than 2% of total gene expression were combined and assigned the label "other".

The 100 most upregulated genes in RG compared to water were categorized based on molecular function. Overall, 61.54% of genes were categorized under the following molecular functions: Enzyme regulator activity (30.77%) and hydrolase activity (30.77%). Enzyme regulatory activity and hydrolase activity comprised the majority of top upregulated genes despite having less than 2% of genes in the entire transcriptome. Protein binding and transferase activity were also

represented among the top upregulated genes despite comprising less than 2% of the whole transcriptome.

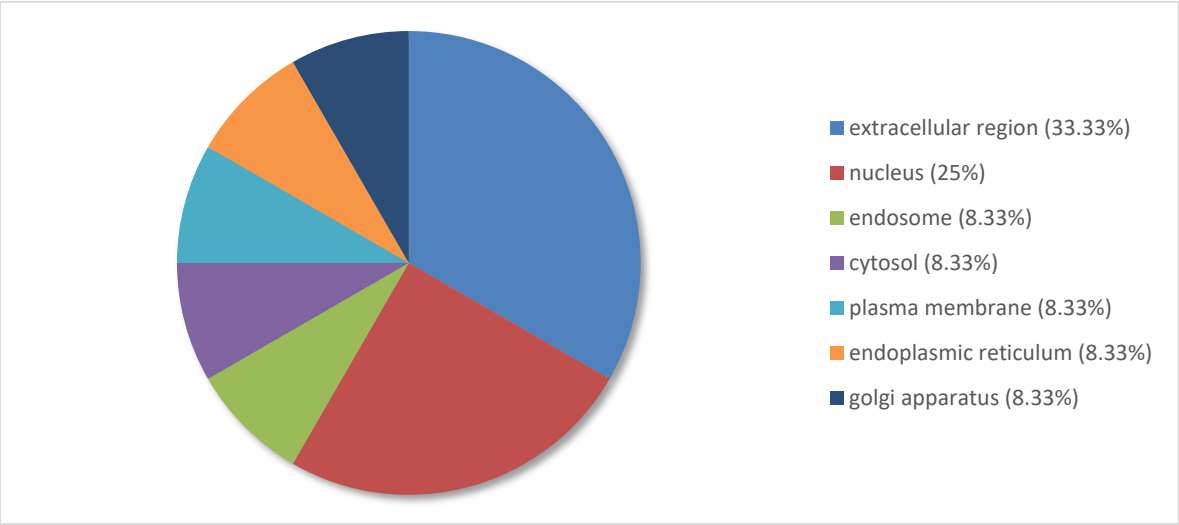

Figure 6c. Percentage of the top 100 upregulated transcripts in *Pinus banksiana* resistant samples compared to the controls categorized by Cellular Component. A total of 100 transcripts from the resistant samples compared to water controls were grouped by Gene Ontology terms within the cellular component category using Omicsbox (BLAST2GO). Terms with lower than 2% of total gene expression were combined and assigned the label "other".

The 100 most upregulated genes in RG compared to water were annotated and categorized based on cellular compartment. Overall, 58.33% of genes were categorized under the following cell compartments: Extracellular region (33.33%) and nucleus (25%). Other organelles had an equal distribution of expressed genes. In contrast to the whole transcriptome, the nucleus comprised a very large portion of expressed genes.

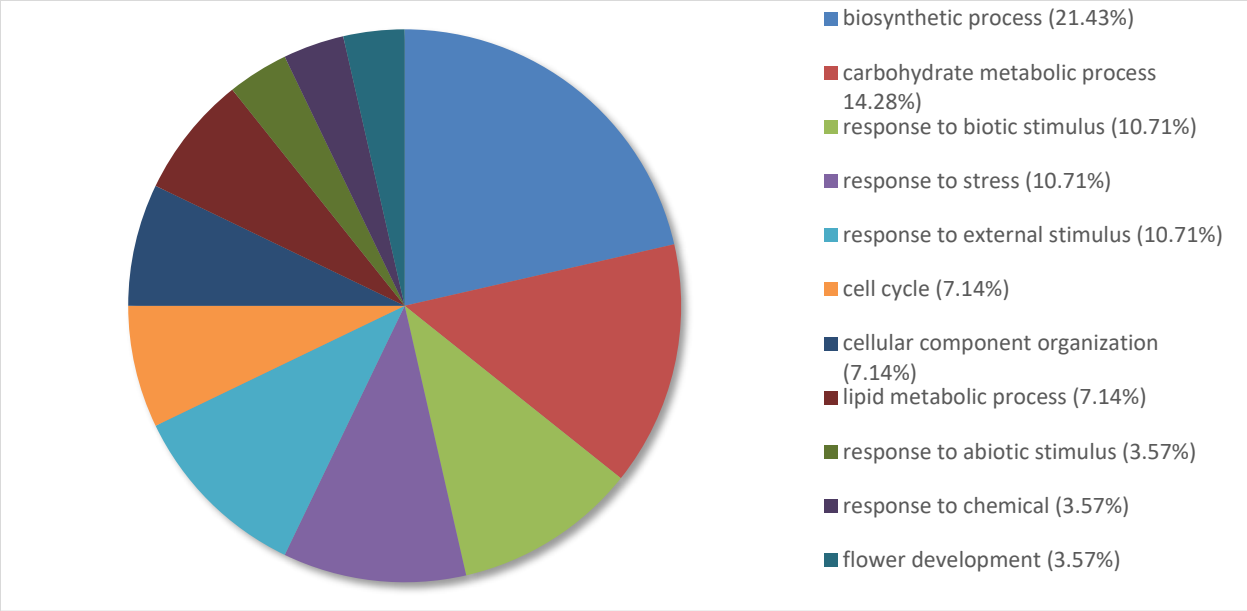

Figure 7a. Percentage of the top 100 downregulated transcripts in *Pinus banksiana* resistant samples compared to water controls categorized by Biological Processes. A total of 100 transcripts from the resistant samples compared to the water controls were grouped by Gene Ontology terms within the biological processes category using Omicsbox (BLAST2GO). Terms with lower than 2% of total gene expression were combined and assigned the label "other".

The 100 most downregulated genes in RG compared to water were annotated and categorized based on biological process. They were categorized under the following categories: Biosynthetic process (21.43%), carbohydrate metabolic process (14.28%), response to biotic stimulus (10.71%), and response to stress (10.71%). Biosynthetic process had the largest proportion of expressed genes despite having less than 2% of expressed genes in the whole transcriptome analysis. In contrast to the whole transcriptome analysis, carbohydrate metabolic process and cell cycle had a larger proportion of expressed genes whereas response to abiotic stimulus and response to chemical had a lower proportion of expressed genes. 3 of the top 5 categories are classified under the response to stimulus category.

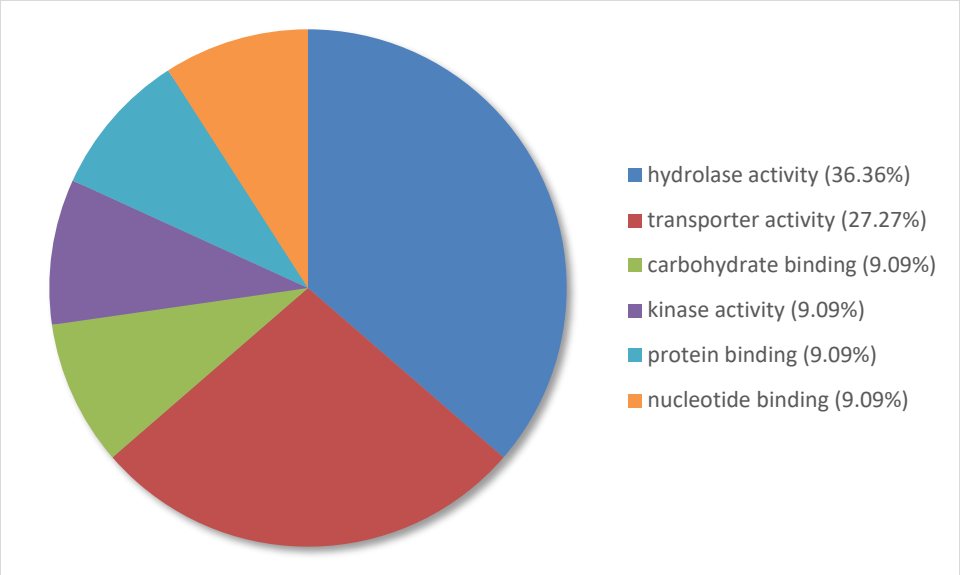

Figure 7b. Percentage of the top 100 downregulated transcripts in *Pinus banksiana* resistant samples compared to water controls categorized by Molecular Function. A total of 100 transcripts from the resistant samples compared to the water controls were grouped by Gene Ontology within the Molecular function category using Omicsbox (BLAST2GO). Terms with lower than 2% of total gene expression were combined and assigned the label "other".

The 100 most downregulated genes in RG were annotated and categorized based on metabolic process. They were categorized under the following terms: Hydrolase activity (36.36%) and transporter activity (27.27%). These categories had a lower proportion of expressed genes in the whole transcriptome analysis and Hydrolase activity represented less than 2% of expressed genes. The other categories had an equal distribution of genes.

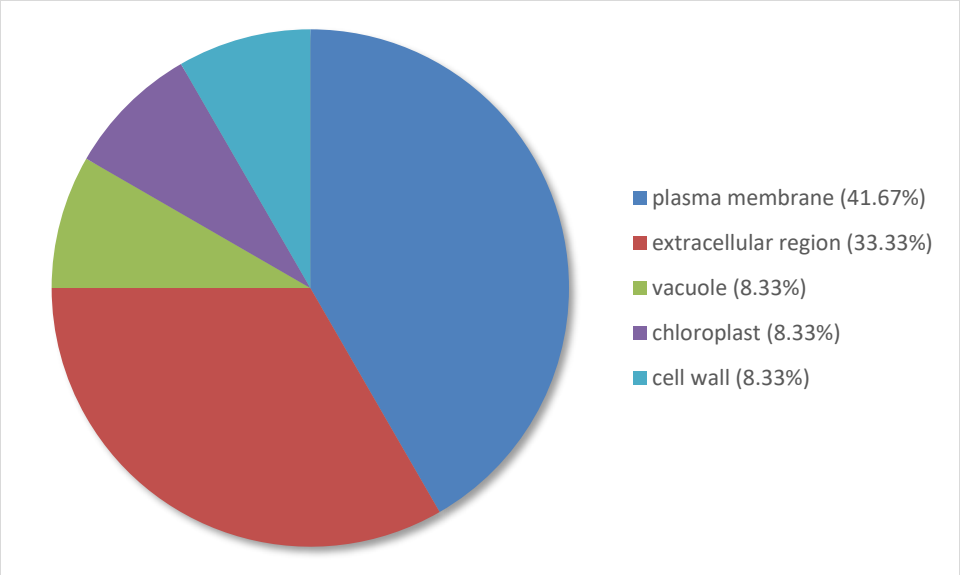

Figure 7c. Percentage of the top 100 downregulated transcripts in *Pinus banksiana* resistant samples compared to water controls categorized by Cellular Component. A total of 100 transcripts from the resistant genotype compared to the water controls were grouped by Gene Ontology terms in the Cellular Component category using Omicsbox (BLAST2GO). Terms with lower than 2% of total gene expression were combined and assigned the label "other".

The 100 most downregulated genes in RG were annotated and categorized based on Cellular Compartment. They were categorized under the following categories: plasma membrane (41.67%) and extracellular region (33.33%). There were five categories represented which is lower than the whole transcriptome analysis which had 10 or more categories.

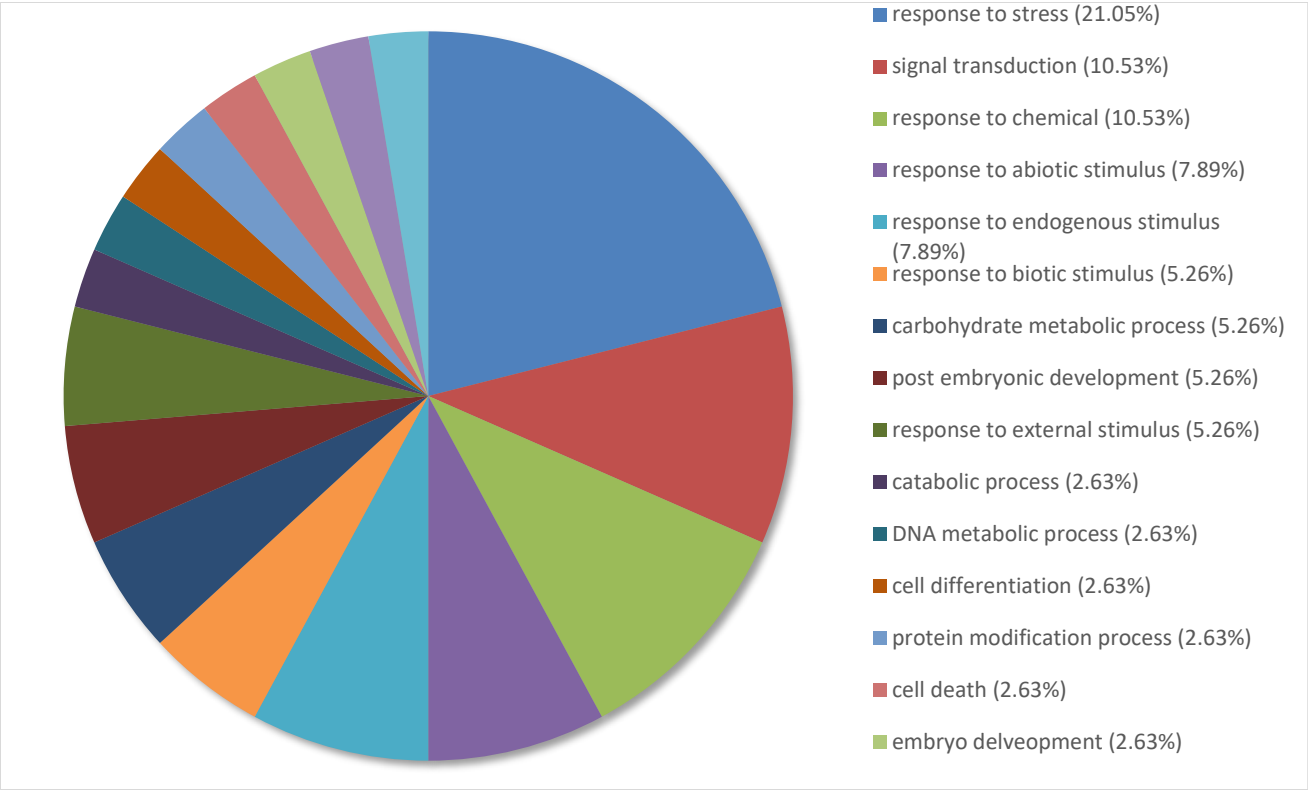

Figure 8a. Percentage of the top 100 upregulated transcripts in *Pinus banksiana* susceptible samples compared to the controls categorized by Biological Processes. A total of 100 transcripts from the susceptible samples compared to water controls were grouped by Gene Ontology terms within the biological processes category using Omicsbox (BLAST2GO). Terms with lower than 2% of total gene expression were combined and assigned the label "other".

The 100 most upregulated genes in SG compared to water were annotated and categorized based on biological processes. Overall, 57.71% of genes were categorized under the following biological processes: Response to stress (21.05%), signal transduction (10.53%), response to chemicals (10.35%), response to abiotic stimulus (7.89%) and response to endogenous stimulus (7.89%). Response to chemical, response to abiotic stimulus, response to endogenous stimulus and response to biotic stimulus are classified under the parent category response to stimulus. DNA metabolic process had a low percentage of genes despite having the highest proportion of genes in the whole transcriptome. In contrast, embryo development and post embryonic development were represented despite having less than 2% of expressed genes in the entire transcriptome.

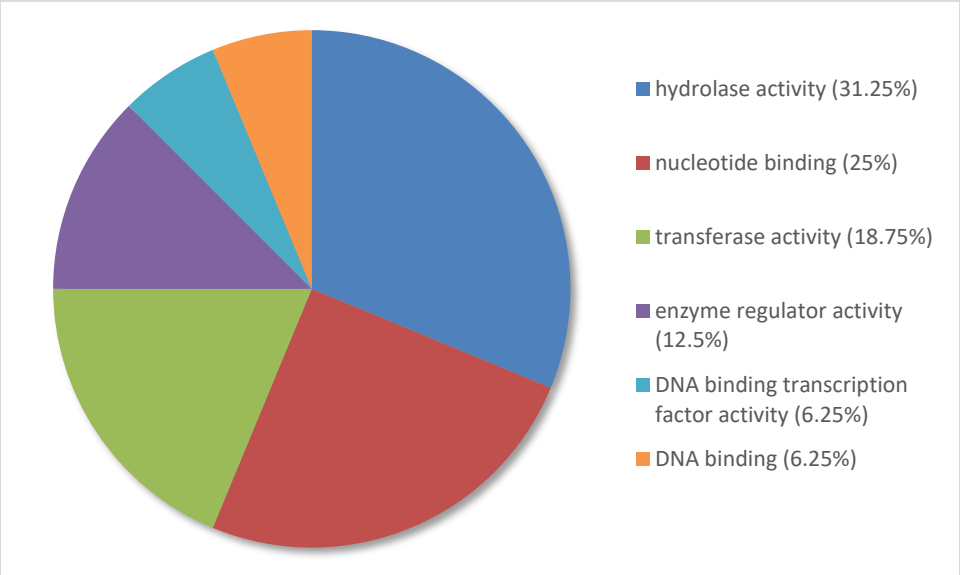

Figure 8b: Percentage of the top 100 upregulated transcripts in *Pinus banksiana* susceptible samples compared to the controls categorized by Molecular Function. A total of 100 transcripts from the susceptible samples compared to the water controls were grouped by Gene Ontology terms within the molecular function category using Omicsbox (BLAST2GO). Terms with lower than 2% of total gene expression were combined and assigned the label "other".

The 100 most upregulated genes in SG compared to water were annotated and categorized based on molecular function. In general, 56.25% of genes fell under the following categories: Hydrolase activity (31.25%) and nucleotide binding (25%). These categories comprised the majority of expressed genes despite having less than 2% of expressed genes in the entire transcriptome. Enzyme regulatory activity was also represented despite having less than 2% of expressed genes.

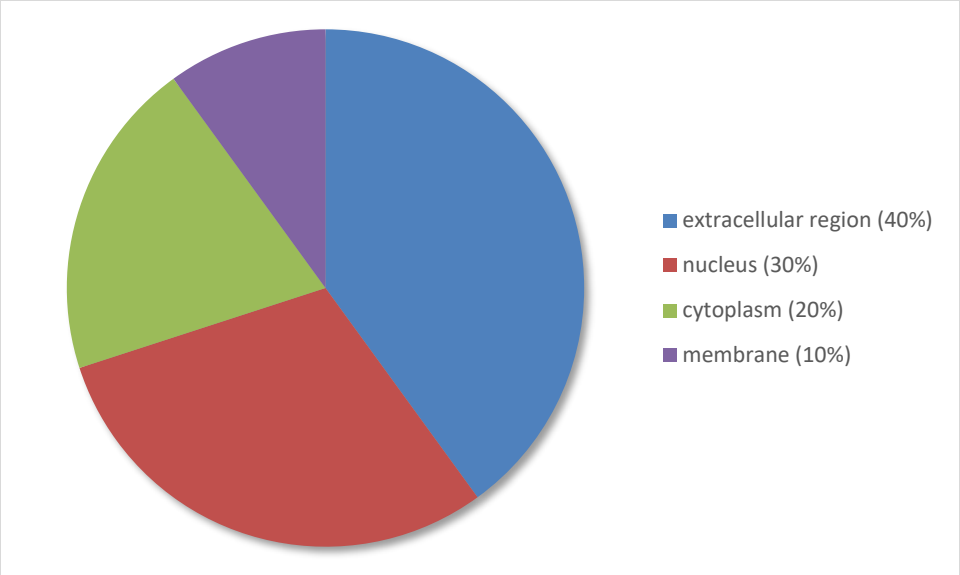

Figure 8c. Percentage of the top 100 upregulated transcripts in Pinus banksiana susceptible samples compared to the controls categorized by Cellular Component. A total of 100 transcripts from the susceptible samples compared to the water controls were grouped by gene Ontology terms within the Cellular Component category using Omicsbox (BLAST2GO). Terms with lower than 2% of total gene expression were combined and assigned the label "other".

For cellular compartment, the 100 most upregulated genes in SG were annotated and categorized. The majority of expressed genes were categorized under the following categories: Extracellular region (40%), nucleus (30%). All of the genes expressed were distributed among 4 categories which was lower than the whole transcriptome analysis which had at least 11 categories.

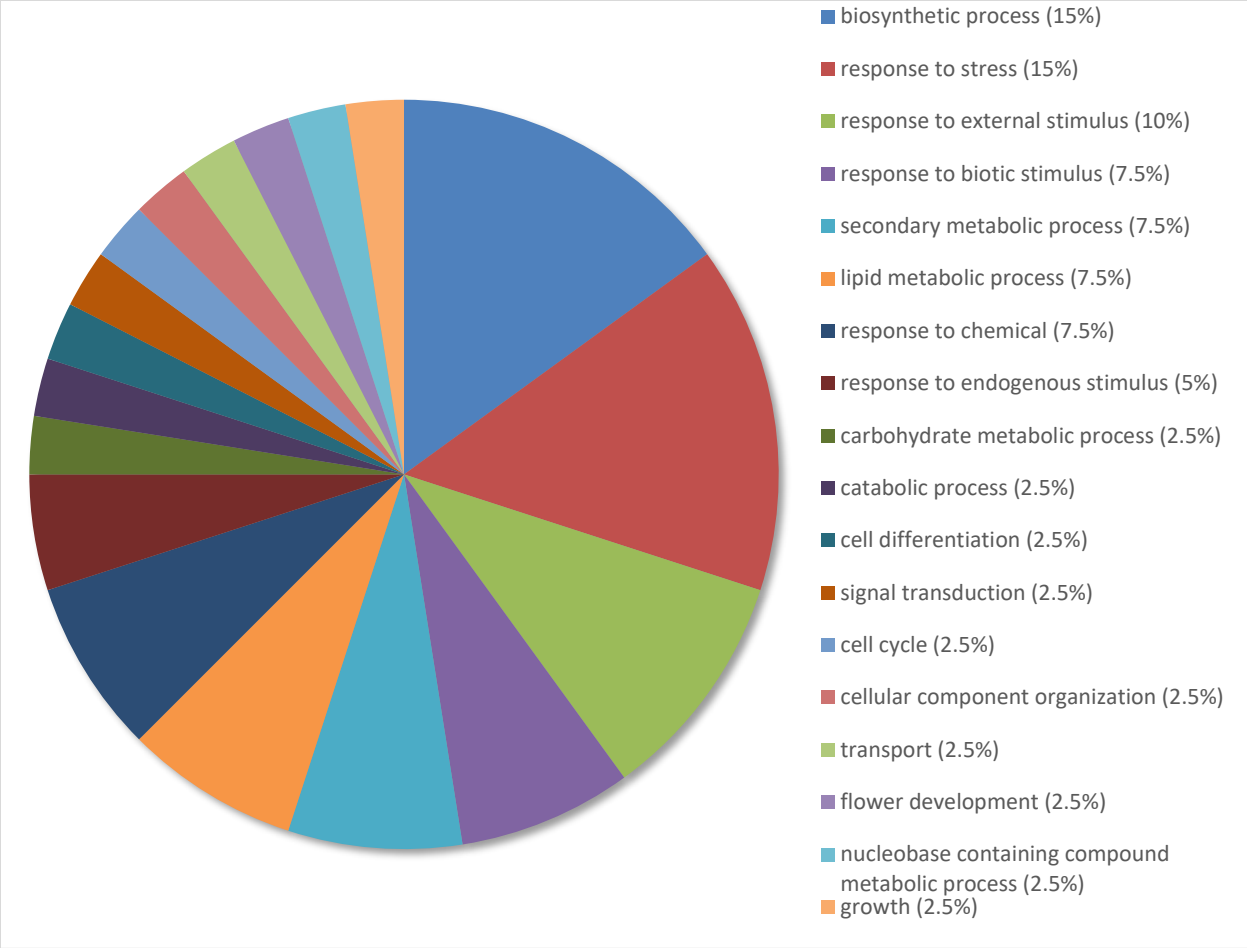

Figure 9a. Percentage of the top 100 downregulated transcripts in Pinus banksiana susceptible samples compared to water controls categorized by Biological Processes. A total of 100 transcripts from the susceptible genotype compared to the water controls were grouped by gene Ontology terms within the Biological Processes category using Omicsbox (BLAST2GO). Terms with lower than 2% of total gene expression were combined and assigned the label "other".

The 100 most downregulated genes in SG were annotated and categorized based on metabolic process. They were categorized under the following categories: biosynthetic process (15%), response to stress (15%), response to external stimulus (10%) and response to biotic stimulus (7.5%). In contrast to the whole transcriptome analysis, biosynthetic process has the largest proportion of gene expression. Response to stress, response to external stimulus and response to biotic stimulus fall under the parent category response to stimulus. 10 categories had 2.5% of expressed genes.

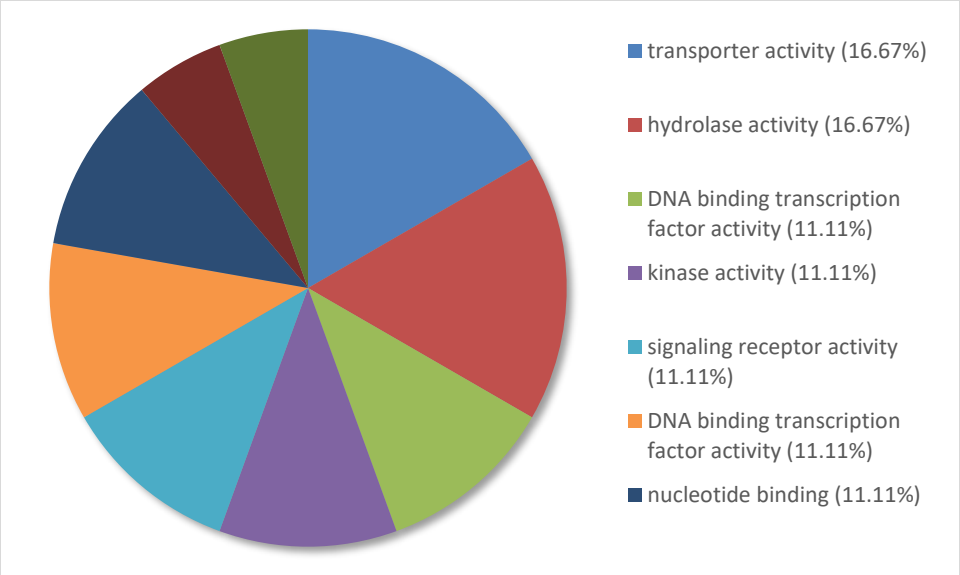

Figure 9b. Percentage of the top 100 downregulated transcripts in Pinus banksiana susceptible samples compared to controls categorized by Molecular Function. A total of 100 transcripts from the susceptible genotype compared to the water controls were grouped by gene Ontology terms within the molecular function category using Omicsbox (BLAST2GO). Terms with lower than 2% of total gene expression were combined and assigned the label "other".

The 100 most downregulated genes in SG were annotated and categorized based on metabolic process. Overall, 55.56% of genes were categorized under the following categories: transporter activity (16.67%), hydrolase activity (16.67%), DNA binding transcription factor activity (11.11%) and kinase activity (11.11%). In contrast to the whole transcriptome analysis, transporter and hydrolase activity comprised a considerably larger proportion of expressed genes. Hydrolase activity and signalling receptor activity comprised less than 2% of expressed genes in the whole transcriptome.

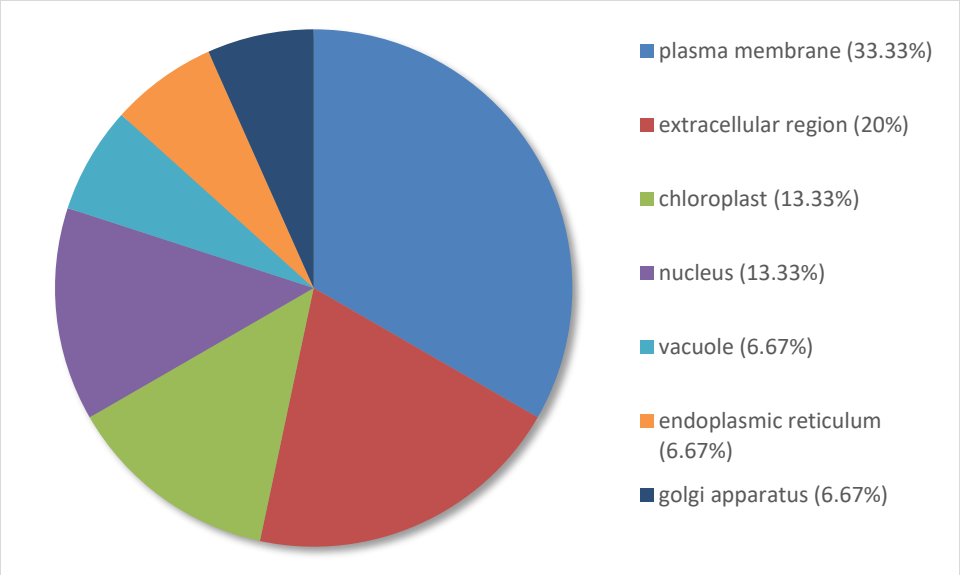

Figure 9c. Percentage of the top 100 downregulated transcripts in Pinus banksiana susceptible samples compared to the controls categorized by terms in Cellular Component. A total of 100 transcripts from the susceptible samples compared to the water controls were grouped by gene ontology terms within the Cellular Component category using Omicsbox (BLAST2GO). Terms with lower than 2% of total gene expression were combined and assigned the label "other".

The 100 most downregulated genes in SG were annotated and categorized based on cellular compartment. Overall, 53.33% of genes were distributed to the following terms: Plasma membrane (33.33%) and extracellular region (20%).

2.3.5 Top 25 differentially expressed genes for pairwise comparisons

Tables of the top 100 upregulated and downregulated genes were compiled from corresponding pairwise comparisons. Genes with the highest or lowest expression were correlated to nickel stress and can be used to partially describe the genetic response to nickel. Protein descriptions with the "predicted protein" label indicated no assignment of any closely related protein or relevant GO terms from the UniProt database. Gene ontology terms and functional categorizations were assigned by the Omics Box/BLAST2GO program.

Table 6a. Top 25 upregulated genes from nickel resistant samples compared to the controls in *Pinus banksiana*

Rank	Gene ID	Res 1	Res 2	Res 3	Water 1	Water 2	Water 3	logFC	Adj. P. Value	UniProt Description
0	TRINITY_DN2786_c0_g1	767.81	197.57	545.86	0	0	0	13.96	0.00116	Predicted Protein
1	TRINITY_DN5716_c0_g1	2328.59	913.58	3881.87	0	7.03	0.41	13.34	0.00029	Predicted Protein
2	TRINITY_DN57079_c0_g1	339.53	238.75	261.65	0	0	0	13.30	0.00002	Predicted Protein
3	TRINITY_DN5965_c1_g1	1173.34	760.7	1106.06	0.33	0	0	13.28	0.00009	Predicted Protein
4	TRINITY_DN258556_c0_g1	280.75	98.46	494.55	0	0	0	13.09	0.00181	Predicted Protein
5	TRINITY_DN1368_c0_g1	1156.77	736.4	2060.57	0	1.3	0.07	12.99	0.00047	Predicted Protein
6	TRINITY_DN2832_c0_g1	334.2	111.71	258.08	0	0	0	12.93	0.00056	Predicted Protein
7	TRINITY_DN1628_c0_g1	646.38	288.02	710.02	0	0.32	0	12.82	0.00065	Trypsin inhibitor [Cleaved into: Trypsin inhibitor chain A; Trypsin inhibitor chain B]
8	TRINITY_DN7061_c1_g1	158.35	218.82	172.81	0	0	0	12.69	0.00000	Predicted Protein
9	TRINITY_DN690_c0_g1	494.67	136.83	407.74	0.05	0	0	12.50	0.00181	Predicted Protein
10	TRINITY_DN5795_c0_g1	753.52	420.03	412.9	0	0.84	0	12.43	0.00032	Predicted Protein
11	TRINITY_DN1520_c0_g1	398.05	358.51	936.72	0.02	0.65	0	11.81	0.00043	Trypsin inhibitor [Cleaved into: Trypsin inhibitor chain A; Trypsin inhibitor chain B]
12	TRINITY_DN3861_c0_g1	179.52	38.1	108.51	0	0	0	11.70	0.00251	Predicted Protein
13	TRINITY_DN40097_c0_g1	440.62	297.68	1698.09	0	3.39	0.69	11.62	0.00080	Predicted Protein
14	TRINITY_DN2463_c0_g1	301.76	196.16	568.86	0	0.04	0.11	11.56	0.00056	Predicted Protein
15	TRINITY_DN4524_c0_g3	64.05	74.91	115.6	0	0	0	11.54	0.00002	Predicted Protein
16	TRINITY_DN792_c0_g1	149.05	126.17	86.37	0	0.03	0	11.54	0.00004	ACT domain-containing protein ACR4 (Protein ACT DOMAIN REPEATS 4)
17	TRINITY_DN792_c0_g1	149.05	126.17	86.37	0	0.03	0	11.54	0.00004	ACT domain-containing protein ACR5 (Protein ACT DOMAIN REPEATS 5)
18	TRINITY_DN129489_c0_g1	125.97	40.97	102.59	0	0	0	11.53	0.00085	Predicted Protein
19	TRINITY_DN2914_c0_g1	134.07	79.52	144.69	0	0.03	0	11.51	0.00014	Protein TIFY 10b, OsTIFY10b (Jasmonate ZIM

										domain-containing protein 7, OsJAZ7) (OsJAZ6)
20	TRINITY_DN2914_c0_g1	134.07	79.52	144.69	0	0.03	0	11.51	0.00014	Protein TIFY 3B (Jasmonate ZIM domain-containing protein 12)
21	TRINITY_DN3536_c0_g1	51.58	119.55	84.19	0	0	0	11.51	0.00001	Predicted Protein
22	TRINITY_DN1537_c0_g1	64.53	90.63	76.46	0	0	0	11.44	0.00000	Predicted Protein
23	TRINITY_DN2075_c1_g1	81.81	56.05	84.87	0	0	0	11.38	0.00005	Predicted Protein
24	TRINITY_DN12750_c0_g1	93.87	62.85	64.95	0	0	0	11.37	0.00005	Predicted Protein
25	TRINITY_DN3685_c0_g2	524.13	169.45	298.36	0.01	0.58	0	11.33	0.00171	Copia protein (Gag-int-pol protein) [Cleaved into: Copia VLP protein; Copia protease, EC 3.4.23.-]

Table 6b. Top 25 downregulated genes from nickel resistant samples compared to the control in *Pinus banksiana*

Rank	Gene ID	Res 1	Res 2	Res 3	Water 1	Water 2	Water 3	logFC	Adj. P. Value	UniProt Description
0	TRINITY_DN1118_c0_g1	0	0	0	27.63	15.12	24.7	-11.36	4.86E-05	Flavonol synthase/flavanone 3-hydroxylase, FLS, EC 1.14.11.9, EC 1.14.20.6
1	TRINITY_DN26931_c0_g1	0.16	0	0	65.61	45.82	36.39	-11.19	9.47E-05	Probable aquaporin PIP2-8 (Plasma membrane intrinsic protein 2-8, AtPIP2;8) (Plasma membrane intrinsic protein 3b, PIP3b)
2	TRINITY_DN432_c0_g1	0	0.3	0	77.54	17.58	69.88	-11.15	0.002533	Predicted Protein
3	TRINITY_DN4059_c0_g1	0	0	0	20.09	12.1	19.58	-10.99	4.10E-05	Predicted Protein
4	TRINITY_DN30654_c0_g1	0	0	0	14.69	11.78	14.4	-10.67	1.63E-05	Predicted Protein
5	TRINITY_DN2314_c0_g1	0.03	0.13	0	40.88	14.56	52.04	-10.43	0.001066	Predicted Protein
6	TRINITY_DN69830_c0_g4	0	0	0	10.13	7.29	18.59	-10.38	0.000101	Predicted Protein
7	TRINITY_DN129793_c0_g1	0	0	0	8.28	13.37	9.36	-10.22	9.45E-06	Putative UPF0481 protein At3g02645
8	TRINITY_DN40558_c0_g1	0.04	0	0.05	36.31	14.48	19.64	-10.08	0.000432	Predicted Protein
9	TRINITY_DN522_c0_g3	0	0	0	8.24	4.71	17.93	-10.05	0.000408	Predicted Protein
10	TRINITY_DN1550_c0_g1	0	0.07	0	18.5	9.11	17.44	-9.99	0.000209	Predicted Protein
11	TRINITY_DN113586_c0_g1	0	0	0	7.25	5.74	13.28	-9.94	8.70E-05	Predicted Protein
12	TRINITY_DN25689_c0_g1	0.06	0.09	0	26.01	16.36	31.07	-9.92	0.000136	Predicted Protein
13	TRINITY_DN26605_c0_g1	0	0	0	6.61	7.11	10.35	-9.87	2.28E-05	Predicted Protein
14	TRINITY_DN31123_c0_g2	0	0	0	6.35	8.14	8.67	-9.82	1.28E-05	Predicted Protein
15	TRINITY_DN4890_c0_g1	0	0	0.17	15.59	12.05	25.46	-9.82	0.000174	Predicted Protein
16	TRINITY_DN5062_c0_g2	0	0	0	10.4	7.97	3.99	-9.72	0.000193	Predicted Protein
17	TRINITY_DN3390_c0_g1	0	0	0	9.96	3.94	7.77	-9.69	0.000273	Predicted Protein
18	TRINITY_DN6314_c0_g1	0	0	0	7.61	6.68	5.98	-9.66	2.86E-05	Predicted Protein
19	TRINITY_DN2507_c0_g1	0	0	0.61	32.43	13.12	23.67	-9.65	0.000952	Predicted Protein
20	TRINITY_DN53932_c0_g1	0.01	0	0.2	17.81	11.58	17.09	-9.61	0.00016	Predicted Protein
21	TRINITY_DN20386_c0_g1	0	0	0	7.77	6	5.13	-9.55	5.04E-05	Predicted Protein
22	TRINITY_DN17540_c0_g1	0	0	0	10.32	6.62	3.33	-9.55	0.000363	Predicted Protein

23	TRINITY_DN51950_c1_g1	0	0	0	6.24	5.15	7.26	-9.53	3.46E-05	Predicted Protein
24	TRINITY_DN59077_c1_g1	0	0.2	0	11.37	9.17	20.15	-9.52	0.000196	Predicted Protein
25	TRINITY_DN26_c1_g1	0	0	0	5.86	4.64	7.86	-9.49	5.04E-05	Alpha-galactosidase, EC 3.2.1.22 (Alpha-D-galactoside galactohydrolase) (Melibiase)

Table 7a. Top 25 upregulated genes from nickel susceptible samples compared to the controls in *Pinus banksiana*

Rank	Gene ID	Sus 1	Sus 2	Sus 3	Water 1	Water 2	Water 3	logFC	Adj. P. Value	Uniprot Description
0	TRINITY_DN2786_c0_g1	856.36	272.59	231.03	0	0	0	12.818	9.58E-05	Predicted Protein
1	TRINITY_DN5965_c1_g1	1181.56	905.23	1030.95	0.33	0	0	12.749	8.20E-06	Predicted Protein
2	TRINITY_DN2075_c1_g1	233.73	192.67	517.7	0	0	0	12.435	3.40E-06	Predicted Protein
3	TRINITY_DN57079_c0_g1	1015.8	115.56	157.97	0	0	0	12.307	0.000978	Predicted Protein
4	TRINITY_DN7061_c1_g1	223.03	244.97	330	0	0	0	12.302	6.15E-08	Predicted Protein
5	TRINITY_DN2832_c0_g1	409.8	198.4	215.56	0	0	0	12.282	6.33E-06	Predicted Protein
6	TRINITY_DN1628_c0_g1	1029.68	393.25	376.84	0	0.32	0	11.958	0.000183	Trypsin inhibitor [Cleaved into: Trypsin inhibitor chain A; Trypsin inhibitor chain B]
7	TRINITY_DN258556_c0_g1	451.94	114.99	118.68	0	0	0	11.777	0.000117	Predicted Protein
8	TRINITY_DN5795_c0_g1	706.72	659.33	762.96	0	0.84	0	11.760	2.45E-05	Predicted Protein
9	TRINITY_DN4524_c0_g3	321.7	70.3	142.87	0	0	0	11.475	8.63E-05	Predicted Protein
10	TRINITY_DN34759_c0_g1	1034.78	337.83	229.04	0	0.56	0	11.360	0.000835	Predicted Protein
11	TRINITY_DN7289_c0_g1	467.02	181.08	31.83	0	0	0	11.355	0.001583	Predicted Protein
12	TRINITY_DN14305_c0_g1	39.09	227.66	256.23	0	0	0	11.312	7.76E-05	Predicted Protein
13	TRINITY_DN3861_c0_g1	42.86	138.8	258.86	0	0	0	11.129	3.22E-05	Predicted Protein
14	TRINITY_DN1368_c0_g1	3066.68	660.38	763.89	0	1.3	0.07	11.127	0.010716	Predicted Protein
15	TRINITY_DN24881_c0_g1	223.93	40.37	165.79	0	0	0	11.115	0.000164	Predicted Protein
16	TRINITY_DN690_c0_g1	349.88	209.87	134.26	0.05	0	0	11.063	2.91E-05	Predicted Protein
17	TRINITY_DN1518_c0_g1	60.21	106.22	199.6	0	0	0	11.036	2.67E-06	Predicted Protein
18	TRINITY_DN1481_c0_g1	248.24	432.11	226.95	0	0.41	0	10.971	2.52E-05	Predicted Protein
19	TRINITY_DN2463_c0_g1	702.31	342.75	369.29	0	0.04	0.11	10.957	3.86E-05	Predicted Protein
20	TRINITY_DN8563_c1_g1	139.01	83.26	93.31	0	0	0	10.944	1.76E-06	Predicted Protein
21	TRINITY_DN9801_c0_g1	90.72	141.47	74.39	0	0	0	10.878	7.09E-07	Predicted Protein
22	TRINITY_DN2496_c0_g1	134.27	107.85	191.85	0	0.08	0	10.632	3.88E-06	Predicted Protein
23	TRINITY_DN4477_c1_g1	64.27	90.49	89.56	0	0	0	10.595	8.85E-08	Predicted Protein
24	TRINITY_DN1520_c0_g1	1683.13	371.18	268.6	0.02	0.65	0	10.588	0.007249	Trypsin inhibitor [Cleaved into: Trypsin inhibitor chain A; Trypsin inhibitor chain B]

25	TRINITY_DN3069_c0_g1	228.16	277.31	149.25	0	0.37	0	10.563	3.66E-05	Predicted Protein

Table 7b. Top 25 downregulated genes from nickel susceptible samples compared to the control in *Pinus banksiana*

Rank	Gene ID	Sus 1	Sus 2	Sus 3	Water 1	Water 2	Water 3	logFC	Adj. P. Value	UniProt Description
0	TRINITY_DN432_c0_g1	0	0	0	77.54	17.58	69.88	-12.147	8.42E-05	Predicted Protein
1	TRINITY_DN2314_c0_g1	0	0	0	40.88	14.56	52.04	-11.582	2.29E-05	Predicted Protein
2	TRINITY_DN4176_c0_g1	0	0.14	0.04	61.56	18.42	66.16	-11.488	5.99E-05	Chalcone synthase, EC 2.3.1.74 (Naringenin-chalcone synthase)
3	TRINITY_DN24626_c0_g1	0	0.04	0.03	21.48	21.87	17.99	-10.913	2.30E-07	Predicted Protein
4	TRINITY_DN26931_c0_g1	0	0	0.55	65.61	45.82	36.39	-10.864	2.13E-05	Probable aquaporin PIP2-8 (Plasma membrane intrinsic protein 2-8, AtPIP2;8) (Plasma membrane intrinsic protein 3b, PIP3b)
5	TRINITY_DN4059_c0_g1	0	0	0	20.09	12.1	19.58	-10.661	1.53E-06	Predicted Protein
6	TRINITY_DN4890_c0_g1	0	0	0	15.59	12.05	25.46	-10.643	1.24E-06	Predicted Protein
7	TRINITY_DN53932_c0_g1	0	0.04	0	17.81	11.58	17.09	-10.514	1.10E-06	Predicted Protein
8	TRINITY_DN2202_c0_g1	0	0	0	12.61	15.48	16.45	-10.433	1.05E-07	Predicted Protein
9	TRINITY_DN30654_c0_g1	0	0	0	14.69	11.78	14.4	-10.336	4.72E-07	Predicted Protein
10	TRINITY_DN20386_c0_g2	0	0	0	27.65	4.28	16.45	-10.308	0.000156	Predicted Protein
11	TRINITY_DN1934_c0_g1	0	0	0	16.23	6.2	17.34	-10.203	1.25E-05	Predicted Protein
12	TRINITY_DN5585_c0_g1	0	0.34	0.59	81.26	16.83	119.24	-10.081	0.002538	Predicted Protein
13	TRINITY_DN69830_c0_g4	0	0.04	0	10.13	7.29	18.59	-10.047	2.81E-06	Predicted Protein
14	TRINITY_DN40558_c0_g1	0.08	0.1	0	36.31	14.48	19.64	-10.006	2.74E-05	Predicted Protein
15	TRINITY_DN6996_c0_g5	0	0	0	12.87	8.76	10.4	-9.985	1.17E-06	Predicted Protein
16	TRINITY_DN216_c0_g1	0.1	0.12	0.05	38.41	25.04	25.45	-9.863	3.90E-06	Fatty acyl-CoA reductase 2, chloroplastic, AtFAR2, EC 1.2.1.84 (Fatty acid reductase 2) (Male sterility protein 2)
17	TRINITY_DN293_c0_g1	0.2	0.93	0.54	83.3	131.42	164.86	-9.758	1.23E-05	Delta-selinene-like synthase, chloroplastic, PsTPS-Sell, EC 4.2.3.76
18	TRINITY_DN293_c0_g1	0.2	0.93	0.54	83.3	131.42	164.86	-9.758	1.23E-05	Alpha-humulene synthase, EC 4.2.3.104 (Terpene synthase TPS-Hum, PgTPS-Hum)

19	TRINITY_DN293_c0_g1	0.2	0.93	0.54	83.3	131.42	164.86	-9.758	1.23E-05	Delta-selinene synthase, EC 4.2.3.71, EC 4.2.3.76 (Agfdsel1)
20	TRINITY_DN522_c0_g3	0	0	0	8.24	4.71	17.93	-9.728	1.28E-05	Predicted Protein
21	TRINITY_DN37470_c0_g1	0	0	0	13.75	5.47	8.44	-9.722	9.79E-06	Predicted Protein
22	TRINITY_DN59077_c1_g1	0	0	0.09	11.37	9.17	20.15	-9.717	3.35E-06	Predicted Protein
23	TRINITY_DN2880_c0_g2	0	0	0	19.16	1.84	13.12	-9.650	0.000464	Predicted Protein
24	TRINITY_DN185135_c0_g1	0	0	0	10.52	6.31	8.09	-9.618	2.17E-06	Predicted Protein
25	TRINITY_DN1400_c0_g1	0	0.21	0.12	24.93	11.67	26.83	-9.607	2.19E-05	Subtilisin-like protease SBT5.6, EC 3.4.21.- (Subtilase subfamily 5 member 6, AtSBT5.6)

2.4 Discussion

2.4.1 Effects of excess nickel on *Pinus banksiana* seedlings

Pinus banksiana seedlings exhibited moderate overall resistance in response to excess nickel. Treatment with 3200 mg/kg $NiSO_4$ lead to the death of all but one plant, confirming the limitations of nickel resistance as previously stipulated by an in situ study in the Greater Sudbury Region (Moarefi & Nkongolo, 2022). The presence of more resistant genotype (RG) seedlings than susceptible genotype (SG) seedlings at the 1600 mg/kg dose suggests moderate nickel tolerance and genetic variability within the sampled group. In a similar manner to the nickel avoider *Acer rubrum*, only three plants were classified as susceptible and had a delayed onset of symptoms (K. Nkongolo et al., 2018). In metal contaminated sites in Sudbury, *Pinus banksiana* was found to have moderate genetic diversity and low gene flow which may have been factors that contributed to heavy metal resistance (Vandeligt et al., 2011). In contrast, other pine species such as *Pinus Resinosa* which had significantly lower genetic diversity and higher rates of inbreeding (Vandeligt et al., 2011; Ranger et al., 2008). Ranger *et al.*, 2008 found that *Pinus banksiana* populations had no correlation between genetic diversity and metal accumulation. However, newer trees involved in the regreening program had a significantly higher genetic diversity.

2.4.2 Differential Gene Expression (DEG) Analysis

DEG analysis of *Pinus banksiana* was able to provide information on the similarities that exists between the transcriptome of each genotype. At a high stringency, there was a lack of differentially expressed genes between RG and SG, indicating a similar pattern of gene expression in response to nickel stress (table 3). When compared to other pairwise analyses, the number of DEGs observed at the low stringency was the lowest, suggesting that mechanisms of nickel resistance

may be driven by a small proportion of genes with low expression (table 3). Nkongolo *et al.*, (2018) found a similar result between the resistant and susceptible genotypes of *Acer rubrum*, indicating that both species have a similar pattern of gene expression between contrasting genotypes (K. Nkongolo et al., 2018). However, both species do not share the same heavy metal tolerance strategy. Nickel avoiders such as *Acer rubrum* are expected to exhibit a lower level of gene expression in aerial tissue due to the minimal amount of nickel accumulation and interaction that occurs (Kalubi et al., 2015; K. Nkongolo et al., 2018). In contrast, *Pinus banksiana* is able to accumulate nickel to the needles, roots and branches albeit to a lesser extant than would be required to be classified as a hyperaccumulator (Gratton et al., 2000; Moarefi & Nkongolo, 2022). Other nickel accumulators such as *Populus tremuloides* or *Betula papyrifera* had a significantly higher number of DEGs at both stringency levels (Czajka & Nkongolo, 2022; Theriault et al., 2016). This finding suggests that there were large differences in accumulation or tolerance mechanisms between *Pinus banksiana* and other accumulators. It is possible that the gene expression associated with resistance occurs in the root cells, as *Pinus banksiana* does not exclusively accumulate nickel to the needles (Moarefi & Nkongolo, 2022). Possible resistance mechanisms in roots may involve the transporter IREG2 and the chelator NRAMP which function in nickel sequestration to the vacuole and chelation, respectively (Merlot et al., 2014; Nishida et al., 2020; Boyd & Nkongolo, 2020; Milner et al., 2014). Conducting a transcriptome analysis on roots could provide a more comprehensive overview of gene expression and explain the observed discrepancies at the high stringency level. The smaller number of total sequences produced in SG samples compared to RG samples may be associated with plants sustaining tissue and DNA damage (Stable 1). The abundance of DEGs in SG compared to the control indicate a significant deviation from the control, surpassing even that of RG compared to water (table 5). The large deviations exhibited by SG

indicate that excess nickel elicited larger changes in gene expression compared to RG. A similar pattern of gene expression was observed for SG in *Betula papyrifera* but not for *Acer rubrum* or *Populus tremuloides* (Theriault et al., 2016; Czajka & Nkongolo, 2022; K. Nkongolo et al., 2018).

2.4.3 Gene Ontology of the top 100 DEGs in response to excess nickel

To further describe the transcriptome in response to excess nickel, analysis of the top differentially expressed genes (DEGs) were used to filter highly regulated mechanisms and processes from those with lower, background expression. The top DEGs experience the highest amount of regulation, thereby serving as reliable indicators of mechanisms that are most likely to be involved in nickel tolerance. Gene ontology of the top DEGs can categorize these processes into discernable functions with interpretive value. The highest proportion of upregulated genes in RG compared to the control and SG compared to the control were associated with the response to stress, implicating the prominence of stress mitigation in nickel tolerance (fig 6a, fig 8a). Commonly reported symptoms of nickel stress include oxidative damage, photoinhibition, loss of water retention, cellular senescence, and growth inhibition (Rizwan et al., 2017; Boisvert et al., 2007; Llamas et al., 2008; Reis et al., 2017; Çelik & Akdaş, 2019; Pavlova, 2017; Yadav, 2022). Under adverse conditions, processes associated with stress mitigation can counteract symptoms by maintaining the homeostasis of substances, minimizing tissue damage and ensuring the proper functioning of enzymes (R. Wang et al., 2015; Gantayat et al., 2017; Rizvi & Khan, 2019). Some stress response mechanisms specific to nickel include the upregulation of antioxidant enzymes, antioxidant production, cell wall thickening and proline accumulation (Rizwan et al., 2017; Demirezen Yilmaz & Uruç Parlak, 2011; G. Wang et al., 2022; Fourati et al., 2019). Genes that are categorized in response to chemicals, to abiotic stimulus and to biotic stimulus may be linked to the stress response for two distinct reasons. Annotation of the top

regulated genes revealed that many of the genes involved in the stress response were multifaceted and functionally related under the same parent term (table 6a-7b). The large proportion of upregulated genes involved in signal transduction indicated the significance of cellular communication in the mediation of physiological changes (fig 6a, fig 8a) (Luo et al., 2016). Multiple studies on nickel afflicted plants have characterized the involvement of signalling in stress mitigation, stress related crosstalk and growth regulation (Sirhindi et al., 2016; Valivand et al., 2019; Mahawar et al., 2018; Kazemi et al., 2010; Wiszniewska et al., 2018; Nazir et al., 2019). Signalling pathways that are induced by nickel stress may include auxin, cytokinin and ethylene (Kolbert et al., 2020).

The terms with the highest proportion of downregulated genes in RG compared to water and SG compared to water were associated with the biosynthetic process, the carbohydrate metabolic process and the response to stress (fig 7a, fig 9a). The biosynthetic process is an expansive category that encompasses numerous products and entities (Ashburner et al., 2000; The Gene Ontology Consortium, 2021). In response to excess nickel, the plant may elicit changes to the biosynthetic process to streamline the production of specific substances to confer higher tolerance. Downregulation of biosynthesis could reduce the production of substances such as ethylene which have the potential to hinder nickel tolerance and accelerate senescence when produced in excess (Stearns et al., 2005; Kolbert et al., 2020). The synthesis of substances that further exasperate tissue damage under compromised conditions such as hydrogen peroxide may also be downregulated to preserve tissue integrity and ensure proper organelle functioning (Jahan et al., 2020). In response to heavy metals, the downregulation of genes involved in the carbohydrate metabolic process depends on the physiological requirements of the plant. The reduced breakdown of structural polymers such as cellulose and pectin have been shown to

maintain the strength of the cell wall (Jia et al., 2019; J.-L. Fan et al., 2011). Conversely, the preservation of constituent monomers and other intermediates may have a role in the regulation of metabolism (C. Li et al., 2020).

Under the same nickel treatment regimen, the transcriptomes of *Populus tremuloides, Betula papyrifera* and *Acer rubrum* elicited the majority of gene expression in nickel transport, cellular component organization and the carbohydrate metabolic process (Czajka & Nkongolo, 2022; Theriault et al., 2016; K. Nkongolo et al., 2018). Gene expression associated with Metabolic Function were similar among the different species. Unlike the previously mentioned species, the plasma membrane comprised the largest portion of gene expression for the cellular component term (fig 6c-9c). The plasma membrane is the second layer that interacts with heavy metals and is thus affected by nickel stress. Excess nickel induces the production of malondialdehyde which causes lipid peroxidation and membrane instability (P. Kumar et al., 2015). Receptors, ligands and other intermediates on the plasma membrane may be involved in signal transduction and the response to stress (Qin et al., 2019; M. Yu et al., 2020; Shimomura, 2006). Additionally, genes that are associated with the stress response may be involved in maintaining membrane integrity and preventing electrolyte leakage (Llamas et al., 2008; Altaf et al., 2022). The small proportion of genes associated with transport indicate that the majority of genes were not associated with nickel transporters (fig 6a-9c). Unlike *Pinus banksiana*, the transcriptomes of the aforementioned angiosperms had the majority of genes associated with the ribosome which was attributed to increased protein translation (Czajka & Nkongolo, 2022; K. Nkongolo et al., 2018; Theriault et al., 2016). Overall, the large functional differences between the transcriptomes of angiosperms and *Pinus banksiana* demonstrate that *Pinus banksiana* deals with excess nickel differently from angiosperms.

2.4.3 Annotation of the top 100 upregulated genes between the resistant genotype and the control

GO annotation of the top DEGs in RG compared to water can elucidate the function of genes and the molecular mechanisms that differentiate RG from untreated plants. Although the annotation of the top 100 genes is informative, it only accounts for a fraction of total expressed genes and is not an exhaustive list that encompasses all highly expressed genes. Genes encoding trypsin inhibitors and cysteine proteinase inhibitors were identified among the top upregulated genes (table 6a, S6a). Trypsin inhibitors and cysteine proteinase inhibitors are proteases that downregulate serine protease and cysteine proteinase activity, respectively (Hou & Lin, 2002; X. Zhang et al., 2008). The upregulation of different proteases is a response to various stressors such as drought, herbivory and heavy metal toxicity (Y. Zhao et al., 2018; Guerra et al., 2015; Major & Constabel, 2008; X. Zhang et al., 2008; S. Khan et al., 2017). Excess nickel can cause an overproduction of ROS, which can damage proteins and cause misfolding, resulting in an increase in protease activity (Schützendübel & Polle, 2002; Jacques et al., 2015). High amounts of nickel stress can cause decreases in protein content, increases in protein aggregation and unsustainable levels of protein breakdown which may compromise cell viability (Rizwan et al., 2017; Arefifard et al., 2014; J. Li et al., 2008; Radisky et al., 2006). The upregulation of trypsin inhibitors and cysteine proteinase inhibitors could be a counteractive measure to elevated levels of protease activity caused by nickel toxicity. In addition to proteinase inhibition, the cysteine proteinase inhibitor Cystatin in *Brassica juncea* has been reported to have the ability to chelate nickel (S. Khan et al., 2017).

Another identified gene encodes a RING-H2 finger protein which is involved in the ubiquitin proteasome pathway (S6a). The RING-H2 finger protein is a E3 ubiquitin ligase that initiates the

ubiquitin proteasome pathway by recognizing misfolded or non-functional proteins caused by stressors such as excess nickel (Qi et al., 2020; Van Hoewyk et al., 2018). Damaged proteins that are processed though the ubiquitin proteasome system (UPS) pathway are eventually degraded in the proteasome (Park et al., 2018). The UPS can aid in the modulation of stress signalling by regulating the amount of proteins and transcription factors involved in the stress response (Z. Zhang et al., 2015). In other plants, increased expression of E3 ubiquitin ligases counteracted heavy metal stress by elevating the expression of antioxidant enzymes, reducing ROS and repressing the transportation of heavy metals via chelation (C.-X. Liu et al., 2022; Ahammed et al., 2021). Under high salinity and drought stress, the RING-H2 finger protein can also regulate ABA synthesis which is a hormone involved in stress mitigation and stress associated signalling (Ko et al., 2006; Zeng et al., 2014).

Several top upregulated genes encode products involved in the jasmonic acid mediated signalling pathway (table 6a, S6a). Two identified genes encode TIFY Jasmonate ZIM-domain proteins which actively represses Jasmonate signalling unless degraded by the ubiquitin-proteasome pathway (Chung & Howe, 2009; Hakata et al., 2017). Another identified gene encodes a Jasmonate induced oxygenase that negatively regulates jasmonate signalling by converting jasmonate to the inactive conjugate 12-hydroxyjasmonate (Smirnova et al., 2017). Jasmonates are stress induced hormones that reduce cell replication, cell size and photosynthetic activity in lieu of driving tissue repair and increasing the production of defense molecules such as jasmonate inducible proteins (Noir et al., 2013; Sirhindi et al., 2016). Some studies reported the use of jasmonates in the alleviation of heavy metal toxicity whereas other studies reported decreased tolerance (Azeem, 2018; Verma et al., 2020; Rakwal & Komatsu, 2001). Additionally, studies have also used jasmonate inhibitors to alleviate heavy metal toxicity (Maksymiec & Krupa, 2006;

Gupta et al., 2000). The culmination of various studies suggest that the physiological effect of genes associated with the Jasmonic acid mediated signalling pathway is dependent on the growth priority and the state of photosynthesis in the plant.

2.4.4 Annotation of the top 100 downregulated genes between the resistant genotype and the control

GO annotation of top downregulated genes in RG compared to water can characterize genes with reduced expression in the resistant genotype (table 6b, S6b). Genes encoding subtilisin-like proteases were identified among the top downregulated genes (S6b). Subtilisin-like proteases are serine type endopeptidases that facilitate the breakdown of peptide bonds using serine as a nucleophilic center (Golldack et al., 2003). Stressors such as heavy metals and drought causes protein damage and dysfunction, eliciting the response of subtilisin-like proteases (Golldack et al., 2003; Xiao et al., 2019). Downregulation of subtilisin-like proteases preserves cell viability by reducing the level of protein breakdown and maintaining the proteome. The reduction in protein breakdown prevents the inhibition of various processes that may have occurred if protease activity was left unchecked (J. Li et al., 2008; Radisky et al., 2006). Downregulation of this gene is consistent with the proposed function of the previously described trypsin inhibitor genes which also inhibit protein breakdown (table 6a).

Several top downregulated genes encode enzymes involved in the flavonoid biosynthetic process (table 6b, S6b). One of the identified genes encodes flavonol synthase which catalyzes the production of flavonol (F. Xu et al., 2012). Another identified gene encodes chalcone synthase, an enzyme that catalyzes the production of naringenin chalcone which serves as an initial precursor to flavonoids (Burbulis et al., 1996). Additionally, an identified gene encodes an anthocyanidin

reductase which converts anthocyanidin to flavan-3-ol (Xie et al., 2003; Takos et al., 2006). Downregulation of these enzymes reduces the production of flavonoids which have broad impacts on plant physiology and the stress response (Mahajan et al., 2011; Burbulis et al., 1996; Besseau et al., 2007; M. Wang et al., 2021; Baozhu et al., 2022). Under various stressors, flavanols have been implicated in scavenging ROS, regulating auxin levels and improving growth (Verdan et al., 2011; Muhlemann et al., 2018; H. Tan et al., 2019). Downregulation of flavonoid production could also be a response to dysregulated iron homeostasis caused by nickel toxicity. Excess nickel causes a severe disruption of iron homeostasis by obstructing the initial uptake of iron into root cells and reducing the iron transportation from roots to shoots (Ghasemi et al., 2009; Rahman et al., 2005). Decreased levels of iron causes the competitive inhibition of photosystem II, diminished chlorophyll function and reduced chlorophyll production (El-Sheekh, 1993; Mohanty et al., 1989; Ghasemi et al., 2009). Flavonols and to a lesser extent flavan-3-ols have a high binding affinity to iron (Verdan et al., 2011; M. Guo et al., 2007; Chobot et al., 2009; Kubicova et al., 2022; Melidou et al., 2005). The downregulation of iron chelators could increase the availability of iron ions and maintain iron homeostasis, thereby counteracting a prominent symptom of nickel toxicity. In some studies, the flavonol quercetin inhibited iron absorption and uptake in animals (Lesjak et al., 2014, 2019). The role of flavonol in nickel tolerance has yet to be investigated.

Two genes encoding a probable PIP2-8 aquaporin were identified among the top downregulated genes (table 6b, S6b). PIP2-8 aquaporins are transporters with a broad specificity that transport water and small solutes between cells (J. Bai et al., 2021). Downregulation of aquaporins may be a response to multiple symptoms caused by nickel toxicity which include decreased water content, reduced transpiration and a disturbance in metal homeostasis (Llamas et al., 2008; Reis et al., 2017; Ghasemi et al., 2009; Rubio et al., 1994). Decreased aquaporin expression could potentially

decrease the intracellular transportation of heavy metals, retain water content and maintain the proper homeostasis of other metals (Barozzi et al., 2019; Kholodova et al., 2011).

A gene encoding the WALLS ARE THIN1 (WAT1) protein was identified (S6b). WAT1 is a vacuolar auxin transporter that exports auxin from the vacuole to the cytoplasm and is an integral component of intracellular auxin homeostasis (Ranocha et al., 2013). Excess nickel can inhibit growth and development by decreasing the distribution of auxin throughout the shoots (Lešková et al., 2020). Downregulation of WAT1 may exasperate growth inhibition by further reducing intracellular levels of auxin (Hanika et al., 2021; Ranocha et al., 2013). It is also possible that downregulation of WAT1 may elicit an increase in salicylic acid synthesis and signalling which is involved in various defense pathways (Denancé et al., 2013; D. Wang et al., 2007). In many plants, salicylic acid was reported to alleviate heavy metal stress by increasing plasma membrane stability, chlorophyl content and antioxidant enzyme activity (Sinha et al., 2015; H. Wang et al., 2009; Yusuf et al., 2012).

Genes encoding cellulose synthase A subunits were identified among the top downregulated genes and are involved in the synthesis of cellulose (S6b) (Taylor et al., 2004). In *Oryza sativa*, silenced cellulose synthase A subunit genes conferred cadmium resistance (X.-Q. Song et al., 2013). The authors attributed the cadmium resistance to possible reductions in the thickness and organization of the cell wall and xylem vasculature. Alterations to the morphology of the xylem decreased cadmium accumulation in the xylem sap, thereby reducing the root to shoot translocation of cadmium. It is plausible that these physical changes can also affect the accumulation of other heavy metals such as nickel.

2.4.5 Annotation of the top 100 upregulated genes between the susceptible genotype and the control

Annotation of top DEGs in SG compared to the water control can describe important mechanisms associated with the susceptible genotype and can provide insights on the high number of DEGs detected in the comparison. Genes expressed within the susceptible genotype are more likely to be associated with cell death and the mitigation of tissue damage based on physical observations from the phenotype (fig 1). Many genes may also be associated with senescence and the controlled progression of cell death, depending on the utility of a particular mechanism (Grbić & Bleecker, 1995; He et al., 2002). Genes encoding a Class V chitinase were identified among the top upregulated genes (STable 7a). Class V chitinase catalyzes the degradation of poly-N-acetyl-D-glucosamine (chitin) into constituent monomers (J. Chen et al., 2018). In several species, increased chitinase expression was correlated with a concerted defense response toward several heavy metals (Békésiová et al., 2008). Increased expression of chitinases also conferred broad resistance to various stressors which include bacterial pathogens, fungal pathogens, wounding and salinity (Dana et al., 2006; Boava et al., 2011; P. Li et al., 2018). However, the exact mechanism of action toward abiotic stresses has yet to be described.

A gene encoding UDP-glycosyltransferase was identified in the top upregulated genes of SG compared to the control (STable 7b). UDP-glycosyltransferase facilitates the transfer of glucose to abscisic acid (ABA), producing the inactive conjugate abscisic acid-glucose ester (ABA-GE) (Sun et al., 2017). ABA conversion to ABA-GE negatively regulates ABA synthesis and subsequently reduces ABA signalling. Decreased ABA signalling may have an impact on facets of plant physiology that specifically respond to heavy metals such as water conservation, stomatal closure, transpiration rate and crosstalk with other stress related hormones (Choudhary et al., 2010;

Hsu & Kao, 2003; R. Li et al., 2022; Q. Tao et al., 2021; Wiszniewska et al., 2018; B. Deng et al., 2022). In some plants, increased ABA have been found to reduce root to shoot translocation and decrease IRT1 which is a nonspecific transporter associated with the initial uptake of nickel (S. K. Fan et al., 2014; F. J. Zhao et al., 2006). Nonetheless, overexpression of ABA can impede growth and cell division to elicit the stress response (Tung et al., 2008; Estrada-Melo et al., 2015; H. Y. Lee et al., 2015). Additionally, ABA is a positive regulator of senescence which may impact growth outcomes, especially in response to heavy metal stress (I. C. Lee et al., 2011). UDP-glycosyltransferase could therefore function to recover plant growth and reduce senescence in lieu of the ABA mediated stress response (Negin et al., 2019; H. Y. Lee et al., 2015). Reduced ABA content has also been reported immediately after the alleviation of a stressor such as drought, suggesting that a similar phenomenon may have occurred in this instance (Ma et al., 2021; X. Zhao et al., 2023).

2.4.6 Annotation of the top 100 downregulated genes between the susceptible genotype and the control

GO annotation of the top downregulated genes in SG compared to water can provide information on genes and mechanisms with reduced expression. Among the top downregulated genes is a gene that encodes fatty acyl-coA reductase (FAR) (table 7b). FAR catalyzes the conversion of fatty acyl-coA to fatty alcohols, which are intermediates of extracellular lipid compounds such as cuticular wax and suberin (Doan et al., 2012; X. Zhang et al., 2022). The deposition of extracellular lipid compounds on the surface of leaves can regulate transpiration by forming a protective barrier that limits permeability and water intake (Y. Wang et al., 2018). In some plants, decreased wax content lead to considerable increases in water permeability, although this function

varies greatly among different species and tissues (Suresh et al., 2022). FAR may potentially be involved in water retention in response to water loss caused by nickel toxicity.

Another identified gene encodes the nonspecific phospholipase C2 (NPC2) which is responsible for glycerolipid metabolism and the conversion of phospholipids to DAG (STable 7b) (Ngo et al., 2018; Peters et al., 2010). Downregulation of NPC2 prevents the conversion of phospholipids to DAG, thereby increasing the presence of available phospholipids (Nakamura et al., 2005). In the absence of a stressor, an adequate balance of phospholipid synthesis and degradation is maintained (K. Yoon et al., 2012). Plasma membrane degradation caused by excess nickel could be further exasperated by enzymes that reduce the available pool of phospholipids (Braidot et al., 1993). The retainment of phospholipids mediated by NPC may result in enhanced stability of cell membranes amidst ROS damage (Nakamura et al., 2005). Furthermore, downregulation of NPC2 can also reduce oxidative stress by decreasing the conversion of DAG to phosphatidic acid (Baldanzi et al., 2016; D'Ambrosio et al., 2018).

Genes encoding MYB transcription factors were identified in the top downregulated genes of SG compared to water (STable 7b). In addition to being involved in seed development, MYB transcription factors regulate the synthesis of trichomes and mucilage (S. F. Li et al., 2020; Machado et al., 2009). Several plant species have shown a positive correlation between trichome production and nickel tolerance, possibly due to nickel accumulating at the base of trichomes stalks (de la Fuente et al., 2007; Krämer et al., 1997). In *Arabidopsis thaliana*, overexpression of MYB12 was found to increase flavonol production as an activator for several genes in the flavonol biosynthesis pathway (Mehrtens et al., 2005). Downregulation of MYB123 suggests decreased flavonol production which aligns with the downregulation of flavonoid related genes as previously described in section 2.4.4.

A gene encoding the Homeobox-leucine zipper (HDZIP) protein was identified among the top downregulated genes (STable 7b). HDZIP is a transcription factor involved in growth and development (Y. Wang et al., 2003; Johannesson et al., 2003). In *Arabidopsis thaliana*, HDZIP increases the sensitivity and positive regulation of ABA (Johannesson et al., n.d.). Downregulation of HDZIP could increase growth by reducing ABA signalling and the associated crosstalk involved with delays in germination (Johannesson et al., 2003). Decreased expression of HDZIP aligns with the upregulation of UDP-glycosyltransferase as described in section 2.4.5. Both genes function to regulate ABA expression in response to nickel stress.

2.5 Conclusion

A comprehensive transcriptome analysis of *Pinus banksiana* was performed in response to excess nickel. The gene expression of each genotype responding to excess nickel was assessed based on various attributes provided by the transcriptome analysis. Nickel resistant plants had 35-51 million sequences whereas nickel susceptible plants had 24-28 million sequences. The de novo transcript assembly identified 581037 transcripts and 435293 genes. At a high stringency, there were no differentially expressed genes between nickel resistant and susceptible genotypes, indicating no significant difference in gene expression. This finding suggests that DEGs may be expressed at a low stringency or occur in the roots. There were 4128 upregulated genes and 3754 downregulated genes in the nickel resistant genotype compared to the control. The response to stress and response to chemical terms comprised the highest proportion of upregulated gene expression whereas the biosynthetic process and carbohydrate metabolic process terms had the highest proportion of downregulated gene expression. The majority of upregulated genes were expressed in the extracellular region and the nucleus whereas the majority of downregulated genes were expressed in the plasma membrane and extracellular region. For the susceptible genotype compared to the

control, there were 37116 upregulated genes and 12053 downregulated genes. The terms with the highest proportion of upregulated genes were the response to stress, response to chemical and signal transduction. The terms with the highest proportion of downregulated genes were the biosynthetic process, response to stress and response to external stimulus. The majority of upregulated genes were expressed in the extracellular region and the nucleus whereas the majority of downregulated genes were expressed in the plasma membrane and extracellular region. Notable top upregulated and downregulated genes were mostly associated with the stress response and included genes encoding trypsin inhibitors, RING-H2 finger proteins, aquaporin proteins, Jasmonate ZIM-domain proteins, ABA related proteins and enzymes involved in the flavonoid biosynthetic process. There were no identified genes that encoded nickel transporters or chelators and mechanisms for nickel resistance could not be elucidated. Transcriptome analysis of *Pinus banksiana* was able to provide detailed information on gene expression and the tolerance mechanisms that respond to nickel toxicity.

Chapter 3: Transcriptome analysis of copper resistant and copper susceptible Jack Pine (*Pinus banksiana*)

3.1 Introduction

Understanding plant resistance to copper is an important step to efficiently revitalize areas afflicted by mining and industrial pollution. Plant resistance to copper is especially important for areas that are poised to increase copper production and exportation. Many facets of plant development and physiology are reliant on copper and the role it plays as an essential ion. Proteins that utilize copper are associated with photosynthesis, cellular respiration, cell wall fortification, growth modulation, apoptosis and antioxidative functions (Ghuge et al., 2015; Shahbaz et al., 2015; Garcia-Molina et al., 2011; Chamseddine et al., 2008). Excess copper causes a variety of symptoms that may damage tissue and impede development. In root cells, excess copper competitively inhibits the uptake of essential ions such as iron, manganese and zinc resulting in disturbed ion homeostasis (S.-L. Lin & Wu, 1994; Ivanov et al., 2016; Martins & Mourato, 2006). Excess copper can replace iron in the binding site of plastoquinone QA of Photosystem II, leading to diminished electron transfer during photosynthesis (Jegerschoeld et al., 1995). Copper toxicity leads to decreased chlorophyll and thylakoid membranes content, which impedes photosynthesis and contribute to chlorosis (Pätsikkä et al., 2002). Decreased nitric oxide production is another symptom of copper toxicity which results in diminished auxin production, cytokinin activity and mitotic activity in root cells. Copper induced production of ROS may also lead to oxidative stress, lipid peroxidation, plant tissue damage and organelle death (Opdenakker et al., 2012; X. Wang et al., 2018; R. Sharma et al., 2019; Nair et al., 2014).

The genetic and physiological basis of copper resistance have been partially described from the literature. In *Arabidopsis thaliana,* the downregulation of COPT1, COPT2, ZIP2 and ZIP4

indicate a decrease in the initial uptake of copper into the root cells (Sancenón et al., 2004; del Pozo et al., 2010; Wintz et al., 2003). Upregulation of the HMA5 transporter in *Arabidopsis thaliana* and *Oryza sativa* suggests increased copper mobilization from the roots and increased root to shoot translocation (Andrés-Colás et al., 2006, p. 5; del Pozo et al., 2010; F. Deng et al., 2013). In *Arabidopsis thaliana*, upregulation of HMA1 and HMA6/PAA1 transporters suggests increased root to shoot translocation and copper transport to the chloroplasts (del Pozo et al., 2010; Boutigny et al., 2014; S. Lee et al., 2007). The HMA8/PAA2 transporter was also upregulated, demonstrating the increased transport of copper to the thylakoid lumen and plastocyanin (del Pozo et al., 2010; Mayerhofer et al., 2016; Tapken et al., 2012). Collectively, the higher amount of copper delivery to the chloroplast stroma, thylakoid lumen and plastocyanin may suggest increased photosynthesis (Tapken et al., 2012, 2015). Similarly, the increased expression of AtHMA7 encourages copper transport to the Golgi apparatus and ethylene receptors located in the ER, suggesting enhanced growth to counteract symptoms of copper toxicity (B. Zhang et al., 2014). In *Oryza sativa*, OsHMA9 was upregulated in the xylem and phloem, indicating increased xylem and phloem loading (S. Lee et al., 2007). Genes encoding the chelators MT2a and MT2b were upregulated in the root tips, shoots and phloem area which indicated elevated metallothionein production for copper chelation in those respective areas (Zhou & Goldsbrough, 1995; W.-J. Guo et al., 2003).

Currently, the response of conifers to heavy metals are elusive and under researched in comparison to angiosperms. Transcriptome analysis of copper resistant trees will be a valuable tool to uncover physiological mechanisms associated with copper resistance or tolerance. *Pinus banksiana* was selected as a candidate for transcriptome analysis due to its successful utilization in the Sudbury regreening program (Beckett & Spiers, n.d.; Lu et al., 2014; K. K. Nkongolo et al., 2013). In

addition to being a hardy and resilient tree, *Pinus banksiana* was observed to have a moderate genetic diversity and low gene flow in metal contaminated sites (Vandeligt et al., 2011; Ranger et al., 2008). Furthermore, newer population of *Pinus banksiana* that were used in the regreening program had a significantly higher genetic diversity in comparison to older populations.

The objective of this study was to 1) Comprehensively map and describe the transcriptome of Jack Pine (*Pinus banksiana*). 2) Use transcriptome analysis and gene ontology to describe the gene expression of genotypes responding to excess copper. 3) Evaluate variances in gene expression between genotypes responding to excess copper.

3.2 Materials and methods

3.2.1 Plant treatment, damage rating and collection

The collection of plant material and preparatory growth conditions followed the same protocol as described in section: 2.2 Materials and Methods. 45 seedlings were given 4 different treatments in a completely randomized block design. 15 seedlings were treated with 50 mL of 1300 mg/kg copper (II) sulphate pentahydrate which represented the in field concentration detected in the soil of metal contaminated areas from a local survey. 15 seedlings were treated with 50 mL of 2600 mg/kg copper (II) sulphate pentahydrate which represented twice the dosage of the in field concentration taken from the same local survey. 5 seedlings were treated with 1300 mg/kg of K_2SO_4 which represented the positive control corresponding to the maximum in field concentration of copper (II) sulphate pentahydrate. 5 seedlings were treated with 2600 mg/kg of K_2SO_4 which represented the positive control corresponding to double the concentration. The post treatment incubation and allocation of damage ratings followed the same protocol as described in section 2.2 Materials and Methods.

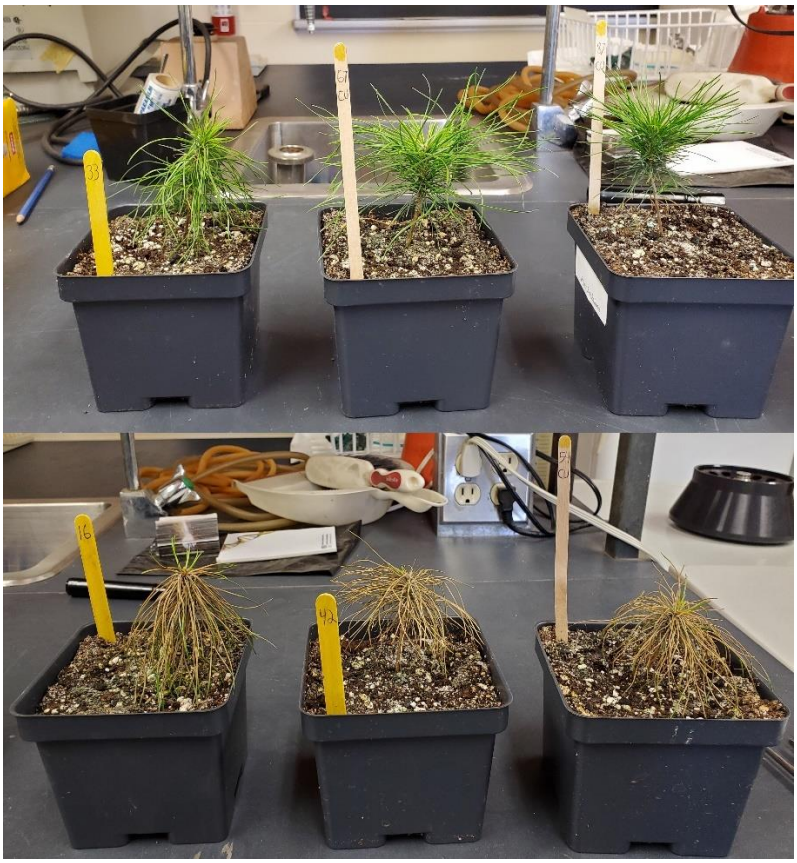

Figure 10. Damage rating of Pinus banksiana seedlings after treatment with 1300 mg/kg of copper. Selected seedlings underwent treatment and were assigned damage ratings based on various attributes. The top image shows seedlings assigned to the resistant group and the lower image shows seedlings assigned to the susceptible group.

3.2.2 Transcriptome analysis of *Pinus banksiana*

RNA Extraction and Quality Control, RNA sequencing and Transcriptome Assembly, Annotation of *Pinus banksiana* using BLAT matching, Quantification of gene expression and quality control (QC) analysis, Differential gene expression (DGE) analysis of pairwise comparisons, Analysis of top upregulated and downregulated genes follow the same procedure as detailed in sections 2.2.2-2.2.7.

3.3 Results

3.3.1 Transcript assembly and QC analysis of sequences

The FastQC program analyzes the raw reads generated from Illumina sequencing evaluates the quality of the data. 0 sequences were flagged as poor quality. Copper resistant plants had a total of 31-49 million sequences and copper susceptible plants had a total of 21-29 million sequences. Both treatment groups had an average sequence length of 51 bases. Copper resistant individuals had a deduplicated percentage of 21-27%, indicating that duplicated gene expression contributed to a large proportion of gene expression. Copper susceptible individuals had a deduplicated percentage ranging from 37-59%, indicating that a significantly large portion of gene expression was from duplicated gene expression. In one circumstance, duplicated gene expression comprised a larger portion of gene expression than non duplicated gene expression. The trinity program facilitated transcript assembly, producing a total of 581037 transcripts and 435293 genes. For copper resistant individuals, 78-83% of genes were mapped to the transcript assembly and for copper susceptible individuals, 50-62% of genes were mapped. 126460 genes out of 435293 genes fulfilled the CPM related parameters and were used for differential gene expression analysis.

3.3.2 Differential gene expression (DGE) analysis between genotypes

The clustering between samples was visually assessed using a multidimensional scale plot and hierarchical cluster map. The water and potassium control groups clustered within the same region, indicating no significant difference in gene expression between the treatment groups and that the presence of the potassium control did not significantly affect the treatment regimen (Sfig 2a-2b). Clustering between the resistant genotype (RG) and susceptible genotype (SG) was low, indicating that gene expression was significantly different between the two genotypes. For RG

and the water control, clustering occurred within the same region and overlapped, demonstrating a similar pattern of gene expression. Clustering did not occur between SG and the water control. DEGs that fulfilled the high stringency cut off (two fold and FDR 0.05) were considered for downstream DGE analysis due to the high level of confidence associated with the false discovery rate (FDR). The low stringency cutoff has some statistical basis for consideration due to having a p value of 0.01. Nevertheless, the higher FDR threshold indicates that the expression of a particular gene has a higher probability of being a false positive, leading to reduced statistical confidence.

Table 8. Differentially expressed genes from the copper resistant genotype compared to the copper susceptible genotype in *Pinus banksiana*

Cutoff	**Standard (two fold and FDR 0.05)**	**Low Stringency (two fold and p value 0.01)**
Upregulated genes	6213	6431
Downregulated genes	29038	29605
Total genes	35251	36036

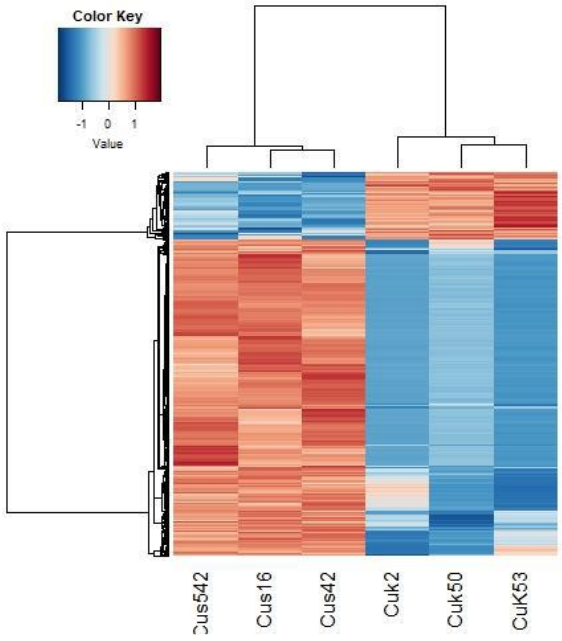

Figure 11a. Heatmap of differentially expressed genes from the copper resistant genotype compared to the copper susceptible genotype in Pinus banksiana. Differentially expressed gene

values are based on the Log2 normalized FC, with red cells representing upregulation and blue cells representing downregulation. Cus542, Cus16 and Cus42 are copper susceptible samples. Cur872, Cur33 and Cur67 are copper resistant samples.

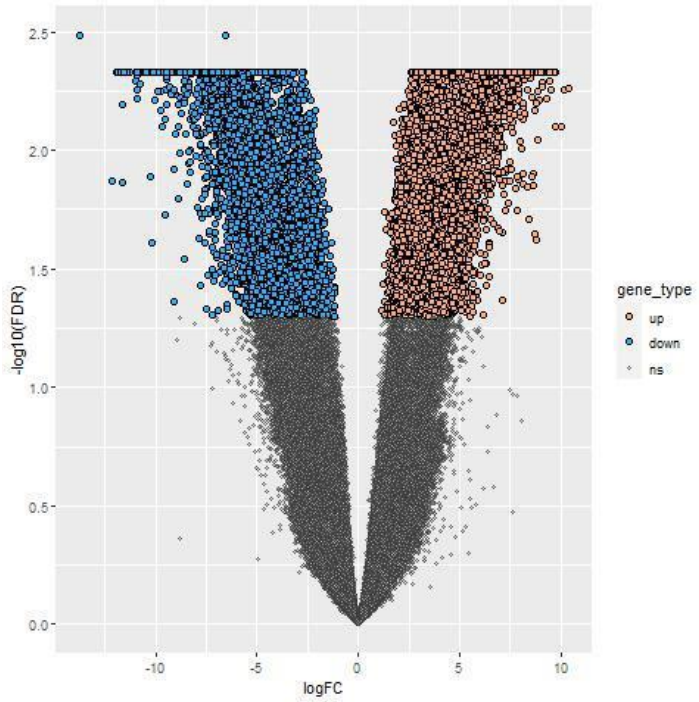

Figure 11b. Volcano plot of differentially expressed genes from the copper resistant genotype compared to the copper susceptible genotype in Pinus banksiana. Brown points represent upregulated gene expression whereas blue points represent downregulated gene expression when compared to the susceptible genotype. Grey points indicate no significant difference from the susceptible genotype. Log10(FDR) is the log10 of the false discovery rate. The border between the no significant points and the differentially regulated genes represents the false discovery rate of 0.05 (two fold).

Table 9. Differentially expressed genes from the copper resistant genotype compared to the water controls in *Pinus banksiana*

Cutoff	**Standard (two fold and FDR 0.05)**	**Low Stringency (two fold and p value 0.01)**
Upregulated genes	1	1138
Downregulated genes	0	1250
Total genes	1	2388

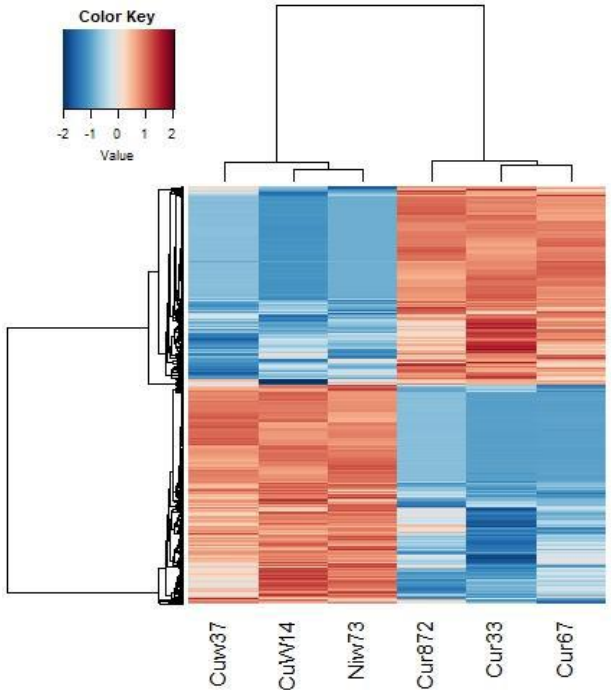

Figure 12a. Heatmap of differentially expressed genes from the copper resistant genotype compared to water controls in Pinus banksiana. Differentially expressed gene values are based on the Log2 normalized FC, with red cells representing upregulation and blue cells representing downregulation. Cur872, Cur33 and Cur67 represent copper resistant samples. Cuw37, CuW14 and Niw73 represent water controls.

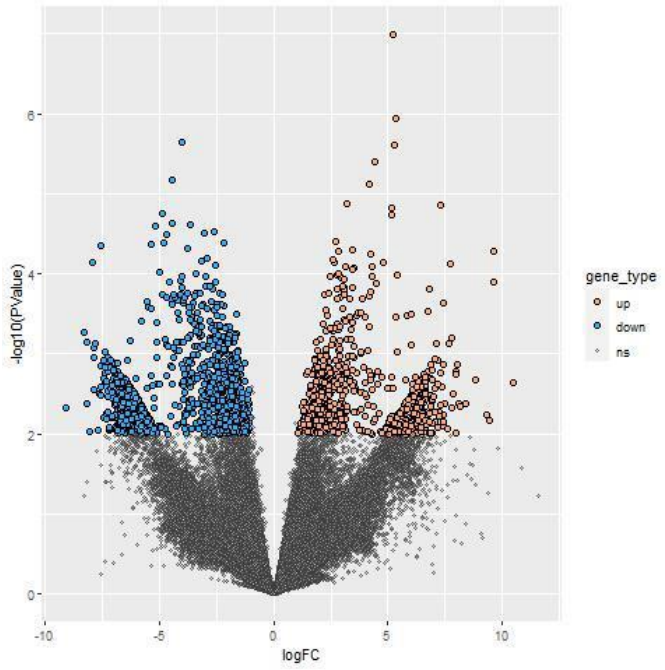

Figure 12b. Volcano plot of differentially expressed genes from the copper resistant genotype compared to the controls in Pinus banksiana. Brown points represent upregulated gene

expression whereas blue points represent downregulated gene expression when compared to the susceptible genotype. Grey points represent genes with no significantly different expression from the water controls. Log10(FDR) is the log10 of the false discovery rate. The border between the nonsignificant points and the differentially regulated genes represents a false discovery rate of 0.05 (two fold).

Table 10. Differentially expressed genes from the copper susceptible genotype compared to the water controls in *Pinus banksiana*

Cutoff	**Standard (two fold and FDR 0.05)**	**Low Stringency (two fold and pvalue 0.01)**
Upregulated genes	27584	31972
Downregulated genes	10065	12130
Total genes	37649	44102

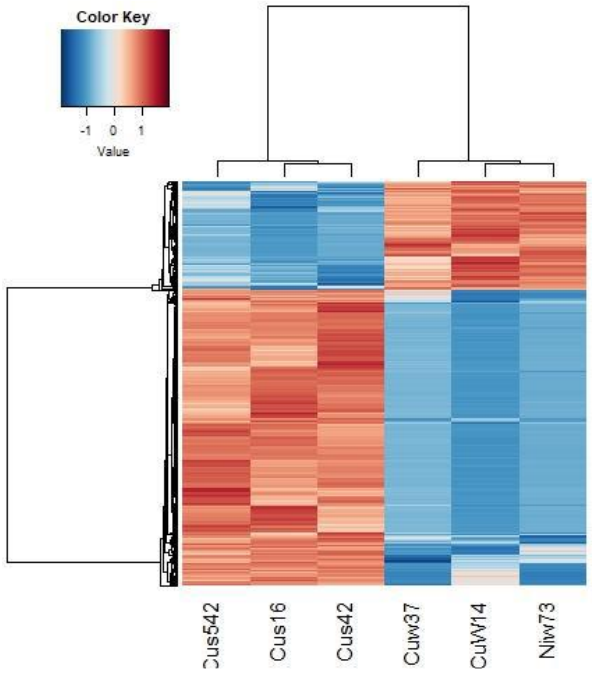

Figure 13a. Heatmap of differentially expressed genes from the copper susceptible genotype compared to water controls in Pinus banksiana. Differentially expressed gene values are based on the Log2 normalized FC, with red cells representing upregulation and blue cells representing downregulation. Cus542, Cus16, Cus42 represent copper resistant samples. Cuw37, CuW14 and Niw73 represent water controls.

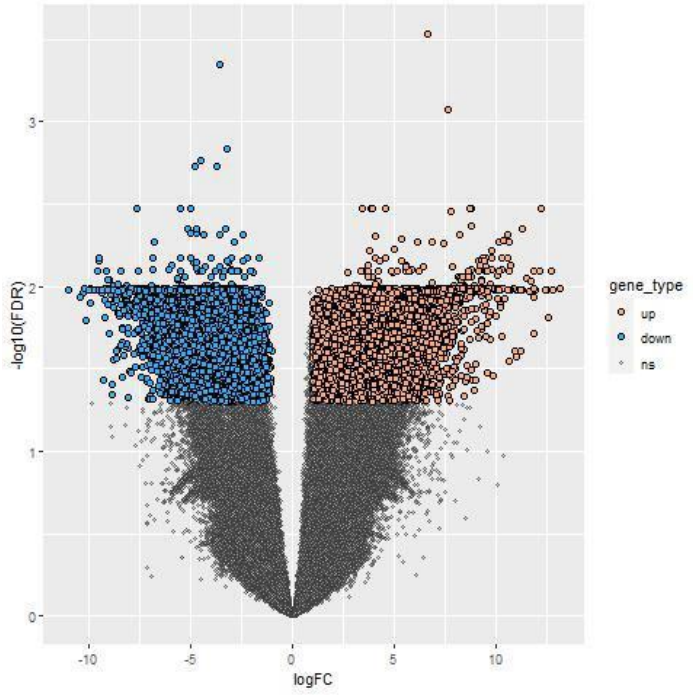

Figure 13b. Volcano plot of differentially expressed genes from the copper susceptible genotype compared to water controls in Pinus banksiana. Brown points represent upregulated gene expression whereas blue points represent downregulated gene expression when compared to the susceptible genotype. Grey points indicate no significant difference in expression from the susceptible genotype. Log10(FDR) is the log10 of the false discovery rate. The border between the no significant points and the differentially regulated genes represents the false discovery rate of 0.05 (two fold).

3.3.4 Gene ontology of the top 100 differential expressed genes for *Pinus banksiana*

Figures 14a-14c show the top upregulated genes of RG compared to SG distributed into different terms within the Biological processes, Molecular functions and Cellular Component categories. The response to stress term (16.67%) comprised the largest proportion of gene expression followed by the biosynthetic process (12.5%), response to chemical (12.5%), signal transduction (8.33%), post-embryonic development (8.33%) and the lipid metabolic process (8.33%). These terms represented 66.66% of expressed genes. Lipid metabolic process comprised a large proportion of expressed genes despite having a low proportion of genes in the whole transcriptome. Response to stress, response to chemical, response to light stimulus and response to endogenous stimulus

share the parent term response to stimulus. Biosynthetic process, post-embryonic development, cell cycle, cellular component organization, response to light stimulus, fruit ripening, secondary metabolic process, photosynthesis, and nucleobase containing compound metabolic process were highly represented terms in the top upregulated transcripts despite comprising less than 2% of expressed genes in the whole transcriptome. For metabolic function, 50% of expressed genes were associated with nucleotide binding followed by transporter activity (25%) and kinase activity (25%). Transporter activity comprised a large proportion of expressed genes despite having a lower percentage distribution in the whole transcriptome. In the cellular component category, the membrane term comprised the largest portion of the top upregulated genes. The thylakoid organelle is represented in the top upregulated genes despite comprising less than 2% of the whole transcriptome.

Figures 15a-15c show the top downregulated genes depicting a different pattern of gene expression. 22.22% of genes were distributed to the carbohydrate metabolic process term whereas the other terms represented 11.11% of expressed genes. In contrast to the whole transcriptome, carbohydrate metabolic process comprised the largest portion of gene expression in top downregulated genes. Response to stress, response to chemical, response to external stimulus and response to endogenous stimulus shared the parent term response to stimuli. Cellular component organization, response to external stimulus and fruit ripening were represented in the top downregulated gene expression despite having less than 2% of expressed genes in the whole transcriptome. In the metabolic function category, 66.67% of expressed genes were allocated to the terms hydrolase activity (33.33%), DNA-binding transcription factor activity (16.67%) and transferase activity (16.67%). DNA binding transcription factor activity comprised a larger portion of expressed genes in the top downregulated transcripts compared to the whole

transcriptome. Hydrolase activity and enzyme regulatory activity were represented despite comprising less than 2% of expressed genes in the whole transcriptome. For the cellular component category, 50% of expressed genes was associated with the extracellular region followed by the terms membrane (25%) and nucleus (25%).

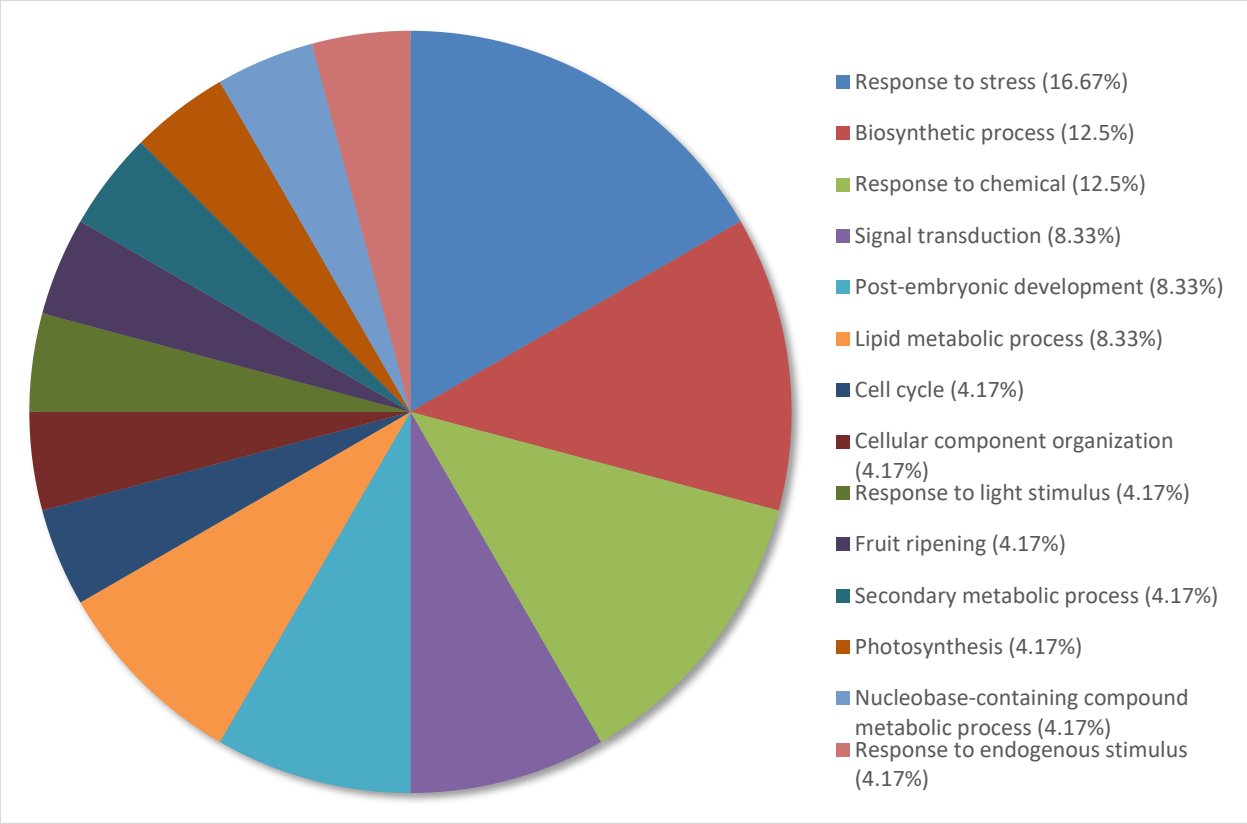

Figure 14a. Percentage of the top 100 Upregulated transcripts in Pinus banksiana resistant samples compared to susceptible samples categorized by Biological Processes. The top 100 most upregulated genes from the resistant samples compared to the susceptible samples were grouped by Gene Ontology terms within the Biological Processes category using Omicsbox/BLAST2GO. Terms with lower than 2% of total gene expression were combined together and assigned the label “other”.

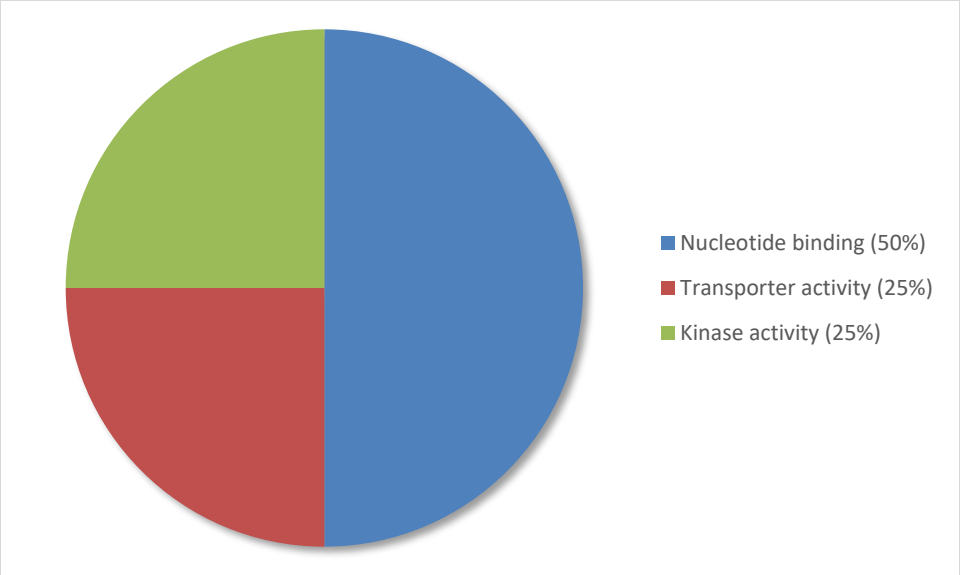

Figure 14b. Percentage of the top 100 Upregulated transcripts in Pinus banksiana resistant samples compared to susceptible samples categorized by Molecular Function. The top 100 most upregulated genes from the resistant samples compared to the susceptible samples were grouped by Gene Ontology terms within the Molecular Function category using Omicsbox/BLAST2GO. Terms with lower than 2% of total gene expression were combined together and assigned the label "other".

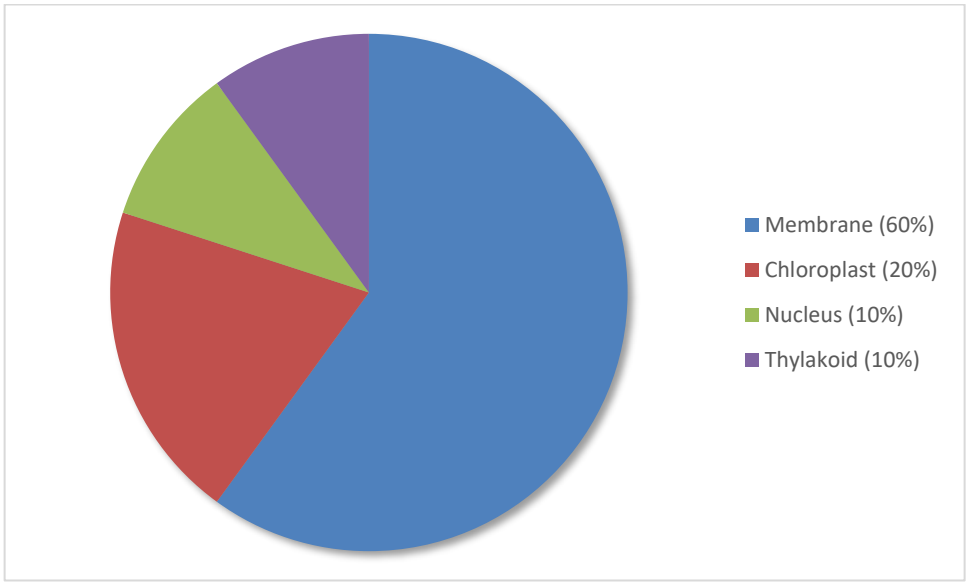

Figure 14c. Percentage of the top 100 Upregulated transcripts in Pinus banksiana resistant samples compared to susceptible samples categorized by Cellular Component. The top 100 most upregulated genes from the resistant samples compared to the susceptible samples were grouped by Gene Ontology terms within the Cellular Component category using Omicsbox/BLAST2GO. Terms with lower than 2% of total gene expression were combined together and assigned the

label “other”.

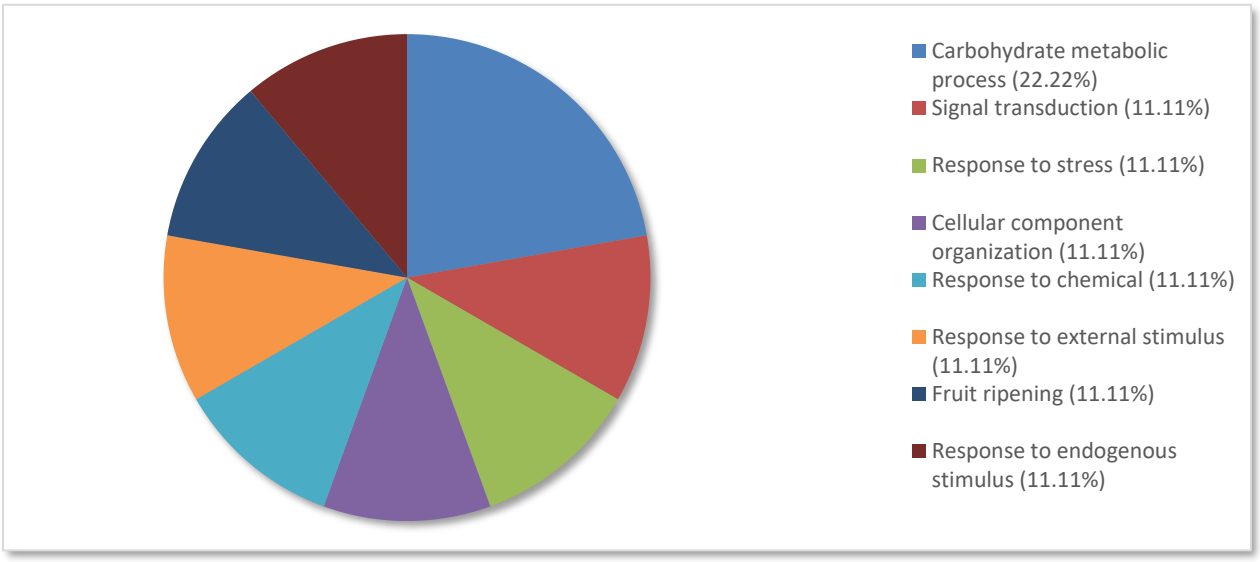

Figure 15a. Percentage of the top 100 downregulated transcripts in Pinus banksiana resistant samples compared to susceptible samples categorized by Biological Processes. The top 100 most downregulated genes from the resistant samples compared to the susceptible samples were annotated and distributed into categories based on Biological Processes using Omicsbox/BLAST2GO. Categories with gene expression lower than 2% were summed together and assigned the label “other”.

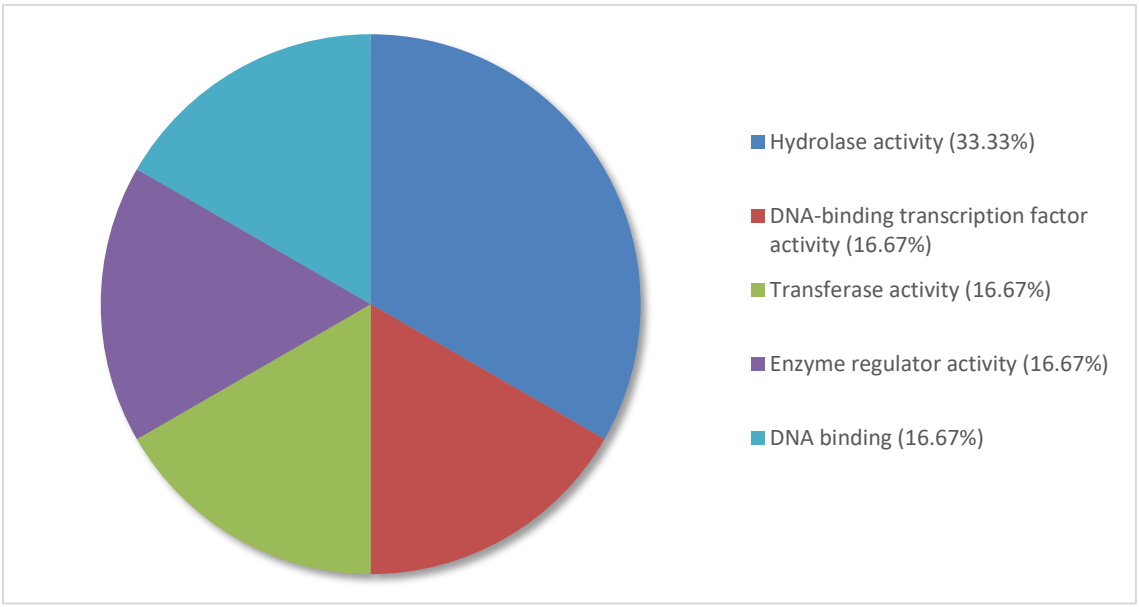

Figure 15b. Percentage of the top 100 downregulated transcripts in Pinus banksiana resistant samples compared to susceptible samples categorized by Molecular Function. The top 100 most downregulated genes from the resistant samples compared to the susceptible samples were annotated and distributed into categories based on Molecular Function using

Omicsbox/BLAST2GO. Categories with gene expression lower than 2% were summed together and assigned the label “other”.

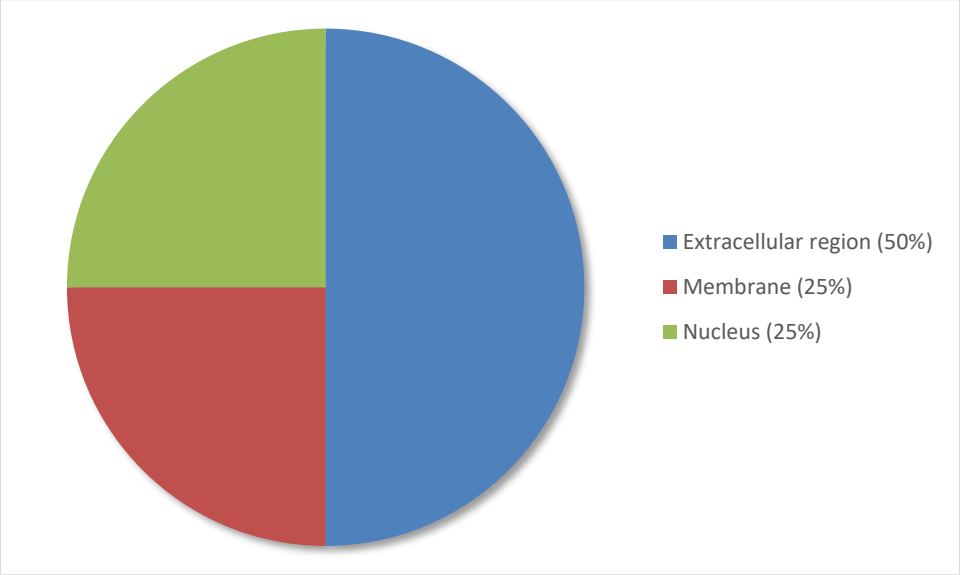

Figure 15c. Percentage of the top 100 downregulated transcripts in Pinus banksiana resistant samples compared to susceptible samples categorized by Cellular Component. The top 100 most downregulated genes from the resistant samples compared to the susceptible samples were annotated and distributed into categories based on Cellular Component using Omicsbox/BLAST2GO. Categories with gene expression lower than 2% were summed together and assigned the label “other”.

Figures 16a-17c shows the proportion of top upregulated and downregulated genes from SG compared to the water controls distributed to different subcategory terms within Biological Processes, Molecular Function and Cellular Component categories. In the Biological processes category, 63.63% of upregulated genes were distributed to the following subcategories: Response to stress (24.24%), carbohydrate metabolic process (12.12%), response to biotic stimulus (9.09%), response to chemical (9.09%) and response to endogenous stimulus (9.09%). 5 of the top 10 categories fall under the parent term response to stimulus. Unlike the whole transcriptome, carbohydrate metabolic process comprised a larger proportion of gene expression and DNA metabolic process comprised a low proportion of gene expression. Response to light stimulus, fruit ripening, post embryonic development and biosynthetic process were categories that were

represented in the top upregulated genes despite comprising less than 2% of expressed genes in the whole transcriptome. For molecular function, 61.54% of expressed genes were distributed to the following categories: Hydrolase activity (38.46%) and transferase activity (23.08%). Hydrolase activity and transferase activity are categories that fall under the parent category catalytic activity whereas nucleotide binding and DNA binding categories are associated with nucleotide function. Hydrolase activity, transferase activity and enzyme regulator activity were categories that were largely represented in the top upregulated genes but comprised less than 2% of expressed genes in the whole transcriptome. In the cellular component category, 66.67% of expressed genes were distributed to the following subcategories: Extracellular region (41.67%) and Nucleus (25%). Genes in the Nucleus term had a large proportion of expressed genes despite comprising less than 2% of expressed genes in the whole transcriptome.

Top downregulated genes in figures 17a-17c depicts a different pattern of gene distribution within subcategories in comparison to top upregulated genes. For the Biological processes category, 52.17% of downregulated genes were allocated to the following terms: Biosynthetic process (17.39%), response to stress (13.04%), lipid metabolic process (13.04%), response to biotic stimulus (8.70%). Lipid metabolic process and carbohydrate process had a larger proportion of top downregulated genes in comparison to the proportion of expressed genes in the whole transcriptome. Biosynthetic process, lipid metabolic process, carbohydrate metabolic process and catabolic process are prominent subcategories that fall under the parent term metabolic processes. The terms biosynthetic process, cellular component organization, secondary metabolic process, flower development and nucleobase containing compound metabolic processes were largely represented in the top downregulated genes but comprised less than 2% of expressed genes in the whole transcriptome. For the metabolic process category, 69.23% of expressed genes were

categorized under hydrolase activity (46.15%) and transporter activity (23.08%). Transporter activity had a higher representation in the top downregulated genes than in the whole transcriptome. The terms hydrolase activity, transferase activity and protein binding were largely represented in the top downregulated genes despite comprising a low proportion of genes in the whole transcriptome. Nucleus and the cell wall were terms that had a higher proportion of expressed genes in the top downregulated genes in comparison to the entire transcriptome.

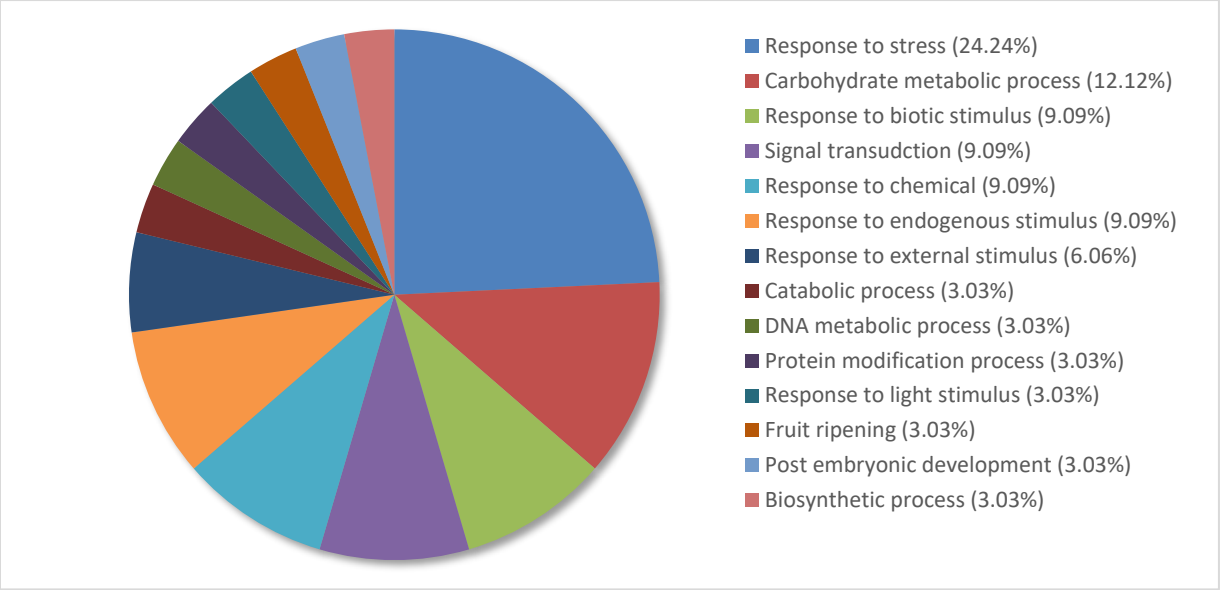

Figure 16a. Percentage of the top 100 upregulated transcripts in Pinus banksiana susceptible samples compared to water controls categorized by Biological Processes. The top 100 most upregulated genes from the susceptible samples compared to the water controls were annotated and distributed into categories based on Biological Processes using Omicsbox/BLAST2GO. Categories with gene expression lower than 2% were summed together and assigned the label "other".

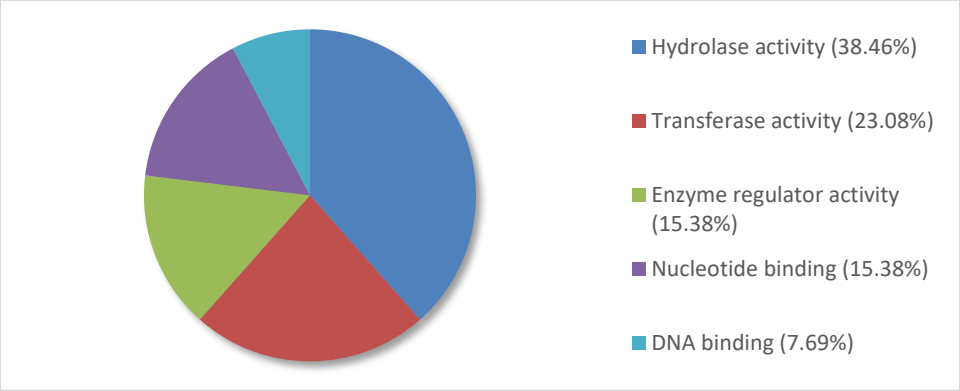

Figure 16b. Percentage of the top 100 upregulated transcripts in Pinus banksiana susceptible samples compared to water controls categorized by Molecular Function. The top 100 most upregulated genes from the susceptible samples compared to the water controls were annotated and distributed into categories based on Molecular Function using Omicsbox/BLAST2GO Categories with gene expression lower than 2% were summed together and assigned the label "other".

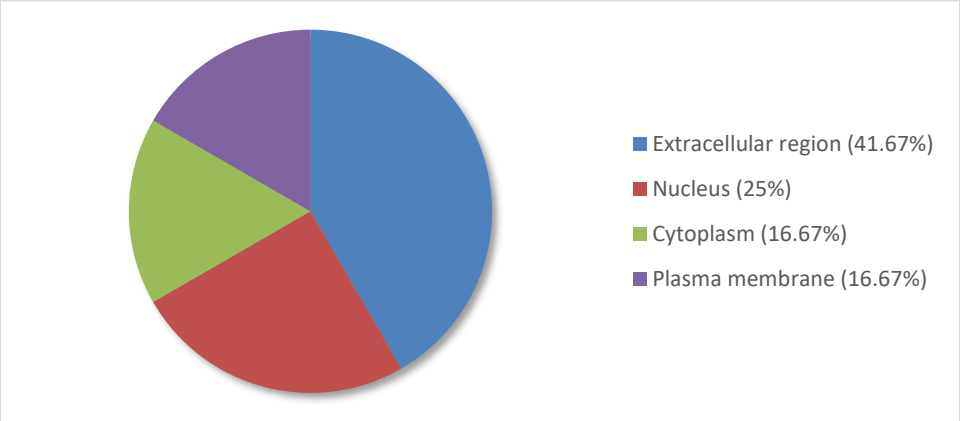

Figure 16c. Percentage of the top 100 upregulated transcripts in Pinus banksiana susceptible samples compared to water controls categorized by Cellular Component. The top 100 most upregulated genes from the susceptible samples compared to the water controls were annotated and distributed into categories based on Cellular Component using Omicsbox/BLAST2GO. Categories with gene expression lower than 2% were summed together and assigned the label "other".

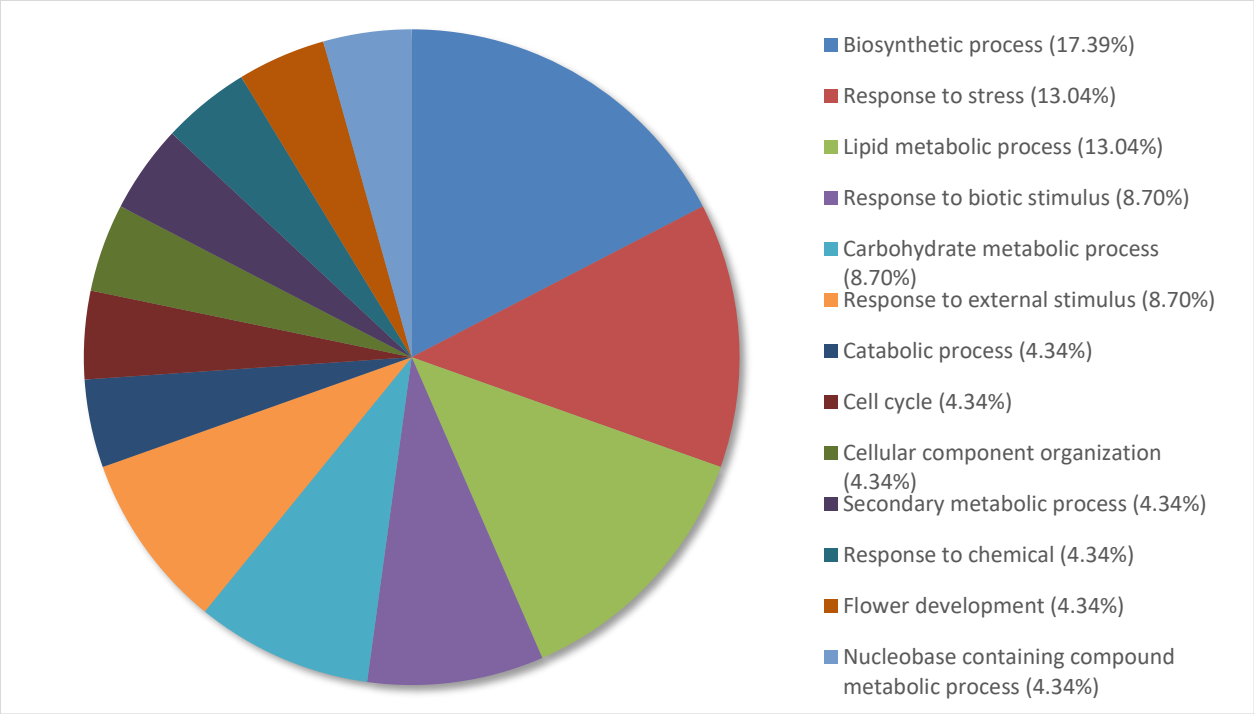

Figure 17a. Percentage of the top 100 downregulated transcripts in Pinus banksiana susceptible samples compared to water controls categorized by Biological Processes. The top 100 most downregulated genes from the susceptible samples compared to the water controls were annotated and distributed into categories based on Biological Processes using Omicsbox/BLAST2GO. Categories with gene expression lower than 2% were summed together and assigned the label "other".

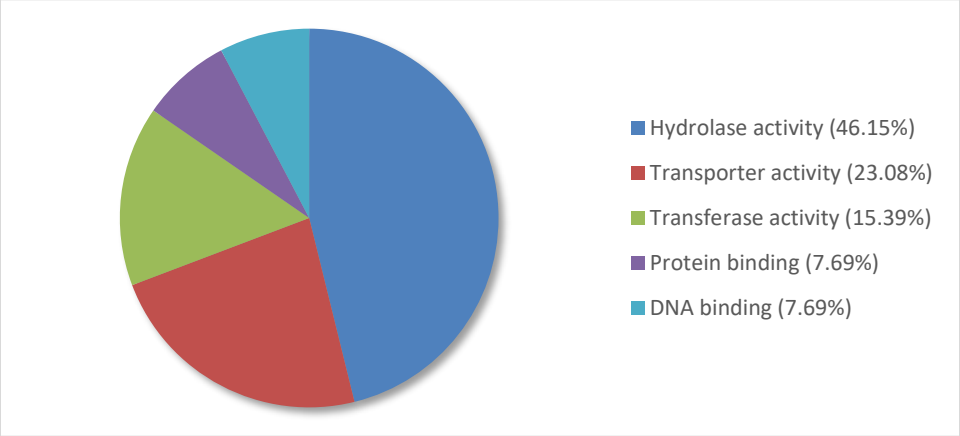

Figure 17b. Percentage of the top 100 downregulated transcripts in Pinus banksiana susceptible samples compared to water controls categorized by Molecular Function. The top 100 most downregulated genes from the susceptible samples compared to the water controls were annotated and distributed into categories based on Molecular Function using

Omicsbox/BLAST2GO. Categories with gene expression lower than 2% were summed together and assigned the label “other”.

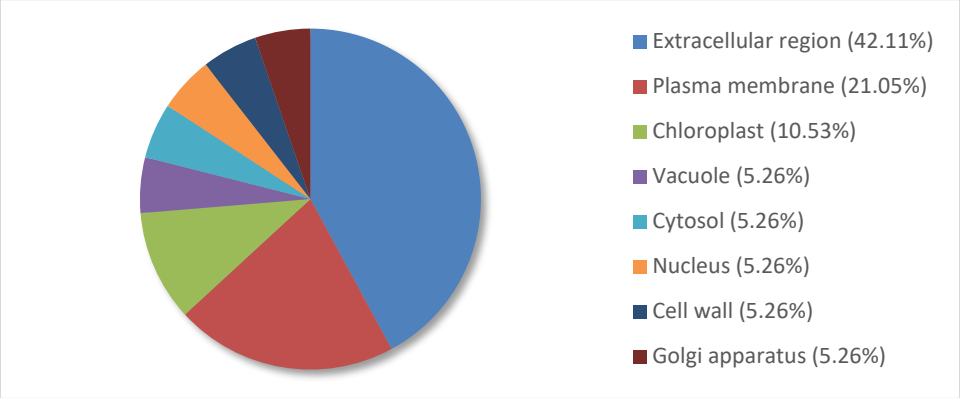

Figure 17c. Percentage of the top 100 downregulated transcripts in Pinus banksiana susceptible samples compared to water controls categorized by Cellular Component. The top 100 most downregulated genes from the susceptible samples compared to the water controls were annotated and distributed into categories based on Cellular Component using Omicsbox/BLAST2GO. Categories with gene expression lower than 2% were summed together and assigned the label “other”.

3.3.5 Top 25 differentially expressed genes between pairwise comparisons

Table 11: Identified candidate genes from the top upregulated genes in copper resistant vs copper susceptible *Pinus banksiana*

Rank	Gene ID	Res 1	Res 2	Res 3	Sus 1	Sus 2	Sus 3	logFC	Adj. P. Value	UniProt Description
80	TRINITY_DN6541_c0_g1	251.91	62.08	39.98	4.26	0.53	3.88	6.93	0.00080	Heavy metal-associated isoprenylated plant protein 20, AtHIP20, AtHIPP20
81	TRINITY_DN6541_c0_g1	251.91	62.08	39.98	4.26	0.53	3.88	6.93	0.00080	Heavy metal-associated isoprenylated plant protein 26, AtHIP26, AtHIPP26 (Farnesylated protein 6, AtFP6)
87	TRINITY_DN55790_c0_g1	6.62	5.2	3.26	0	0.87	0	6.90	0.00072	Pleiotropic drug resistance protein 1 (NtPDR1)

Table 12a. Top 25 upregulated genes from copper resistant samples compared to copper susceptible samples in *Pinus banksiana*

Rank	Gene ID	Res 1	Res 2	Res 3	Sus 1	Sus 2	Sus 3	logFC	Adj. P. Value	UniProt Description
0	TRINITY_DN35689_c0_g1	12.05	7.41	11.07	0	0	0	9.21	0.00002	Predicted Protein
1	TRINITY_DN10618_c0_g1	17.42	2.72	9.6	0	0	0	8.82	0.00181	Predicted Protein
2	TRINITY_DN91621_c0_g2	13.93	4.82	5.68	0	0	0	8.78	0.00025	Predicted Protein
3	TRINITY_DN199894_c0_g2	9.44	9.02	1.99	0	0	0	8.45	0.00117	Predicted Protein
4	TRINITY_DN28042_c0_g3	4.91	8.95	2.74	0	0	0	8.26	0.00022	Cytochrome P450 750A1, EC 1.14.-.- (Cytochrome P450 CYPC)
5	TRINITY_DN7900_c0_g1	6	6.27	3.22	0	0	0	8.25	0.00007	Predicted Protein
6	TRINITY_DN2617_c0_g1	8.29	4.5	3.27	0	0	0	8.24	0.00017	Predicted Protein
7	TRINITY_DN20922_c0_g1	3.17	6.13	4.05	0	0	0	8.02	0.00004	Predicted Protein
8	TRINITY_DN236262_c0_g1	11.08	1.85	3.41	0	0	0	7.96	0.00197	Predicted Protein
9	TRINITY_DN95006_c0_g1	6.22	4.28	1.99	0	0	0	7.87	0.00033	Predicted Protein
10	TRINITY_DN219929_c1_g1	2.74	4.62	4.69	0	0	0	7.86	0.00003	Predicted Protein
11	TRINITY_DN4529_c0_g1	3	7.73	1.66	0	0	0	7.73	0.00069	1,8-cineole synthase, chloroplastic, EC 4.2.3.108 (Terpene synthase TPS-Cin, PgTPS-Cin)
12	TRINITY_DN13781_c0_g3	16.16	15.27	4.31	0	0	1.35	7.73	0.00318	Predicted Protein
13	TRINITY_DN216_c0_g1	58.07	22.76	12.46	0.07	0.49	0.97	7.72	0.00440	Fatty acyl-CoA reductase 2, chloroplastic, AtFAR2, EC 1.2.1.84 (Fatty acid reductase 2) (Male sterility protein 2)
14	TRINITY_DN9994_c0_g1	8.13	1.94	2.38	0	0	0	7.67	0.00114	Predicted Protein
15	TRINITY_DN5226_c2_g1	3.74	2.06	5.32	0	0	0	7.66	0.00014	Predicted Protein
16	TRINITY_DN57458_c1_g1	2.43	3.07	4.49	0	0	0	7.58	0.00004	Predicted Protein
17	TRINITY_DN3869_c0_g1	3.23	4.31	2.12	0	0	0	7.58	0.00009	Predicted Protein
18	TRINITY_DN47098_c0_g1	7.77	2.08	1.81	0	0	0	7.58	0.00131	Predicted Protein
19	TRINITY_DN19214_c1_g2	3.44	3.21	2.82	0	0	0	7.57	0.00004	Predicted Protein
20	TRINITY_DN40558_c0_g2	1.22	7.95	3.16	0	0	0	7.57	0.00127	Predicted Protein
21	TRINITY_DN18490_c0_g1	2.06	7.43	1.88	0	0	0	7.57	0.00066	Predicted Protein
22	TRINITY_DN9649_c1_g3	0.84	8.97	3.91	0	0	0	7.54	0.00382	Predicted Protein
23	TRINITY_DN148688_c0_g2	6.51	3.72	1.03	0	0	0	7.54	0.00203	Predicted Protein

24	TRINITY_DN100_c0_g2	7.29	15.7	4.96	0	0.41	0.08	7.53	0.00072	Predicted Protein
25	TRINITY_DN178176_c0_g1	3.36	4.4	1.77	0	0	0	7.53	0.00017	Predicted Protein

Table 12b. Top 25 downregulated genes from copper resistant samples compared to copper susceptible samples in *Pinus banksiana*

Rank	Gene ID	Res 1	Res 2	Res 3	Sus 1	Sus 2	Sus 3	logFC	Adj. P. Value	UniProt Description
0	TRINITY_DN3519_c0_g1	0	0	0	191.35	54.37	115.22	-11.34	0.00021	Predicted Protein
1	TRINITY_DN43547_c0_g1	0	0	0	162.58	38.33	61.13	-10.81	0.00035	Predicted Protein
2	TRINITY_DN2824_c0_g1	0	0.03	0	90.93	154.91	84.36	-10.53	0.00000	Polygalacturonase, PG, EC 3.2.1.15 (Pectinase)
3	TRINITY_DN2824_c0_g1	0	0.03	0	90.93	154.91	84.36	-10.53	0.00000	Probable polygalacturonase At1g80170, PG, EC 3.2.1.15 (Pectinase At1g80170)
4	TRINITY_DN1315_c0_g1	0.43	0.06	0.31	763.2	1448.5	490.5	-10.28	0.00001	Beta-glucosidase 12, EC 3.2.1.21
5	TRINITY_DN1315_c0_g1	0.43	0.06	0.31	763.2	1448.5	490.5	-10.28	0.00001	Furcatin hydrolase, FH, EC 3.2.1.161
6	TRINITY_DN1315_c0_g1	0.43	0.06	0.31	763.2	1448.5	490.5	-10.28	0.00001	Non-cyanogenic beta-glucosidase, EC 3.2.1.21
7	TRINITY_DN1315_c0_g1	0.43	0.06	0.31	763.2	1448.5	490.5	-10.28	0.00001	Beta-glucosidase 27, Os8bglu27, EC 3.2.1.21
8	TRINITY_DN1315_c0_g1	0.43	0.06	0.31	763.2	1448.5	490.5	-10.28	0.00001	Beta-glucosidase 11, Os4bglu11, EC 3.2.1.21
9	TRINITY_DN1315_c0_g1	0.43	0.06	0.31	763.2	1448.5	490.5	-10.28	0.00001	Beta-glucosidase 24, Os6bglu24, EC 3.2.1.21
10	TRINITY_DN1315_c0_g1	0.43	0.06	0.31	763.2	1448.5	490.5	-10.28	0.00001	Beta-glucosidase 13, Os4bglu13, EC 3.2.1.21
11	TRINITY_DN67935_c0_g1	0	0	0	16.39	97.3	73.99	-10.13	0.00080	Predicted Protein
12	TRINITY_DN702_c0_g1	0	0.03	0	59.4	116.45	27.95	-9.93	0.00006	Cytochrome P450 71AU50, EC 1.14.-.-
13	TRINITY_DN702_c0_g1	0	0.03	0	59.4	116.45	27.95	-9.93	0.00006	Cytochrome P450 750A1, EC 1.14.-.- (Cytochrome P450 CYPC)
14	TRINITY_DN2358_c0_g1	0	0	0	81.45	89.01	7.38	-9.91	0.00287	Predicted Protein
15	TRINITY_DN31159_c0_g1	0	0	0	32.73	41.22	41.42	-9.83	0.00001	Predicted Protein
16	TRINITY_DN157611_c0_g2	0	0	0	22.19	59.12	26.75	-9.60	0.00002	Predicted Protein
17	TRINITY_DN10725_c0_g1	0	0	0	29.76	70.11	14.01	-9.55	0.00010	Predicted Protein
18	TRINITY_DN30360_c0_g2	0	0	0	98.39	13.66	18.36	-9.53	0.00190	Predicted Protein
19	TRINITY_DN251401_c0_g1	0	0	0	93.47	11.8	22.49	-9.52	0.00209	Predicted Protein
20	TRINITY_DN27632_c0_g2	0	0	0	8.22	77.05	47.39	-9.45	0.00238	Predicted Protein
21	TRINITY_DN10160_c0_g1	0	0	0	14.16	73.48	23.65	-9.41	0.00024	Predicted Protein
22	TRINITY_DN1453_c1_g4	0	0	0	36.74	50.95	10.28	-9.37	0.00016	Predicted Protein

23	TRINITY_DN57079_c0_g1	6.63	0	0	223.25	327.76	184.27	-9.36	0.00049	Predicted Protein
24	TRINITY_DN3979_c0_g1	0.05	0.01	0	52.76	91.37	16.98	-9.28	0.00028	Predicted Protein
25	TRINITY_DN4524_c0_g3	0	0	5.98	113.8	426.21	83.05	-9.21	0.00327	Predicted Protein

Table 13a. Top 25 upregulated genes from copper susceptible samples compared to water controls in *Pinus banksiana*

Rank	Gene ID	Sus 1	Sus 2	Sus 3	Water 1	Water 2	Water 3	logFC	Adj. P. Value	UniProt Description
0	TRINITY_DN2786_c0_g1	670.58	354.91	364.1	0	0	0	13.15	8.45E-06	Predicted Protein
1	TRINITY_DN1628_c0_g1	1238.41	1180.01	590.75	0	0.32	0	12.80	2.48E-05	Trypsin inhibitor [Cleaved into: Trypsin inhibitor chain A; Trypsin inhibitor chain B]
2	TRINITY_DN258556_c0_g1	248.22	356.86	541.07	0	0	0	12.77	1.88E-05	Predicted Protein
3	TRINITY_DN1368_c0_g1	1712.84	2189.53	1629.49	0	1.3	0.07	12.73	2.67E-06	Predicted Protein
4	TRINITY_DN5716_c0_g1	2481.86	3248.79	5881.21	0	7.03	0.41	12.53	6.37E-04	Predicted Protein
5	TRINITY_DN2832_c0_g1	358.6	494.32	122.28	0	0	0	12.49	3.11E-05	Predicted Protein
6	TRINITY_DN5391_c1_g1	496.98	221.21	166.02	0	0	0	12.43	3.94E-05	Predicted Protein
7	TRINITY_DN57079_c0_g1	223.25	327.76	184.27	0	0	0	12.22	1.57E-07	Predicted Protein
8	TRINITY_DN5965_c1_g1	799.48	842.36	692.63	0.33	0	0	12.12	2.95E-06	Predicted Protein
9	TRINITY_DN50999_c1_g1	333.04	156.25	133.24	0	0	0	11.95	1.73E-05	Predicted Protein
10	TRINITY_DN55243_c0_g1	115.54	286.47	226.14	0	0	0	11.88	1.05E-05	Predicted Protein
11	TRINITY_DN1520_c0_g1	1020.58	623.65	1427.83	0.02	0.65	0	11.86	1.18E-03	Trypsin inhibitor [Cleaved into: Trypsin inhibitor chain A; Trypsin inhibitor chain B]
12	TRINITY_DN5795_c0_g1	851.63	854.34	325.97	0	0.84	0	11.83	2.09E-04	Predicted Protein
13	TRINITY_DN7061_c1_g1	194.74	291.48	98.46	0	0	0	11.82	2.94E-06	Predicted Protein
14	TRINITY_DN8563_c1_g1	131.04	322.9	115.04	0	0	0	11.71	4.77E-06	Predicted Protein
15	TRINITY_DN4524_c0_g3	113.8	426.21	83.05	0	0	0	11.63	9.67E-05	Predicted Protein
16	TRINITY_DN257933_c1_g1	201.53	169.25	77.24	0	0	0	11.48	4.34E-06	Predicted Protein
17	TRINITY_DN3536_c0_g1	122.8	169.34	90.42	0	0	0	11.28	3.13E-07	Predicted Protein
18	TRINITY_DN237688_c0_g1	211.18	103.61	72.51	0	0	0	11.25	1.84E-05	Predicted Protein
19	TRINITY_DN7685_c0_g1	509.79	347.25	228.34	0	0.41	0	11.24	6.78E-05	Predicted Protein
20	TRINITY_DN14732_c0_g1	372.88	97.02	31.35	0	0	0	11.18	1.92E-03	Predicted Protein
21	TRINITY_DN12750_c0_g1	166.37	64.69	116.96	0	0	0	11.11	3.61E-05	Predicted Protein
22	TRINITY_DN2463_c0_g1	818.33	234.67	289.22	0	0.04	0.11	11.02	2.24E-03	Predicted Protein
23	TRINITY_DN3069_c0_g1	313.54	458.61	155.11	0	0.37	0	10.98	6.68E-05	Predicted Protein
24	TRINITY_DN2221_c0_g1	664.03	226.26	181.23	0	0.68	0	10.90	1.96E-03	Predicted Protein

25	TRINITY_DN3092_c0_g1	661.05	923.49	459.73	0.14	0.35	0	10.88	6.47E-06	Glucan endo-1,3-beta-glucosidase, acidic isoform, EC 3.2.1.39 ((1->3)-beta-glucan endohydrolase, (1->3)-beta-glucanase) (Beta-1,3-endoglucanase)

Table 13b. Top 25 downregulated genes from copper susceptible samples compared to water controls in *Pinus banksiana*

Rank	Gene ID	Sus 1	Sus 2	Sus 3	Water 1	Water 2	Water 3	logFC	Adj. P. value	UniProt Description
0	TRINITY_DN293_c0_g1	0.02	0	4.27	83.3	131.42	164.86	-11.03	5.8E-05	Delta-selinene-like synthase, chloroplastic, PsTPS-Sell, EC 4.2.3.76
1	TRINITY_DN293_c0_g1	0.02	0	4.27	83.3	131.42	164.86	-11.03	5.8E-05	Alpha-humulene synthase, EC 4.2.3.104 (Terpene synthase TPS-Hum, PgTPS-Hum)
2	TRINITY_DN293_c0_g1	0.02	0	4.27	83.3	131.42	164.86	-11.03	5.8E-05	Delta-selinene synthase, EC 4.2.3.71, EC 4.2.3.76 (Agfdsel1)
3	TRINITY_DN5038_c0_g2	0.21	0.18	1.49	147.03	102.4	230.91	-10.45	2.0E-04	Predicted Protein
4	TRINITY_DN1269_c0_g1	0	0	0.13	32.25	13.5	37.33	-10.30	1.4E-04	Predicted Protein
5	TRINITY_DN4890_c0_g1	0	0	0	15.59	12.05	25.46	-10.25	7.2E-06	Predicted Protein
6	TRINITY_DN2314_c0_g1	0.03	0.05	0.05	40.88	14.56	52.04	-10.14	7.2E-04	Predicted Protein
7	TRINITY_DN8038_c0_g1	0.16	0.3	0.98	122.65	81.13	105.38	-10.02	7.8E-05	Probable aquaporin PIP2-8 (Plasma membrane intrinsic protein 2-8, AtPIP2;8) (Plasma membrane intrinsic protein 3b, PIP3b)
8	TRINITY_DN26931_c0_g1	1.66	0	0	65.61	45.82	36.39	-9.96	3.1E-04	Probable aquaporin PIP2-8 (Plasma membrane intrinsic protein 2-8, AtPIP2;8) (Plasma membrane intrinsic protein 3b, PIP3b)
9	TRINITY_DN10618_c0_g1	0	0	0	17.92	13.75	10	-9.96	9.8E-06	Predicted Protein
10	TRINITY_DN4059_c0_g1	0.07	0	0	20.09	12.1	19.58	-9.78	1.7E-05	Predicted Protein
11	TRINITY_DN159567_c0_g1	0	0	0	11.89	6.31	15.47	-9.60	2.5E-05	WAT1-related protein At5g07050
12	TRINITY_DN34182_c0_g1	0	0	0	11.56	9.9	10.5	-9.59	2.7E-06	Predicted Protein
13	TRINITY_DN129749_c0_g1	0	0	0	9.6	9.98	11.12	-9.52	1.5E-06	Predicted Protein
14	TRINITY_DN129793_c0_g1	0	0	0	8.28	13.37	9.36	-9.48	1.2E-06	Putative UPF0481 protein At3g02645
15	TRINITY_DN2617_c0_g1	0	0	0	12.84	6.76	7.48	-9.34	2.4E-05	Predicted Protein
16	TRINITY_DN11362_c0_g1	0	0.76	0.54	39.53	30.88	57.71	-9.33	1.4E-04	Predicted Protein
17	TRINITY_DN4176_c0_g1	0.47	0	0.44	61.56	18.42	66.16	-9.31	3.9E-03	Chalcone synthase, EC 2.3.1.74 (Naringenin-chalcone synthase)
18	TRINITY_DN2507_c0_g1	0	1.1	0	32.43	13.12	23.67	-9.23	6.4E-04	Predicted Protein
19	TRINITY_DN113586_c0_g1	0	0	0	7.25	5.74	13.28	-9.21	1.3E-05	Predicted Protein

20	TRINITY_DN1400_c0_g1	0.07	0.06	0.21	24.93	11.67	26.83	-9.20	2.6E-04	Subtilisin-like protease SBT5.6, EC 3.4.21.- (Subtilase subfamily 5 member 6, AtSBT5.6)
21	TRINITY_DN26605_c0_g1	0	0	0	6.61	7.11	10.35	-9.13	2.9E-06	Predicted Protein
22	TRINITY_DN7878_c0_g1	0.4	1.2	1.38	124.44	78.86	175.53	-9.11	5.2E-05	Predicted Protein
23	TRINITY_DN1514_c0_g1	0.27	0.75	1.81	82.92	99.69	154.44	-9.11	4.5E-06	Germin-like protein 8-14 (Germin-like protein 1) (Germin-like protein 5, OsGER5)
24	TRINITY_DN21458_c0_g1	0	0	0	8.31	6.63	7.86	-9.11	4.5E-06	Predicted Protein
25	TRINITY_DN69830_c0_g4	0.03	0.09	0.04	10.13	7.29	18.59	-9.10	4.0E-05	Predicted Protein

3.4 Discussion

3.4.1 Effects of excess Copper on *Pinus banksiana* seedlings

For the 1300 mg/kg dose, seedlings in the resistant group sustained no damage and had a similar appearance to the water controls and the potassium controls. Only three seedlings were given a resistant damage rating and many seedlings were considered susceptible or moderately susceptible. The post treatment physical attributes of the sampling group had a similar outcome as the heavy metal accumulator *Populus tremuloides* when subjected to nickel stress (Czajka & Nkongolo, 2022).

3.4.2 DGE analysis of copper genotypes

A transcriptome analysis of *Pinus banksiana* treated with excess copper was performed to evaluate differences in global gene expression between different genotypes. Analyzing the transcriptome of resistant and susceptible seedlings can provide valuable insight on the molecular mechanisms associated with copper resistance or susceptibility in *Pinus banksiana*. The high number of DEGs in RG compared to SG at high stringency indicated that copper resistant plants had a significantly different pattern of gene expression compared to copper susceptible plants (table 8). Notably, the large proportion of downregulated genes compared to upregulated genes suggests a decline in many cellular processes. The similar number of DEGs at low stringency suggests that the majority of genes were high stringency and elicited a high level of expression (table 8). In RG compared to water, the very low number of DEGs at a high stringency indicates a similar pattern of gene expression between resistant plants and untreated plants (table 9). It can be inferred that the gene expression of the resistant genotype mostly emulated untreated conditions and that copper resistance may be orchestrated by a small number of molecular mechanisms. Many studies have

demonstrated the significance of a single transporter or chelator gene on copper resistance and overall growth outcomes (Andrés-Colás et al., 2006; S. Lee et al., 2007; W.-J. Guo et al., 2008). Some genes were differentially expressed at a low stringency, implying that expressed genes with a high false discovery rate may also be associated with copper resistance (table 9). The large deviation in gene expression for SG compared to both RG and the water group suggests that there may be genetic and molecular factors contributing to copper susceptibility (table 10, table 8). The number of DEGs was also considerably higher in SG compared to water, implying that copper susceptibility was characterized by a large deviation from untreated conditions. This raises the possibility that DEGs in SG were associated with coping mechanisms responding to copper induced stress and tissue damage. This pattern of gene expression was also observed in *Populus tremuloides* when exposed to excess nickel (Czajka & Nkongolo, 2022).

3.4.3 Identification of candidate genes associated with copper resistance in *Pinus banksiana*

Analysis of the top upregulated genes revealed two promising candidate genes that may be involved in copper resistance mechanisms for *Pinus banksiana*. A candidate gene encoding a heavy metal-associated isoprenylated plant (HIPP) protein was identified (table 11). HIPP proteins are metallochaperones that chelate and deliver heavy metal ions to various proteins across cellular compartments (de Abreu-Neto et al., 2013). The conserved protein structure of HIPP family proteins is comprised of a cysteine rich heavy metal associated (HMA) domain facilitating the binding of heavy metals and an isoprenylaton site involved in cellular compartment localization and signal transduction (Tehseen et al., 2010; de Abreu-Neto et al., 2013; Barth et al., 2009). Structural variation within the isoprenylated site offers the functional diversity needed to facilitate cellular compartment localization and protein targeting (Barth et al., 2009; Gao et al., 2009). In yeast, the overexpression of HIPP conferred resistance to copper, cadmium and zinc (khan et al.,

2019). Additionally, overexpression of HIPP in *Arabidopsis thaliana* conferred cadmium resistance (Suzuki et al., 2002). Studies that demonstrated the binding of HIPP to copper, cadmium and zinc in plants corroborates the function of HIPP in the detoxification of heavy metals (Gao et al., 2009; Dykema et al., 1999). The capture of copper ions by cysteine rich chelators is an essential mechanism that prevents excess copper from inhibiting enzymes, causing protein misfolding and generating ROS (X. Zhang et al., 2015). Although the specific protein targeted by AtHIPP20 are currently unknown, possible targets of metallochaperone mediated ion delivery include transporters, enzymes or other chaperones (khan et al., 2019).

Another identified candidate gene encodes the Pleiotropic drug resistance (PDR) protein, which is an ATP-binding cassette (ABC) transporter (table 11) (Crouzet et al., 2013). ABC transporters are membrane localized transporters that facilitate the movement of a large diversity of entities via an ATP hydrolysis motif (Fernandez et al., 2012; Ogasawara et al., 2020). The conserved protein region of ABC transporters include two nucleotide binding folds associated with ATP hydrolysis and two hydrophobic membrane domains involved in the determination of substrate specificity (Moody et al., 2002; Fernandez et al., 2012). The broad substrate specificity of PDR proteins often includes heavy metals, resulting in its involvement in heavy metal homeostasis as it pertains to the cytosol and the region external to the membrane (D.-Y. Kim et al., 2007). In addition to heavy metal, PDR is also able to transport phytohormones, antifungal agents, and metabolites with antimicrobial properties (Kang et al., 2010; H. Zhang et al., 2020; Pierman et al., 2017). In *Arabidopsis thaliana*, overexpression of AtPDR8 conferred cadmium resistance and reduced total cadmium content by exporting cadmium from the cytosol to the apoplast (D.-Y. Kim et al., 2007). Similarly, upregulated AtPDR12 expression increased lead export from the cytosol which subsequently decreased lead content and contributed to lead resistance (M. Lee et al., 2005). A

possible role of PDR in copper detoxification may involve utilizing a similar efflux mechanism to export copper away from the cytosol and plasma membrane. The suppression of PDR in certain species treated with cadmium or lead resulted in severe growth defects, establishing PDR as a crucial component in heavy metal detoxification (He Li et al., 2022; M. Lee et al., 2005). Hormones such as Jasmonic acid and ABA induced the upregulation of Ospdr9, suggesting that PDR may also play a secondary role in mediating the general stress response (Moons, 2003; H. Zhang et al., 2020). Further research is needed to describe how PDR contributes to copper detoxification in *Pinus banksiana*.

3.4.4 GO Annotation of the top 25 upregulated genes between the resistant genotype and the susceptible genotype

Many of the top upregulated genes in RG compared to SG were involved in the stress response and may contribute to copper tolerance (table 12a). Among the top upregulated genes was a gene encoding terpene synthase (TPS) (table 12a). TPS synthesizes 1,8-cineole and other terpenoids that partake in a variety of defense functions such as thermoregulation, resin assisted wound sealing, and plant to plant signalling (Keeling et al., 2011; Kaitera et al., 2021; E. Sharma et al., 2017). In response to heavy metals, terpenoids may scavenge ROS, mainly exerting its protective effect on membranes (Loreto et al., 2001). Terpenoids can also enhance the stability and rigidity of the chloroplast membrane by increasing the hydrophobic bonding between lipids (Velikova et al., 2011; Siwko et al., 2007). Enhancing the stability of membranes is a protective mechanism for resisting ROS mediated damage and lipid peroxidation caused by copper toxicity (S. Wang et al., 2021; Farghaly et al., 2022).

A gene encoding a Fatty acyl-CoA reductase (FAR) was also identified among the top upregulated genes (table 12a). FAR catalyzes the synthesis of fatty alcohols from fatty acyl-coA and serves an integral part in the acyl-reduction pathway (Kunst & Samuels, 2003). In response to heavy metals, fatty alcohols are used as components for larger extracellular lipid compounds such as cuticular wax and suberin (Doan et al., 2012; X. Zhang et al., 2022). When secreted onto the surface of leaves, cuticular wax and suberin form a hydrophobic barrier that blocks and protects cells against copper induced water loss (Y. Wang et al., 2018; Mostofa & Fujita, 2013). The negative regulation of water transpiration is crucial to counteract water loss and drought which could induce further tissue damage (Mostofa & Fujita, 2013).

Genes encoding Early light-induced proteins (ELIP) were also identified (STable 12a). ELIPs are photoactive proteins that regulate chloroplast content, counteract the photoinhibition of photosystem II and safeguards photosynthesis machinery (X. Liu et al., 2020; L. Tao et al., 2011). Copper stress decreases chloroplast concentration, diminishes thylakoid membranes and replaces the iron cofactor in plastoquinone QA of photosystem II (Pätsikkä et al., 2002). Notably, the inhibition of plastoquinone QA results in a reduction of electron transfer and subsequent light absorption (Jegerschoeld et al., 1995; Pätsikkä et al., 2002). The collective effect of copper on chloroplast function may result in photodamage and ROS mediated damage (Caspi et al., 1999; Lindahl et al., 1997). Upregulation of ELIP may potentially serve a photoprotective role to preserve chloroplast function and light absorption, although the exact mechanism of action has yet to be described (L. Tao et al., 2011).

3.4.5 GO annotation of the top 25 downregulated genes between the resistant genotype and the susceptible genotype

Several top downregulated genes encode enzymes involved in carbohydrate metabolism (table 12b). An identified gene encodes polygalactuornase (pectinase), which facilitates the hydrolysis of the alpha-1,4 glycosidic bonds present in polygalacturnoan (pectin) (table 12b) (Atkinson et al., 2012). Pectin is an essential component of the cell wall and is responsible for cell to cell adhesion (Orfila et al., 2002). Pectinase downregulation could potentially contribute to copper tolerance by preserving pectin content, thereby maintaining the integrity of the cell wall. In multiple plants, downregulation of pectinase improved tolerance to multiple stressors by decreasing cell expansion, cell separation and increasing cell density (Atkinson et al., 2012; H. Liu et al., 2014; Ohara et al., 2021). Multiple identified genes encode for beta glucosidase which is an enzyme that facilitates the conversion of cellobiose to glucose (table 12b) (Chuenchor et al., 2008). Beta glucosidase is an integral component of cellulose breakdown and was found to be expressed in the cell wall of some plants (Nematollahi & Roux, 1999; Sasaki & Nagayama, 1997). As the most abundant component of the cell wall, cellulose provides the tensile and turgor pressure required to maintain structural integrity (McCann & Roberts, 1994; Y. Zhang et al., 2021). Downregulation of beta glucosidase upregulates cellulose production and also contributes to the maintenance of the cell wall in response to various stressors (Kalluri et al., 2016; M. Zheng et al., 2019). The cell wall plays a crucial role in copper detoxification by acting as a site of sequestration and heavy metal distribution (Ren et al., 2020; Y.-Y. Cao et al., 2019). The role of pectinase and beta glucosidase in maintaining the integrity of the cell wall is supported by the upregulation of the PDR transporter candidate gene, which has been previously shown to transport cadmium from the cytosol to the apoplast (table 11) (D.-Y. Kim et al., 2007).

A gene encoding a trypsin inhibitor was identified in the top downregulated genes (STable 12b). Trypsin inhibitors mitigate the activity of serine proteases and prevent the breakdown of associated proteins (Hou & Lin, 2002). Protein damage and misfolding caused by heavy metal binding and ROS interaction induces the production of serine proteases (Schützendübel & Polle, 2002; Jacques et al., 2015). Downregulation of trypsin inhibitors suggests that higher levels of serine protease activity were needed to breakdown damage or misfolded proteins thereby improving cell viability. Other studies reported variation in trypsin inhibitor activity in response to excess copper, suggesting that the activity is dependent on the extent protein damage present (Karmous et al., 2014; Guerra et al., 2015).

3.4.6 GO annotation of the top 25 upregulated genes between the susceptible genotype and the control

In addition to stress related mechanisms triggered by excess copper, the examination of highly upregulated genes between SG and water could reveal genes associated with plant cell death and necrosis. Among the top upregulated genes were genes encoding the trypsin inhibitor, which was previously found to be downregulated in RG compared to SG (table 13a, table 12b). In contrast to the RG genotype, there was an upregulation in trypsin inhibitors which may indicate a larger amount of serine protease activity present in SG (table 13a, table 12b). Increased ROS production and undesired copper binding causes protein misfolding and damage which can elicit serine protease activity (Schützendübel & Polle, 2002; Jacques et al., 2015). Overexpression of serine protease may damage plant tissue and cause a further reduction in protein content (W. B. Jiang et al., 1999). The upregulation of trypsin inhibitors could therefore be a protective strategy to conserve protein content and delay senescence (Radisky et al., 2006; Azeez et al., 2007). Upregulation of trypsin inhibitors in other plants has also been reported in response to other

stressors such as drought and fungal infection (Guretzki & Papenbrock, 2014; Tubajika & Damann, 2001).

In contrast to RG compared to SG, many of the top upregulated genes encoded beta glucosidase (table 13a, S13a, 12b). The upregulation of beta glucosidase increases the conversion of cellobiose and other sugars to glucose, implying a metabolic related function. An adverse side effect of upregulated beta glucosidase is decreased cellulose content which may compromise the strength and integrity of the cell wall (Y. Jiang et al., 2022). Some studies demonstrated that beta glucosidase may play a possible role in the stress response by regulating ABA levels (K. H. Lee et al., 2006; Liang et al., 2020; Z.-Y. Xu et al., 2012). Other studies reported a correlation between beta glucosidase overexpression and the production of antioxidant flavonols which may also contribute to stress alleviation (Baba et al., 2017).

3.4.7 GO annotation of the top 25 downregulated genes between the susceptible genotype and the control

Among the top downregulated genes in SG compared to the control were genes encoding the probable aquaporin proteins PIP2-8 (table 13b). Aquaporins are membrane bound channels that serve as an important point of entry for water, nutrients, and heavy metals (Lopez-Zaplana et al., 2022). The broad specificity of Aquaporins provides a potential point of regulation to control the transport of heavy metals. Downregulation of aquaporins could also be a response to increased transpiration and water loss caused by heavy metals (Kholodova et al., 2011).

A gene encoding the WALLS ARE THIN1 (WAT1) protein was also identified among the top downregulated genes (table 13b). WAT1 is an auxin transporter that is localized to the vacuole, facilitating the movement of auxin to the cytoplasm (Ranocha et al., 2013). Excess copper can

deregulate auxin homeostasis and distribution which can negatively impact various aspects of plant development (Y. Song et al., 2017; Yuan et al., 2013). In particular, the deregulation of auxin can affect cell division, cell elongation, leaf morphogenesis and hormone crosstalk, (Ku et al., 2009; DEMASON & CHAWLA, 2006; Y. Song et al., 2017). In response to copper stress, the downregulation of WAT1 could be strategy to safeguard growth by altering the transport and intracellular distribution of auxin. However, the response of WAT1 to copper specifically is not fully understood. Downregulation of WAT1 may also regulate salicylic acid synthesis which coordinates the stress response (Denancé et al., 2013; D. Wang et al., 2007).

3.5 Conclusion

A comprehensive transcriptome analysis was conducted on copper treated *Pinus banksiana* to understand the genetic response of different genotypes to copper. Across all plants, there was a total of 21-49 million expressed sequences. 435293 genes were identified from 581037 total transcripts. There were 19789 DEGs between RG and SG at a high stringency, indicating significant differences in gene expression between resistant and susceptible plants. The low number of DEGs between RG and the water control indicated a similar pattern of gene expression. SG had a large number of DEGs compared to both RG and the control, suggesting that SG had a different set of coping mechanisms from the aforementioned groups.

Gene Ontology of the top upregulated genes in RG compared to SG showed that the response to stress had the highest proportion of expressed genes. For top downregulated genes, the carbohydrate metabolic process term had the highest percentage expressed genes. The candidate genes AtHIPP20 and AtHIPP26 encodes a metallochaperone. The candidate gene NtPDR1 encodes an ATP binding cassette transporter. Other identified top upregulated genes were associated with the coordination of the stress response and included TPS, AtFAR2 and ELIP1.

Top downregulated genes included polygalacturonase and beta glucosidase, suggesting a possible role in the strengthening of the cell wall and the sequestration of copper ions. This study demonstrated the strong utility of transcriptome analysis for elucidating the genetic response of plants and associated genotypes to copper stress. The identified candidate genes should be further researched to evaluate potential applications in various industries.

Chapter 4: General conclusions

The objectives of this research were to 1) Comprehensively map and characterize the transcriptome of Jack Pine (*Pinus banksiana*), 2) Assess the gene expression of distinct genotypes exposed to nickel ion toxicity, and 3) Assess the gene expression of distinct genotypes exposed to copper ion toxicity.

Transcriptome analysis is an indispensable asset to researchers, providing a means to assess genetic responses to different biotic and abiotic stressors, analyze different phenotypes and discover the molecular mechanisms associated with a particular outcome. Additionally, Gene Ontology can be used to establish a molecular basis and rational for genetic changes that occur within a given genotype.

Pinus banksiana seedlings were treated with 1600 mg/kg of nickel sulphate. RNA sequencing was performed followed by de novo transcript assembly. Gene ontology was used to map and characterize the transcriptome of untreated plants. To assess highly regulated mechanisms and filter out terms with background expression, gene ontology was used to characterize the top differentially expressed genes between the genotypes. Both the tolerant and susceptible genotype had a significantly different pattern of gene expression from the control. The stress response term had the highest proportion of upregulated gene expression. The terms with the

highest proportion of downregulated gene expression were the biosynthetic process and carbohydrate metabolic process. The majority of upregulated gene expression was localized to the extracellular region and nucleus whereas the majority of downregulated gene expression occurred in the plasma membrane and extracellular region. Annotation of the top upregulated and downregulated genes identified highly regulated genes in the tolerant genotype which included genes that encoded Trypsin inhibitors, Jasmonate ZIM domain-containing proteins, a RING-H2 finger protein, and enzymes involved in the flavonol synthesis pathway. Many of the identified genes were involved in the coordination of the stress response. There were no differentially expressed genes observed between tolerant and susceptible genotypes, indicating the absence of mechanisms associated with nickel resistance.

The second study followed a similar protocol as the first study except the seedlings were treated with 1300 mg/kg of copper sulphate. Gene Ontology was used to provide information on the mechanisms involved in the top differentially expressed genes between the genotypes. The copper resistant genotype had a significantly different pattern of gene expression compared to the copper susceptible genotype. The response to stress term had the highest proportion of upregulated gene expression whereas for downregulated gene expression the carbohydrate metabolic process term had the highest percentage of expressed genes. Upregulated gene expression was mostly localized to the membrane while the extracellular region accounted for the majority of downregulated gene expression. Annotation of the top differentially regulated genes revealed possible mechanisms associated with copper resistance and copper tolerance. Genes that could potentially confer copper resistance include ATHIP genes which encoded a metallochaperone and NtPDR1 encoding an ATP binding cassette transporter. Genes that may be involved in copper tolerance mechanisms included genes that encode terpene synthase, fatty

acyl-CoA reductase and early light induced proteins. The downregulation of genes encoding pectinase and beta glucosidase suggests strengthening of the cell wall to facilitate copper sequestration.

Future studies

Future research can be conducted to complement and further describe the mechanisms associated with heavy metal resistance. A study on global DNA methylation could be conducted to investigate the role of epigenetics in nickel resistance and copper resistance. A transcriptome analysis of copper resistant plants compared to nickel tolerant plants should be performed to analyze differences in gene expression and mechanisms that occur in response to both metals. Assessment of the identified candidate genes and corresponding physiological parameters can also be conducted to develop relevant plant technologies. These studies may include the administration of the nickel at different doses and the assessment of metal accumulation or sequestration. Finally, a study using third generation sequencing can be done to assess the transcriptome using longer reads.

References

Adhikari, T., & Kumar, A. (2012). Phytoaccumulation and Tolerance of *Riccinus Communis* L. to Nickel. *International Journal of Phytoremediation*, *14*(5), 481–492. https://doi.org/10.1080/15226514.2011.604688

Ahammed, G. J., Li, C.-X., Li, X., Liu, A., Chen, S., & Zhou, J. (2021). Overexpression of tomato RING E3 ubiquitin ligase gene SlRING1 confers cadmium tolerance by attenuating cadmium accumulation and oxidative stress. *Physiologia Plantarum*, *173*(1), 449–459. https://doi.org/10.1111/ppl.13294

Alexander, M. E., & Cruz, M. G. (2012). Modelling the effects of surface and crown fire behaviour on serotinous cone opening in jack pine and lodgepole pine forests. *International Journal of Wildland Fire*, *21*(6), 709. https://doi.org/10.1071/wf11153

Alloway, B. J., & Tills, A. R. (1984). Copper deficiency in world crops. *Outlook on Agriculture*, *13*(1), 32–42. https://doi.org/10.1177/003072708401300105

Altaf, M. A., Hao, Y., He, C., Mumtaz, M. A., Shu, H., Fu, H., & Wang, Z. (2022). Physiological and Biochemical Responses of Pepper (Capsicum annuum L.) Seedlings to Nickel Toxicity. *Frontiers in Plant Science*, *13*. https://www.frontiersin.org/articles/10.3389/fpls.2022.950392

Amari, T., Lutts, S., Taamali, M., Lucchini, G., Sacchi, G. A., Abdelly, C., & Ghnaya, T. (2016). Implication of citrate, malate and histidine in the accumulation and transport of nickel in Mesembryanthemum crystallinum and Brassica juncea. *Ecotoxicology and Environmental Safety*, *126*, 122–128. https://doi.org/10.1016/j.ecoenv.2015.12.029

Andreazza, R., Okeke, B. C., Pieniz, S., Bento, F. M., & Camargo, F. A. O. (2013). Biosorption and Bioreduction of Copper from Different Copper Compounds in Aqueous Solution. *Biological Trace Element Research*, *152*(3), 411–416. https://doi.org/10.1007/s12011-013-9625-8

Andrés-Colás, N., Sancenón, V., Rodríguez-Navarro, S., Mayo, S., Thiele, D. J., Ecker, J. R., Puig, S., & Peñarrubia, L. (2006). The Arabidopsis heavy metal P-type ATPase HMA5 interacts with metallochaperones and functions in copper detoxification of roots. *The Plant Journal*, *45*(2), 225–236. https://doi.org/10.1111/j.1365-313x.2005.02601.x

Antala, S., & Dempski, R. E. (2012). The Human ZIP4 Transporter Has Two Distinct Binding Affinities and Mediates Transport of Multiple Transition Metals. *Biochemistry*, *51*(5), 963–973. https://doi.org/10.1021/bi201553p

Arefifard, M., Mahdieh, M., & Amirjani, M. (2014). Study of the effect of nickel heavy metals on some physiological parameters of Catharanthus roseus. *Natural Product Research*, *28*(18), 1499–1502. https://doi.org/10.1080/14786419.2014.913240

Ashburner, M., Ball, C. A., Blake, J. A., Botstein, D., Butler, H., Cherry, J. M., Davis, A. P., Dolinski, K., Dwight, S. S., Eppig, J. T., Harris, M. A., Hill, D. P., Issel-Tarver, L.,

Kasarskis, A., Lewis, S., Matese, J. C., Richardson, J. E., Ringwald, M., Rubin, G. M., & Sherlock, G. (2000). Gene Ontology: Tool for the unification of biology. *Nature Genetics*, *25*(1), Article 1. https://doi.org/10.1038/75556

Ashworth, D., & Alloway, B. (2008). Influence of Dissolved Organic Matter on the Solubility of Heavy Metals in Sewage-Sludge-Amended Soils. *Communications in Soil Science and Plant Analysis*, *39*. https://doi.org/10.1080/00103620701826787

Atafar, Z., Mesdaghinia, A., Nouri, J., Homaee, M., Yunesian, M., Ahmadimoghaddam, M., & Mahvi, A. H. (2008). Effect of fertilizer application on soil heavy metal concentration. *Environmental Monitoring and Assessment*, *160*(1), 83. https://doi.org/10.1007/s10661-008-0659-x

Atkinson, R. G., Sutherland, P. W., Johnston, S. L., Gunaseelan, K., Hallett, I. C., Mitra, D., Brummell, D. A., Schröder, R., Johnston, J. W., & Schaffer, R. J. (2012). Down-regulation of POLYGALACTURONASE1 alters firmness, tensile strength and water loss in apple (Malus x domestica) fruit. *BMC Plant Biology*, *12*(1), 129. https://doi.org/10.1186/1471-2229-12-129

Auguy, F., Fahr, M., Moulin, P., Brugel, A., Laplaze, L., Mzibri, M. E., Filali-Maltouf, A., Doumas, P., & Smouni, A. (2013). Lead Tolerance and Accumulation in Hirschfeldia incana, a Mediterranean Brassicaceae from Metalliferous Mine Spoils. *PLoS ONE*, *8*(5), e61932. https://doi.org/10.1371/journal.pone.0061932

Azeem, U. (2018). Ameliorating Nickel Stress by Jasmonic Acid Treatment in Zea mays L. *Russian Agricultural Sciences*, *44*(3), 209–215. https://doi.org/10.3103/S1068367418030035

Azeez, A., Sane, A. P., Bhatnagar, D., & Nath, P. (2007). Enhanced expression of serine proteases during floral senescence in Gladiolus. *Phytochemistry*, *68*(10), 1352–1357. https://doi.org/10.1016/j.phytochem.2007.02.027

Baba, S. A., Vishwakarma, R. A., & Ashraf, N. (2017). Functional Characterization of CsBGlu12, a β-Glucosidase from Crocus sativus, Provides Insights into Its Role in Abiotic Stress through Accumulation of Antioxidant Flavonols. *The Journal of Biological Chemistry*, *292*(11), 4700–4713. https://doi.org/10.1074/jbc.M116.762161

Babin-Fenske, J., & Anand, M. (2011). Patterns of insect communities along a stress gradient following decommissioning of a Cu–Ni smelter. *Environmental Pollution*, *159*(10), 3036–3043. https://doi.org/10.1016/j.envpol.2011.04.011

Baccouch, S., Chaoui, A., & El Ferjani, E. (2001). Nickel toxicity induces oxidative damage In *Zea mays* roots. *Journal of Plant Nutrition*, *24*(7), 1085–1097. https://doi.org/10.1081/PLN-100103805

Bačkor, M., Pawlik-Skowrońska, B., Bud'ová, J., & Skowroński, T. (2007). Response to copper and cadmium stress in wild-type and copper tolerant strains of the lichen alga Trebouxia

erici: Metal accumulation, toxicity and non-protein thiols. *Plant Growth Regulation*, *52*(1), 17–27. https://doi.org/10.1007/s10725-007-9173-3

Baginsky, C., Brito, B., Imperial, J., Ruiz-Argüeso, T., & Palacios, J. M. (2005). Symbiotic Hydrogenase Activity in Bradyrhizobium sp. (Vigna) Increases Nitrogen Content in Vigna unguiculata Plants. *Applied and Environmental Microbiology*, *71*(11), 7536–7538. https://doi.org/10.1128/aem.71.11.7536-7538.2005

Bai, C., Reilly, C. C., & Wood, B. W. (2006). Nickel Deficiency Disrupts Metabolism of Ureides, Amino Acids, and Organic Acids of Young Pecan Foliage. *Plant Physiology*, *140*(2), 433–443. https://doi.org/10.1104/pp.105.072983

Bai, J., Wang, X., Yao, X., Chen, X., Lu, K., Hu, Y., Wang, Z., Mu, Y., Zhang, L., & Dong, H. (2021). Rice aquaporin OsPIP2;2 is a water-transporting facilitator in relevance to drought-tolerant responses. *Plant Direct*, *5*(8), e338. https://doi.org/10.1002/pld3.338

Baker, A. J. M. (1981). Accumulators and excluders -strategies in the response of plants to heavy metals. *Journal of Plant Nutrition*, *3*(1–4), 643–654. https://doi.org/10.1080/01904168109362867

Baklanov, I. A. (2011). Heterogeneity of epidermal cells in relation to nickel accumulation in hyperaccumulator plants belonging to the genus Alyssum L. *Cell and Tissue Biology*, *5*(6), 603–611. https://doi.org/10.1134/s1990519x11060034

Baldanzi, G., Bettio, V., Malacarne, V., & Graziani, A. (2016). Diacylglycerol Kinases: Shaping Diacylglycerol and Phosphatidic Acid Gradients to Control Cell Polarity. *Frontiers in Cell and Developmental Biology*, *4*. https://www.frontiersin.org/articles/10.3389/fcell.2016.00140

Ballabio, C., Panagos, P., Lugato, E., Huang, J.-H., Orgiazzi, A., Jones, A., Fernández-Ugalde, O., Borrelli, P., & Montanarella, L. (2018). Copper distribution in European topsoils: An assessment based on LUCAS soil survey. *Science of The Total Environment*, *636*, 282–298. https://doi.org/10.1016/j.scitotenv.2018.04.268

Baloun, J., Nevrtalova, E., Kovacova, V., Hudzieczek, V., Cegan, R., Vyskot, B., & Hobza, R. (2014). Characterization of the HMA7 gene and transcriptomic analysis of candidate genes for copper tolerance in two Silene vulgaris ecotypes. *Journal of Plant Physiology*, *171*(13), 1188–1196. https://doi.org/10.1016/j.jplph.2014.04.014

Baozhu, L., Ruonan, F., Yanting, F., Runan, L., Hui, Z., Tingting, C., Jiong, L., Han, L., Xiang, Z., & Chun-peng, S. (2022). The flavonoid biosynthesis regulator PFG3 confers drought stress tolerance in plants by promoting flavonoid accumulation. *Environmental and Experimental Botany*, *196*, 104792. https://doi.org/10.1016/j.envexpbot.2022.104792

Baran, U., & Ekmekçi, Y. (2021). Correction to: Physiological, photochemical, and antioxidant responses of wild and cultivated Carthamus species exposed to nickel toxicity and evaluation of their usage potential in phytoremediation. *Environmental Science and Pollution Research*, *28*(43), 61869–61870. https://doi.org/10.1007/s11356-021-16513-7

Barcelos, J. P. Q., Reis, H. P. G., Godoy, C. V., Gratão, P. L., Furlani Junior, E., Putti, F. F., Campos, M., & Reis, A. R. (2018). Impact of foliar nickel application on urease activity, antioxidant metabolism and control of powdery mildew (Microsphaera diffusa) in soybean plants. *Plant Pathology*, *67*(7), 1502–1513. https://doi.org/10.1111/ppa.12871

Barozzi, F., Papadia, P., Stefano, G., Renna, L., Brandizzi, F., Migoni, D., Fanizzi, F. P., Piro, G., & Di Sansebastiano, G.-P. (2019). Variation in Membrane Trafficking Linked to SNARE AtSYP51 Interaction With Aquaporin NIP1;1. *Frontiers in Plant Science*, *9*. https://www.frontiersin.org/articles/10.3389/fpls.2018.01949

Barth, O., Vogt, S., Uhlemann, R., Zschiesche, W., & Humbeck, K. (2009). Stress induced and nuclear localized HIPP26 from Arabidopsis thaliana interacts via its heavy metal associated domain with the drought stress related zinc finger transcription factor ATHB29. *Plant Molecular Biology*, *69*(1), 213–226. https://doi.org/10.1007/s11103-008-9419-0

Barton, A. M., & Grenier, D. J. (2008). Dynamics of jack pine at the southern range boundary in downeast Maine. *Canadian Journal of Forest Research*, *38*(4), 733–743. https://doi.org/10.1139/x07-176

Bastow, E. L., Garcia de la Torre, V. S., Maclean, A. E., Green, R. T., Merlot, S., Thomine, S., & Balk, J. (2018). Vacuolar Iron Stores Gated by NRAMP3 and NRAMP4 Are the Primary Source of Iron in Germinating Seeds. *Plant Physiology*, *177*(3), 1267–1276. https://doi.org/10.1104/pp.18.00478

Batool, S. (2018). Effect of nickel toxicity on growth, photosynthetic pigments and dry matter yield of Cicer arietinum L. varieties. *Asian J Agri & Biol*, *6*(2), 143–148.

Becher, M., Talke, I. N., Krall, L., & Krämer, U. (2004). Cross-species microarray transcript profiling reveals high constitutive expression of metal homeostasis genes in shoots of the zinc hyperaccumulator Arabidopsis halleri. *The Plant Journal*, *37*(2), 251–268. https://doi.org/10.1046/j.1365-313X.2003.01959.x

Beckett, P., & Spiers, G. (n.d.). *Sudbury, Canada -40 years of a Community Regreening on a Smelter-Impacted Landscape Before After*. https://www.atlanticclra.ca/wp-content/uploads/2018/11/Beckett-Presentation.pdf

Békésiová, B., Hraška, Š., Libantová, J., Moravčíková, J., & Matušíková, I. (2008). Heavy-metal stress induced accumulation of chitinase isoforms in plants. *Molecular Biology Reports*, *35*(4), 579–588. https://doi.org/10.1007/s11033-007-9127-x

Bernal, M., Casero, D., Singh, V., Wilson, G. T., Grande, A., Yang, H., Dodani, S. C., Pellegrini, M., Huijser, P., Connolly, E. L., Merchant, S. S., & Krämer, U. (2012). Transcriptome Sequencing Identifies SPL7-Regulated Copper Acquisition Genes FRO4/FRO5 and the Copper Dependence of Iron Homeostasis in Arabidopsis. *The Plant Cell*, *24*(2), 738–761. https://doi.org/10.1105/tpc.111.090431

Besseau, S., Hoffmann, L., Geoffroy, P., Lapierre, C., Pollet, B., & Legrand, M. (2007). Flavonoid Accumulation in Arabidopsis Repressed in Lignin Synthesis Affects Auxin Transport and Plant Growth. *The Plant Cell*, *19*(1), 148–162. https://doi.org/10.1105/tpc.106.044495

Bhagi-Damodaran, A., Michael, M. A., Zhu, Q., Reed, J., Sandoval, B. A., Mirts, E. N., Chakraborty, S., Moënne-Loccoz, P., Zhang, Y., & Lu, Y. (2016). Why copper is preferred over iron for oxygen activation and reduction in haem-copper oxidases. *Nature Chemistry*, *9*(3), 257–263. https://doi.org/10.1038/nchem.2643

Bhuiyan, M. S. U., Min, S. R., Jeong, W. J., Sultana, S., Choi, K. S., Lee, Y., & Liu, J. R. (2011). Overexpression of AtATM3 in Brassica juncea confers enhanced heavy metal tolerance and accumulation. *Plant Cell, Tissue and Organ Culture (PCTOC)*, *107*(1), 69–77. https://doi.org/10.1007/s11240-011-9958-y

Binder, B. M., O'Malley, R. C., Wang, W., Moore, J. M., Parks, B. M., Spalding, E. P., & Bleecker, A. B. (2004). Arabidopsis Seedling Growth Response and Recovery to Ethylene. A Kinetic Analysis. *Plant Physiology*, *136*(2), 2913–2920. https://doi.org/10.1104/pp.104.050369

Boava, L. P., Cristofani-Yaly, M., Stuart, R. M., & Machado, M. A. (2011). Expression of defense-related genes in response to mechanical wounding and Phytophthora parasitica infection in Poncirus trifoliata and Citrus sunki. *Physiological and Molecular Plant Pathology*, *76*(2), 119–125. https://doi.org/10.1016/j.pmpp.2011.07.004

Boisvert, S., Joly, D., Leclerc, S., Govindachary, S., Harnois, J., & Carpentier, R. (2007). Inhibition of the oxygen-evolving complex of photosystem II and depletion of extrinsic polypeptides by nickel. *BioMetals*, *20*(6), 879–889. https://doi.org/10.1007/s10534-007-9081-z

Boutigny, S., Sautron, E., Finazzi, G., Rivasseau, C., Frelet-Barrand, A., Pilon, M., Rolland, N., & Seigneurin-Berny, D. (2014). HMA1 and PAA1, two chloroplast-envelope PIB-ATPases, play distinct roles in chloroplast copper homeostasis. *Journal of Experimental Botany*, *65*(6), 1529–1540. https://doi.org/10.1093/jxb/eru020

Boyd, M., & Nkongolo, K. (2020). Expression of Genes Associated with Nickel Resistance in White Spruce (*Picea glauca*) under Nickel Stress: Analysis of AT2G16800 and *NRAMP* Genes. *American Journal of Plant Sciences*, *11*(08), 1163–1174. https://doi.org/10.4236/ajps.2020.118082

Braidot, E., Vianello, A., Petrussa, E., & Macrí, F. (1993). Dissipation of the electrochemical proton gradient in phospholipase-induced degradation of plant mitochondria and microsomes. *Plant Science*, *90*(1), 31–39. https://doi.org/10.1016/0168-9452(93)90153-Q

Brown, P. H., Welch, R. M., & Cary, E. E. (1987). Nickel: A Micronutrient Essential for Higher Plants. *Plant Physiology*, *85*(3), 801–803. https://doi.org/10.1104/pp.85.3.801

Brown, S. L., Chaney, R. L., Angle, J. S., & Baker, A. J. M. (1995). Zinc and Cadmium Uptake by Hyperaccumulator Thlaspi caerulescens Grown in Nutrient Solution. *Soil Science Society of America Journal*, *59*(1), 125–133. https://doi.org/10.2136/sssaj1995.03615995005900010020x

Burbulis, I. E., Iacobucci, M., & Shirley, B. W. (1996). A null mutation in the first enzyme of flavonoid biosynthesis does not affect male fertility in Arabidopsis. *The Plant Cell*, *8*(6), 1013–1025. https://doi.org/10.1105/tpc.8.6.1013

Cao, J., Li, X., Lv, Y., & Ding, L. (2015). Comparative analysis of the phytocyanin gene family in 10 plant species: A focus on Zea mays. *Frontiers in Plant Science*, *6*. https://doi.org/10.3389/fpls.2015.00515

Cao, Y.-Y., Qi, C.-D., Li, S., Wang, Z., Wang, X., Wang, J., Ren, S., Li, X., Zhang, N., & Guo, Y.-D. (2019). Melatonin Alleviates Copper Toxicity via Improving Copper Sequestration and ROS Scavenging in Cucumber. *Plant and Cell Physiology*, *60*(3), 562–574. https://doi.org/10.1093/pcp/pcy226

Caspi, V., Droppa, M., Horváth, G., Malkin, S., Marder, J. B., & Raskin, V. I. (1999). The effect of copper on chlorophyll organization during greening of barley leaves. *Photosynthesis Research*, *62*(2), 165–174. https://doi.org/10.1023/A:1006397714430

Cataldo, D. A., Garland, T. R., & Wildung, R. E. (1978). Nickel in Plants: I. Uptake Kinetics Using Intact Soybean Seedlings. *Plant Physiology*, *62*(4), 563–565. https://doi.org/10.1104/pp.62.4.563

Çelik, Ö., & Akdaş, E. Y. (2019). Tissue-specific transcriptional regulation of seven heavy metal stress-responsive miRNAs and their putative targets in nickel indicator castor bean (R. communis L.) plants. *Ecotoxicology and Environmental Safety*, *170*, 682–690. https://doi.org/10.1016/j.ecoenv.2018.12.006

Chamseddine, M., Wided, B. A., Guy, H., Marie-Edith, C., & Fatma, J. (2008). Cadmium and copper induction of oxidative stress and antioxidative response in tomato (Solanum lycopersicon) leaves. *Plant Growth Regulation*, *57*(1), 89–99. https://doi.org/10.1007/s10725-008-9324-1

Chatzopoulou, F., Sanmartin, M., Mellidou, I., Pateraki, I., Koukounaras, A., Tanou, G., Kalamaki, M. S., Veljović-Jovanović, S., Antić, T. C., Kostas, S., Tsouvaltzis, P., Grumet, R., & Kanellis, A. K. (2020). Silencing of ascorbate oxidase results in reduced growth, altered ascorbic acid levels and ripening pattern in melon fruit. *Plant Physiology and Biochemistry*, *156*, 291–303. https://doi.org/10.1016/j.plaphy.2020.08.040

Chen, C., Rodriguez, I. B., Chen, Y. L., Zehr, J. P., Chen, Y., Hsu, S. D., Yang, S., & Ho, T. (2022). Nickel superoxide dismutase protects nitrogen fixation in Trichodesmium. *Limnology and Oceanography Letters*, *7*(4), 363–371. https://doi.org/10.1002/lol2.10263

Chen, D., Shao, M., Sun, S., Liu, T., Zhang, H., Qin, N., Zeng, R., & Song, Y. (2019). Enhancement of Jasmonate-Mediated Antiherbivore Defense Responses in Tomato by

Acetic Acid, a Potent Inducer for Plant Protection. *Frontiers in Plant Science*, *10*. https://doi.org/10.3389/fpls.2019.00764

Chen, D., Zhang, H., Wang, Q., Shao, M., Li, X., Chen, D., Zeng, R., & Song, Y. (2020). Intraspecific variations in cadmium tolerance and phytoaccumulation in giant duckweed (Spirodela polyrhiza). *Journal of Hazardous Materials*, *395*, 122672. https://doi.org/10.1016/j.jhazmat.2020.122672

Chen, J., Piao, Y., Liu, Y., Li, X., & Piao, Z. (2018). Genome-wide identification and expression analysis of chitinase gene family in Brassica rapa reveals its role in clubroot resistance. *Plant Science*, *270*, 257–267. https://doi.org/10.1016/j.plantsci.2018.02.017

Chen, S., Yao, Q., Chen, X., Liu, J., Chen, D., Ou, T., Liu, J., Dong, Z., Zheng, Z., & Fang, K. (2021). Tree-ring recorded variations of 10 heavy metal elements over the past 168 years in southeastern China. *Elementa: Science of the Anthropocene*, *9*(1). https://doi.org/10.1525/elementa.2020.20.00075

Chiang, H.-C., Lo, J.-C., & Yeh, K.-C. (2006). Genes associated with heavy metal tolerance and accumulation in Zn/Cd hyperaccumulator Arabidopsis halleri: A genomic survey with cDNA microarray. *Environmental Science & Technology*, *40*(21), 6792–6798. https://doi.org/10.1021/es061432y

Chobot, V., Huber, C., Trettenhahn, G., & Hadacek, F. (2009). (±)-Catechin: Chemical Weapon, Antioxidant, or Stress Regulator? *Journal of Chemical Ecology*, *35*(8), 980–996. https://doi.org/10.1007/s10886-009-9681-x

Choudhary, S. P., Bhardwaj, R., Gupta, B. D., Dutt, P., Gupta, R. K., Kanwar, M., & Dutt, P. (2010). Changes induced by Cu2+ and Cr6+ metal stress in polyamines, auxins, abscisic acid titers and antioxidative enzymes activities of radish seedlings. *Brazilian Journal of Plant Physiology*, *22*, 263–270. https://doi.org/10.1590/S1677-04202010000400006

Chu, C.-C., Lee, W.-C., Guo, W.-Y., Pan, S.-M., Chen, L.-J., Li, H., & Jinn, T.-L. (2005). A Copper Chaperone for Superoxide Dismutase That Confers Three Types of Copper/Zinc Superoxide Dismutase Activity in Arabidopsis. *Plant Physiology*, *139*(1), 425–436. https://doi.org/10.1104/pp.105.065284

Chuenchor, W., Pengthaisong, S., Robinson, R. C., Yuvaniyama, J., Oonanant, W., Bevan, D. R., Esen, A., Chen, C.-J., Opassiri, R., Svasti, J., & Cairns, J. R. K. (2008). Structural Insights into Rice BGlu1 β-Glucosidase Oligosaccharide Hydrolysis and Transglycosylation. *Journal of Molecular Biology*, *377*(4), 1200–1215. https://doi.org/10.1016/j.jmb.2008.01.076

Chung, H. S., & Howe, G. A. (2009). A Critical Role for the TIFY Motif in Repression of Jasmonate Signaling by a Stabilized Splice Variant of the JASMONATE ZIM-Domain Protein JAZ10 in Arabidopsis. *The Plant Cell*, *21*(1), 131–145. https://doi.org/10.1105/tpc.108.064097

Cohu, C. M., Abdel-Ghany, S. E., Gogolin Reynolds, K. A., Onofrio, A. M., Bodecker, J. R., Kimbrel, J. A., Niyogi, K. K., & Pilon, M. (2009). Copper Delivery by the Copper Chaperone for Chloroplast and Cytosolic Copper/Zinc-Superoxide Dismutases: Regulation and Unexpected Phenotypes in an Arabidopsis Mutant. *Molecular Plant*, *2*(6), 1336–1350. https://doi.org/10.1093/mp/ssp084

Constabel, C. P., Bergey, D. R., & Ryan, C. A. (1995). Systemin activates synthesis of wound-inducible tomato leaf polyphenol oxidase via the octadecanoid defense signaling pathway. *Proceedings of the National Academy of Sciences*, *92*(2), 407–411. https://doi.org/10.1073/pnas.92.2.407

Corso, M., Schvartzman, M. S., Guzzo, F., Souard, F., Malkowski, E., Hanikenne, M., & Verbruggen, N. (2018). Contrasting cadmium resistance strategies in two metallicolous populations of Arabidopsis halleri. *New Phytologist*, *218*(1), 283–297. https://doi.org/10.1111/nph.14948

Coursolle, C., Bigras, F. J., & Margolis, H. A. (2002). Effects of Root Freezing on the Physiology and Growth of Picea glauca, Picea mariana and Pinus banksiana Seedlings Under Different Soil Moisture Regimes. *Scandinavian Journal of Forest Research*, *17*(3), 206–217. https://doi.org/10.1080/028275802753742873

Cox, D. D., Slaton, N. A., Ross, W. J., & Roberts, T. L. (2018). Trifoliolate Leaflet Chloride Concentrations for Characterizing Soybean Yield Loss from Chloride Toxicity. *Agronomy Journal*, *110*(4), 1589–1599. https://doi.org/10.2134/agronj2017.12.0725

Croser, C., Renault, S., Franklin, J., & Zwiazek, J. (2001). The effect of salinity on the emergence and seedling growth of Picea mariana, Picea glauca, and Pinus banksiana. *Environmental Pollution*, *115*(1), 9–16. https://doi.org/10.1016/s0269-7491(01)00097-5

Crouzet, J., Roland, J., Peeters, E., Trombik, T., Ducos, E., Nader, J., & Boutry, M. (2013). NtPDR1, a plasma membrane ABC transporter from Nicotiana tabacum, is involved in diterpene transport. *Plant Molecular Biology*, *82*(1), 181–192. https://doi.org/10.1007/s11103-013-0053-0

Ćurguz, V. G., Raičević, V., Veselinović, M., Tabakovic-Tošić, M., & Vilotić, D. (2012). *Influence of Heavy Metals on Seed Germination and Growth of Picea abies L. Karst*. 8.

Czajka, K. M., & Nkongolo, K. (2022). Transcriptome analysis of trembling aspen (Populus tremuloides) under nickel stress. *PLoS ONE*, *17*(10), e0274740. https://doi.org/10.1371/journal.pone.0274740

da Silva, C. P., de Almeida, T. E., Zittel, R., de Oliveira Stremel, T. R., Domingues, C. E., Kordiak, J., & de Campos, S. X. (2016). Translocation of metal ions from soil to tobacco roots and their concentration in the plant parts. *Environmental Monitoring and Assessment*, *188*(12), 663. https://doi.org/10.1007/s10661-016-5679-3

D'Ambrosio, J. M., Gonorazky, G., Sueldo, D. J., Moraga, J., Di Palma, A. A., Lamattina, L., Collado, I. G., & Laxalt, A. M. (2018). The sesquiterpene botrydial from Botrytis cinerea

induces phosphatidic acid production in tomato cell suspensions. *Planta*, *247*(4), 1001–1009. https://doi.org/10.1007/s00425-018-2843-8

Dana, M. de las M., Pintor-Toro, J. A., & Cubero, B. (2006). Transgenic Tobacco Plants Overexpressing Chitinases of Fungal Origin Show Enhanced Resistance to Biotic and Abiotic Stress Agents. *Plant Physiology*, *142*(2), 722–730. https://doi.org/10.1104/pp.106.086140

Davidson, J., & Gunn, J. (2012). *Effects of Land Cover Disturbance on Stream Invertebrate Diversity and Metal Concentrations in a Small Urban Industrial Watershed*. Human and Ecological Risk Assessment: An International Journal. https://www.tandfonline.com/doi/full/10.1080/10807039.2012.707935

de Abreu-Neto, J. B., Turchetto-Zolet, A. C., de Oliveira, L. F. V., Bodanese Zanettini, M. H., & Margis-Pinheiro, M. (2013). Heavy metal-associated isoprenylated plant protein (HIPP): Characterization of a family of proteins exclusive to plants. *The FEBS Journal*, *280*(7), 1604–1616. https://doi.org/10.1111/febs.12159

de la Fuente, V., Rodríguez, N., Díez-Garretas, B., Rufo, L., Asensi, A., & Amils, R. (2007). Nickel distribution in the hyperaccumulator Alyssum serpyllifolium Desf. Spp. From the Iberian Peninsula. *Plant Biosystems - An International Journal Dealing with All Aspects of Plant Biology*, *141*(2), 170–180. https://doi.org/10.1080/11263500701401422

DeForest, D. K., Brix, K. V., & Adams, W. J. (2007). Assessing metal bioaccumulation in aquatic environments: The inverse relationship between bioaccumulation factors, trophic transfer factors and exposure concentration. *Aquatic Toxicology (Amsterdam, Netherlands)*, *84*(2), 236–246. https://doi.org/10.1016/j.aquatox.2007.02.022

del Pozo, T., Cambiazo, V., & González, M. (2010). Gene expression profiling analysis of copper homeostasis in Arabidopsis thaliana. *Biochemical and Biophysical Research Communications*, *393*(2), 248–252. https://doi.org/10.1016/j.bbrc.2010.01.111

Delhaize, E., Ryan, P. R., & Randall, P. J. (1993). Aluminum Tolerance in Wheat (Triticum aestivum L.) (II. Aluminum-Stimulated Excretion of Malic Acid from Root Apices). *Plant Physiology*, *103*(3), 695–702. https://doi.org/10.1104/pp.103.3.695

Demason, D. A., & Chawla, R. (2006). Auxin/gibberellin interactions in pea leaf morphogenesis. *Botanical Journal of the Linnean Society*, *150*(1), 45–59. https://doi.org/10.1111/j.1095-8339.2006.00491.x

Demirevska-Kepova, K., Simova-Stoilova, L., Stoyanova, Z., Hölzer, R., & Feller, U. (2004). Biochemical changes in barley plants after excessive supply of copper and manganese. *Environmental and Experimental Botany*, *52*(3), 253–266. https://doi.org/10.1016/j.envexpbot.2004.02.004

Demirezen Yilmaz, D., & Uruç Parlak, K. (2011). Antioxidative parameters in the opposite-leaved pondweed (*Gronlendia densa*) in response to nickel stress. *Chemical Speciation & Bioavailability*, *23*(2), 71–79. https://doi.org/10.3184/095422911X13026931812524

Denancé, N., Ranocha, P., Oria, N., Barlet, X., Rivière, M.-P., Yadeta, K. A., Hoffmann, L., Perreau, F., Clément, G., Maia-Grondard, A., van den Berg, G. C. M., Savelli, B., Fournier, S., Aubert, Y., Pelletier, S., Thomma, B. P. H. J., Molina, A., Jouanin, L., Marco, Y., & Goffner, D. (2013). Arabidopsis wat1 (walls are thin1)-mediated resistance to the bacterial vascular pathogen, Ralstonia solanacearum, is accompanied by cross-regulation of salicylic acid and tryptophan metabolism. *The Plant Journal*, *73*(2), 225–239. https://doi.org/10.1111/tpj.12027

Deng, B., Zhang, W., & Yang, H. (2022). Abscisic Acid Decreases Cell Death in Malus hupehensis Rehd. Under Cd Stress by Reducing Root Cd2+ Influx and Leaf Transpiration. *Journal of Plant Growth Regulation*, *41*(2), 639–646. https://doi.org/10.1007/s00344-021-10327-0

Deng, F., Yamaji, N., Xia, J., & Ma, J. F. (2013). A Member of the Heavy Metal P-Type ATPase OsHMA5 Is Involved in Xylem Loading of Copper in Rice. *Plant Physiology*, *163*(3), 1353–1362. https://doi.org/10.1104/pp.113.226225

Deng, T.-H.-B., Chen, J.-Q., Geng, K.-R., van der Ent, A., Tang, Y.-T., Wen, D., Wang, X., Li, L., Du, R.-Y., Morel, J.-L., & Qiu, R.-L. (2021). Quantification of nickel and cobalt mobility and accumulation via the phloem in the hyperaccumulator Noccaea caerulescens (Brassicaceae). *Metallomics*, *13*(4). https://doi.org/10.1093/mtomcs/mfab012

DeVolder, P. S., Brown, S. L., Hesterberg, D., & Pandya, K. (2003). Metal Bioavailability and Speciation in a Wetland Tailings Repository Amended with Biosolids Compost, Wood Ash, and Sulfate. *Journal of Environmental Quality*, *32*(3), 851–864. https://doi.org/10.2134/jeq2003.8510

Dey, S., Mazumder, P. B., & Paul, S. B. (2015). Copper-induced changes in growth and antioxidative mechanisms of tea plant (Camellia sinensis (L.) O. Kuntze). *African Journal of Biotechnology*, *14*(7), Article 7. https://doi.org/10.4314/ajb.v14i7

Di Palma, L., Ferrantelli, P., Merli, C., Petrucci, E., & Pitzolu, I. (2007). Influence of Soil Organic Matter on Copper Extraction from Contaminated Soil. *Soil and Sediment Contamination: An International Journal*, *16*(3), 323–335. https://doi.org/10.1080/15320380701285758

Dion, M., Loranger, S., Kennedy, G., Courchesne, F., & Zayed, J. (1993). Evaluation of black spruce (Picea mariana) as a bioindicator of aluminum contamination. *Water, Air, & Soil Pollution*, *71*(1–2), 29–41. https://doi.org/10.1007/BF00475510

Doan, T. T. P., Domergue, F., Fournier, A. E., Vishwanath, S. J., Rowland, O., Moreau, P., Wood, C. C., Carlsson, A. S., Hamberg, M., & Hofvander, P. (2012). Biochemical characterization of a chloroplast localized fatty acid reductase from Arabidopsis thaliana. *Biochimica et Biophysica Acta (BBA) - Molecular and Cell Biology of Lipids*, *1821*(9), 1244–1255. https://doi.org/10.1016/j.bbalip.2011.10.019

Ducic, T., Leinemann, L., Finkeldey, R., & Polle, A. (2006). Uptake and translocation of manganese in seedlings of two varieties of Douglas fir (Pseudotsuga menziesii var.

Viridis and glauca). *New Phytologist*, *170*(1), 11–20. https://doi.org/10.1111/j.1469-8137.2006.01666.x

Dudal, Y., Sévenier, G., Dupont, L., & Guillon, E. (2005). Fate of the metal-binding soluble organic matter throughout a soil profile. *Soil Science*, *170*(9), 707–715. https://doi.org/10.1097/01.ss.0000185909.03213.6b

Dunemann, L., Von Wirén, N., Schulz, R., & Marschner, H. (1991). Speciation analysis of nickel in soil solutions and availability to oat plants. *Plant and Soil*, *133*(2), 263–269. https://doi.org/10.1007/bf00009198

Dykema, P. E., Sipes, P. R., Marie, A., Biermann, B. J., Crowell, D. N., & Randall, S. K. (1999). A new class of proteins capable of binding transition metals. *Plant Molecular Biology*, *41*(1), 139–150. https://doi.org/10.1023/A:1006367609556

Echevarria, G., Massoura, S. T., Sterckeman, T., Becquer, T., Schwartz, C., & Morel, J. L. (2006). Assessment and control of the bioavailability of nickel in soils. *Environmental Toxicology and Chemistry*, *25*(3), 643. https://doi.org/10.1897/05-051r.1

El-Khatib, A. A., Youssef, N. A., Barakat, N. A., & Samir, N. A. (2020). Responses of *Eucalyptus globulus* and *Ficus nitida* to different potential of heavy metal air pollution. *International Journal of Phytoremediation*, *22*(10), 986–999. https://doi.org/10.1080/15226514.2020.1719031

El-Sheekh, M. M. (1993). Inhibition of Photosystem II in the Green Alga Scenedesmus obliquus by Nickel. *Biochemie Und Physiologie Der Pflanzen*, *188*(6), 363–372. https://doi.org/10.1016/s0015-3796(11)80139-3

Estrada-Melo, A. C., Chao, Reid, M. S., & Jiang, C.-Z. (2015). Overexpression of an ABA biosynthesis gene using a stress-inducible promoter enhances drought resistance in petunia. *Horticulture Research*, *2*, 15013. https://doi.org/10.1038/hortres.2015.13

Fackler, J. P., Fetchin, J. A., & Fries, D. C. (1972). Sulfur chelates. XV. Sulfur addition and abstraction reactions of dithioaryl acid complexes of zinc(II), nickel(II), palladium(II), and platinum(II) and the x-ray crystal structures of bis(trithioperoxycumato)zinc(II) and dithiocumato(trithioperoxycumato)nickel(II). *Journal of the American Chemical Society*, *94*(21), 7323–7333. https://doi.org/10.1021/ja00776a011

Fan, H., & Zhou, W. (2009). Screening of Amaranth Cultivars (Amaranthus mangostanus L.) for Cadmium Hyperaccumulation. *Agricultural Sciences in China*, *8*(3), 342–351. https://doi.org/10.1016/s1671-2927(08)60218-7

Fan, J.-L., Wei, X.-Z., Wan, L.-C., Zhang, L.-Y., Zhao, X.-Q., Liu, W.-Z., Hao, H.-Q., & Zhang, H.-Y. (2011). Disarrangement of actin filaments and Ca2+ gradient by CdCl2 alters cell wall construction in Arabidopsis thaliana root hairs by inhibiting vesicular trafficking. *Journal of Plant Physiology*, *168*(11), 1157–1167. https://doi.org/10.1016/j.jplph.2011.01.031

Fan, S. K., Fang, X. Z., Guan, M. Y., Ye, Y. Q., Lin, X. Y., Du, S. T., & Jin, C. W. (2014). Exogenous abscisic acid application decreases cadmium accumulation in Arabidopsis plants, which is associated with the inhibition of IRT1-mediated cadmium uptake. *Frontiers in Plant Science*, *5*. https://www.frontiersin.org/articles/10.3389/fpls.2014.00721

Farghaly, F. A., Hamada, A. M., & Radi, A. A. (2022). Phyto-remedial of excessive copper and evaluation of its impact on the metabolic activity of Zea mays. *Cereal Research Communications*, *50*(4), 973–985. https://doi.org/10.1007/s42976-022-00259-0

Fasani, E., DalCorso, G., Zorzi, G., Agrimonti, C., Fragni, R., Visioli, G., & Furini, A. (2021). Overexpression of ZNT1 and NRAMP4 from the Ni Hyperaccumulator Noccaea caerulescens Population Monte Prinzera in Arabidopsis thaliana Perturbs Fe, Mn, and Ni Accumulation. *International Journal of Molecular Sciences*, *22*(21), 11896. https://doi.org/10.3390/ijms222111896

Fernandez, L. R., Vandenbussche, G., Roosens, N., Govaerts, C., Goormaghtigh, E., & Verbruggen, N. (2012). Metal binding properties and structure of a type III metallothionein from the metal hyperaccumulator plant Noccaea caerulescens. *Biochimica et Biophysica Acta (BBA) - Proteins and Proteomics*, *1824*(9), 1016–1023. https://doi.org/10.1016/j.bbapap.2012.05.010

Fourati, E., Vogel-Mikuš, K., Bettaieb, T., Kavčič, A., Kelemen, M., Vavpetič, P., Pelicon, P., Abdelly, C., & Ghnaya, T. (2019). Physiological response and mineral elements accumulation pattern in Sesuvium portulacastrum L. subjected in vitro to nickel. *Chemosphere*, *219*, 463–471. https://doi.org/10.1016/j.chemosphere.2018.12.081

Franklin, J. A., Zwiazek, J. J., Renault, S., & Croser, C. (2002). Growth and elemental composition of jack pine (Pinus banksiana) seedlings treated with sodium chloride and sodium sulfate. *Trees*, *16*(4), 325–330. https://doi.org/10.1007/s00468-002-0175-5

Gajewska, E., & Skłodowska, M. (2006). Effect of nickel on ROS content and antioxidative enzyme activities in wheat leaves. *BioMetals*, *20*(1), 27–36. https://doi.org/10.1007/s10534-006-9011-5

Gantayat, S., Mania, S., Pradhan, C., & Das, A. B. (2017). Ionic Stress Induced Cytotoxic Effect of Cadmium and Nickel Ions on Roots of *Allium cepa* L. *Cytologia*, *83*(2), 143–148. https://doi.org/10.1508/cytologia.83.143

Gao, W., Xiao, S., Li, H.-Y., Tsao, S.-W., & Chye, M.-L. (2009). Arabidopsis thaliana acyl-CoA-binding protein ACBP2 interacts with heavy-metal-binding farnesylated protein AtFP6. *New Phytologist*, *181*(1), 89–102. https://doi.org/10.1111/j.1469-8137.2008.02631.x

Garcia, L., Welchen, E., Gey, U., Arce, A. L., Steinebrunner, I., & Gonzalez, D. H. (2015). The cytochrome c oxidase biogenesis factor AtCOX17 modulates stress responses in Arabidopsis. *Plant, Cell & Environment*, *39*(3), 628–644. https://doi.org/10.1111/pce.12647

Garcia-Molina, A., Andrés-Colás, N., Perea-García, A., del Valle-Tascón, S., Peñarrubia, L., & Puig, S. (2011). The intracellular Arabidopsis COPT5 transport protein is required for photosynthetic electron transport under severe copper deficiency. *The Plant Journal*, *65*(6), 848–860. https://doi.org/10.1111/j.1365-313X.2010.04472.x

Garcia-Molina, A., Andrés-Colás, N., Perea-García, A., Neumann, U., Dodani, S. C., Huijser, P., Peñarrubia, L., & Puig, S. (2013). The Arabidopsis COPT6 Transport Protein Functions in Copper Distribution Under Copper-Deficient Conditions. *Plant and Cell Physiology*, *54*(8), 1378–1390. https://doi.org/10.1093/pcp/pct088

Gendre, D., Czernic, P., Conéjéro, G., Pianelli, K., Briat, J.-F., Lebrun, M., & Mari, S. (2006). TcYSL3, a member of the YSL gene family from the hyper-accumulator Thlaspi caerulescens, encodes a nicotianamine-Ni/Fe transporter. *The Plant Journal*, *49*(1), 1–15. https://doi.org/10.1111/j.1365-313x.2006.02937.x

Ghasemi, R., Ghaderian, S. M., & Krämer, U. (2009). Interference of nickel with copper and iron homeostasis contributes to metal toxicity symptoms in the nickel hyperaccumulator plant Alyssum inflatum. *New Phytologist*, *184*(3), 566–580. https://doi.org/10.1111/j.1469-8137.2009.02993.x

Ghuge, S., Tisi, A., Carucci, A., Rodrigues-Pousada, R., Franchi, S., Tavladoraki, P., Angelini, R., & Cona, A. (2015). Cell Wall Amine Oxidases: New Players in Root Xylem Differentiation under Stress Conditions. *Plants*, *4*(3), 489–504. https://doi.org/10.3390/plants4030489

Gimeno-García, E., Andreu, V., & Boluda, R. (1996). Heavy metals incidence in the application of inorganic fertilizers and pesticides to rice farming soils. *Environmental Pollution*, *92*(1), 19–25. https://doi.org/10.1016/0269-7491(95)00090-9

Golldack, D., Vera, P., & Dietz, K.-J. (2003). Expression of subtilisin-like serine proteases in Arabidopsis thaliana is cell-specific and responds to jasmonic acid and heavy metals with developmental differences. *Physiologia Plantarum*, *118*(1), 64–73. https://doi.org/10.1034/j.1399-3054.2003.00087.x

Gratton, W. S., Nkongolo, K. K., & Spiers, G. A. (2000). Heavy Metal Accumulation in Soil and Jack Pine (Pinus banksiana) Needles in Sudbury, Ontario, Canada. *Bulletin of Environmental Contamination and Toxicology*, *64*(4), 550–557. https://doi.org/10.1007/s001280000038

Grbić, V., & Bleecker, A. B. (1995). Ethylene regulates the timing of leaf senescence in Arabidopsis. *The Plant Journal*, *8*(4), 595–602. https://doi.org/10.1046/j.1365-313X.1995.8040595.x

Greenwood, M., Livingston, W., Day, M. E., Kenaley, S., White, A., & Brissette, J. (2002). Contrasting modes of survival by jack and pitch pine at a common range limit. *Canadian Journal of Forest Research*, *32*, 1662–1674. https://doi.org/10.1139/x02-088

Guerra, F. P., Reyes, L., Vergara-Jaque, A., Campos-Hernández, C., Gutiérrez, A., Pérez-Díaz, J., Pérez-Díaz, R., Blaudez, D., & Ruíz-Lara, S. (2015). Populus deltoides Kunitz trypsin inhibitor 3 confers metal tolerance and binds copper, revealing a new defensive role against heavy metal stress. *Environmental and Experimental Botany*, *115*, 28–37. https://doi.org/10.1016/j.envexpbot.2015.02.005

Guo, J., Xu, L., Su, Y., Wang, H., Gao, S., Xu, J., & Que, Y. (2013). ScMT2-1-3, a Metallothionein Gene of Sugarcane, Plays an Important Role in the Regulation of Heavy Metal Tolerance/Accumulation. *BioMed Research International*, *2013*, 1–12. https://doi.org/10.1155/2013/904769

Guo, M., Perez, C., Wei, Y., Rapoza, E., Su, G., Bou-Abdallah, F., & Chasteen, N. D. (2007). Iron-binding properties of plant phenolics and cranberry's bio-effects. *Dalton Transactions (Cambridge, England : 2003)*, *43*, 4951–4961. https://doi.org/10.1039/b705136k

Guo, T., Zhang, J., Christie, P., & Li, X. (2006). Effects of Arbuscular Mycorrhizal Fungi and Ammonium: Nitrate Ratios on Growth and Pungency of Onion Seedlings. *Journal of Plant Nutrition*, *29*(6), 1047–1059. https://doi.org/10.1080/01904160600689175

Guo, W.-J., Bundithya, W., & Goldsbrough, P. B. (2003). Characterization of the Arabidopsis Metallothionein Gene Family: Tissue-Specific Expression and Induction during Senescence and in Response to Copper. *The New Phytologist*, *159*(2), 369–381.

Guo, W.-J., Meetam, M., & Goldsbrough, P. B. (2008). Examining the Specific Contributions of Individual Arabidopsis Metallothioneins to Copper Distribution and Metal Tolerance. *Plant Physiology*, *146*(4), 1697–1706. https://doi.org/10.1104/pp.108.115782

Gupta, V., Willits, M. G., & Glazebrook, J. (2000). Arabidopsis thaliana EDS4 Contributes to Salicylic Acid (SA)-Dependent Expression of Defense Responses: Evidence for Inhibition of Jasmonic Acid Signaling by SA. *Molecular Plant-Microbe Interactions®*, *13*(5), 503–511. https://doi.org/10.1094/MPMI.2000.13.5.503

Guretzki, S., & Papenbrock, J. (2014). Characterization of Lablab purpureus Regarding Drought Tolerance, Trypsin Inhibitor Activity and Cyanogenic Potential for Selection in Breeding Programmes. *Journal of Agronomy and Crop Science*, *200*(1), 24–35. https://doi.org/10.1111/jac.12043

Hakata, M., Muramatsu, M., Nakamura, H., Hara, N., Kishimoto, M., Iida-Okada, K., Kajikawa, M., Imai-Toki, N., Toki, S., Nagamura, Y., Yamakawa, H., & Ichikawa, H. (2017). Overexpression of TIFY genes promotes plant growth in rice through jasmonate signaling. *Bioscience, Biotechnology, and Biochemistry*, *81*(5), 906–913. https://doi.org/10.1080/09168451.2016.1274638

Hall, J. L. (2002). Cellular mechanisms for heavy metal detoxification and tolerance. *Journal of Experimental Botany*, *53*(366), 1–11. https://doi.org/10.1093/jexbot/53.366.1

Hanika, K., Schipper, D., Chinnappa, S., Oortwijn, M., Schouten, H. J., Thomma, B. P. H. J., & Bai, Y. (2021). Impairment of Tomato WAT1 Enhances Resistance to Vascular Wilt Fungi Despite Severe Growth Defects. *Frontiers in Plant Science*, *12*. https://www.frontiersin.org/articles/10.3389/fpls.2021.721674

Harada, E., Yamaguchi, Y., Koizumi, N., & Hiroshi, S. (2002). Cadmium stress induces production of thiol compounds and transcripts for enzymes involved in sulfur assimilation pathways in Arabidopsis. *Journal of Plant Physiology*, *159*(4), 445–448. https://doi.org/10.1078/0176-1617-00733

Hart, S. A., & Chen, H. Y. H. (2008). Fire, logging and overstory affect understory abundance, diversity, and composition in boreal forest. *Ecological Monographs*, *78*(1), 123–140. https://doi.org/10.1890/06-2140.1

Hashem, A., Abd_Allah, E. F., Alqarawi, A. A., & Egamberdieva, D. (2016). Bioremediation of adverse impact of cadmium toxicity on Cassia italica Mill by arbuscular mycorrhizal fungi. *Saudi Journal of Biological Sciences*, *23*(1), 39–47. https://doi.org/10.1016/j.sjbs.2015.11.007

He Li, Chao Li, Di Sun, & Zhimin Yang. (2022). OsPDR20 is an ABCG metal transporter regulating cadmium accumulation in rice. *Journal of Environmental Sciences (China)*. https://doi.org/10.1016/j.jes.2022.09.021

He, Y., Fukushige, H., Hildebrand, D. F., & Gan, S. (2002). Evidence Supporting a Role of Jasmonic Acid in Arabidopsis Leaf Senescence. *Plant Physiology*, *128*(3), 876–884. https://doi.org/10.1104/pp.010843

Helaoui, S., Boughattas, I., El Kribi-Boukhris, S., Mkhinini, M., Alphonse, V., Livet, A., Bousserrhine, N., & Banni, M. (2022). Assessing the effects of nickel on, e.g., Medicago sativa L. nodules using multidisciplinary approach. *Environmental Science and Pollution Research*. https://doi.org/10.1007/s11356-022-21311-w

Herren, T., & Feller, U. (1997). Influence of increased zinc levels on phloem transport in wheat shoots. *Journal of Plant Physiology*, *150*(1), 228–231. https://doi.org/10.1016/S0176-1617(97)80208-8

Höhner, R., Pribil, M., Herbstová, M., Lopez, L. S., Kunz, H.-H., Li, M., Wood, M., Svoboda, V., Puthiyaveetil, S., Leister, D., & Kirchhoff, H. (2020). Plastocyanin is the long-range electron carrier between photosystem II and photosystem I in plants. *Proceedings of the National Academy of Sciences*, *117*(26), 15354–15362. https://doi.org/10.1073/pnas.2005832117

Hoppen, C., Müller, L., Hänsch, S., Uzun, B., Milić, D., Meyer, A. J., Weidtkamp-Peters, S., & Groth, G. (2019). Soluble and membrane-bound protein carrier mediate direct copper transport to the ethylene receptor family. *Scientific Reports*, *9*(1). https://doi.org/10.1038/s41598-019-47185-6

Hou, W.-C., & Lin, Y.-H. (2002). Sweet potato (Ipomoea batatas (L.) Lam) trypsin inhibitors, the major root storage proteins, inhibit one endogenous serine protease activity. *Plant Science*, *163*(4), 733–739. https://doi.org/10.1016/S0168-9452(02)00168-1

Hsu, Y. T., & Kao, C. H. (2003). Role of abscisic acid in cadmium tolerance of rice (Oryza sativa L.) seedlings. *Plant, Cell & Environment*, *26*(6), 867–874. https://doi.org/10.1046/j.1365-3040.2003.01018.x

Huang, C., Chui, Y., Gong, M., & Chana, F. (2020). Mechanical behaviour of wood compressed in radial direction: Part II. Influence of temperature and moisture content. *Journal of Bioresources and Bioproducts*, *5*(4), 266–275. https://doi.org/10.1016/j.jobab.2020.10.005

Huang, M., Barbour, S. L., Elshorbagy, A., Zettl, J., & Si, B. C. (2013). Effects of Variably Layered Coarse Textured Soils on Plant Available Water and Forest Productivity. *Procedia Environmental Sciences*, *19*, 148–157. https://doi.org/10.1016/j.proenv.2013.06.017

Huang, S., Yamaji, N., Sakurai, G., Mitani-Ueno, N., Konishi, N., & Ma, J. F. (2022). A pericycle-localized silicon transporter for efficient xylem loading in rice. *New Phytologist*, *234*(1), 197–208. https://doi.org/10.1111/nph.17959

Hutchinson, T. C., & Gunderman, D. (1998). The Contamination and Recovery of Natural Ecosystems by Smelting and Mining Activities at Sudbury, Ontario. In I. Linkov & R. Wilson (Eds.), *Air Pollution in the Ural Mountains* (pp. 363–373). Springer Netherlands. https://doi.org/10.1007/978-94-011-5208-2_33

Hutchinson, T. C., & Symington, M. S. (1997). Persistence of metal stress in a forested ecosystem near Sudbury, 66 years after closure of the O'Donnell roast bed. *Journal of Geochemical Exploration*, *58*(2–3), 323–330. https://doi.org/10.1016/s0375-6742(96)00067-2

Ingle, R. A., Mugford, S. T., Rees, J. D., Campbell, M. M., & Smith, J. A. C. (2005). Constitutively High Expression of the Histidine Biosynthetic Pathway Contributes to Nickel Tolerance in Hyperaccumulator Plants. *The Plant Cell*, *17*(7), 2089–2106. https://doi.org/10.1105/tpc.104.030577

Intawongse, M., & Dean, J. R. (2006). Uptake of heavy metals by vegetable plants grown on contaminated soil and their bioavailability in the human gastrointestinal tract. *Food Additives and Contaminants*, *23*(1), 36–48. https://doi.org/10.1080/02652030500387554

Irtelli, B., Petrucci, W. A., & Navari-Izzo, F. (2008). Nicotianamine and histidine/proline are, respectively, the most important copper chelators in xylem sap of Brassica carinata under conditions of copper deficiency and excess. *Journal of Experimental Botany*, *60*(1), 269–277. https://doi.org/10.1093/jxb/ern286

Ivanov, Y. V., Kartashov, A. V., Ivanova, A. I., Savochkin, Y. V., & Kuznetsov, V. V. (2016). Effects of copper deficiency and copper toxicity on organogenesis and some

physiological and biochemical responses of Scots pine (Pinus sylvestris L.) seedlings grown in hydroculture. *Environmental Science and Pollution Research*, *23*(17), 17332–17344. https://doi.org/10.1007/s11356-016-6929-1

Jacques, S., Ghesquière, B., De Bock, P.-J., Demol, H., Wahni, K., Willems, P., Messens, J., Van Breusegem, F., & Gevaert, K. (2015). Protein Methionine Sulfoxide Dynamics in Arabidopsis thaliana under Oxidative Stress[S]. *Molecular & Cellular Proteomics*, *14*(5), 1217–1229. https://doi.org/10.1074/mcp.M114.043729

Jahan, M. S., Guo, S., Baloch, A. R., Sun, J., Shu, S., Wang, Y., Ahammed, G. J., Kabir, K., & Roy, R. (2020). Melatonin alleviates nickel phytotoxicity by improving photosynthesis, secondary metabolism and oxidative stress tolerance in tomato seedlings. *Ecotoxicology and Environmental Safety*, *197*, 110593. https://doi.org/10.1016/j.ecoenv.2020.110593

Jain, S., Muneer, S., Guerriero, G., Liu, S., Vishwakarma, K., Chauhan, D. K., Dubey, N. K., Tripathi, D. K., & Sharma, S. (2018). Tracing the role of plant proteins in the response to metal toxicity: A comprehensive review. *Plant Signaling & Behavior*, *13*(9), e1507401. https://doi.org/10.1080/15592324.2018.1507401

Jara-Marini, M. E., Soto-Jiménez, M. F., & Páez-Osuna, F. (2009). Trophic relationships and transference of cadmium, copper, lead and zinc in a subtropical coastal lagoon food web from SE Gulf of California. *Chemosphere*, *77*(10), 1366–1373. https://doi.org/10.1016/j.chemosphere.2009.09.025

Jegerschoeld, C., Arellano, J. B., Schroeder, W. P., van Kan, P. J. M., Baron, M., & Styring, S. (1995). Copper(II) Inhibition of Electron Transfer through Photosystem II Studied by EPR Spectroscopy. *Biochemistry*, *34*(39), 12747–12754. https://doi.org/10.1021/bi00039a034

Jewiss, T. (2013). *The mining history of the Sudbury area | Earth Sciences Museum*. Earth Sciences Museum. https://uwaterloo.ca/earth-sciences-museum/resources/mining-canada/mining-history-sudbury-area

Jia, H., Wang, X., Wei, T., Zhou, R., Muhammad, H., Hua, L., Ren, X., Guo, J., & Ding, Y. (2019). Accumulation and fixation of Cd by tomato cell wall pectin under Cd stress. *Environmental and Experimental Botany*, *167*, 103829. https://doi.org/10.1016/j.envexpbot.2019.103829

Jiang, W. B., Lers, A., Lomaniec, E., & Aharoni, N. (1999). Senescence-related serine protease in parsley. *Phytochemistry*, *50*(3), 377–382. https://doi.org/10.1016/S0031-9422(98)00546-9

Jiang, Y., Yin, H., Wang, D., Zhong, Y., & Deng, Y. (2022). Exploring the mechanism of Akebia trifoliata fruit cracking based on cell-wall metabolism. *Food Research International*, *157*, 111219. https://doi.org/10.1016/j.foodres.2022.111219

Jogawat, A., Yadav, B., Chhaya, & Narayan, O. P. (2021). Metal transporters in organelles and their roles in heavy metal transportation and sequestration mechanisms in plants. *Physiologia Plantarum*, ppl.13370. https://doi.org/10.1111/ppl.13370

Johannesson, H., Wang, Y., Hanson, J., & Engström, P. (n.d.). *The Arabidopsis thaliana homeobox gene ATHB5 is a potential regulator of abscisic acid responsiveness in developing seedlings*.

Johannesson, H., Wang, Y., Hanson, J., & Engström, P. (2003). The Arabidopsis thaliana homeobox gene ATHB5 is a potential regulator of abscisic acid responsiveness in developing seedlings. *Plant Molecular Biology*, *51*(5), 719–729. https://doi.org/10.1023/A:1022567625228

Jourand, P., Ducousso, M., Reid, R., Majorel, C., Richert, C., Riss, J., & Lebrun, M. (2010). Nickel-tolerant ectomycorrhizal Pisolithus albus ultramafic ecotype isolated from nickel mines in New Caledonia strongly enhance growth of the host plant Eucalyptus globulus at toxic nickel concentrations. *Tree Physiology*, *30*(10), 1311–1319. https://doi.org/10.1093/treephys/tpq070

Jouvin, D., Weiss, D. J., Mason, T. F. M., Bravin, M. N., Louvat, P., Zhao, F., Ferec, F., Hinsinger, P., & Benedetti, M. F. (2012). Stable Isotopes of Cu and Zn in Higher Plants: Evidence for Cu Reduction at the Root Surface and Two Conceptual Models for Isotopic Fractionation Processes. *Environmental Science & Technology*, *46*(5), 2652–2660. https://doi.org/10.1021/es202587m

Jung, H., Gayomba, S. R., Rutzke, M. A., Craft, E., Kochian, L. V., & Vatamaniuk, O. K. (2012). COPT6 Is a Plasma Membrane Transporter That Functions in Copper Homeostasis in Arabidopsis and Is a Novel Target of SQUAMOSA Promoter-binding Protein-like 7. *Journal of Biological Chemistry*, *287*(40), 33252–33267. https://doi.org/10.1074/jbc.m112.397810

Jutsz, A. M., & Gnida, A. (2015). Mechanisms of stress avoidance and tolerance by plants used in phytoremediation of heavy metals. *Archives of Environmental Protection*, *41*(4), 104–114. https://doi.org/10.1515/aep-2015-0045

Kaitera, J., Piispanen, J., & Bergmann, U. (2021). Terpene and resin acid contents in Scots pine stem lesions colonized by the rust fungus Cronartium pini. *Forest Pathology*, *51*(4), e12700. https://doi.org/10.1111/efp.12700

Kalluri, U. C., Payyavula, R. S., Labbé, J. L., Engle, N., Bali, G., Jawdy, S. S., Sykes, R. W., Davis, M., Ragauskas, A., Tuskan, G. A., & Tschaplinski, T. J. (2016). Down-Regulation of KORRIGAN-Like Endo-β-1,4-Glucanase Genes Impacts Carbon Partitioning, Mycorrhizal Colonization and Biomass Production in Populus. *Frontiers in Plant Science*, *7*. https://www.frontiersin.org/articles/10.3389/fpls.2016.01455

Kalubi, K. N., Mehes-Smith, M., Narendrula, R., Michael, P., & Omri, A. (2015). Molecular analysis of red maple (Acer rubrum) populations from a reclaimed mining region in

Northern Ontario (Canada): Soil metal accumulation and translocation in plants. *Ecotoxicology*, *24*(3), 636–647. https://doi.org/10.1007/s10646-014-1411-7

Kang, J., Hwang, J.-U., Lee, M., Kim, Y.-Y., Assmann, S. M., Martinoia, E., & Lee, Y. (2010). PDR-type ABC transporter mediates cellular uptake of the phytohormone abscisic acid. *Proceedings of the National Academy of Sciences*, *107*(5), 2355–2360. https://doi.org/10.1073/pnas.0909222107

Karmous, I., Chaoui, A., Jaouani, K., Sheehan, D., El Ferjani, E., Scoccianti, V., & Crinelli, R. (2014). Role of the ubiquitin-proteasome pathway and some peptidases during seed germination and copper stress in bean cotyledons. *Plant Physiology and Biochemistry*, *76*, 77–85. https://doi.org/10.1016/j.plaphy.2013.12.025

Kashian, D. M., Barnes, B. V., & Walker, W. S. (2003). Ecological Species Groups of Landform-Level Ecosystems Dominated by Jack Pine in Northern Lower Michigan, USA. *Plant Ecology*, *166*(1), 75–91.

Kaur, H., & Manchanda, J. S. (2019). Copper induced iron deficiency in wheat (Triticum aestivum L). *Journal of Plant Nutrition*, *42*(20), 2824–2843. https://doi.org/10.1080/01904167.2019.1659323

Kazemi, N., Khavari-Nejad, R. A., Fahimi, H., Saadatmand, S., & Nejad-Sattari, T. (2010). Effects of exogenous salicylic acid and nitric oxide on lipid peroxidation and antioxidant enzyme activities in leaves of Brassica napus L. under nickel stress. *Scientia Horticulturae*, *126*(3), 402–407. https://doi.org/10.1016/j.scienta.2010.07.037

Keeling, C. I., Weisshaar, S., Ralph, S. G., Jancsik, S., Hamberger, B., Dullat, H. K., & Bohlmann, J. (2011). Transcriptome mining, functional characterization, and phylogeny of a large terpene synthase gene family in spruce (Picea spp.). *BMC Plant Biology*, *11*, 43. https://doi.org/10.1186/1471-2229-11-43

Keller, W., Yan, N. D., Gunn, J. M., & Heneberry, J. (2007). Recovery of Acidified Lakes: Lessons From Sudbury, Ontario, Canada. In P. Brimblecombe, H. Hara, D. Houle, & M. Novak (Eds.), *Acid Rain—Deposition to Recovery* (pp. 317–322). Springer Netherlands. https://doi.org/10.1007/978-1-4020-5885-1_35

Kenkel, N. C., Hendrie, M. L., & Bella, I. E. (1997). A long-term study ofPinus banksianapopulation dynamics. *Journal of Vegetation Science*, *8*(2), 241–254. https://doi.org/10.2307/3237353

Khan, M. A. R., Bolan, N. S., & MacKay, A. D. (2005). Adsorption and Desorption of Copper in Pasture Soils. *Communications in Soil Science and Plant Analysis*, *36*(17–18), 2461–2487. https://doi.org/10.1080/00103620500255824

Khan, S., Khan, N. A., & Bano, B. (2017). In-sights into the effect of heavy metal stress on the endogenous mustard cystatin. *International Journal of Biological Macromolecules*, *105*, 1138–1147. https://doi.org/10.1016/j.ijbiomac.2017.07.146

khan, I. ullah, Rono, J. K., Zhang, B. Q., Liu, X. S., Wang, M. Q., Wang, L. L., Wu, X. C., Chen, X., Cao, H. W., & Yang, Z. M. (2019). Identification of novel rice (Oryza sativa) HPP and HIPP genes tolerant to heavy metal toxicity. *Ecotoxicology and Environmental Safety*, *175*, 8–18. https://doi.org/10.1016/j.ecoenv.2019.03.040

Khare, D., Mitsuda, N., Lee, S., Song, W., Hwang, D., Ohme-Takagi, M., Martinoia, E., Lee, Y., & Hwang, J. (2016). Root avoidance of toxic metals requires the GeBP-LIKE 4 transcription factor in Arabidopsis thaliana. *New Phytologist*, *213*(3), 1257–1273. https://doi.org/10.1111/nph.14242

Khawla, K., Besma, K., Enrique, M., & Mohamed, H. (2019). Accumulation of trace elements by corn (Zea mays) under irrigation with treated wastewater using different irrigation methods. *Ecotoxicology and Environmental Safety*, *170*, 530–537. https://doi.org/10.1016/j.ecoenv.2018.12.025

Kholodova, V., Volkov, K., Abdeyeva, A., & Kuznetsov, V. (2011). Water status in Mesembryanthemum crystallinum under heavy metal stress. *Environmental and Experimental Botany*, *71*(3), 382–389. https://doi.org/10.1016/j.envexpbot.2011.02.007

Kim, D.-Y., Bovet, L., Maeshima, M., Martinoia, E., & Lee, Y. (2007). The ABC transporter AtPDR8 is a cadmium extrusion pump conferring heavy metal resistance. *The Plant Journal*, *50*(2), 207–218. https://doi.org/10.1111/j.1365-313X.2007.03044.x

Kim, S., Takahashi, M., Higuchi, K., Tsunoda, K., Nakanishi, H., Yoshimura, E., Mori, S., & Nishizawa, N. K. (2005). Increased Nicotianamine Biosynthesis Confers Enhanced Tolerance of High Levels of Metals, in Particular Nickel, to Plants. *Plant and Cell Physiology*, *46*(11), 1809–1818. https://doi.org/10.1093/pcp/pci196

Kintlová, M., Blavet, N., Cegan, R., & Hobza, R. (2017). Transcriptome of barley under three different heavy metal stress reaction. *Genomics Data*, *13*, 15–17. https://doi.org/10.1016/j.gdata.2017.05.016

Klaumann, S., Nickolaus, S. D., Fürst, S. H., Starck, S., Schneider, S., Ekkehard Neuhaus, H., & Trentmann, O. (2011). The tonoplast copper transporter COPT5 acts as an exporter and is required for interorgan allocation of copper in Arabidopsis thaliana. *New Phytologist*, *192*(2), 393–404. https://doi.org/10.1111/j.1469-8137.2011.03798.x

Ko, J.-H., Yang, S. H., & Han, K.-H. (2006). Upregulation of an Arabidopsis RING-H2 gene, XERICO, confers drought tolerance through increased abscisic acid biosynthesis. *The Plant Journal*, *47*(3), 343–355. https://doi.org/10.1111/j.1365-313X.2006.02782.x

Kohler, A., Blaudez, D., Chalot, M., & Martin, F. (2004). Cloning and expression of multiple metallothioneins from hybrid poplar. *New Phytologist*, *164*(1), 83–93. https://doi.org/10.1111/j.1469-8137.2004.01168.x

Kolbert, Z., Oláh, D., Molnár, Á., Szőllősi, R., Erdei, L., & Ördög, A. (2020). Distinct redox signalling and nickel tolerance in Brassica juncea and Arabidopsis thaliana.

Ecotoxicology and Environmental Safety, *189*, 109989. https://doi.org/10.1016/j.ecoenv.2019.109989

Kozhevnikova, A. D., Seregin, I. V., & Schat, H. (2020). Accumulation of Nickel by Excluder Thlaspi arvense and Hyperaccumulator Noccaea caerulescens upon Short-Term and Long-Term Exposure. *Russian Journal of Plant Physiology*, *67*(2), 303–311. https://doi.org/10.1134/S1021443720020089

Kozhevnikova, A. D., Seregin, I. V., & Schat, H. (2021). Translocation of Ni and Zn in Odontarrhena corsica and Noccaea caerulescens: The effects of exogenous histidine and Ni/Zn interactions. *Plant and Soil*, *468*(1–2), 295–318. https://doi.org/10.1007/s11104-021-05080-y

Kramer, D. M., Holness, D. L., Haynes, E., McMillan, K., Berriault, C., Kalenge, S., & Lightfoot, N. (2017). From awareness to action: Sudbury, mining and occupational disease in a time of change. *Work, 58*(2), 149–162. https://doi.org/10.3233/WOR-172610

Krämer, U., Cotter-Howells, J. D., Charnock, J. M., Baker, A. J. M., & Smith, J. A. C. (1996). Free histidine as a metal chelator in plants that accumulate nickel. *Nature*, *379*(6566), 635–638. https://doi.org/10.1038/379635a0

Krämer, U., Grime, G. W., Smith, J. A. C., Hawes, C. R., & Baker, A. J. M. (1997). Micro-PIXE as a technique for studying nickel localization in leaves of the hyperaccumulator plant Alyssum lesbiacum. *Nuclear Instruments and Methods in Physics Research Section B: Beam Interactions with Materials and Atoms*, *130*(1), 346–350. https://doi.org/10.1016/S0168-583X(97)00368-6

Krämer, U., Pickering, I. J., Prince, R. C., Raskin, I., & Salt, D. E. (2000). Subcellular Localization and Speciation of Nickel in Hyperaccumulator and Non-Accumulator Thlaspi Species. *Plant Physiology*, *122*(4), 1343–1354.

Ku, S.-J., Park, J.-Y., Ha, S.-B., & Kim, J. (2009). Overexpression of IAA1 with domain II mutation impairs cell elongation and cell division in inflorescences and leaves of Arabidopsis. *Journal of Plant Physiology*, *166*(5), 548–553. https://doi.org/10.1016/j.jplph.2008.07.006

Kubicova, L., Bachmann, G., Weckwerth, W., & Chobot, V. (2022). (±)-Catechin—A Mass-Spectrometry-Based Exploration Coordination Complex Formation with FeII and FeIII. *Cells*, *11*(6), Article 6. https://doi.org/10.3390/cells11060958

Kulikova, A. L., Kuznetsova, N. A., & Kholodova, V. P. (2011). Effect of copper excess in environment on soybean root viability and morphology. *Russian Journal of Plant Physiology*, *58*(5), 836–843. https://doi.org/10.1134/s102144371105013x

Kumar, G., Kushwaha, H. R., Panjabi-Sabharwal, V., Kumari, S., Joshi, R., Karan, R., Mittal, S., Pareek, S. L. S., & Pareek, A. (2012). Clustered metallothionein genes are co-regulated in rice and ectopic expression of OsMT1e-Pconfers multiple abiotic stress tolerance in

tobacco via ROS scavenging. *BMC Plant Biology*, *12*(1). https://doi.org/10.1186/1471-2229-12-107

Kumar, P., Rouphael, Y., Cardarelli, M., & Colla, G. (2015). Effect of nickel and grafting combination on yield, fruit quality, antioxidative enzyme activities, lipid peroxidation, and mineral composition of tomato. *Journal of Plant Nutrition and Soil Science*, *178*(6), 848–860. https://doi.org/10.1002/jpln.201400651

Kunst, L., & Samuels, A. L. (2003). Biosynthesis and secretion of plant cuticular wax. *Progress in Lipid Research*, *42*(1), 51–80. https://doi.org/10.1016/S0163-7827(02)00045-0

Küpper, H., Küpper, F., & Spiller, M. (1996). Environmental relevance of heavy metal-substituted chlorophylls using the example of water plants. *Journal of Experimental Botany*, *47*(2), 259–266. https://doi.org/10.1093/jxb/47.2.259

Küpper, H., Lombi, E., Zhao, F., Wieshammer, G., & McGrath, S. P. (2001). Cellular compartmentation of nickel in the hyperaccumulators Alyssum lesbiacum, Alyssum bertolonii and Thlaspi goesingense. *Journal of Experimental Botany*, *52*(365), 2291–2300. https://doi.org/10.1093/jexbot/52.365.2291

Lee, H. Y., Jang, G., Um, T., Kim, J.-K., Lee, J. S., & Do Choi, Y. (2015). The soluble ABA receptor PYL8 regulates drought resistance by controlling ABA signaling in Arabidopsis. *Plant Biotechnology Reports*, *9*(5), 319–330. https://doi.org/10.1007/s11816-015-0366-3

Lee, I. C., Hong, S. W., Whang, S. S., Lim, P. O., Nam, H. G., & Koo, J. C. (2011). Age-Dependent Action of an ABA-Inducible Receptor Kinase, RPK1, as a Positive Regulator of Senescence in Arabidopsis Leaves. *Plant and Cell Physiology*, *52*(4), 651–662. https://doi.org/10.1093/pcp/pcr026

Lee, K. H., Piao, H. L., Kim, H.-Y., Choi, S. M., Jiang, F., Hartung, W., Hwang, I., Kwak, J. M., Lee, I.-J., & Hwang, I. (2006). Activation of Glucosidase via Stress-Induced Polymerization Rapidly Increases Active Pools of Abscisic Acid. *Cell*, *126*(6), 1109–1120. https://doi.org/10.1016/j.cell.2006.07.034

Lee, M., Lee, K., Lee, J., Noh, E. W., & Lee, Y. (2005). AtPDR12 Contributes to Lead Resistance in Arabidopsis. *Plant Physiology*, *138*(2), 827–836. https://doi.org/10.1104/pp.104.058107

Lee, S., & Kang, B. S. (2005). Phytochelatin is not a primary factor in determining copper tolerance. *Journal of Plant Biology*, *48*(1), 32–38. https://doi.org/10.1007/bf03030562

Lee, S., Kim, Y.-Y., Lee, Y., & An, G. (2007). Rice P1B-Type Heavy-Metal ATPase, OsHMA9, Is a Metal Efflux Protein. *Plant Physiology*, *145*(3), 831–842. https://doi.org/10.1104/pp.107.102236

Lequeux, H., Hermans, C., Lutts, S., & Verbruggen, N. (2010). Response to copper excess in Arabidopsis thaliana: Impact on the root system architecture, hormone distribution, lignin

accumulation and mineral profile. *Plant Physiology and Biochemistry*, *48*(8), 673–682. https://doi.org/10.1016/j.plaphy.2010.05.005

Lesjak, M., Balesaria, S., Skinner, V., Debnam, E. S., & Srai, S. K. S. (2019). Quercetin inhibits intestinal non-haem iron absorption by regulating iron metabolism genes in the tissues. *European Journal of Nutrition*, *58*(2), 743–753. https://doi.org/10.1007/s00394-018-1680-7

Lesjak, M., Hoque, R., Balesaria, S., Skinner, V., Debnam, E. S., Srai, S. K. S., & Sharp, P. A. (2014). Quercetin Inhibits Intestinal Iron Absorption and Ferroportin Transporter Expression In Vivo and In Vitro. *PLoS ONE*, *9*(7), e102900. https://doi.org/10.1371/journal.pone.0102900

Lešková, A., Zvarík, M., Araya, T., & Giehl, R. F. H. (2020). Nickel Toxicity Targets Cell Wall-Related Processes and PIN2-Mediated Auxin Transport to Inhibit Root Elongation and Gravitropic Responses in Arabidopsis. *Plant and Cell Physiology*, *61*(3), 519–535. https://doi.org/10.1093/pcp/pcz217

Letelier, M. E., Lepe, A. M., Faúndez, M., Salazar, J., Marín, R., Aracena, P., & Speisky, H. (2005). Possible mechanisms underlying copper-induced damage in biological membranes leading to cellular toxicity. *Chemico-Biological Interactions*, *151*(2), 71–82. https://doi.org/10.1016/j.cbi.2004.12.004

Li, C., Liu, Y., Tian, J., Zhu, Y., & Fan, J. (2020). Changes in sucrose metabolism in maize varieties with different cadmium sensitivities under cadmium stress. *PLOS ONE*, *15*(12), e0243835. https://doi.org/10.1371/journal.pone.0243835

Li, J., Brader, G., & Palva, E. T. (2008). Kunitz Trypsin Inhibitor: An Antagonist of Cell Death Triggered by Phytopathogens and Fumonisin B1 in Arabidopsis. *Molecular Plant*, *1*(3), 482–495. https://doi.org/10.1093/mp/ssn013

Li, P., Zhang, Y., Wu, X., & Liu, Y. (2018). Drought stress impact on leaf proteome variations of faba bean (Vicia faba L.) in the Qinghai–Tibet Plateau of China. *3 Biotech*, *8*(2), 110. https://doi.org/10.1007/s13205-018-1088-3

Li, R., Wu, L., Shao, Y., Hu, Q., & Zhang, H. (2022). Melatonin alleviates copper stress to promote rice seed germination and seedling growth via crosstalk among various defensive response pathways. *Plant Physiology and Biochemistry*, *179*, 65–77. https://doi.org/10.1016/j.plaphy.2022.03.016

Li, S. F., Allen, P. J., Napoli, R. S., Browne, R. G., Pham, H., & Parish, R. W. (2020). MYB–bHLH–TTG1 Regulates Arabidopsis Seed Coat Biosynthesis Pathways Directly and Indirectly via Multiple Tiers of Transcription Factors. *Plant and Cell Physiology*, *61*(5), 1005–1018. https://doi.org/10.1093/pcp/pcaa027

Li, W., Lacey, R. F., Ye, Y., Lu, J., Yeh, K.-C., Xiao, Y., Li, L., Wen, C.-K., Binder, B. M., & Zhao, Y. (2017). Triplin, a small molecule, reveals copper ion transport in ethylene

signaling from ATX1 to RAN1. *PLOS Genetics*, *13*(4), e1006703. https://doi.org/10.1371/journal.pgen.1006703

Li, X., Lin, M., Hu, P., Lai, N., Huang, Z., & Chen, L. (2021). Copper Toxicity Differentially Regulates the Seedling Growth, Copper Distribution, and Photosynthetic Performance of Citrus sinensis and Citrus grandis. *Journal of Plant Growth Regulation*. https://doi.org/10.1007/s00344-021-10516-x

Liang, B., Zheng, Y., Wang, J., Zhang, W., Fu, Y., Kai, W., Xu, Y., Yuan, B., Li, Q., & Leng, P. (2020). Overexpression of the persimmon abscisic acid β-glucosidase gene (DkBG1) alters fruit ripening in transgenic tomato. *The Plant Journal*, *102*(6), 1220–1233. https://doi.org/10.1111/tpj.14695

Lin, S.-L., & Wu, L. (1994). Effects of copper concentration on mineral nutrient uptake and copper accumulation in protein of copper-tolerant and nontolerant Lotus purshianus L. *Ecotoxicology and Environmental Safety*, *29*(2), 214–228. https://doi.org/10.1016/0147-6513(94)90021-3

Lin, Y.-F., Severing, E. I., te Lintel Hekkert, B., Schijlen, E., & Aarts, M. G. M. (2014). A comprehensive set of transcript sequences of the heavy metal hyperaccumulator Noccaea caerulescens. *Frontiers in Plant Science*, *5*, 261. https://doi.org/10.3389/fpls.2014.00261

Lindahl, M., Funk, C., Webster, J., Bingsmark, S., Adamska, I., & Andersson, B. (1997). Expression of ELIPs and PS II-S protein in spinach during acclimative reduction of the Photosystem II antenna in response to increased light intensities. *Photosynthesis Research*, *54*(3), 227–236. https://doi.org/10.1023/A:1005920730947

Liu, C.-X., Yang, T., Zhou, H., Ahammed, G. J., Qi, Z.-Y., & Zhou, J. (2022). The E3 Ubiquitin Ligase Gene Sl1 Is Critical for Cadmium Tolerance in Solanum lycopersicum L. *Antioxidants*, *11*(3), 456. https://doi.org/10.3390/antiox11030456

Liu, H., Ma, Y., Chen, N., Guo, S., Liu, H., Guo, X., Chong, K., & Xu, Y. (2014). Overexpression of stress-inducible OsBURP16, the β subunit of polygalacturonase 1, decreases pectin content and cell adhesion and increases abiotic stress sensitivity in rice. *Plant, Cell & Environment*, *37*(5), 1144–1158. https://doi.org/10.1111/pce.12223

Liu, X., Zhang, Y., Yang, H., Liang, Y., Li, X., Oliver, M. J., & Zhang, D. (2020). Functional Aspects of Early Light-Induced Protein (ELIP) Genes from the Desiccation-Tolerant Moss Syntrichia caninervis. *International Journal of Molecular Sciences*, *21*(4), Article 4. https://doi.org/10.3390/ijms21041411

Llamas, A., Ullrich, C. I., & Sanz, A. (2008). Ni2+ toxicity in rice: Effect on membrane functionality and plant water content. *Plant Physiology and Biochemistry*, *46*(10), 905–910. https://doi.org/10.1016/j.plaphy.2008.05.006

Lopez-Zaplana, A., Martinez-Garcia, N., Carvajal, M., & Bárzana, G. (2022). Relationships between aquaporins gene expression and nutrient concentrations in melon plants

(Cucumis melo L.) during typical abiotic stresses. *Environmental and Experimental Botany*, *195*, 104759. https://doi.org/10.1016/j.envexpbot.2021.104759

Loreto, F., Mannozzi, M., Maris, C., Nascetti, P., Ferranti, F., & Pasqualini, S. (2001). Ozone Quenching Properties of Isoprene and Its Antioxidant Role in Leaves. *Plant Physiology*, *126*(3), 993–1000. https://doi.org/10.1104/pp.126.3.993

Lu, P., Parker, W. H., Cherry, M., Colombo, S., Parker, W. C., Man, R., & Roubal, N. (2014). Survival and growth patterns of white spruce (*Picea glauca* [M oench] Voss) rangewide provenances and their implications for climate change adaptation. *Ecology and Evolution*, *4*(12), 2360–2374. https://doi.org/10.1002/ece3.1100

Luo, Z.-B., He, J., Polle, A., & Rennenberg, H. (2016). Heavy metal accumulation and signal transduction in herbaceous and woody plants: Paving the way for enhancing phytoremediation efficiency. *Biotechnology Advances*, *34*(6), 1131–1148. https://doi.org/10.1016/j.biotechadv.2016.07.003

Ma, Y., Cao, J., Chen, Q., He, J., Liu, Z., Wang, J., Li, X., & Yang, Y. (2021). Abscisic acid receptors maintain abscisic acid homeostasis by modulating UGT71C5 glycosylation activity. *Journal of Integrative Plant Biology*, *63*(3), 543–552. https://doi.org/10.1111/jipb.13030

Machado, A., Wu, Y., Yang, Y., Llewellyn, D. J., & Dennis, E. S. (2009). The MYB transcription factor GhMYB25 regulates early fibre and trichome development. *The Plant Journal*, *59*(1), 52–62. https://doi.org/10.1111/j.1365-313X.2009.03847.x

Mahajan, M., Ahuja, P. S., & Yadav, S. K. (2011). Post-Transcriptional Silencing of Flavonol Synthase mRNA in Tobacco Leads to Fruits with Arrested Seed Set. *PLOS ONE*, *6*(12), e28315. https://doi.org/10.1371/journal.pone.0028315

Mahawar, L., Kumar, R., & Shekhawat, G. S. (2018). Evaluation of heme oxygenase 1 (HO 1) in Cd and Ni induced cytotoxicity and crosstalk with ROS quenching enzymes in two to four leaf stage seedlings of Vigna radiata. *Protoplasma*, *255*(2), 527–545. https://doi.org/10.1007/s00709-017-1166-0

Major, I. T., & Constabel, C. P. (2008). Functional Analysis of the Kunitz Trypsin Inhibitor Family in Poplar Reveals Biochemical Diversity and Multiplicity in Defense against Herbivores. *Plant Physiology*, *146*(3), 888–903. https://doi.org/10.1104/pp.107.106229

Maksymiec, W., & Krupa, Z. (2006). The effects of short-term exposition to Cd, excess Cu ions and jasmonate on oxidative stress appearing in Arabidopsis thaliana. *Environmental and Experimental Botany*, *57*(1), 187–194. https://doi.org/10.1016/j.envexpbot.2005.05.006

Mansilla, N., Welchen, E., & Gonzalez, D. H. (2019). Arabidopsis SCO Proteins Oppositely Influence Cytochrome c Oxidase Levels and Gene Expression during Salinity Stress. *Plant and Cell Physiology*, *60*(12), 2769–2784. https://doi.org/10.1093/pcp/pcz166

Marastoni, L., Lucini, L., Miras-Moreno, B., Trevisan, M., Sega, D., Zamboni, A., & Varanini, Z. (2020). Changes in physiological activities and root exudation profile of two grapevine rootstocks reveal common and specific strategies for Fe acquisition. *Scientific Reports*, *10*(1). https://doi.org/10.1038/s41598-020-75317-w

Mari, S., Gendre, D., Pianelli, K., Ouerdane, L., Lobinski, R., Briat, J.-F., Lebrun, M., & Czernic, P. (2006a). Root-to-shoot long-distance circulation of nicotianamine and nicotianamine-nickel chelates in the metal hyperaccumulator Thlaspi caerulescens. *Journal of Experimental Botany*, *57*(15), 4111–4122. https://doi.org/10.1093/jxb/erl184

Mari, S., Gendre, D., Pianelli, K., Ouerdane, L., Lobinski, R., Briat, J.-F., Lebrun, M., & Czernic, P. (2006b). Root-to-shoot long-distance circulation of nicotianamine and nicotianamine-nickel chelates in the metal hyperaccumulator Thlaspi caerulescens. *Journal of Experimental Botany*, *57*(15), 4111–4122. https://doi.org/10.1093/jxb/erl184

Martins, L. L., & Mourato, M. P. (2006). Effect of Excess Copper on Tomato Plants: Growth Parameters, Enzyme Activities, Chlorophyll, and Mineral Content. *Journal of Plant Nutrition*, *29*(12), 2179–2198. https://doi.org/10.1080/01904160600972845

Marziah, M., & Lam, C. H. (1987). Micronutrients. *Journal of Plant Nutrition*, *10*(9–16), 2089–2094. https://doi.org/10.1080/01904168709363759

Mayerhofer, H., Sautron, E., Rolland, N., Catty, P., Seigneurin-Berny, D., Pebay-Peyroula, E., & Ravaud, S. (2016). Structural Insights into the Nucleotide-Binding Domains of the P1B-type ATPases HMA6 and HMA8 from Arabidopsis thaliana. *PLOS ONE*, *11*(11), e0165666. https://doi.org/10.1371/journal.pone.0165666

McCall, J., Gunn, J., & Struik, H. (1995). Photo interpretive study of recovery of damaged lands near the metal smelters of Sudbury, Canada. *Water, Air, & Soil Pollution*, *85*(2), 847–852. https://doi.org/10.1007/bf00476935

McCann, M. C., & Roberts, K. (1994). Changes in cell wall architecture during cell elongation. *Journal of Experimental Botany*, *45*(Special_Issue), 1683–1691. https://doi.org/10.1093/jxb/45.Special_Issue.1683

McCord, J. M., & Fridovich, I. (1969). Superoxide Dismutase. *Journal of Biological Chemistry*, *244*(22), 6049–6055. https://doi.org/10.1016/S0021-9258(18)63504-5

McLeod, T., & MacDonald, G. (1997). Postglacial range expansion and population growth of Picea mariana, Picea glauca and Pinus banksiana in the western interior of Canada. *Journal of Biogeography*, *24*(6), 865–881. https://doi.org/10.1046/j.1365-2699.1997.00151.x

Mehrtens, F., Kranz, H., Bednarek, P., & Weisshaar, B. (2005). The Arabidopsis Transcription Factor MYB12 Is a Flavonol-Specific Regulator of Phenylpropanoid Biosynthesis. *Plant Physiology*, *138*(2), 1083–1096. https://doi.org/10.1104/pp.104.058032

Melidou, M., Riganakos, K., & Galaris, D. (2005). Protection against nuclear DNA damage offered by flavonoids in cells exposed to hydrogen peroxide: The role of iron chelation. *Free Radical Biology and Medicine*, *39*(12), 1591–1600. https://doi.org/10.1016/j.freeradbiomed.2005.08.009

Merlot, S., Hannibal, L., Martins, S., Martinelli, L., Amir, H., Lebrun, M., & Thomine, S. (2014). The metal transporter PgIREG1 from the hyperaccumulator Psychotria gabriellae is a candidate gene for nickel tolerance and accumulation. *Journal of Experimental Botany*, *65*(6), 1551–1564. https://doi.org/10.1093/jxb/eru025

Milner, M. J., Craft, E., Yamaji, N., Koyama, E., Ma, J. F., & Kochian, L. V. (2012). Characterization of the high affinity Zn transporter from Noccaea caerulescens, NcZNT1, and dissection of its promoter for its role in Zn uptake and hyperaccumulation. *New Phytologist*, *195*(1), 113–123. https://doi.org/10.1111/j.1469-8137.2012.04144.x

Milner, M. J., Mitani-Ueno, N., Yamaji, N., Yokosho, K., Craft, E., Fei, Z., Ebbs, S., Clemencia Zambrano, M., Ma, J. F., & Kochian, L. V. (2014). Root and shoot transcriptome analysis of two ecotypes ofNoccaea caerulescensuncovers the role ofNcNramp1in Cd hyperaccumulation. *The Plant Journal*, *78*(3), 398–410. https://doi.org/10.1111/tpj.12480

Mira, H., Martínez-García, F., & Peñarrubia, L. (2001). Evidence for the plant-specific intercellular transport of the Arabidopsis copper chaperone CCH. *The Plant Journal*, *25*(5), 521–528. https://doi.org/10.1046/j.1365-313x.2001.00985.x

Miri, M., Ehrampoush, M. H., Reza Ghaffari, H., Aval, H. E., Rezai, M., Najafpour, F., Abaszadeh Fathabadi, Z., Aval, M. Y., & Ebrahimi, A. (2016). Atmospheric Heavy Metals Biomonitoring Using a Local Pinus eldarica Tree. *Health Scope*, *6*(1). https://doi.org/10.17795/jhealthscope-39241

Mnasri, M., Ghabriche, R., Fourati, E., Zaier, H., Sabally, K., Barrington, S., Lutts, S., Abdelly, C., & Ghnaya, T. (2015). Cd and Ni transport and accumulation in the halophyte Sesuvium portulacastrum: Implication of organic acids in these processes. *Frontiers in Plant Science*, *6*. https://doi.org/10.3389/fpls.2015.00156

Moarefi, N., & Nkongolo, K. K. (2022). Contrasting tolerance and gene expression between white pine (Pinus strobus) and jack pine (P. banksiana) exposed to an increasing nickel concentration. *Ecological Genetics and Genomics*, *24*, 100124. https://doi.org/10.1016/j.egg.2022.100124

Mohanty, N., Vass, I., & Demeter, S. (1989). Impairment of photosystem 2 activity at the level of secondary quinone electron acceptor in chloroplasts treated with cobalt, nickel and zinc ions. *Physiologia Plantarum*, *76*(3), 386–390. https://doi.org/10.1111/j.1399-3054.1989.tb06208.x

Montiel-Rozas, M. M., Madejón, E., & Madejón, P. (2016). Effect of heavy metals and organic matter on root exudates (low molecular weight organic acids) of herbaceous species: An assessment in sand and soil conditions under different levels of contamination. *Environmental Pollution*, *216*, 273–281. https://doi.org/10.1016/j.envpol.2016.05.080

Moody, J. E., Millen, L., Binns, D., Hunt, J. F., & Thomas, P. J. (2002). Cooperative, ATP-dependent Association of the Nucleotide Binding Cassettes during the Catalytic Cycle of ATP-binding Cassette Transporters *. *Journal of Biological Chemistry*, *277*(24), 21111–21114. https://doi.org/10.1074/jbc.C200228200

Moons, A. (2003). Ospdr9, which encodes a PDR-type ABC transporter, is induced by heavy metals, hypoxic stress and redox perturbations in rice roots 1. *FEBS Letters*, *553*(3), 370–376. https://doi.org/10.1016/S0014-5793(03)01060-3

Morel, M., Crouzet, J., Gravot, A., Auroy, P., Leonhardt, N., Vavasseur, A., & Richaud, P. (2008). AtHMA3, a P1B-ATPase Allowing Cd/Zn/Co/Pb Vacuolar Storage in Arabidopsis. *Plant Physiology*, *149*(2), 894–904. https://doi.org/10.1104/pp.108.130294

Morita, A., Yanagisawa, O., Takatsu, S., Maeda, S., & Hiradate, S. (2008). Mechanism for the detoxification of aluminum in roots of tea plant (Camellia sinensis (L.) Kuntze). *Phytochemistry*, *69*(1), 147–153. https://doi.org/10.1016/j.phytochem.2007.06.007

Mostofa, M. G., & Fujita, M. (2013). Salicylic acid alleviates copper toxicity in rice (Oryza sativa L.) seedlings by up-regulating antioxidative and glyoxalase systems. *Ecotoxicology*, *22*(6), 959–973. https://doi.org/10.1007/s10646-013-1073-x

Możdżeń, K., Wanic, T., Rut, G., Łaciak, T., & Rzepka, A. (2017). Toxic effects of high copper content on physiological processes in Pinus sylvestris L. *Photosynthetica*, *55*(1), 193–200. https://doi.org/10.1007/s11099-016-0229-3

Muhlemann, J. K., Younts, T. L. B., & Muday, G. K. (2018). Flavonols control pollen tube growth and integrity by regulating ROS homeostasis during high-temperature stress. *Proceedings of the National Academy of Sciences*, *115*(47), E11188–E11197. https://doi.org/10.1073/pnas.1811492115

Mukta, R. H., Khatun, M. R., & Nazmul Huda, A. K. M. (2019). Calcium induces phytochelatin accumulation to cope with chromium toxicity in rice (*Oryza sativa* L.). *Journal of Plant Interactions*, *14*(1), 295–302. https://doi.org/10.1080/17429145.2019.1629034

Muniz, P., Danulat, E., Yannicelli, B., García-Alonso, J., Medina, G., & Bícego, M. C. (2004). Assessment of contamination by heavy metals and petroleum hydrocarbons in sediments of Montevideo Harbour (Uruguay). *Environment International*, *29*(8), 1019–1028. https://doi.org/10.1016/S0160-4120(03)00096-5

Nag, K., & Joardar, D. S. (1976). Metal complexes of sulfur–nitrogen chelating agents. V. 2-N-Ethylaminocyclopentene-1-dithiocarboxylic acid complexes of Ni(II), Pd(II), Pt(II), Co(II), Co(III), and Cu(I). *Canadian Journal of Chemistry*, *54*(17), 2827–2831. https://doi.org/10.1139/v76-400

Nair, P. M., Gopalakrishnan, & Chung, I. M. (2014). Impact of copper oxide nanoparticles exposure on Arabidopsis thaliana growth, root system development, root lignificaion, and molecular level changes. *Environmental Science and Pollution Research International*, *21*(22), 12709–12722. https://doi.org/10.1007/s11356-014-3210-3

Nakamura, Y., Awai, K., Masuda, T., Yoshioka, Y., Takamiya, K., & Ohta, H. (2005). A Novel Phosphatidylcholine-hydrolyzing Phospholipase C Induced by Phosphate Starvation in Arabidopsis*. *Journal of Biological Chemistry*, *280*(9), 7469–7476. https://doi.org/10.1074/jbc.M408799200

Narendrula, R., Nkongolo, K. K., & Beckett, P. (2011). Comparative Soil Metal Analyses in Sudbury (Ontario, Canada) and Lubumbashi (Katanga, DR-Congo). *Bulletin of Environmental Contamination and Toxicology*, *88*(2), 187–192. https://doi.org/10.1007/s00128-011-0485-7

Natasha, Shahid, M., Saleem, M., Anwar, H., Khalid, S., Tariq, T. Z., Murtaza, B., Amjad, M., & Naeem, M. A. (2020). A multivariate analysis of comparative effects of heavy metals on cellular biomarkers of phytoremediation using Brassica oleracea. *International Journal of Phytoremediation*, *22*(6), 617–627. https://doi.org/10.1080/15226514.2019.1701980

Nazir, F., Hussain, A., & Fariduddin, Q. (2019). Interactive role of epibrassinolide and hydrogen peroxide in regulating stomatal physiology, root morphology, photosynthetic and growth traits in Solanum lycopersicum L. under nickel stress. *Environmental and Experimental Botany*, *162*, 479–495. https://doi.org/10.1016/j.envexpbot.2019.03.021

Negin, B., Yaaran, A., Kelly, G., Zait, Y., & Moshelion, M. (2019). Mesophyll Abscisic Acid Restrains Early Growth and Flowering But Does Not Directly Suppress Photosynthesis. *Plant Physiology*, *180*(2), 910–925. https://doi.org/10.1104/pp.18.01334

Nematollahi, W. P., & Roux, S. J. (1999). A Novel β-Glucosidase from the Cell Wall of Maize (Zea mays L.): Rapid Purification and Partial Characterization. *Journal of Plant Physiology*, *155*(4), 462–469. https://doi.org/10.1016/S0176-1617(99)80040-6

Ngo, A. H., Lin, Y.-C., Liu, Y., Gutbrod, K., Peisker, H., Dörmann, P., & Nakamura, Y. (2018). A pair of nonspecific phospholipases C, NPC2 and NPC6, are involved in gametophyte development and glycerolipid metabolism in Arabidopsis. *New Phytologist*, *219*(1), 163–175. https://doi.org/10.1111/nph.15147

Ngu, T. T., Krecisz, S., & Stillman, M. J. (2010). Bismuth binding studies to the human metallothionein using electrospray mass spectrometry. *Biochemical and Biophysical Research Communications*, *396*(2), 206–212. https://doi.org/10.1016/j.bbrc.2010.04.053

Nguyen, C., Soulier, A. J., Masson, P., Bussière, S., & Cornu, J. Y. (2016). Accumulation of Cd, Cu and Zn in shoots of maize (Zea mays L.) exposed to 0.8 or 20 nM Cd during vegetative growth and the relation with xylem sap composition. *Environmental Science and Pollution Research*, *23*(4), 3152–3164. https://doi.org/10.1007/s11356-015-5782-y

Nishida, S., Kato, A., Tsuzuki, C., Yoshida, J., & Mizuno, T. (2015). Induction of Nickel Accumulation in Response to Zinc Deficiency in Arabidopsis thaliana. *International Journal of Molecular Sciences*, *16*(12), 9420–9430. https://doi.org/10.3390/ijms16059420

Nishida, S., Tanikawa, R., Ishida, S., Yoshida, J., Mizuno, T., Nakanishi, H., & Furuta, N. (2020). Elevated Expression of Vacuolar Nickel Transporter Gene IREG2 Is Associated With Reduced Root-to-Shoot Nickel Translocation in Noccaea japonica. *Frontiers in Plant Science*, *11*. https://doi.org/10.3389/fpls.2020.00610

Nishida, S., Tsuzuki, C., Kato, A., Aisu, A., Yoshida, J., & Mizuno, T. (2011). AtIRT1, the Primary Iron Uptake Transporter in the Root, Mediates Excess Nickel Accumulation in Arabidopsis thaliana. *Plant and Cell Physiology*, *52*(8), 1433–1442. https://doi.org/10.1093/pcp/pcr089

Nkongolo, K. K., Spiers, G., Beckett, P., Narendrula, R., Theriault, G., Tran, A., & Kalubi, K. N. (2013). Long-Term Effects of Liming on Soil Chemistry in Stable and Eroded Upland Areas in a Mining Region. *Water, Air, & Soil Pollution*, *224*(7), 1618. https://doi.org/10.1007/s11270-013-1618-x

Nkongolo, K., Theriault, G., & Michael, P. (2018). Differential levels of gene expression and molecular mechanisms between red maple (*Acer rubrum*) genotypes resistant and susceptible to nickel toxicity revealed by transcriptome analysis. *Ecology and Evolution*, *8*(10), 4876–4890. https://doi.org/10.1002/ece3.4045

Noir, S., Bömer, M., Takahashi, N., Ishida, T., Tsui, T.-L., Balbi, V., Shanahan, H., Sugimoto, K., & Devoto, A. (2013). Jasmonate Controls Leaf Growth by Repressing Cell Proliferation and the Onset of Endoreduplication while Maintaining a Potential Stand-By Mode. *Plant Physiology*, *161*(4), 1930–1951. https://doi.org/10.1104/pp.113.214908

Nouet, C., Charlier, J.-B., Carnol, M., Bosman, B., Farnir, F., Motte, P., & Hanikenne, M. (2015). Functional analysis of the threeHMA4copies of the metal hyperaccumulatorArabidopsis halleri. *Journal of Experimental Botany*, *66*(19), 5783–5795. https://doi.org/10.1093/jxb/erv280

Ogasawara, F., Kodan, A., & Ueda, K. (2020). ABC proteins in evolution. *FEBS Letters*, *594*(23), 3876–3881. https://doi.org/10.1002/1873-3468.13945

Ohara, T., Takeuchi, H., Sato, J., Nakamura, A., Ichikawa, H., Yokoyama, R., Nishitani, K., Minami, E., Satoh, S., & Iwai, H. (2021). Structural Alteration of Rice Pectin Affects Cell Wall Mechanical Strength and Pathogenicity of the Rice Blast Fungus Under Weak Light Conditions. *Plant and Cell Physiology*, *62*(4), 641–649. https://doi.org/10.1093/pcp/pcab019

Oorts, K. (2013). Copper. In B. J. Alloway (Ed.), *Heavy Metals in Soils* (Vol. 22, pp. 367–394). Springer Netherlands. https://doi.org/10.1007/978-94-007-4470-7_13

Opdenakker, K., Remans, T., Keunen, E., Vangronsveld, J., & Cuypers, A. (2012). Exposure of Arabidopsis thaliana to Cd or Cu excess leads to oxidative stress mediated alterations in MAPKinase transcript levels. *Environmental and Experimental Botany*, *83*, 53–61. https://doi.org/10.1016/j.envexpbot.2012.04.003

Orfila, C., Huisman, M. M., Willats, W. G., van Alebeek, G.-J. W., Schols, H. A., Seymour, G. B., & Knox, P. J. (2002). Altered cell wall disassembly during ripening of Cnr tomato fruit: Implications for cell adhesion and fruit softening. *Planta*, *215*(3), 440–447. https://doi.org/10.1007/s00425-002-0753-1

Ouzounidou, G., Asfi, M., Sotirakis, N., Papadopoulou, P., & Gaitis, F. (2008). Olive mill wastewater triggered changes in physiology and nutritional quality of tomato (Lycopersicon esculentum Mill.) depending on growth substrate. *Journal of Hazardous Materials*, *158*(2), 523–530. https://doi.org/10.1016/j.jhazmat.2008.01.100

Pabian, S. E., Rummel, S. M., Sharpe, W. E., & Brittingham, M. C. (2012). Terrestrial Liming As a Restoration Technique for Acidified Forest Ecosystems. *International Journal of Forestry Research*, *2012*, 1–10. https://doi.org/10.1155/2012/976809

Page, V., & Feller, U. (2005). Selective Transport of Zinc, Manganese, Nickel, Cobalt and Cadmium in the Root System and Transfer to the Leaves in Young Wheat Plants. *Annals of Botany*, *96*(3), 425–434. https://doi.org/10.1093/aob/mci189

Panou-Filotheou, H. (2001). Effects of Copper Toxicity on Leaves of Oregano (Origanum vulgare subsp. Hirtum). *Annals of Botany*, *88*(2), 207–214. https://doi.org/10.1006/anbo.2001.1441

Park, Y. C., Moon, J.-C., Chapagain, S., Oh, D. G., Kim, J. J., & Jang, C. S. (2018). Role of salt-induced RING finger protein 3 (OsSIRP3), a negative regulator of salinity stress response by modulating the level of its target proteins. *Environmental and Experimental Botany*, *155*, 21–30. https://doi.org/10.1016/j.envexpbot.2018.06.017

Parker, G. H. (2004). Tissue metal levels in Muskrat (Ondatra zibethica) collected near the Sudbury (Ontario) ore-smelters; prospects for biomonitoring marsh pollution. *Environmental Pollution*, *129*(1), 23–30. https://doi.org/10.1016/j.envpol.2003.10.003

Pätsikkä, E., Kairavuo, M., Šeršen, F., Aro, E.-M., & Tyystjärvi, E. (2002). Excess Copper Predisposes Photosystem II to Photoinhibition in Vivo by Outcompeting Iron and Causing Decrease in Leaf Chlorophyll. *Plant Physiology*, *129*(3), 1359–1367. https://doi.org/10.1104/pp.004788

Pavlova, D. (2017). Nickel effect on root-meristem cell division in Plantago lanceolata (Plantaginaceae) seedlings. *Australian Journal of Botany*, *65*(5), 446. https://doi.org/10.1071/bt17054

Pawlik-Skowronska, B., di Toppi, L. S., Favali, M. A., Fossati, F., Pirszel, J., & Skowronski, T. (2002). Lichens respond to heavy metals by phytochelatin synthesis. *New Phytologist*, *156*(1), 95–102. https://doi.org/10.1046/j.1469-8137.2002.00498.x

Pazalja, M., Salihović, M., Sulejmanović, J., Smajović, A., Begić, S., Špirtović-Halilović, S., & Sher, F. (2021). Heavy metals content in ashes of wood pellets and the health risk assessment related to their presence in the environment. *Scientific Reports*, *11*(1), Article 1. https://doi.org/10.1038/s41598-021-97305-4

Persans, M. W., Nieman, K., & Salt, D. E. (2001). Functional activity and role of cation-efflux family members in Ni hyperaccumulation in Thlaspi goesingense. *Proceedings of the National Academy of Sciences, 98*(17), 9995–10000. https://doi.org/10.1073/pnas.171039798

Peters, C., Li, M., Narasimhan, R., Roth, M., Welti, R., & Wang, X. (2010). Nonspecific Phospholipase C NPC4 Promotes Responses to Abscisic Acid and Tolerance to Hyperosmotic Stress in Arabidopsis. *The Plant Cell*, *22*(8), 2642–2659. https://doi.org/10.1105/tpc.109.071720

Pető, A., Lehotai, N., Lozano-Juste, J., León, J., Tari, I., Erdei, L., & Kolbert, Z. (2011). Involvement of nitric oxide and auxin in signal transduction of copper-induced morphological responses in Arabidopsis seedlings. *Annals of Botany*, *108*(3), 449–457. https://doi.org/10.1093/aob/mcr176

Pianelli, K., Mari, S., Marquès, L., Lebrun, M., & Czernic, P. (2005). Nicotianamine Over-accumulation Confers Resistance to Nickel in Arabidopsis thaliana. *Transgenic Research*, *14*(5), 739–748. https://doi.org/10.1007/s11248-005-7159-3

Picault, N., Cazalé, A. C., Beyly, A., Cuiné, S., Carrier, P., Luu, D. T., Forestier, C., & Peltier, G. (2006). Chloroplast targeting of phytochelatin synthase in Arabidopsis: Effects on heavy metal tolerance and accumulation. *Biochimie*, *88*(11), 1743–1750. https://doi.org/10.1016/j.biochi.2006.04.016

Pierman, B., Toussaint, F., Bertin, A., Lévy, D., Smargiasso, N., De Pauw, E., & Boutry, M. (2017). Activity of the purified plant ABC transporter NtPDR1 is stimulated by diterpenes and sesquiterpenes involved in constitutive and induced defenses. *Journal of Biological Chemistry*, *292*(47), 19491–19502. https://doi.org/10.1074/jbc.M117.811935

Pisaric, M. F. J., St-Onge, S. M., & Kokelj, S. V. (2009). Tree-ring Reconstruction of Early-growing Season Precipitation from Yellowknife, Northwest Territories, Canada. *Arctic, Antarctic, and Alpine Research*, *41*(4), 486–496. https://doi.org/10.1657/1938-4246-41.4.486

Pollard, A. J., Reeves, R. D., & Baker, A. J. M. (2014). Facultative hyperaccumulation of heavy metals and metalloids. *Plant Science*, *217–218*, 8–17. https://doi.org/10.1016/j.plantsci.2013.11.011

Qi, Z.-Y., Ahammed, G. J., Jiang, C.-Y., Li, C.-X., & Zhou, J. (2020). The E3 ubiquitin ligase gene SlRING1 is essential for plant tolerance to cadmium stress in Solanum lycopersicum. *Journal of Biotechnology*, *324*, 239–247. https://doi.org/10.1016/j.jbiotec.2020.11.008

Qin, T., Tian, Q., Wang, G., & Xiong, L. (2019). LOWER TEMPERATURE 1 Enhances ABA Responses and Plant Drought Tolerance by Modulating the Stability and Localization of C2-Domain ABA-Related Proteins in Arabidopsis. *Molecular Plant*, *12*(9), 1243–1258. https://doi.org/10.1016/j.molp.2019.05.002

R. Benatti, M., Yookongkaew, N., Meetam, M., Guo, W., Punyasuk, N., AbuQamar, S., & Goldsbrough, P. (2014). Metallothionein deficiency impacts copper accumulation and redistribution in leaves and seeds of A rabidopsis. *New Phytologist*, *202*(3), 940–951. https://doi.org/10.1111/nph.12718

Radisky, E. S., Lee, J. M., Lu, C.-J. K., & Koshland, D. E. (2006). Insights into the serine protease mechanism from atomic resolution structures of trypsin reaction intermediates. *Proceedings of the National Academy of Sciences*, *103*(18), 6835–6840. https://doi.org/10.1073/pnas.0601910103

Rahman, H., Sabreen, S., Alam, S., & Kawai, S. (2005). Effects of Nickel on Growth and Composition of Metal Micronutrients in Barley Plants Grown in Nutrient Solution. *Journal of Plant Nutrition*, *28*(3), 393–404. https://doi.org/10.1081/PLN-200049149

Rahmati Ishka, M., & Vatamaniuk, O. K. (2020). Copper deficiency alters shoot architecture and reduces fertility of both gynoecium and androecium in Arabidopsis thaliana. *Plant Direct*, *4*(11). https://doi.org/10.1002/pld3.288

Rakwal, R., & Komatsu, S. (2001). Jasmonic acid-induced necrosis and drastic decreases in ribulose-1,5-bisphosphate carboxylase/oxygenase in rice seedlings under light involves reactive oxygen species. *Journal of Plant Physiology*, *158*(6), 679–688. https://doi.org/10.1078/0176-1617-00372

Ramos, J., Naya, L., Gay, M., Abián, J., & Becana, M. (2008). Functional Characterization of an Unusual Phytochelatin Synthase, LjPCS3, of Lotus japonicus. *Plant Physiology*, *148*(1), 536–545. https://doi.org/10.1104/pp.108.121715

Ranger, M., Nkongolo, K. K., Michael, P., & Beckett, P. (2008). Genetic Differentiation of Jack Pine (Pinus banksiana) and Red Pine (P. resinosa) Populations From Metal Contaminated Areas in Northern Ontario (Canada) Using ISSR Markers. *Silvae Genetica*, *57*(1–6), 333–340. https://doi.org/10.1515/sg-2008-0049

Ranocha, P., Dima, O., Nagy, R., Felten, J., Corratgé-Faillie, C., Novák, O., Morreel, K., Lacombe, B., Martinez, Y., Pfrunder, S., Jin, X., Renou, J.-P., Thibaud, J.-B., Ljung, K., Fischer, U., Martinoia, E., Boerjan, W., & Goffner, D. (2013). Arabidopsis WAT1 is a vacuolar auxin transport facilitator required for auxin homoeostasis. *Nature Communications*, *4*(1), Article 1. https://doi.org/10.1038/ncomms3625

Rastogi, A., Al-Abed, S. R., & Dionysiou, D. D. (2009). Effect of inorganic, synthetic and naturally occurring chelating agents on Fe(II) mediated advanced oxidation of chlorophenols. *Water Research*, *43*(3), 684–694. https://doi.org/10.1016/j.watres.2008.10.045

Reich, P. B., Rich, R. L., Lu, X., Wang, Y.-P., & Oleksyn, J. (2014). Biogeographic variation in evergreen conifer needle longevity and impacts on boreal forest carbon cycle projections. *Proceedings of the National Academy of Sciences*, *111*(38), 13703–13708. https://doi.org/10.1073/pnas.1216054110

Reis, A. R. dos, de Queiroz Barcelos, J. P., de Souza Osório, C. R. W., Santos, E. F., Lisboa, L. A. M., Santini, J. M. K., dos Santos, M. J. D., Furlani Junior, E., Campos, M., de Figueiredo, P. A. M., Lavres, J., & Gratão, P. L. (2017). A glimpse into the physiological, biochemical and nutritional status of soybean plants under Ni-stress conditions. *Environmental and Experimental Botany*, *144*, 76–87. https://doi.org/10.1016/j.envexpbot.2017.10.006

Ren, C., Qi, Y., Huang, G., Yao, S., You, J., & Hu, H. (2020). Contributions of root cell wall polysaccharides to Cu sequestration in castor (Ricinus communis L.) exposed to different Cu stresses. *Journal of Environmental Sciences*, *88*, 209–216. https://doi.org/10.1016/j.jes.2019.08.012

Riesen, O., & Feller, U. (2005). Redistribution of Nickel, Cobalt, Manganese, Zinc, and Cadmium via the Phloem in Young and Maturing Wheat. *Journal of Plant Nutrition*, *28*(3), 421–430. https://doi.org/10.1081/PLN-200049153

Rizvi, A., & Khan, M. S. (2019). Heavy metal-mediated toxicity to maize: Oxidative damage, antioxidant defence response and metal distribution in plant organs. *International Journal of Environmental Science and Technology*, *16*(8), 4873–4886. https://doi.org/10.1007/s13762-018-1916-3

Rizwan, M., Imtiaz, M., Dai, Z., Mehmood, S., Adeel, M., Liu, J., & Tu, S. (2017). Nickel stressed responses of rice in Ni subcellular distribution, antioxidant production, and osmolyte accumulation. *Environmental Science and Pollution Research*, *24*(25), 20587–20598. https://doi.org/10.1007/s11356-017-9665-2

Robson, A. D., Hartley, R. D., & Jarvis, S. C. (1981). Effect of Copper Deficiency on Phenolic and Other Constituents of Wheat Cell Walls. *New Phytologist*, *89*(3), 361–371. https://doi.org/10.1111/j.1469-8137.1981.tb02317.x

Romero, P., Gabrielli, A., Sampedro, R., Perea-García, A., Puig, S., & Lafuente, M. T. (2021). Identification and molecular characterization of the high-affinity copper transporters family in Solanum lycopersicum. *International Journal of Biological Macromolecules*, *192*, 600–610. https://doi.org/10.1016/j.ijbiomac.2021.10.032

Rosatto, S., Mariotti, M., Romeo, S., & Roccotiello, E. (2021). Root and Shoot Response to Nickel in Hyperaccumulator and Non-Hyperaccumulator Species. *Plants*, *10*(3), 508. https://doi.org/10.3390/plants10030508

Rousell, D. H., Fedorowich, J. S., & Dressler, B. O. (2003). Sudbury Breccia (Canada): A product of the 1850 Ma Sudbury Event and host to footwall Cu–Ni–PGE deposits. *Earth-Science Reviews*, *60*(3–4), 147–174. https://doi.org/10.1016/s0012-8252(02)00091-0

Rubio, M. I., Escrig, I., Martínez-Cortina, C., López-Benet, F. J., & Sanz, A. (1994). Cadmium and nickel accumulation in rice plants. Effects on mineral nutrition and possible interactions of abscisic and gibberellic acids. *Plant Growth Regulation*, *14*(2), 151–157. https://doi.org/10.1007/BF00025217

Rudolph, & Laidly. (1990). *Silvics of North America*. U.S. Government Printing Office.

Rumney, R. H. M., Preston, M. D., Jones, T., Basiliko, N., & Gunn, J. (2021). Soil amendment improves carbon sequestration by trees on severely damaged acid and metal impacted landscape, but total storage remains low. *Forest Ecology and Management*, *483*, 118896. https://doi.org/10.1016/j.foreco.2020.118896

Rutherford, J. E., & Mellow, R. J. (1994). The effects of an abandoned roast yard on the fish and macroinvertebrate communities of surrounding beaver ponds. *Hydrobiologia*, *294*(3), 219–228. https://doi.org/10.1007/bf00021295

Sabella, E., Aprile, A., Tenuzzo, B. A., Carata, E., Panzarini, E., Luvisi, A., De Bellis, L., & Vergine, M. (2022). Effects of Cadmium on Root Morpho-Physiology of Durum Wheat. *Frontiers in Plant Science*, *13*. https://doi.org/10.3389/fpls.2022.936020

Salinitro, M., Zappi, A., Casolari, S., Locatelli, M., Tassoni, A., & Melucci, D. (2022). The Design of Experiment as a Tool to Model Plant Trace-Metal Bioindication Abilities. *Molecules*, *27*(6), 1844. https://doi.org/10.3390/molecules27061844

Sancenón, V., Puig, S., Mateu-Andrés, I., Dorcey, E., Thiele, D. J., & Peñarrubia, L. (2004). The Arabidopsis Copper Transporter COPT1 Functions in Root Elongation and Pollen Development*. *Journal of Biological Chemistry*, *279*(15), 15348–15355. https://doi.org/10.1074/jbc.M313321200

Sánchez-Mata, D., de la Fuente, V., Rufo, L., Rodríguez, N., & Amils, R. (2013). Localization of Nickel in Tissues of Streptanthus polygaloides Gray (Cruciferae) and Endemic Nickel Hyperaccumulators from California. *Biological Trace Element Research*, *157*(1), 75–83. https://doi.org/10.1007/s12011-013-9868-4

Sasaki, I., & Nagayama, H. (1997). Induction of β-Glucosidase in Botrytis cinerea by Cell Wall Fractions of the Host Plant. *Bioscience, Biotechnology, and Biochemistry*, *61*(7), 1073–1076. https://doi.org/10.1271/bbb.61.1073

Sastre, I., Vicente, M. A., & Lobo, M. C. (2001). Behaviour of cadmium and nickel in a soil amended with sewage sludge. *Land Degradation & Development*, *12*(1), 27–33. https://doi.org/10.1002/ldr.421

Sautron, E., Mayerhofer, H., Giustini, C., Pro, D., Crouzy, S., Ravaud, S., Pebay-Peyroula, E., Rolland, N., Catty, P., & Seigneurin-Berny, D. (2015). HMA6 and HMA8 are two chloroplast Cu+-ATPases with different enzymatic properties. *Bioscience Reports*, *35*(3). https://doi.org/10.1042/bsr20150065

Sauvé, S., McBride, M. B., Norvell, W. A., & Hendershot, W. H. (1997). Copper Solubility and Speciation of In Situ Contaminated Soils: Effects of Copper Level, pH and Organic Matter. *Water, Air, and Soil Pollution*, *100*(1), 133–149. https://doi.org/10.1023/A:1018312109677

Schaaf, G., Honsbein, A., Meda, A. R., Kirchner, S., Wipf, D., & von Wirén, N. (2006). AtIREG2 Encodes a Tonoplast Transport Protein Involved in Iron-dependent Nickel Detoxification in Arabidopsis thaliana Roots. *Journal of Biological Chemistry*, *281*(35), 25532–25540. https://doi.org/10.1074/jbc.m601062200

Scheiber, I. F., Pilátová, J., Malych, R., Kotabova, E., Krijt, M., Vyoral, D., Mach, J., Léger, T., Camadro, J.-M., Prášil, O., Lesuisse, E., & Sutak, R. (2019). Copper and iron metabolism in Ostreococcus tauri – the role of phytotransferrin, plastocyanin and a chloroplast copper-transporting ATPase. *Metallomics*, *11*(10), 1657–1666. https://doi.org/10.1039/c9mt00078j

Schindler, M. (2014). A mineralogical and geochemical study of slag from the historical O'Donnell roast yards, Sudbury, Ontario, Canada. *The Canadian Mineralogist*, *52*(3), 433–452. https://doi.org/10.3749/canmin.52.3.433

Schreffler, A. M., & Sharpe, W. E. (2003). Effects of lime, fertilizer, and herbicide on forest soil and soil solution chemistry, hardwood regeneration, and hardwood growth following shelterwood harvest. *Forest Ecology and Management*, *177*(1–3), 471–484. https://doi.org/10.1016/S0378-1127(02)00452-8

Schützendübel, A., & Polle, A. (2002). Plant responses to abiotic stresses: Heavy metal-induced oxidative stress and protection by mycorrhization. *Journal of Experimental Botany*, *53*(372), 1351–1365. https://doi.org/10.1093/jxb/53.372.1351

Seigneurin-Berny, D., Gravot, A., Auroy, P., Mazard, C., Kraut, A., Finazzi, G., Grunwald, D., Rappaport, F., Vavasseur, A., Joyard, J., Richaud, P., & Rolland, N. (2006). HMA1, a New Cu-ATPase of the Chloro plast Envelope, Is Essential for Growth under Adverse Light Conditions. *Journal of Biological Chemistry*, *281*(5), 2882–2892. https://doi.org/10.1074/jbc.m508333200

Seliga, H. (1999). Antioxidative activity of copper in root nodules of yellow lupin plants. *Acta Physiologiae Plantarum*, *21*(4), 427–431. https://doi.org/10.1007/s11738-999-0016-x

Seregin, I. V., Erlikh, N. T., & Kozhevnikova, A. D. (2014). Nickel and zinc accumulation capacities and tolerance to these metals in the excluder Thlaspi arvense and the hyperaccumulator Noccaea caerulescens. *Russian Journal of Plant Physiology*, *61*(2), 204–214. https://doi.org/10.1134/s1021443714020137

Seregin, I. V., Kozhevnikova, A. D., Zhukovskaya, N. V., & Schat, H. (2015). Cadmium tolerance and accumulation in Excluder Thlaspi arvense and various accessions of hyperaccumulator Noccaea caerulescens. *Russian Journal of Plant Physiology*, *62*(6), 837–846. https://doi.org/10.1134/s1021443715050131

Shahbaz, M., Ravet, K., Peers, G., & Pilon, M. (2015). Prioritization of copper for the use in photosynthetic electron transport in developing leaves of hybrid poplar. *Frontiers in Plant Science*, *6*. https://doi.org/10.3389/fpls.2015.00407

Sharma, E., Anand, G., & Kapoor, R. (2017). Terpenoids in plant and arbuscular mycorrhiza-reinforced defence against herbivorous insects. *Annals of Botany*, *119*(5), 791–801. https://doi.org/10.1093/aob/mcw263

Sharma, R., Bhardwaj, R., Thukral, A. K., Al-Huqail, A. A., Siddiqui, M. H., & Ahmad, P. (2019). Oxidative stress mitigation and initiation of antioxidant and osmoprotectant responses mediated by ascorbic acid in Brassica juncea L. subjected to copper (II) stress. *Ecotoxicology and Environmental Safety*, *182*, 109436. https://doi.org/10.1016/j.ecoenv.2019.109436

Sharpe, M., Hwang, H., Schroeder, D., Ryu, S. R., & Lieffers, V. J. (2017). Prescribed fire as a tool to regenerate live and dead serotinous jack pine (Pinus banksiana) stands. *International Journal of Wildland Fire*, *26*(6), 478. https://doi.org/10.1071/wf17046

Shikanai, T., Müller-Moulé, P., Munekage, Y., Niyogi, K. K., & Pilon, M. (2003). PAA1, a P-Type ATPase of Arabidopsis, Functions in Copper Transport in Chloroplasts. *The Plant Cell*, *15*(6), 1333–1346. https://doi.org/10.1105/tpc.011817

Shimomura, S. (2006). Identification of a Glycosylphosphatidylinositol-anchored Plasma Membrane Protein Interacting with the C-terminus of Auxin-binding Protein 1: A Photoaffinity Crosslinking Study. *Plant Molecular Biology*, *60*(5), 663–677. https://doi.org/10.1007/s11103-005-5471-1

Shin, L.-J., Lo, J.-C., & Yeh, K.-C. (2012). Copper Chaperone Antioxidant Protein1 Is Essential for Copper Homeostasis. *Plant Physiology*, *159*(3), 1099–1110. https://doi.org/10.1104/pp.112.195974

Shukla, T., Khare, R., Kumar, S., Lakhwani, D., Sharma, D., Asif, M. H., & Trivedi, P. K. (2018). Differential transcriptome modulation leads to variation in arsenic stress response in Arabidopsis thaliana accessions. *Journal of Hazardous Materials*, *351*, 1–10. https://doi.org/10.1016/j.jhazmat.2018.02.031

Sinha, P., Shukla, A. K., & Sharma, Y. K. (2015). Amelioration of Heavy-Metal Toxicity in Cauliflower by Application of Salicylic Acid. *Communications in Soil Science and Plant Analysis*, *46*(10), 1309–1319. https://doi.org/10.1080/00103624.2015.1033543

Siqueira Freitas, D., Wurr Rodak, B., Rodrigues dos Reis, A., de Barros Reis, F., Soares de Carvalho, T., Schulze, J., Carbone Carneiro, M. A., & Guimarães Guilherme, L. R. (2018). Hidden Nickel Deficiency? Nickel Fertilization via Soil Improves Nitrogen Metabolism and Grain Yield in Soybean Genotypes. *Frontiers in Plant Science*, *9*. https://doi.org/10.3389/fpls.2018.00614

Sirhindi, G., Mir, M. A., Abd-Allah, E. F., Ahmad, P., & Gucel, S. (2016). Jasmonic Acid Modulates the Physio-Biochemical Attributes, Antioxidant Enzyme Activity, and Gene Expression in Glycine max under Nickel Toxicity. *Frontiers in Plant Science*, *7*, 591. https://doi.org/10.3389/fpls.2016.00591

Siriwong, W., Amonpattaratkit, P., & Klysubun, W. (2020). XAS analysis of copper binding in soils. *Journal of Metals, Materials and Minerals*, *30*(2). https://doi.org/10.55713/jmmm.v30i2.646

Siwko, M. E., Marrink, S. J., de Vries, A. H., Kozubek, A., Schoot Uiterkamp, A. J. M., & Mark, A. E. (2007). Does isoprene protect plant membranes from thermal shock? A molecular dynamics study. *Biochimica et Biophysica Acta (BBA) - Biomembranes*, *1768*(2), 198–206. https://doi.org/10.1016/j.bbamem.2006.09.023

Smirnova, E., Marquis, V., Poirier, L., Aubert, Y., Zumsteg, J., Ménard, R., Miesch, L., & Heitz, T. (2017). Jasmonic Acid Oxidase 2 Hydroxylates Jasmonic Acid and Represses Basal Defense and Resistance Responses against Botrytis cinerea Infection. *Molecular Plant*, *10*(9), 1159–1173. https://doi.org/10.1016/j.molp.2017.07.010

Soares, M. R., Casagrande, J. C., & Mouta, E. R. (2011). Nickel adsorption by variable charge soils: Effect of pH and ionic strength. *Brazilian Archives of Biology and Technology*, *54*(1), 207–220. https://doi.org/10.1590/S1516-89132011000100025

Song, J., Yang, Y. Q., Zhu, S. H., Chen, G. C., Yuan, X. F., Liu, T. T., Yu, X. H., & Shi, J. Y. (2013). Spatial distribution and speciation of copper in root tips of cucumber revealed by μ-XRF and μ-XANES. *Biologia Plantarum*, *57*(3), 581–586. https://doi.org/10.1007/s10535-013-0317-1

Song, W.-Y., Yamaki, T., Yamaji, N., Ko, D., Jung, K.-H., Fujii-Kashino, M., An, G., Martinoia, E., Lee, Y., & Ma, J. F. (2014). A rice ABC transporter, OsABCC1, reduces arsenic accumulation in the grain. *Proceedings of the National Academy of Sciences*, *111*(44), 15699–15704. https://doi.org/10.1073/pnas.1414968111

Song, X.-Q., Liu, L.-F., Jiang, Y.-J., Zhang, B.-C., Gao, Y.-P., Liu, X.-L., Lin, Q.-S., Ling, H.-Q., & Zhou, Y.-H. (2013). Disruption of Secondary Wall Cellulose Biosynthesis Alters Cadmium Translocation and Tolerance in Rice Plants. *Molecular Plant*, *6*(3), 768–780. https://doi.org/10.1093/mp/sst025

Song, Y., Zhou, L., Yang, S., Wang, C., Zhang, T., & Wang, J. (2017). Dose-dependent sensitivity of Arabidopsis thaliana seedling root to copper is regulated by auxin homeostasis. *Environmental and Experimental Botany*, *139*, 23–30. https://doi.org/10.1016/j.envexpbot.2017.04.003

Stearns, J. C., Shah, S., Greenberg, B. M., Dixon, D. G., & Glick, B. R. (2005). Tolerance of transgenic canola expressing 1-aminocyclopropane-1-carboxylic acid deaminase to growth inhibition by nickel. *Plant Physiology and Biochemistry*, *43*(7), 701–708. https://doi.org/10.1016/j.plaphy.2005.05.010

Stolarska, A., Wrobel, J., Wozniak, A., & Marska, B. (2007). Effect of zinc and copper soil contamination on the transpiration intensity and stomal index of winter crop wheat seedlings. *Journal of Elementology*, *12*(1). http://agro.icm.edu.pl/agro/element/bwmeta1.element.agro-article-5a60db0b-4547-417b-845b-4322d69799bc

Sun, Y., Ji, K., Liang, B., Du, Y., Jiang, L., Wang, J., Kai, W., Zhang, Y., Zhai, X., Chen, P., Wang, H., & Leng, P. (2017). Suppressing ABA uridine diphosphate glucosyltransferase (SlUGT75C1) alters fruit ripening and the stress response in tomato. *The Plant Journal*, *91*(4), 574–589. https://doi.org/10.1111/tpj.13588

Suresh, K., Zeisler-Diehl, V. V., Wojciechowski, T., & Schreiber, L. (2022). Comparing anatomy, chemical composition, and water permeability of suberized organs in five plant species: Wax makes the difference. *Planta*, *256*(3), 1–13. https://doi.org/10.1007/s00425-022-03975-3

Suzuki, N., Yamaguchi, Y., Koizumi, N., & Sano, H. (2002). Functional characterization of a heavy metal binding protein CdI19 from Arabidopsis. *The Plant Journal*, *32*(2), 165–173. https://doi.org/10.1046/j.1365-313X.2002.01412.x

Szunyog, G., Laskai, A., Szűcs, D., Sóvágó, I., & Várnagy, K. (2019). A comparative study on the nickel binding ability of peptides containing separate cysteinyl residues. *Dalton Transactions*, *48*(44), 16800–16811. https://doi.org/10.1039/c9dt03055g

Takos, A. M., Ubi, B. E., Robinson, S. P., & Walker, A. R. (2006). Condensed tannin biosynthesis genes are regulated separately from other flavonoid biosynthesis genes in apple fruit skin. *Plant Science*, *170*(3), 487–499. https://doi.org/10.1016/j.plantsci.2005.10.001

Tan, H., Man, C., Xie, Y., Yan, J., Chu, J., & Huang, J. (2019). A Crucial Role of GA-Regulated Flavonol Biosynthesis in Root Growth of Arabidopsis. *Molecular Plant*, *12*(4), 521–537. https://doi.org/10.1016/j.molp.2018.12.021

Tan, P., Zeng, C., Wan, C., Liu, Z., Dong, X., Peng, J., Lin, H., Li, M., Liu, Z., & Yan, M. (2021). Metabolic Profiles of Brassica juncea Roots in Response to Cadmium Stress. *Metabolites*, *11*(6), 383. https://doi.org/10.3390/metabo11060383

Tan, X. W., Ikeda, H., & Oda, M. (2000). Effects of nickel concentration in the nutrient solution on the nitrogen assimilation and growth of tomato seedlings in hydroponic culture supplied with urea or nitrate as the sole nitrogen source. *Scientia Horticulturae*, *84*(3–4), 265–273. https://doi.org/10.1016/s0304-4238(99)00107-7

Tao, L., Zeba, N., Ashrafuzzaman, M., & Hong, C. B. (2011). Heavy metal stress-inducible early light-inducible gene CaELIP from hot pepper (Capsicum annuum) shows broad expression patterns under various abiotic stresses and circadian rhythmicity. *Environmental and Experimental Botany*, *72*(2), 297–303. https://doi.org/10.1016/j.envexpbot.2011.04.009

Tao, Q., Jupa, R., Dong, Q., Yang, X., Liu, Y., Li, B., Yuan, S., Yin, J., Xu, Q., Li, T., & Wang, C. (2021). Abscisic acid-mediated modifications in water transport continuum are involved in cadmium hyperaccumulation in Sedum alfredii. *Chemosphere*, *268*, 129339. https://doi.org/10.1016/j.chemosphere.2020.129339

Tapken, W., Kim, J., Nishimura, K., Wijk, K. J., & Pilon, M. (2014). The Clp protease system is required for copper ion-dependent turnover of the PAA 2/ HMA 8 copper transporter in chloroplasts. *New Phytologist*, *205*(2), 511–517. https://doi.org/10.1111/nph.13093

Tapken, W., Ravet, K., & Pilon, M. (2012). Plastocyanin Controls the Stabilization of the Thylakoid Cu-transporting P-type ATPase PAA2/HMA8 in Response to Low Copper in Arabidopsis. *The Journal of Biological Chemistry*, *287*(22), 18544–18550. https://doi.org/10.1074/jbc.M111.318204

Tapken, W., Ravet, K., Shahbaz, M., & Pilon, M. (2015). Regulation of Cu delivery to chloroplast proteins. *Plant Signaling & Behavior*, *10*(7), e1046666. https://doi.org/10.1080/15592324.2015.1046666

Tavladoraki, P., Cona, A., & Angelini, R. (2016). Copper-Containing Amine Oxidases and FAD-Dependent Polyamine Oxidases Are Key Players in Plant Tissue Differentiation and Organ Development. *Frontiers in Plant Science*, *7*. https://doi.org/10.3389/fpls.2016.00824

Taylor, N. G., Gardiner, J. C., Whiteman, R., & Turner, S. R. (2004). Cellulose synthesis in the Arabidopsis secondary cell wall. *Cellulose*, *11*(3), 329–338. https://doi.org/10.1023/B:CELL.0000046405.11326.a8

Tchounwou, P. B., Yedjou, C. G., Patlolla, A. K., & Sutton, D. J. (2012). Heavy Metal Toxicity and the Environment. In A. Luch (Ed.), *Molecular, Clinical and Environmental Toxicology* (Vol. 101, pp. 133–164). Springer Basel. https://doi.org/10.1007/978-3-7643-8340-4_6

Tehseen, M., Cairns, N., Sherson, S., & Cobbett, C. S. (2010). Metallochaperone-like genes in Arabidopsis thaliana†. *Metallomics*, *2*(8), 556–564. https://doi.org/10.1039/c003484c

Teptina, A. Yu., & Paukov, A. G. (2015). Nickel accumulation by species of Alyssum and Noccaea (Brassicaceae) from ultramafic soils in the Urals, Russia. *Australian Journal of Botany*, *63*(2), 78. https://doi.org/10.1071/bt14265

Tewari, R. K., Kumar, P., & Sharma, P. N. (2006). Antioxidant responses to enhanced generation of superoxide anion radical and hydrogen peroxide in the copper-stressed mulberry plants. *Planta*, *223*(6), 1145–1153. https://doi.org/10.1007/s00425-005-0160-5

Thakur, S., & Sharma, S. S. (2015). Characterization of seed germination, seedling growth, and associated metabolic responses of Brassica juncea L. cultivars to elevated nickel concentrations. *Protoplasma*, *253*(2), 571–580. https://doi.org/10.1007/s00709-015-0835-0

The Gene Ontology Consortium. (2021). The Gene Ontology resource: Enriching a GOld mine. *Nucleic Acids Research*, *49*(D1), D325–D334. https://doi.org/10.1093/nar/gkaa1113

Theriault, G., Michael, P., & Nkongolo, K. (2016). Comprehensive Transcriptome Analysis of Response to Nickel Stress in White Birch (Betula papyrifera). *PLOS ONE*, *11*(4), e0153762. https://doi.org/10.1371/journal.pone.0153762

Thounaojam, T. C., Panda, P., Mazumdar, P., Kumar, D., Sharma, G. D., Sahoo, L., & Sanjib, P. (2012). Excess copper induced oxidative stress and response of antioxidants in rice. *Plant Physiology and Biochemistry*, *53*, 33–39. https://doi.org/10.1016/j.plaphy.2012.01.006

Tiberg, C., Sjöstedt, C., Persson, I., & Gustafsson, J. P. (2013). Phosphate effects on copper(II) and lead(II) sorption to ferrihydrite. *Geochimica et Cosmochimica Acta*, *120*, 140–157. https://doi.org/10.1016/j.gca.2013.06.012

Tubajika, K. M., & Damann, K. E. (2001). Sources of Resistance to Aflatoxin Production in Maize. *Journal of Agricultural and Food Chemistry*, *49*(5), 2652–2656. https://doi.org/10.1021/jf001333i

Tung, S. A., Smeeton, R., White, C. A., Black, C. R., Taylor, I. B., Hilton, H. W., & Thompson, A. J. (2008). Over-expression of LeNCED1 in tomato (Solanum lycopersicum L.) with the rbcS3C promoter allows recovery of lines that accumulate very high levels of abscisic acid and exhibit severe phenotypes. *Plant, Cell & Environment*, *31*(7), 968–981. https://doi.org/10.1111/j.1365-3040.2008.01812.x

Turra, G. L., Agostini, R. B., Fauguel, C. M., Presello, D. A., Andreo, C. S., González, J. M., & Campos-Bermudez, V. A. (2015). Structure of the novel monomeric glyoxalase I fromZea mays. *Acta Crystallographica Section D Biological Crystallography*, *71*(10), 2009–2020. https://doi.org/10.1107/s1399004715015205

Tweiten, M. A. (2016). *The response of a jack pine forest to late-Holocene climate variability in northwestern Wisconsin—Michael A. Tweiten, Sara C. Hotchkiss, Robert K. Booth, Randy R. Calcote, Elizabeth A. Lynch, 2009*. The Holocene. https://journals.sagepub.com/doi/abs/10.1177/0959683609340993

Ueno, D., Milner, M. J., Yamaji, N., Yokosho, K., Koyama, E., Clemencia Zambrano, M., Kaskie, M., Ebbs, S., Kochian, L. V., & Ma, J. F. (2011). Elevated expression of TcHMA3 plays a key role in the extreme Cd tolerance in a Cd-hyperaccumulating ecotype of Thlaspi caerulescens. *The Plant Journal*, *66*(5), 852–862. https://doi.org/10.1111/j.1365-313x.2011.04548.x

Uraguchi, S., Kamiya, T., Sakamoto, T., Kasai, K., Sato, Y., Nagamura, Y., Yoshida, A., Kyozuka, J., Ishikawa, S., & Fujiwara, T. (2011). Low-affinity cation transporter (OsLCT1) regulates cadmium transport into rice grains. *Proceedings of the National Academy of Sciences*, *108*(52), 20959–20964. https://doi.org/10.1073/pnas.1116531109

Urra, M., Buezo, J., Royo, B., Cornejo, A., López-Gómez, P., Cerdán, D., Esteban, R., Martínez-Merino, V., Gogorcena, Y., Tavladoraki, P., & Moran, J. F. (2022). The importance of the urea cycle and its relationships to polyamine metabolism during ammonium stress in Medicago truncatula. *Journal of Experimental Botany*, *73*(16), 5581–5595. https://doi.org/10.1093/jxb/erac235

Valivand, M., Amooaghaie, R., & Ahadi, A. (2019). Interplay between hydrogen sulfide and calcium/calmodulin enhances systemic acquired acclimation and antioxidative defense against nickel toxicity in zucchini. *Environmental and Experimental Botany*, *158*, 40–50. https://doi.org/10.1016/j.envexpbot.2018.11.006

Van Assche, F., & Clijsters, H. (1990). Effects of metals on enzyme activity in plants. *Plant, Cell & Environment*, *13*(3), 195–206. https://doi.org/10.1111/j.1365-3040.1990.tb01304.x

van de Mortel, J. E., Almar Villanueva, L., Schat, H., Kwekkeboom, J., Coughlan, S., Moerland, P. D., Ver Loren van Themaat, E., Koornneef, M., & Aarts, M. G. M. (2006). Large Expression Differences in Genes for Iron and Zinc Homeostasis, Stress Response, and Lignin Biosynthesis Distinguish Roots of Arabidopsis thaliana and the Related Metal Hyperaccumulator Thlaspi caerulescens. *Plant Physiology*, *142*(3), 1127–1147. https://doi.org/10.1104/pp.106.082073

Van Hoewyk, D., Taskin, M. B., Yaprak, A. E., Turgay, O. C., & Ergul, A. (2018). Profiling of proteasome activity in Alyssum species on serpentine soils in Turkey reveals possible insight into nickel tolerance and accumulation. *Plant Physiology and Biochemistry*, *124*, 184–189. https://doi.org/10.1016/j.plaphy.2018.01.022

Vandeligt, K. K., Nkongolo, K. K., Mehes, M., & Beckett, P. (2011). Genetic analysis of *Pinus banksiana* and *Pinus resinosa* populations from stressed sites contaminated with metals in Northern Ontario (Canada). *Chemistry and Ecology*, *27*(4), 369–380. https://doi.org/10.1080/02757540.2011.561790

Vatansever, R., ÖzyiĞit, İ. İ., & Filiz, E. (2016). Comparative and phylogenetic analysis of zinc transporter genes/proteins in plants. *TURKISH JOURNAL OF BIOLOGY*, *40*, 600–611. https://doi.org/10.3906/biy-1501-91

Velikova, V., Várkonyi, Z., Szabó, M., Maslenkova, L., Nogues, I., Kovács, L., Peeva, V., Busheva, M., Garab, G., Sharkey, T. D., & Loreto, F. (2011). Increased Thermostability of Thylakoid Membranes in Isoprene-Emitting Leaves Probed with Three Biophysical Techniques. *Plant Physiology*, *157*(2), 905–916. https://doi.org/10.1104/pp.111.182519

Verdan, A. M., Wang, H. C., García, C. R., Henry, W. P., & Brumaghim, J. L. (2011). Iron binding of 3-hydroxychromone, 5-hydroxychromone, and sulfonated morin: Implications for the antioxidant activity of flavonols with competing metal binding sites. *Journal of Inorganic Biochemistry*, *105*(10), 1314–1322. https://doi.org/10.1016/j.jinorgbio.2011.07.006

Verma, G., Srivastava, D., Narayan, S., Shirke, P. A., & Chakrabarty, D. (2020). Exogenous application of methyl jasmonate alleviates arsenic toxicity by modulating its uptake and translocation in rice (Oryza sativa L.). *Ecotoxicology and Environmental Safety*, *201*, 110735. https://doi.org/10.1016/j.ecoenv.2020.110735

Viarengo, A., Bettella, E., Fabbri, R., Burlando, B., & Lafaurie, M. (1997). Heavy metal inhibition of EROD activity in liver microsomes from the bass Dicentrarchus labrax exposed to organic xenobiotics: Role of GSH in the reduction of heavy metal effects.

Marine Environmental Research, *44*(1), 1–11. https://doi.org/10.1016/s0141-1136(96)00097-9

Visioli, G., Gullì, M., & Marmiroli, N. (2014). Noccaea caerulescens populations adapted to grow in metalliferous and non-metalliferous soils: Ni tolerance, accumulation and expression analysis of genes involved in metal homeostasis. *Environmental and Experimental Botany*, *105*, 10–17. https://doi.org/10.1016/j.envexpbot.2014.04.001

Wang, D., Pajerowska-Mukhtar, K., Culler, A. H., & Dong, X. (2007). Salicylic Acid Inhibits Pathogen Growth in Plants through Repression of the Auxin Signaling Pathway. *Current Biology*, *17*(20), 1784–1790. https://doi.org/10.1016/j.cub.2007.09.025

Wang, G., Xiao, Q., Tariq, M., Peng, C., Wu, J., & Zhang, W. (2022). Unveiling the Potential Tolerance and Physiological Response Mechanisms of Wheat after Exposure to Nickel in a Soil–Plant System. *ACS Agricultural Science & Technology*, *2*(5), 941–949. https://doi.org/10.1021/acsagscitech.2c00087

Wang, H., Feng, T., Peng, X., Yan, M., & Tang, X. (2009). Up-regulation of chloroplastic antioxidant capacity is involved in alleviation of nickel toxicity of Zea mays L. by exogenous salicylic acid. *Ecotoxicology and Environmental Safety*, *72*(5), 1354–1362. https://doi.org/10.1016/j.ecoenv.2009.03.008

Wang, H.-Q., Xuan, W., Huang, X.-Y., Mao, C., & Zhao, F.-J. (2020). Cadmium Inhibits Lateral Root Emergence in Rice by Disrupting OsPIN-Mediated Auxin Distribution and the Protective Effect of OsHMA3. *Plant and Cell Physiology*, *62*(1), 166–177. https://doi.org/10.1093/pcp/pcaa150

Wang, L., Yang, L., Yang, F., Li, X., Song, Y., Wang, X., & Hu, X. (2010). Involvements of H2O2 and metallothionein in NO-mediated tomato tolerance to copper toxicity. *Journal of Plant Physiology*, *167*(15), 1298–1306. https://doi.org/10.1016/j.jplph.2010.04.007

Wang, M., Zhang, Y., Zhu, C., Yao, X., Zheng, Z., Tian, Z., & Cai, X. (2021). EkFLS overexpression promotes flavonoid accumulation and abiotic stress tolerance in plant. *Physiologia Plantarum*, *172*(4), 1966–1982. https://doi.org/10.1111/ppl.13407

Wang, R., Wang, J., Zhao, L., Yang, S., & Song, Y. (2015). Impact of heavy metal stresses on the growth and auxin homeostasis of Arabidopsis seedlings. *BioMetals*, *28*(1), 123–132. https://doi.org/10.1007/s10534-014-9808-6

Wang, S., He, T., Xu, F., Li, X., Yuan, L., Wang, Q., & Liu, H. (2021). Analysis of physiological and metabolite response of Celosia argentea to copper stress. *Plant Biology*, *23*(2), 391–399. https://doi.org/10.1111/plb.13160

Wang, X., Zhi, J., Liu, X., Zhang, H., Liu, H., & Xu, J. (2018). Transgenic tobacco plants expressing a P1B-ATPase gene from Populus tomentosa Carr. (PtoHMA5) demonstrate improved cadmium transport. *International Journal of Biological Macromolecules*, *113*, 655–661. https://doi.org/10.1016/j.ijbiomac.2018.02.081

Wang, Y., Henriksson, E., Söderman, E., Henriksson, K. N., Sundberg, E., & Engström, P. (2003). The arabidopsis homeobox gene, ATHB16, regulates leaf development and the sensitivity to photoperiod in Arabidopsis. *Developmental Biology*, *264*(1), 228–239. https://doi.org/10.1016/j.ydbio.2003.07.017

Wang, Y., Sun, Y., You, Q., Luo, W., Wang, C., Zhao, S., Chai, G., Li, T., Shi, X., Li, C., Jetter, R., & Wang, Z. (2018). Three Fatty Acyl-Coenzyme A Reductases, BdFAR1, BdFAR2 and BdFAR3, are Involved in Cuticular Wax Primary Alcohol Biosynthesis in Brachypodium distachyon. *Plant and Cell Physiology*, *59*(3), 527–543. https://doi.org/10.1093/pcp/pcx211

Wang, Y., Xu, L., Chen, Y., Shen, H., Gong, Y., Limera, C., & Liu, L. (2013). Transcriptome Profiling of Radish (Raphanus sativus L.) Root and Identification of Genes Involved in Response to Lead (Pb) Stress with Next Generation Sequencing. *PLoS ONE*, *8*(6), e66539. https://doi.org/10.1371/journal.pone.0066539

Wasay, S. A., Barrington, S. F., & Tokunaga, S. (1998). Remediation of Soils Polluted by Heavy Metals using Salts of Organic Acids and Chelating Agents. *Environmental Technology*, *19*(4), 369–379. https://doi.org/10.1080/09593331908616692

Wei, W., Chai, T., Zhang, Y., Han, L., Xu, J., & Guan, Z. (2009). The Thlaspi caerulescens NRAMP Homologue TcNRAMP3 is Capable of Divalent Cation Transport. *Molecular Biotechnology*, *41*(1), 15–21. https://doi.org/10.1007/s12033-008-9088-x

Weryszko-Chmielewska, E., & Chwil, M. (2005). Lead-Induced Histological and Ultrastructural Changes in the Leaves of Soybean (Glycine max (L.) Merr.). *Soil Science & Plant Nutrition*, *51*(2), 203–212. https://doi.org/10.1111/j.1747-0765.2005.tb00024.x

Wiggenhauser, M., Aucour, A.-M., Bureau, S., Campillo, S., Telouk, P., Romani, M., Ma, J. F., Landrot, G., & Sarret, G. (2021). Cadmium transfer in contaminated soil-rice systems: Insights from solid-state speciation analysis and stable isotope fractionation. *Environmental Pollution*, *269*, 115934. https://doi.org/10.1016/j.envpol.2020.115934

Wildner, G. F., & Henkel, J. (1979). The effect of divalent metal ions on the activity of Mg++ depleted ribulose-1,5-bisphosphate oxygenase. *Planta*, *146*(2), 223–228. https://doi.org/10.1007/BF00388236

Wintz, H., Fox, T., Wu, Y.-Y., Feng, V., Chen, W., Chang, H.-S., Zhu, T., & Vulpe, C. (2003). Expression Profiles of Arabidopsis thaliana in Mineral Deficiencies Reveal Novel Transporters Involved in Metal Homeostasis. *Journal of Biological Chemistry*, *278*(48), 47644–47653. https://doi.org/10.1074/jbc.m309338200

Wiszniewska, A., Muszyńska, E., Hanus-Fajerska, E., Dziurka, K., & Dziurka, M. (2018). Evaluation of the protective role of exogenous growth regulators against Ni toxicity in woody shrub Daphne jasminea. *Planta*, *248*(6), 1365–1381. https://doi.org/10.1007/s00425-018-2979-6

Wuerges, J., Lee, J.-W., Yim, Y.-I., Yim, H.-S., Kang, S.-O., & Carugo, K. D. (2004). Crystal structure of nickel-containing superoxide dismutase reveals another type of active site. *Proceedings of the National Academy of Sciences*, *101*(23), 8569–8574. https://doi.org/10.1073/pnas.0308514101

Xiao, L., Shang, X.-H., Cao, S., Xie, X.-Y., Zeng, W.-D., Lu, L.-Y., Chen, S.-B., & Yan, H.-B. (2019). Comparative physiology and transcriptome analysis allows for identification of lncRNAs imparting tolerance to drought stress in autotetraploid cassava. *BMC Genomics*, *20*(1), 514. https://doi.org/10.1186/s12864-019-5895-7

Xie, D.-Y., Sharma, S. B., Paiva, N. L., Ferreira, D., & Dixon, R. A. (2003). Role of Anthocyanidin Reductase, Encoded by BANYULS in Plant Flavonoid Biosynthesis. *Science*, *299*(5605), 396–399. https://doi.org/10.1126/science.1078540

Xu, F., Li, L., Zhang, W., Cheng, H., Sun, N., Cheng, S., & Wang, Y. (2012). Isolation, characterization, and function analysis of a flavonol synthase gene from Ginkgo biloba. *Molecular Biology Reports*, *39*(3), 2285–2296. https://doi.org/10.1007/s11033-011-0978-9

Xu, F., Vaziriyeganeh, M., & Zwiazek, J. J. (2020). Effects of pH and Mineral Nutrition on Growth and Physiological Responses of Trembling Aspen (Populus tremuloides), Jack Pine (Pinus banksiana), and White Spruce (Picea glauca) Seedlings in Sand Culture. *Plants (Basel, Switzerland)*, *9*(6), E682. https://doi.org/10.3390/plants9060682

Xu, J., Yang, L., Wang, Z., Dong, G., Huang, J., & Wang, Y. (2006). Toxicity of copper on rice growth and accumulation of copper in rice grain in copper contaminated soil. *Chemosphere*, *62*(4), 602–607. https://doi.org/10.1016/j.chemosphere.2005.05.050

Xu, Z.-Y., Lee, K. H., Dong, T., Jeong, J. C., Jin, J. B., Kanno, Y., Kim, D. H., Kim, S. Y., Seo, M., Bressan, R. A., Yun, D.-J., & Hwang, I. (2012). A Vacuolar β-Glucosidase Homolog That Possesses Glucose-Conjugated Abscisic Acid Hydrolyzing Activity Plays an Important Role in Osmotic Stress Responses in Arabidopsis. *The Plant Cell*, *24*(5), 2184–2199. https://doi.org/10.1105/tpc.112.095935

Yadav. (2022). Nickel toxicity on seed germination and growth in radish (Raphanus sativus) and its recovery using copper and boron. *Journal of Environmental Biology*, *30*(3). https://pubmed.ncbi.nlm.nih.gov/20120479/

Yadav, S. K., Singla-Pareek, S. L., Ray, M., Reddy, M. K., & Sopory, S. K. (2005). Methylglyoxal levels in plants under salinity stress are dependent on glyoxalase I and glutathione. *Biochemical and Biophysical Research Communications*, *337*(1), 61–67. https://doi.org/10.1016/j.bbrc.2005.08.263

Yamaji, N., Mitatni, N., & Ma, J. F. (2008). A Transporter Regulating Silicon Distribution in Rice Shoots. *The Plant Cell*, *20*(5), 1381–1389. https://doi.org/10.1105/tpc.108.059311

Yamasaki, H., Abdel-Ghany, S. E., Cohu, C. M., Kobayashi, Y., Shikanai, T., & Pilon, M. (2007). Regulation of Copper Homeostasis by Micro-RNA in Arabidopsis. *Journal of Biological Chemistry*, *282*(22), 16369–16378. https://doi.org/10.1074/jbc.m700138200

Yan, A., Wang, Y., Tan, S. N., Mohd Yusof, M. L., Ghosh, S., & Chen, Z. (2020). Phytoremediation: A Promising Approach for Revegetation of Heavy Metal-Polluted Land. *Frontiers in Plant Science*, *11*, 359. https://doi.org/10.3389/fpls.2020.00359

Yang, K., Miao, G., Wu, W., Lin, D., Pan, B., Wu, F., & Xing, B. (2015). Sorption of Cu2+ on humic acids sequentially extracted from a sediment. *Chemosphere*, *138*, 657–663. https://doi.org/10.1016/j.chemosphere.2015.07.061

Yang, Q., Ma, X., Luo, S., Gao, J., Yang, X., & Feng, Y. (2018). SaZIP4, an uptake transporter of Zn/Cd hyperaccumulator Sedum alfredii Hance. *Environmental and Experimental Botany*, *155*, 107–117. https://doi.org/10.1016/j.envexpbot.2018.06.021

Yang, X., Baligar, V. C., Martens, D. C., & Clark, R. B. (1996). Plant tolerance to nickel toxicity: II nickel effects on influx and transport of mineral nutrients in four plant species. *Journal of Plant Nutrition*, *19*(2), 265–279. https://doi.org/10.1080/01904169609365121

Yang, Z., Wu, Y., Li, Y., Ling, H.-Q., & Chu, C. (2009). OsMT1a, a type 1 metallothionein, plays the pivotal role in zinc homeostasis and drought tolerance in rice. *Plant Molecular Biology*, *70*(1–2), 219–229. https://doi.org/10.1007/s11103-009-9466-1

Yao, X., Cai, Y., Yu, D., & Liang, G. (2018). BHLH104 confers tolerance to cadmium stress in Arabidopsis thaliana. *Journal of Integrative Plant Biology*, *60*(8), 691–702. https://doi.org/10.1111/jipb.12658

Yoon, J., Cao, X., Zhou, Q., & Ma, L. Q. (2006). Accumulation of Pb, Cu, and Zn in native plants growing on a contaminated Florida site. *Science of The Total Environment*, *368*(2–3), 456–464. https://doi.org/10.1016/j.scitotenv.2006.01.016

Yoon, K., Han, D., Li, Y., Sommerfeld, M., & Hu, Q. (2012). Phospholipid:Diacylglycerol Acyltransferase Is a Multifunctional Enzyme Involved in Membrane Lipid Turnover and Degradation While Synthesizing Triacylglycerol in the Unicellular Green Microalga Chlamydomonas reinhardtii. *The Plant Cell*, *24*(9), 3708–3724. https://doi.org/10.1105/tpc.112.100701

Yu, M., Li, R., Cui, Y., Chen, W., Li, B., Zhang, X., Bu, Y., Cao, Y., Xing, J., Jewaria, P. K., Li, X., Bhalerao, R. P., Yu, F., & Lin, J. (2020). The RALF1-FERONIA interaction modulates endocytosis to mediate control of root growth in Arabidopsis. *Development*, *147*(13), dev189902. https://doi.org/10.1242/dev.189902

Yu, X.-Z., Fan, W.-J., & Lin, Y.-J. (2018). Analysis of gene expression profiles for metal tolerance protein in rice seedlings exposed to both the toxic hexavalent chromium and trivalent chromium. *International Biodeterioration & Biodegradation*, *129*, 102–108. https://doi.org/10.1016/j.ibiod.2018.01.011

Yuan, H.-M., & Huang, X. (2016). Inhibition of root meristem growth by cadmium involves nitric oxide-mediated repression of auxin accumulation and signalling in Arabidopsis: Cadmium stress causes root defects via nitric oxide and auxin. *Plant, Cell & Environment*, *39*(1), 120–135. https://doi.org/10.1111/pce.12597

Yuan, H.-M., Xu, H.-H., Liu, W.-C., & Lu, Y.-T. (2013). Copper Regulates Primary Root Elongation Through PIN1-Mediated Auxin Redistribution. *Plant and Cell Physiology*, *54*(5), 766–778. https://doi.org/10.1093/pcp/pct030

Yusuf, M., Fariduddin, Q., Hayat, S., & Ahmad, A. (2011). Nickel: An Overview of Uptake, Essentiality and Toxicity in Plants. *Bulletin of Environmental Contamination and Toxicology*, *86*(1), 1–17. https://doi.org/10.1007/s00128-010-0171-1

Yusuf, M., Fariduddin, Q., Varshney, P., & Ahmad, A. (2012). Salicylic acid minimizes nickel and/or salinity-induced toxicity in Indian mustard (Brassica juncea) through an improved antioxidant system. *Environmental Science and Pollution Research*, *19*(1), 8–18. https://doi.org/10.1007/s11356-011-0531-3

Zaharieva, T. B., & Abadía, J. (2003). Iron deficiency enhances the levels of ascorbate, glutathione, and related enzymes in sugar beet roots. *Protoplasma*, *221*(3), 269–275. https://doi.org/10.1007/s00709-002-0051-6

Zakrzewski, W. T., & Duchesne, I. (2012). Stem biomass model for jack pine (Pinus banksiana Lamb.) in Ontario. *Forest Ecology and Management*, *279*, 112–120. https://doi.org/10.1016/j.foreco.2012.05.012

Zarinkamar, F., Saderi, Z., & Soleimanpour, S. (2013). Excluder Strategies in Response to Pb Toxicity in Matricaria Chamomilla. *Environment and Ecology Research*, *1*(1), 1–11. https://doi.org/10.13189/eer.2013.010101

Zemiani, A., Boldarini, M. T. B., Anami, M. H., de Oliveira, E. F., & da Silva, A. F. (2021). Tolerance of Mentha crispa L. (garden mint) cultivated in cadmium-contaminated oxisol. *Environmental Science and Pollution Research*, *28*(31), 42107–42120. https://doi.org/10.1007/s11356-021-13641-y

Zeng, D.-E., Hou, P., Xiao, F., & Liu, Y. (2014). Overexpressing a novel RING-H2 finger protein gene, OsRHP1, enhances drought and salt tolerance in rice (Oryza sativa L.). *Journal of Plant Biology*, *57*(6), 357–365. https://doi.org/10.1007/s12374-013-0481-z

Zhang, B., Shang, S., Jabeen, Z., & Zhang, G. (2014). Involvement of ethylene in alleviation of Cd toxicity by NaCl in tobacco plants. *Ecotoxicology and Environmental Safety*, *101*, 64–69. https://doi.org/10.1016/j.ecoenv.2013.12.013

Zhang, C., Lu, W., Yang, Y., Shen, Z., Ma, J. F., & Zheng, L. (2018). OsYSL16 is Required for Preferential Cu Distribution to Floral Organs in Rice. *Plant and Cell Physiology*, *59*(10), 2039–2051. https://doi.org/10.1093/pcp/pcy124

Zhang, H., Jing, W., Zheng, J., Jin, Y., Wu, D., Cao, C., Dong, Y., Shi, X., & Zhang, W. (2020). The ATP-binding cassette transporter OsPDR1 regulates plant growth and pathogen resistance by affecting jasmonates biosynthesis in rice. *Plant Science*, *298*, 110582. https://doi.org/10.1016/j.plantsci.2020.110582

Zhang, W., Tong, L., Yuan, Y., Liu, Z., Huang, H., Tan, F., & Qiu, R. (2010). Influence of soil washing with a chelator on subsequent chemical immobilization of heavy metals in a contaminated soil. *Journal of Hazardous Materials*, *178*(1–3), 578–587. https://doi.org/10.1016/j.jhazmat.2010.01.124

Zhang, X., Dippold, M. A., Kuzyakov, Y., & Razavi, B. S. (2019). Spatial pattern of enzyme activities depends on root exudate composition. *Soil Biology and Biochemistry*, *133*, 83–93. https://doi.org/10.1016/j.soilbio.2019.02.010

Zhang, X., Feng, H., Feng, C., Xu, H., Huang, X., Wang, Q., Duan, X., Wang, X., Wei, G., Huang, L., & Kang, Z. (2015). Isolation and characterisation of cDNA encoding a wheat heavy metal-associated isoprenylated protein involved in stress responses. *Plant Biology*, *17*(6), 1176–1186. https://doi.org/10.1111/plb.12344

Zhang, X., Liu, S., & Takano, T. (2008). Two cysteine proteinase inhibitors from Arabidopsis thaliana, AtCYSa and AtCYSb, increasing the salt, drought, oxidation and cold tolerance. *Plant Molecular Biology*, *68*(1), 131–143. https://doi.org/10.1007/s11103-008-9357-x

Zhang, X., Liu, Y., Ayaz, A., Zhao, H., & Lü, S. (2022). The Plant Fatty Acyl Reductases. *International Journal of Molecular Sciences*, *23*(24), Article 24. https://doi.org/10.3390/ijms232416156

Zhang, X., Uroic, M. K., Xie, W.-Y., Zhu, Y.-G., Chen, B.-D., McGrath, S. P., Feldmann, J., & Zhao, F.-J. (2012). Phytochelatins play a key role in arsenic accumulation and tolerance in the aquatic macrophyte Wolffia globosa. *Environmental Pollution (Barking, Essex: 1987)*, *165*, 18–24. https://doi.org/10.1016/j.envpol.2012.02.009

Zhang, Y., Chen, K., Zhao, F.-J., Sun, C., Jin, C., Shi, Y., Sun, Y., Li, Y., Yang, M., Jing, X., Luo, J., & Lian, X. (2018). OsATX1 Interacts with Heavy Metal P1B-Type ATPases and Affects Copper Transport and Distribution. *Plant Physiology*, *178*(1), 329–344. https://doi.org/10.1104/pp.18.00425

Zhang, Y., Yu, J., Wang, X., Durachko, D. M., Zhang, S., & Cosgrove, D. J. (2021). Molecular insights into the complex mechanics of plant epidermal cell walls. *Science*, *372*(6543), 706–711. https://doi.org/10.1126/science.abf2824

Zhang, Y., Zhang, H., Liu, Y., Zhang, Z. L., & Ding, C. K. (2017). Chelating Ability and Microbial Stability of an l-Arginine-Modified Chitosan-Based Environmental Remediation Material. *Journal of Polymers and the Environment*, *26*(3), 885–894. https://doi.org/10.1007/s10924-017-1000-y

Zhang, Z., Li, J., Liu, H., Chong, K., & Xu, Y. (2015). Roles of ubiquitination-mediated protein degradation in plant responses to abiotic stresses. *Environmental and Experimental Botany*, *114*, 92–103. https://doi.org/10.1016/j.envexpbot.2014.07.005

Zhao, F. J., Jiang, R. F., Dunham, S. J., & McGrath, S. P. (2006). Cadmium uptake, translocation and tolerance in the hyperaccumulator Arabidopsis halleri. *New Phytologist*, *172*(4), 646–654. https://doi.org/10.1111/j.1469-8137.2006.01867.x

Zhao, X., Zhang, T., Bai, L., Zhao, S., Guo, Y., & Li, Z. (2023). CKL2 mediates the crosstalk between abscisic acid and brassinosteroid signaling to promote swift growth recovery after stress in Arabidopsis. *Journal of Integrative Plant Biology*, *65*(1), 64–81. https://doi.org/10.1111/jipb.13397

Zhao, Y., Gao, C., Shi, F., Yun, L., Jia, Y., & Wen, J. (2018). Transcriptomic and proteomic analyses of drought responsive genes and proteins in Agropyron mongolicum Keng. *Current Plant Biology*, *14*, 19–29. https://doi.org/10.1016/j.cpb.2018.09.005

Zheng, F., Cui, X., Rivarola, M., Gao, T., Chang, C., & Dong, C.-H. (2017). Molecular association of Arabidopsis RTH with its homolog RTE1 in regulating ethylene signaling. *Journal of Experimental Botany*, *68*(11), 2821–2832. https://doi.org/10.1093/jxb/erx175

Zheng, L., Yamaji, N., Yokosho, K., & Ma, J. F. (2012). YSL16 Is a Phloem-Localized Transporter of the Copper-Nicotianamine Complex That Is Responsible for Copper Distribution in Rice. *The Plant Cell*, *24*(9), 3767–3782. https://doi.org/10.1105/tpc.112.103820

Zheng, M., Liu, X., Lin, J., Liu, X., Wang, Z., Xin, M., Yao, Y., Peng, H., Zhou, D.-X., Ni, Z., Sun, Q., & Hu, Z. (2019). Histone acetyltransferase GCN5 contributes to cell wall integrity and salt stress tolerance by altering the expression of cellulose synthesis genes. *The Plant Journal*, *97*(3), 587–602. https://doi.org/10.1111/tpj.14144

Zhou, J., & Goldsbrough, P. B. (1995). Structure, organization and expression of the metallothionein gene family inArabidopsis. *Molecular and General Genetics MGG*, *248*(3), 318–328. https://doi.org/10.1007/bf02191599

Zhu, Y., Li, G., Singh, J., Khan, A., Fazio, G., Saltzgiver, M., & Xia, R. (2021). Laccase Directed Lignification Is One of the Major Processes Associated With the Defense Response Against Pythium ultimum Infection in Apple Roots. *Frontiers in Plant Science*, *12*. https://doi.org/10.3389/fpls.2021.629776

Appendices

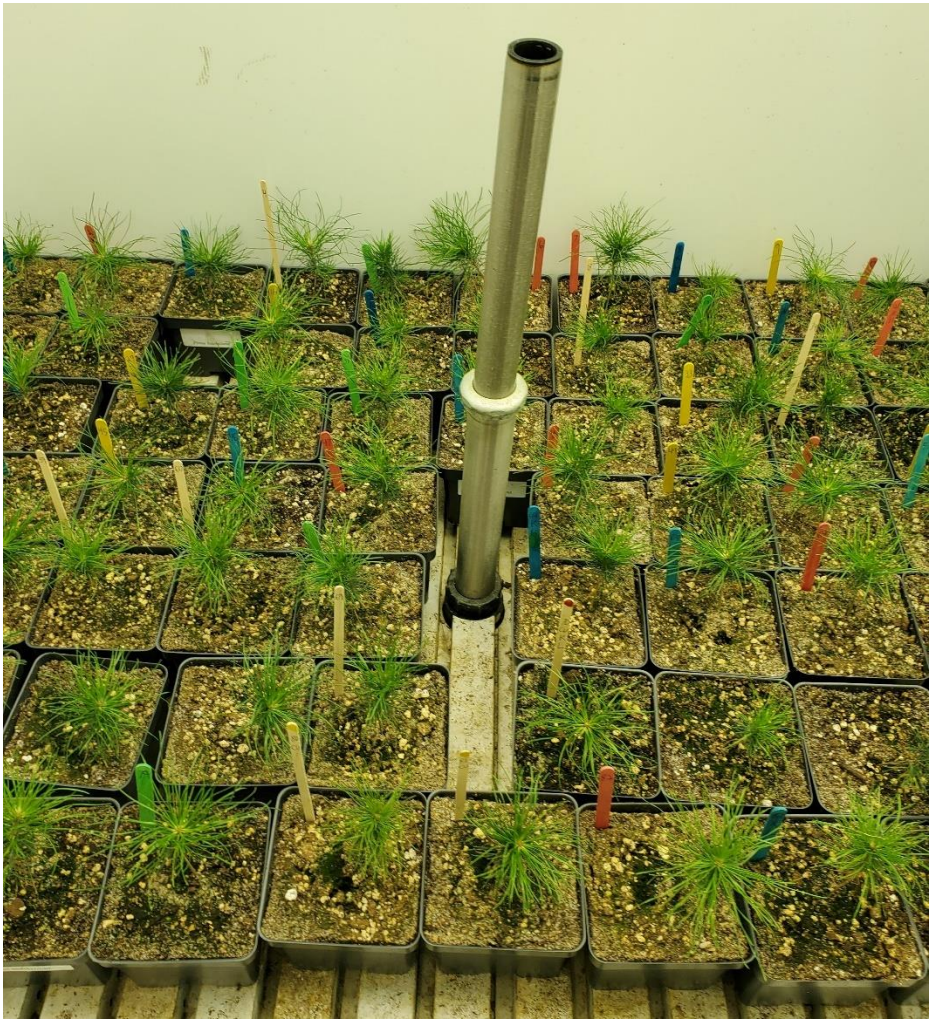

Sfigure 1. *Pinus banksiana* seedlings in a growth chamber prior to heavy metal treatment

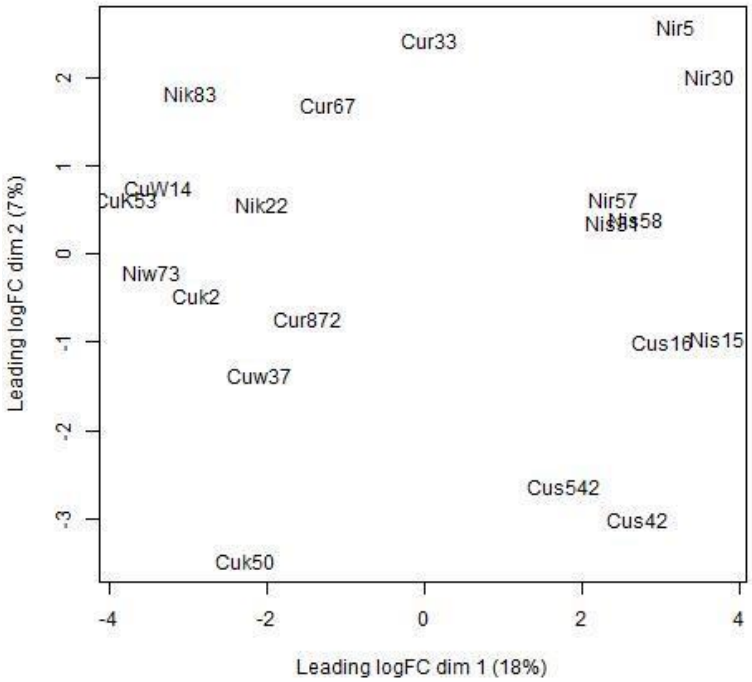

Sfigure 2a. Sample clusters assessed via a multidimensional scale (MDS) plot

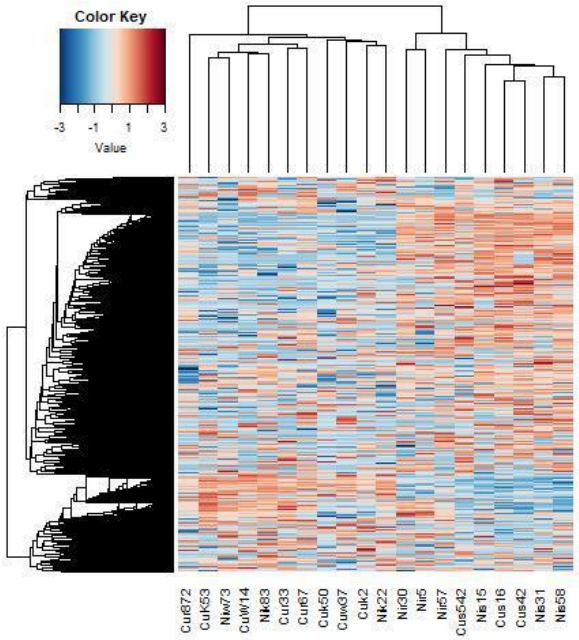

Sfigure 2b. Heatmap of 5000 genes between the samples. Differential gene expression between samples was used to visually assess Hierarchical clustering between the samples.

STable 1. Sequence Data QC verified by FastQC

File name	Total Sequences	Sequences flagged as poor quality	Sequence length	%GC	Total Deduplicated Percentage
Nik22_S20_R1_001.fastq.gz	27542578	0	51	42	20.9
Nik22_S20_R2_001.fastq.gz	27542578	0	51	42	28.26
Nik83_S13_R1_001.fastq.gz	48707028	0	51	43	18.59
Nik83_S13_R2_001.fastq.gz	48707028	0	51	43	26.68
Nir5_S14_R1_001.fastq.gz	43071699	0	51	43	28.06
Nir5_S14_R2_001.fastq.gz	43071699	0	51	46	41.21
Nir30_S15_R1_001.fastq.gz	51430261	0	51	44	24.01
Nir30_S15_R2_001.fastq.gz	51430261	0	51	44	33.2
Nir57_S16_R1_001.fastq.gz	35240520	0	51	43	34.95
Nir57_S16_R2_001.fastq.gz	35240520	0	51	43	41.93
Nis15_S17_R1_001.fastq.gz	27007956	0	51	44	38.07
Nis15_S17_R2_001.fastq.gz	27007956	0	51	44	46.43
Nis31_S18_R1_001.fastq.gz	24852733	0	51	43	42.53
Nis31_S18_R2_001.fastq.gz	24852733	0	51	44	50.41
Nis58_S19_R1_001.fastq.gz	28880651	0	51	43	44.65
Nis58_S19_R2_001.fastq.gz	28880651	0	51	44	52.34
Niw73_S21_R1_001.fastq.gz	32894698	0	51	43	17.31
Niw73_S21_R2_001.fastq.gz	32894698	0	51	44	25.99

STable 6a. Top 100 upregulated genes from nickel resistant samples compared to the water controls in *Pinus banksiana*

Rank	Gene ID	Res 1	Res 2	Res 3	Water 1	Water 2	Water 3	logFC	Adj. P. Value	UniProt Description
0	TRINITY_DN2786_c0_g1	767.81	197.57	545.86	0	0	0	13.96	0.00116	Predicted Protein
1	TRINITY_DN5716_c0_g1	2328.59	913.58	3881.87	0	7.03	0.41	13.34	0.00029	Predicted Protein
2	TRINITY_DN57079_c0_g1	339.53	238.75	261.65	0	0	0	13.30	0.00002	Predicted Protein
3	TRINITY_DN5965_c1_g1	1173.34	760.7	1106.06	0.33	0	0	13.28	0.00009	Predicted Protein
4	TRINITY_DN258556_c0_g1	280.75	98.46	494.55	0	0	0	13.09	0.00181	Predicted Protein
5	TRINITY_DN1368_c0_g1	1156.77	736.4	2060.57	0	1.3	0.07	12.99	0.00047	Predicted Protein
6	TRINITY_DN2832_c0_g1	334.2	111.71	258.08	0	0	0	12.93	0.00056	Predicted Protein
7	TRINITY_DN1628_c0_g1	646.38	288.02	710.02	0	0.32	0	12.82	0.00065	Trypsin inhibitor [Cleaved into: Trypsin inhibitor chain A; Trypsin inhibitor chain B]
8	TRINITY_DN7061_c1_g1	158.35	218.82	172.81	0	0	0	12.69	0.00000	Predicted Protein
9	TRINITY_DN690_c0_g1	494.67	136.83	407.74	0.05	0	0	12.50	0.00181	Predicted Protein
10	TRINITY_DN5795_c0_g1	753.52	420.03	412.9	0	0.84	0	12.43	0.00032	Predicted Protein
11	TRINITY_DN1520_c0_g1	398.05	358.51	936.72	0.02	0.65	0	11.81	0.00043	Trypsin inhibitor [Cleaved into: Trypsin inhibitor chain A; Trypsin inhibitor chain B]
12	TRINITY_DN3861_c0_g1	179.52	38.1	108.51	0	0	0	11.70	0.00251	Predicted Protein
13	TRINITY_DN40097_c0_g1	440.62	297.68	1698.09	0	3.39	0.69	11.62	0.00080	Predicted Protein
14	TRINITY_DN2463_c0_g1	301.76	196.16	568.86	0	0.04	0.11	11.56	0.00056	Predicted Protein
15	TRINITY_DN4524_c0_g3	64.05	74.91	115.6	0	0	0	11.54	0.00002	Predicted Protein
16	TRINITY_DN792_c0_g1	149.05	126.17	86.37	0	0.03	0	11.54	0.00004	ACT domain-containing protein ACR4 (Protein ACT DOMAIN REPEATS 4)
17	TRINITY_DN792_c0_g1	149.05	126.17	86.37	0	0.03	0	11.54	0.00004	ACT domain-containing protein ACR5 (Protein ACT DOMAIN REPEATS 5)
18	TRINITY_DN129489_c0_g1	125.97	40.97	102.59	0	0	0	11.53	0.00085	Predicted Protein
19	TRINITY_DN2914_c0_g1	134.07	79.52	144.69	0	0.03	0	11.51	0.00014	Protein TIFY 10b, OsTIFY10b (Jasmonate ZIM

									domain-containing protein 7, OsJAZ7) (OsJAZ6)
20	TRINITY_DN2914_c0_g1	134.07	79.52	144.69	0	0.03	0	11.51	0.00014	Protein TIFY 3B (Jasmonate ZIM domain-containing protein 12)
21	TRINITY_DN3536_c0_g1	51.58	119.55	84.19	0	0	0	11.51	0.00001	Predicted Protein
22	TRINITY_DN1537_c0_g1	64.53	90.63	76.46	0	0	0	11.44	0.00000	Predicted Protein
23	TRINITY_DN2075_c1_g1	81.81	56.05	84.87	0	0	0	11.38	0.00005	Predicted Protein
24	TRINITY_DN12750_c0_g1	93.87	62.85	64.95	0	0	0	11.37	0.00005	Predicted Protein
25	TRINITY_DN3685_c0_g2	524.13	169.45	298.36	0.01	0.58	0	11.33	0.00171	Copia protein (Gag-int-pol protein) [Cleaved into: Copia VLP protein; Copia protease, EC 3.4.23.-]
26	TRINITY_DN3069_c0_g1	310.77	133.21	112.57	0	0.37	0	11.16	0.00120	Predicted Protein
27	TRINITY_DN4477_c1_g1	58.41	73.47	40.83	0	0	0	11.00	0.00002	Predicted Protein
28	TRINITY_DN9955_c0_g1	42.57	42.66	81.29	0	0	0	10.91	0.00007	Predicted Protein
29	TRINITY_DN3861_c0_g2	73.03	22.1	87.52	0	0	0	10.90	0.00200	Predicted Protein
30	TRINITY_DN2496_c0_g1	164.42	56.24	74.78	0	0.08	0	10.89	0.00111	Predicted Protein
31	TRINITY_DN3195_c0_g2	97.14	27.64	44.27	0	0	0	10.82	0.00125	Predicted Protein
32	TRINITY_DN13148_c0_g2	149.44	53.58	71	0.03	0	0	10.80	0.00087	Predicted Protein
33	TRINITY_DN8563_c1_g1	81.63	24.89	51.8	0	0	0	10.76	0.00105	Predicted Protein
34	TRINITY_DN4828_c0_g1	77.75	87.05	75	0	0.07	0	10.73	0.00002	Predicted Protein
35	TRINITY_DN1453_c1_g4	164.09	61.99	144.64	0	0.3	0	10.72	0.00143	Predicted Protein
36	TRINITY_DN1031_c0_g1	92.79	147.67	132.23	0	0.42	0	10.65	0.00004	Putative cysteine-rich repeat secretory protein 17
37	TRINITY_DN17_c0_g2	50.63	58.32	26.97	0	0	0	10.62	0.00006	RING-H2 finger protein ATL60, EC 2.3.2.27 (RING-type E3 ubiquitin transferase ATL60)
38	TRINITY_DN1299_c1_g1	32.6	35.97	67.12	0	0	0	10.60	0.00007	Predicted Protein
39	TRINITY_DN2516_c0_g1	445.31	249.4	199.81	0.02	0.63	0.07	10.58	0.00032	Predicted Protein
40	TRINITY_DN1518_c0_g1	96.36	25.43	28.14	0	0	0	10.56	0.00213	Predicted Protein
41	TRINITY_DN678_c0_g1	132.68	116.88	131.13	0	0.61	0	10.55	0.00012	Cysteine proteinase inhibitor 6, AtCYS-6 (PIP-M) (PRLI-interacting factor M)

42	TRINITY_DN678_c0_g1	132.68	116.88	131.13	0	0.61	0	10.55	0.00012	Cysteine proteinase inhibitor 3, AtCYS-3
43	TRINITY_DN678_c0_g1	132.68	116.88	131.13	0	0.61	0	10.55	0.00012	Multicystatin, MC
44	TRINITY_DN125473_c0_g2	65.02	24.25	42.52	0	0	0	10.54	0.00058	Predicted Protein
45	TRINITY_DN103008_c0_g1	216.81	147.31	109.01	0.08	0.1	0	10.48	0.00022	Predicted Protein
46	TRINITY_DN6089_c0_g1	96.41	139.06	110.48	0	0.52	0	10.47	0.00004	Predicted Protein
47	TRINITY_DN630_c0_g1	70.97	43.91	146.42	0	0.16	0	10.40	0.00127	Protein SRG1, AtSRG1 (Protein SENESCENCE-RELATED GENE 1)
48	TRINITY_DN630_c0_g1	70.97	43.91	146.42	0	0.16	0	10.40	0.00127	Jasmonate-induced oxygenase 4, EC 1.14.11.- (2-oxoglutarate-dependent dioxygenase JOX4) (Anthocyanidin synthase) (Jasmonic acid oxidase 4)
49	TRINITY_DN630_c0_g1	70.97	43.91	146.42	0	0.16	0	10.40	0.00127	Codeine O-demethylase, EC 1.14.11.32
50	TRINITY_DN630_c0_g1	70.97	43.91	146.42	0	0.16	0	10.40	0.00127	S-norcoclaurine synthase 1, CjNCS1, EC 4.2.1.78
51	TRINITY_DN1958_c0_g1	34.95	25.92	54.49	0	0	0	10.38	0.00015	Predicted Protein
52	TRINITY_DN3889_c0_g1	414.11	167.54	300.23	0	0.98	0.57	10.37	0.00068	Predicted Protein
53	TRINITY_DN4195_c0_g1	47.94	20.18	47.91	0	0	0	10.36	0.00056	Predicted Protein
54	TRINITY_DN50999_c1_g1	44.58	72.78	14	0	0	0	10.35	0.00092	Predicted Protein
55	TRINITY_DN5723_c0_g1	147.25	109.75	89.9	0.01	0.19	0	10.34	0.00014	Predicted Protein
56	TRINITY_DN4424_c0_g1	47.33	16.14	56.98	0	0	0	10.33	0.00157	Predicted Protein
57	TRINITY_DN1307_c0_g1	16.43	96.5	26.64	0	0	0	10.30	0.00055	Germin-like protein 1-1 (Germin-like protein 4, OsGER4)
58	TRINITY_DN1307_c0_g1	16.43	96.5	26.64	0	0	0	10.30	0.00055	Germin-like protein subfamily 2 member 2
59	TRINITY_DN8008_c0_g1	41.17	24.54	37.72	0	0	0	10.26	0.00013	Predicted Protein
60	TRINITY_DN5391_c1_g1	39.5	79.43	11.5	0	0	0	10.24	0.00179	Predicted Protein
61	TRINITY_DN5136_c0_g1	45.05	28.07	26.97	0	0	0	10.21	0.00012	Predicted Protein
62	TRINITY_DN71807_c0_g1	29.61	23.8	49.04	0	0	0	10.21	0.00014	Predicted Protein
63	TRINITY_DN10435_c0_g1	688.04	977.43	155.25	0.18	0.41	0.11	10.17	0.00093	Glucan endo-1,3-beta-glucosidase, acidic isoform,

									EC 3.2.1.39 ((1->3)-beta-glucan endohydrolase, (1->3)-beta-glucanase) (Beta-1,3-endoglucanase)
64	TRINITY_DN1644_c0_g1	42.57	17.5	40.38	0	0	0	10.15	0.00061	NAC transcription factor 47 (NAC domain-containing protein 47, ANAC047) (Protein SPEEDY HYPONASTIC GROWTH)
65	TRINITY_DN1472_c0_g1	212.32	210.54	174.12	0.02	0.16	0.1	10.15	0.00002	Triacylglycerol lipase OBL1, EC 3.1.1.- (Oil body lipase 1, NtOBL1)
66	TRINITY_DN8703_c1_g1	20.94	68.98	20.74	0	0	0	10.14	0.00014	Predicted Protein
67	TRINITY_DN30360_c0_g2	32.32	41.67	19.9	0	0	0	10.09	0.00004	Predicted Protein
68	TRINITY_DN690_c1_g1	36.04	15	46.52	0	0	0	10.06	0.00098	Predicted Protein
69	TRINITY_DN2595_c0_g1	34.43	14.93	48.4	0	0	0	10.06	0.00100	Predicted Protein
70	TRINITY_DN5044_c1_g1	3556.6	1665.87	4959.49	2.92	5.34	0.16	10.06	0.00002	Predicted Protein
71	TRINITY_DN2691_c0_g1	93.28	347.62	74.23	0	0.14	0.33	10.04	0.00108	Predicted Protein
72	TRINITY_DN59057_c0_g1	979.45	270.63	1164.92	0.55	2.6	0	10.03	0.00106	Predicted Protein
73	TRINITY_DN5965_c0_g1	159.21	70.92	203.21	0.07	0.21	0	10.00	0.00161	Predicted Protein
74	TRINITY_DN7685_c0_g1	69.15	75.78	88.19	0	0.41	0	9.99	0.00010	Predicted Protein
75	TRINITY_DN25430_c0_g1	14.61	23.03	66.45	0	0	0	9.99	0.00091	Predicted Protein
76	TRINITY_DN1507_c0_g1	26.74	27.5	28.46	0	0	0	9.97	0.00002	Predicted Protein
77	TRINITY_DN183161_c0_g1	38.89	15.66	33.33	0	0	0	9.96	0.00062	Predicted Protein
78	TRINITY_DN2540_c0_g1	65.96	51.15	17.44	0	0.05	0	9.95	0.00116	Predicted Protein
79	TRINITY_DN257933_c1_g1	22.27	33.69	26.6	0	0	0	9.95	0.00001	Predicted Protein
80	TRINITY_DN15707_c0_g1	40.5	12.74	34.71	0	0	0	9.90	0.00145	Predicted Protein
81	TRINITY_DN122303_c0_g2	43.54	23.48	82.74	0	0	0.06	9.87	0.00149	Predicted Protein
82	TRINITY_DN12875_c0_g1	368	113.74	248.93	0.24	0.34	0	9.86	0.00219	Predicted Protein
83	TRINITY_DN157113_c2_g1	33.92	29.87	15.92	0	0	0	9.85	0.00013	Predicted Protein
84	TRINITY_DN6211_c0_g1	26.02	66.59	9.11	0	0	0	9.84	0.00186	Predicted Protein
85	TRINITY_DN5240_c1_g1	75.64	57.88	47.63	0	0.09	0.03	9.78	0.00014	Predicted Protein
86	TRINITY_DN2454_c0_g2	24.25	22.33	25.85	0	0	0	9.78	0.00003	Predicted Protein

87	TRINITY_DN1456_c0_g1	306.48	253.1	155.47	0.27	0	0.25	9.78	0.00018	Predicted Protein
88	TRINITY_DN26886_c0_g1	61.81	26.91	40.92	0	0.09	0	9.77	0.00069	Predicted Protein
89	TRINITY_DN8619_c0_g1	37.8	12.68	28.14	0	0	0	9.77	0.00109	Predicted Protein
90	TRINITY_DN27427_c0_g1	48.32	16.08	14.95	0	0	0	9.71	0.00155	Predicted Protein
91	TRINITY_DN5616_c1_g1	114.68	86.52	56.74	0	1.17	0	9.70	0.00072	Predicted Protein
92	TRINITY_DN21893_c1_g1	11.63	44.29	22.13	0	0	0	9.67	0.00012	Predicted Protein
93	TRINITY_DN7420_c0_g1	25.09	11.85	36.81	0	0	0	9.66	0.00090	Predicted Protein
94	TRINITY_DN49749_c0_g1	27.49	17.43	20.17	0	0	0	9.61	0.00013	Predicted Protein
95	TRINITY_DN5340_c0_g1	27.6	47.12	22.31	0	0.04	0	9.60	0.00005	Predicted Protein
96	TRINITY_DN3840_c0_g2	40.87	29.93	22.16	0	0.03	0	9.58	0.00017	Predicted Protein
97	TRINITY_DN237688_c0_g1	21.17	36.54	11.77	0	0	0	9.57	0.00015	Predicted Protein
98	TRINITY_DN251401_c0_g1	26.95	28.1	11.66	0	0	0	9.57	0.00020	Predicted Protein
99	TRINITY_DN104547_c0_g1	238.4	83.01	249.46	0.25	0.3	0	9.56	0.00258	Predicted Protein
100	TRINITY_DN395_c0_g1	33.63	33.79	22.39	0.02	0	0	9.54	0.00005	Inositol polyphosphate 5-phosphatase OCRL, EC 3.1.3.36, EC 3.1.3.56 (Inositol polyphosphate 5-phosphatase OCRL-1) (Phosphatidylinositol 3,4,5-triphosphate 5-phosphatase, EC 3.1.3.86)

STable 6b. Top 100 downregulated genes from nickel resistant samples compared to the control in *Pinus banksiana*

Rank	Gene ID	Res 1	Res 2	Res 3	Water 1	Water 2	Water 3	Adj. P. Value	Protein Description
0	TRINITY_DN1118_c0_g1	0	0	0	27.63	15.12	24.7	4.86E-05	Flavonol synthase/flavanone 3-hydroxylase, FLS, EC 1.14.11.9, EC 1.14.20.6
1	TRINITY_DN26931_c0_g1	0.16	0	0	65.61	45.82	36.39	9.47E-05	Probable aquaporin PIP2-8 (Plasma membrane intrinsic protein 2-8, AtPIP2;8) (Plasma membrane intrinsic protein 3b, PIP3b)
2	TRINITY_DN432_c0_g1	0	0.3	0	77.54	17.58	69.88	0.002533	Predicted Protein
3	TRINITY_DN4059_c0_g1	0	0	0	20.09	12.1	19.58	4.10E-05	Predicted Protein
4	TRINITY_DN30654_c0_g1	0	0	0	14.69	11.78	14.4	1.63E-05	Predicted Protein
5	TRINITY_DN2314_c0_g1	0.03	0.13	0	40.88	14.56	52.04	0.001066	Predicted Protein
6	TRINITY_DN69830_c0_g4	0	0	0	10.13	7.29	18.59	0.000101	Predicted Protein
7	TRINITY_DN129793_c0_g1	0	0	0	8.28	13.37	9.36	9.45E-06	Putative UPF0481 protein At3g02645
8	TRINITY_DN40558_c0_g1	0.04	0	0.05	36.31	14.48	19.64	0.000432	Predicted Protein
9	TRINITY_DN522_c0_g3	0	0	0	8.24	4.71	17.93	0.000408	Predicted Protein
10	TRINITY_DN1550_c0_g1	0	0.07	0	18.5	9.11	17.44	0.000209	Predicted Protein
11	TRINITY_DN113586_c0_g1	0	0	0	7.25	5.74	13.28	8.70E-05	Predicted Protein
12	TRINITY_DN25689_c0_g1	0.06	0.09	0	26.01	16.36	31.07	0.000136	Predicted Protein
13	TRINITY_DN26605_c0_g1	0	0	0	6.61	7.11	10.35	2.28E-05	Predicted Protein
14	TRINITY_DN31123_c0_g2	0	0	0	6.35	8.14	8.67	1.28E-05	Predicted Protein
15	TRINITY_DN4890_c0_g1	0	0	0.17	15.59	12.05	25.46	0.000174	Predicted Protein
16	TRINITY_DN5062_c0_g2	0	0	0	10.4	7.97	3.99	0.000193	Predicted Protein
17	TRINITY_DN3390_c0_g1	0	0	0	9.96	3.94	7.77	0.000273	Predicted Protein
18	TRINITY_DN6314_c0_g1	0	0	0	7.61	6.68	5.98	2.86E-05	Predicted Protein
19	TRINITY_DN2507_c0_g1	0	0	0.61	32.43	13.12	23.67	0.000952	Predicted Protein
20	TRINITY_DN53932_c0_g1	0.01	0	0.2	17.81	11.58	17.09	0.00016	Predicted Protein
21	TRINITY_DN20386_c0_g1	0	0	0	7.77	6	5.13	5.04E-05	Predicted Protein
22	TRINITY_DN17540_c0_g1	0	0	0	10.32	6.62	3.33	0.000363	Predicted Protein
23	TRINITY_DN51950_c1_g1	0	0	0	6.24	5.15	7.26	3.46E-05	Predicted Protein
24	TRINITY_DN59077_c1_g1	0	0.2	0	11.37	9.17	20.15	0.000196	Predicted Protein

25	TRINITY_DN26_c1_g1	0	0	0	5.86	4.64	7.86	5.04E-05	Alpha-galactosidase, EC 3.2.1.22 (Alpha-D-galactoside galactohydrolase) (Melibiase)
26	TRINITY_DN3304_c0_g1	0	0	0	9.07	9.08	2.36	0.000767	Predicted Protein
27	TRINITY_DN229927_c0_g1	0	0	0	7.04	3.93	6.56	0.000106	Predicted Protein
28	TRINITY_DN44526_c0_g2	0	0	0	8.45	2.63	7.68	0.000697	Predicted Protein
29	TRINITY_DN185135_c0_g1	0.01	0.04	0	10.52	6.31	8.09	0.00011	Predicted Protein
30	TRINITY_DN69346_c0_g1	0	0	0.11	8.89	9.05	16.12	0.000102	Predicted Protein
31	TRINITY_DN61932_c0_g1	0	0	0	4.25	10.03	4.53	4.75E-05	Predicted Protein
32	TRINITY_DN1400_c0_g1	0.03	0.03	0.07	24.93	11.67	26.83	0.000432	Subtilisin-like protease SBT5.6, EC 3.4.21.- (Subtilase subfamily 5 member 6, AtSBT5.6)
33	TRINITY_DN6996_c0_g5	0	0.12	0	12.87	8.76	10.4	0.000112	Predicted Protein
34	TRINITY_DN28592_c2_g1	0	1.27	0	25.1	13.73	26.65	0.000766	Predicted Protein
35	TRINITY_DN63981_c0_g2	0	0	0	4.48	4.77	7.31	3.70E-05	Predicted Protein
36	TRINITY_DN129749_c0_g1	0	0.12	0	9.6	9.98	11.12	4.47E-05	Predicted Protein
37	TRINITY_DN800_c0_g2	0	0	0	8	2.45	6.55	0.000689	Predicted Protein
38	TRINITY_DN1269_c0_g1	0.15	0.2	0	32.25	13.5	37.33	0.001037	Predicted Protein
39	TRINITY_DN11362_c0_g1	0	0.89	0.23	39.53	30.88	57.71	0.000201	Predicted Protein
40	TRINITY_DN20766_c0_g1	0	0.07	0	10.17	5.57	10.32	0.000218	Subtilisin-like protease SBT1.7, EC 3.4.21.- (Cucumisin-like serine protease) (Subtilase subfamily 1 member 7, AtSBT1.7) (Subtilisin-like serine protease 1, At-SLP1)
41	TRINITY_DN15047_c0_g1	0	0	0	4.32	5.55	5.12	1.96E-05	Predicted Protein
42	TRINITY_DN26605_c0_g2	0	0	0	2.45	6.9	7.85	0.00015	Predicted Protein
43	TRINITY_DN104952_c0_g1	0	0	0	6.71	2.45	6.55	0.000484	Predicted Protein
44	TRINITY_DN4176_c0_g1	0.02	0.33	0.26	61.56	18.42	66.16	0.001525	Chalcone synthase, EC 2.3.1.74 (Naringenin-chalcone synthase)
45	TRINITY_DN24969_c0_g1	0.12	0	0	15.57	5.1	13.9	0.00131	Predicted Protein
46	TRINITY_DN24626_c0_g1	0.12	0.13	0	21.48	21.87	17.99	6.53E-05	Predicted Protein
47	TRINITY_DN121_c0_g3	0.09	0.02	0.11	16.6	18.32	21.49	5.20E-05	Cellulose synthase A catalytic subunit 4 [UDP-forming], AtCesA4, EC 2.4.1.12 (Protein IRREGULAR XYLEM 5, AtIRX5)
48	TRINITY_DN20218_c0_g1	0.02	0.04	0	9.8	8.24	11.28	5.62E-05	Predicted Protein
49	TRINITY_DN5372_c0_g1	0	0	0	7.25	1.67	7.18	0.001777	Predicted Protein
50	TRINITY_DN3173_c0_g2	0	0	0	5.65	2.3	7.09	0.000497	Predicted Protein

51	TRINITY_DN15841_c0_g1	0	0	0	5.23	2.71	6.29	0.000214	Predicted Protein
52	TRINITY_DN1891_c0_g3	0	0	0	6.76	3.67	3.42	0.000191	Predicted Protein
53	TRINITY_DN15910_c0_g1	0.1	0.24	0.09	49.33	33.41	37.21	4.83E-05	Predicted Protein
54	TRINITY_DN7784_c1_g1	0	0	0	8.87	2.18	3.94	0.001207	Predicted Protein
55	TRINITY_DN8038_c0_g1	0.62	0.26	0.25	122.65	81.13	105.38	4.77E-06	Probable aquaporin PIP2-8 (Plasma membrane intrinsic protein 2-8, AtPIP2;8) (Plasma membrane intrinsic protein 3b, PIP3b)
56	TRINITY_DN12836_c0_g1	0	0	0	7	3.29	3.35	0.00028	Alpha carbonic anhydrase 7, AtaCA7, AtalphaCA7, EC 4.2.1.1 (Alpha carbonate dehydratase 7)
57	TRINITY_DN6386_c0_g2	0	0	0	4.88	3.66	4.48	5.51E-05	Predicted Protein
58	TRINITY_DN7751_c0_g1	0	0	0	5.77	2.52	5.12	0.000267	Predicted Protein
59	TRINITY_DN159567_c0_g1	0	0.32	0	11.89	6.31	15.47	0.000621	WAT1-related protein At5g07050
60	TRINITY_DN293_c0_g1	0.59	0.32	0.44	83.3	131.42	164.86	4.44E-07	Delta-selinene-like synthase, chloroplastic, PsTPS-Sell, EC 4.2.3.76
61	TRINITY_DN293_c0_g1	0.59	0.32	0.44	83.3	131.42	164.86	4.44E-07	Alpha-humulene synthase, EC 4.2.3.104 (Terpene synthase TPS-Hum, PgTPS-Hum)
62	TRINITY_DN293_c0_g1	0.59	0.32	0.44	83.3	131.42	164.86	4.44E-07	Delta-selinene synthase, EC 4.2.3.71, EC 4.2.3.76 (Agfdsel1)
63	TRINITY_DN44886_c0_g1	0	0.04	0	6.47	4.31	7.89	0.000134	Predicted Protein
64	TRINITY_DN71967_c0_g1	0	0	0	6.52	2.32	4.44	0.00046	Predicted Protein
65	TRINITY_DN87537_c1_g2	0	0	0	4.36	1.76	7.92	0.000982	Predicted Protein
66	TRINITY_DN63391_c0_g1	0	0	0	6.17	1.74	5.13	0.000994	Predicted Protein
67	TRINITY_DN50988_c0_g1	0.05	0	0	8.96	3.64	8.45	0.000593	Predicted Protein
68	TRINITY_DN36314_c0_g2	0	0	0	7.73	4.68	1.42	0.001863	Putative anthocyanidin reductase, GbANR, EC 1.3.1.-
69	TRINITY_DN647_c0_g2	0	0.07	0.06	15.17	6.47	13.72	0.00068	Purple acid phosphatase 3, EC 3.1.3.2
70	TRINITY_DN256198_c0_g1	0	0	0	7.86	4.47	1.34	0.002153	Predicted Protein
71	TRINITY_DN125084_c0_g3	0.03	0	0	5.87	7.75	3.36	0.000138	Delta-selinene synthase, EC 4.2.3.71, EC 4.2.3.76 (Agfdsel1)
72	TRINITY_DN22583_c0_g1	0	0	0	4.49	3.11	3.47	8.47E-05	Predicted Protein
73	TRINITY_DN98979_c0_g4	0	0	0	3.3	4.07	3.81	2.91E-05	Probable galactinol--sucrose galactosyltransferase 6, EC 2.4.1.82 (Protein DARK INDUCIBLE 10) (Raffinose synthase 6)
74	TRINITY_DN9649_c1_g3	0	0	0	2.73	10.46	1.9	0.000761	Predicted Protein

75	TRINITY_DN11419_c0_g1	0	0	0	5.05	1.36	6.38	0.001738	Predicted Protein
76	TRINITY_DN1911_c0_g1	0	0.03	0.03	7.9	7.77	6.89	5.67E-05	Predicted Protein
77	TRINITY_DN2236_c0_g1	0.2	0	0.25	39.44	18.18	16.02	0.001027	Predicted Protein
78	TRINITY_DN250708_c0_g1	0	0	0	7.84	2	2.38	0.001663	Predicted Protein
79	TRINITY_DN18490_c0_g1	0	0	0	3.72	1.31	8	0.002018	Predicted Protein
80	TRINITY_DN7878_c0_g1	0.25	1.75	0.46	124.44	78.86	175.53	2.73E-06	Predicted Protein
81	TRINITY_DN3227_c0_g1	0	0	0	3.03	2.62	5.23	0.000109	Predicted Protein
82	TRINITY_DN83526_c0_g3	0	0	0	2.83	5.13	3	4.20E-05	Predicted Protein
83	TRINITY_DN1934_c0_g1	0.02	0.03	0.06	16.23	6.2	17.34	0.001139	Predicted Protein
84	TRINITY_DN121_c0_g1	0.18	0.1	0.03	20.19	22.8	24.32	2.97E-05	Cellulose synthase A catalytic subunit 8 [UDP-forming], AtCesA8, EC 2.4.1.12 (Protein IRREGULAR XYLEM 1, AtIRX1) (Protein LEAF WILTING 2)
85	TRINITY_DN121_c0_g1	0.18	0.1	0.03	20.19	22.8	24.32	2.97E-05	Cellulose synthase A catalytic subunit 9 [UDP-forming], EC 2.4.1.12 (OsCesA9)
86	TRINITY_DN2085_c0_g1	0.34	0.57	0.14	100.49	52.63	54.79	3.54E-05	Predicted Protein
87	TRINITY_DN41388_c0_g2	0	0	0.04	3.85	3.14	9.7	0.000494	Predicted Protein
88	TRINITY_DN17036_c0_g1	0.06	0.77	0.19	41.49	43.27	52.52	1.13E-05	Predicted Protein
89	TRINITY_DN19058_c0_g1	0	0	0	2.83	3.41	3.9	3.74E-05	Predicted Protein
90	TRINITY_DN5226_c2_g1	0	0	0	3.04	1.9	6.31	0.000435	Predicted Protein
91	TRINITY_DN61279_c2_g1	0	0	0	5.99	1.98	2.71	0.000712	Probable LRR receptor-like serine/threonine-protein kinase At5g48740, EC 2.7.11.1
92	TRINITY_DN1794_c0_g3	0	0	0	2.16	2.75	6.48	0.000243	Predicted Protein
93	TRINITY_DN31192_c0_g2	0	0	0	3.24	3.3	3.39	4.09E-05	Predicted Protein
94	TRINITY_DN260195_c2_g2	0	0	0	3.29	3.18	3.44	4.45E-05	Predicted Protein
95	TRINITY_DN304016_c0_g1	0	0	0	3.72	2.27	4.05	0.000138	Predicted Protein
96	TRINITY_DN4245_c0_g1	0.06	0.24	0	6.69	11.32	27.52	0.00114	Predicted Protein
97	TRINITY_DN16676_c0_g2	0	0	0	3.9	2.93	2.89	8.31E-05	Predicted Protein
98	TRINITY_DN1794_c0_g1	0	0	0	3.92	2.16	3.82	0.000175	Predicted Protein
99	TRINITY_DN180254_c0_g1	0.01	0	0	4.85	4.11	5.09	7.03E-05	Predicted Protein
100	TRINITY_DN30545_c1_g1	0.08	0.08	0.06	16.07	11.96	18.36	0.000123	Predicted Protein

STable 7a. Top 100 upregulated genes from nickel susceptible samples compared to the controls in *Pinus banksiana*

Rank	Gene ID	Sus 1	Sus 2	Sus 3	Water 1	Water 2	Water 3	logFC	Adj. P. Value	Uniprot Description
0	TRINITY_DN2786_c0_g1	856.36	272.59	231.03	0	0	0	12.82	9.58E-05	Predicted Protein
1	TRINITY_DN5965_c1_g1	1181.56	905.23	1030.95	0.33	0	0	12.75	8.20E-06	Predicted Protein
2	TRINITY_DN2075_c1_g1	233.73	192.67	517.7	0	0	0	12.43	3.40E-06	Predicted Protein
3	TRINITY_DN57079_c0_g1	1015.8	115.56	157.97	0	0	0	12.31	0.000978	Predicted Protein
4	TRINITY_DN7061_c1_g1	223.03	244.97	330	0	0	0	12.30	6.15E-08	Predicted Protein
5	TRINITY_DN2832_c0_g1	409.8	198.4	215.56	0	0	0	12.28	6.33E-06	Predicted Protein
6	TRINITY_DN1628_c0_g1	1029.68	393.25	376.84	0	0.32	0	11.96	0.000183	Trypsin inhibitor [Cleaved into: Trypsin inhibitor chain A; Trypsin inhibitor chain B]
7	TRINITY_DN258556_c0_g1	451.94	114.99	118.68	0	0	0	11.78	0.000117	Predicted Protein
8	TRINITY_DN5795_c0_g1	706.72	659.33	762.96	0	0.84	0	11.76	2.45E-05	Predicted Protein
9	TRINITY_DN4524_c0_g3	321.7	70.3	142.87	0	0	0	11.47	8.63E-05	Predicted Protein
10	TRINITY_DN34759_c0_g1	1034.78	337.83	229.04	0	0.56	0	11.36	0.000835	Predicted Protein
11	TRINITY_DN7289_c0_g1	467.02	181.08	31.83	0	0	0	11.35	0.001583	Predicted Protein
12	TRINITY_DN14305_c0_g1	39.09	227.66	256.23	0	0	0	11.31	7.76E-05	Predicted Protein
13	TRINITY_DN3861_c0_g1	42.86	138.8	258.86	0	0	0	11.13	3.22E-05	Predicted Protein
14	TRINITY_DN1368_c0_g1	3066.68	660.38	763.89	0	1.3	0.07	11.13	0.010716	Predicted Protein
15	TRINITY_DN24881_c0_g1	223.93	40.37	165.79	0	0	0	11.12	0.000164	Predicted Protein
16	TRINITY_DN690_c0_g1	349.88	209.87	134.26	0.05	0	0	11.06	2.91E-05	Predicted Protein
17	TRINITY_DN1518_c0_g1	60.21	106.22	199.6	0	0	0	11.04	2.67E-06	Predicted Protein
18	TRINITY_DN1481_c0_g1	248.24	432.11	226.95	0	0.41	0	10.97	2.52E-05	Predicted Protein
19	TRINITY_DN2463_c0_g1	702.31	342.75	369.29	0	0.04	0.11	10.96	3.86E-05	Predicted Protein
20	TRINITY_DN8563_c1_g1	139.01	83.26	93.31	0	0	0	10.94	1.76E-06	Predicted Protein
21	TRINITY_DN9801_c0_g1	90.72	141.47	74.39	0	0	0	10.88	7.09E-07	Predicted Protein
22	TRINITY_DN2496_c0_g1	134.27	107.85	191.85	0	0.08	0	10.63	3.88E-06	Predicted Protein
23	TRINITY_DN4477_c1_g1	64.27	90.49	89.56	0	0	0	10.60	8.85E-08	Predicted Protein
24	TRINITY_DN1520_c0_g1	1683.13	371.18	268.6	0.02	0.65	0	10.59	0.007249	Trypsin inhibitor [Cleaved into: Trypsin inhibitor

									chain A; Trypsin inhibitor chain B]
25	TRINITY_DN3069_c0_g1	228.16	277.31	149.25	0	0.37	0	10.56	3.66E-05	Predicted Protein
26	TRINITY_DN4424_c0_g1	87.8	59.58	77.9	0	0	0	10.48	7.87E-07	Predicted Protein
27	TRINITY_DN5391_c1_g1	61.43	67.15	96.09	0	0	0	10.47	2.02E-07	Predicted Protein
28	TRINITY_DN257933_c1_g1	66.61	58.29	101.55	0	0	0	10.47	5.11E-07	Predicted Protein
29	TRINITY_DN8013_c1_g2	71.59	52.96	98.07	0	0	0	10.44	8.81E-07	Predicted Protein
30	TRINITY_DN12884_c0_g1	323.26	95.6	86.1	0	0.13	0	10.44	0.000244	Predicted Protein
31	TRINITY_DN129489_c0_g1	212.21	36.49	45.31	0	0	0	10.40	0.00026	Predicted Protein
32	TRINITY_DN16613_c0_g1	49.7	318.88	542.06	0.77	0	0	10.35	0.002258	Predicted Protein
33	TRINITY_DN1307_c0_g1	156.84	44.72	36.31	0	0	0	10.24	0.000104	Germin-like protein 1-1 (Germin-like protein 4, OsGER4)
34	TRINITY_DN1307_c0_g1	156.84	44.72	36.31	0	0	0	10.24	0.000104	Germin-like protein subfamily 2 member 2
35	TRINITY_DN1507_c0_g1	77.69	30.86	83.25	0	0	0	10.14	1.22E-05	Predicted Protein
36	TRINITY_DN9955_c0_g1	212.46	31.95	27.96	0	0	0	10.10	0.000582	Predicted Protein
37	TRINITY_DN12750_c0_g1	57.73	47.71	65.01	0	0	0	10.08	3.98E-07	Predicted Protein
38	TRINITY_DN1453_c1_g4	121.3	205.45	105.17	0	0.3	0	10.06	2.77E-05	Predicted Protein
39	TRINITY_DN17_c0_g2	46.6	43.02	78.55	0	0	0	10.03	7.05E-07	RING-H2 finger protein ATL60, EC 2.3.2.27 (RING-type E3 ubiquitin transferase ATL60)
40	TRINITY_DN3066_c3_g2	66.68	32.1	71.89	0	0	0	10.02	5.15E-06	Predicted Protein
41	TRINITY_DN50999_c1_g1	41.96	50.86	72.52	0	0	0	10.02	2.78E-07	Predicted Protein
42	TRINITY_DN883_c0_g1	779.73	316.71	218.58	0.03	0.73	0	10.01	0.001774	Class V chitinase, AtChiC, EC 3.2.1.14, EC 3.2.1.200
43	TRINITY_DN883_c0_g1	779.73	316.71	218.58	0.03	0.73	0	10.01	0.001774	Class V chitinase CHIT5b, MtCHIT5b, EC 3.2.1.14
44	TRINITY_DN5965_c0_g1	353.05	199.87	227.8	0.07	0.21	0	10.00	5.20E-05	Predicted Protein
45	TRINITY_DN4828_c0_g1	128.64	100.33	56.9	0	0.07	0	9.98	2.49E-05	Predicted Protein
46	TRINITY_DN15754_c0_g2	191.49	88.62	108.22	0	0.27	0	9.97	7.12E-05	Predicted Protein
47	TRINITY_DN5037_c0_g1	45.53	39.39	75.59	0	0	0	9.96	9.27E-07	Probable disease resistance protein At4g33300

48	TRINITY_DN2914_c0_g1	58.11	70.45	90.7	0	0.03	0	9.91	9.50E-07	Protein TIFY 10b, OsTIFY10b (Jasmonate ZIM domain-containing protein 7, OsJAZ7) (OsJAZ6)
49	TRINITY_DN2914_c0_g1	58.11	70.45	90.7	0	0.03	0	9.91	9.50E-07	Protein TIFY 3B (Jasmonate ZIM domain-containing protein 12)
50	TRINITY_DN12858_c0_g1	39.28	60.28	49.32	0	0	0	9.87	1.94E-07	Predicted Protein
51	TRINITY_DN5136_c0_g1	89.54	27.06	46.78	0	0	0	9.86	2.67E-05	Predicted Protein
52	TRINITY_DN1369_c0_g1	30.46	67	55.86	0	0	0	9.86	5.13E-07	Predicted Protein
53	TRINITY_DN5257_c0_g1	51.33	44.59	48.63	0	0	0	9.85	4.01E-07	Disease resistance protein Roq1 (NAD(+) hydrolase RPV1, EC 3.2.2.6) (Recognition of XopQ 1 protein)
54	TRINITY_DN4066_c0_g1	49.38	24.94	85.92	0	0	0	9.84	1.34E-05	Predicted Protein
55	TRINITY_DN103008_c0_g1	157.28	172.42	170.28	0.08	0.1	0	9.84	2.33E-06	Predicted Protein
56	TRINITY_DN25430_c0_g1	61.55	46.45	36.7	0	0	0	9.82	1.97E-06	Predicted Protein
57	TRINITY_DN27427_c0_g1	43.15	55.5	40.21	0	0	0	9.78	3.51E-07	Predicted Protein
58	TRINITY_DN30360_c0_g2	33.45	28.27	96.74	0	0	0	9.78	1.13E-05	Predicted Protein
59	TRINITY_DN3861_c0_g2	23.6	52.74	73.85	0	0	0	9.77	2.41E-06	Predicted Protein
60	TRINITY_DN630_c0_g1	278.35	47.92	62.63	0	0.16	0	9.76	0.000788	Protein SRG1, AtSRG1 (Protein SENESCENCE-RELATED GENE 1)
61	TRINITY_DN630_c0_g1	278.35	47.92	62.63	0	0.16	0	9.76	0.000788	Jasmonate-induced oxygenase 4, EC 1.14.11.- (2-oxoglutarate-dependent dioxygenase JOX4) (Anthocyanidin synthase) (Jasmonic acid oxidase 4)
62	TRINITY_DN630_c0_g1	278.35	47.92	62.63	0	0.16	0	9.76	0.000788	Codeine O-demethylase, EC 1.14.11.32
63	TRINITY_DN630_c0_g1	278.35	47.92	62.63	0	0.16	0	9.76	0.000788	S-norcoclaurine synthase 1, CjNCS1, EC 4.2.1.78
64	TRINITY_DN1456_c0_g1	299.75	199.03	556.22	0.27	0	0.25	9.75	0.000548	Predicted Protein
65	TRINITY_DN1453_c1_g2	80.93	14.5	69.32	0	0	0	9.72	0.000167	Predicted Protein

66	TRINITY_DN1644_c0_g1	42.79	32.77	57.69	0	0	0	9.71	9.39E-07	NAC transcription factor 47 (NAC domain-containing protein 47, ANAC047) (Protein SPEEDY HYPONASTIC GROWTH)
67	TRINITY_DN3884_c0_g2	100.65	203.76	97.89	0.52	0	0	9.70	6.36E-05	Predicted Protein
68	TRINITY_DN122283_c1_g1	21.07	48.55	76.15	0	0	0	9.69	4.43E-06	Predicted Protein
69	TRINITY_DN2126_c0_g1	528.07	419.8	320.85	0.02	0.61	0.1	9.60	0.000201	UDP-glycosyltransferase 75C1, Abscisic acid beta-glucosyltransferase, Indole-3-acetate beta-glucosyltransferase, SlUGT75C1, EC 2.4.1.121, EC 2.4.1.263
70	TRINITY_DN36982_c0_g1	105.05	90.61	162.57	0.4	0	0	9.60	4.09E-05	Predicted Protein
71	TRINITY_DN2364_c0_g1	38.88	35.3	46.73	0	0	0	9.59	3.92E-07	Disease resistance-like protein DSC2, EC 3.2.2.6 (Protein DOMINANT SUPRESSOR OF CAMTA3 NUMBER 2)
72	TRINITY_DN792_c0_g1	55.94	77.28	42.6	0	0.03	0	9.56	3.71E-06	ACT domain-containing protein ACR4 (Protein ACT DOMAIN REPEATS 4)
73	TRINITY_DN792_c0_g1	55.94	77.28	42.6	0	0.03	0	9.56	3.71E-06	ACT domain-containing protein ACR5 (Protein ACT DOMAIN REPEATS 5)
74	TRINITY_DN4963_c0_g1	150.88	121.41	208.93	0.14	0	0.09	9.55	1.62E-05	Predicted Protein
75	TRINITY_DN1663_c0_g1	25.82	31.27	61.98	0	0	0	9.48	1.62E-06	Predicted Protein
76	TRINITY_DN2952_c0_g1	125.84	206.04	85.86	0	0	0.5	9.48	0.000134	Predicted Protein
77	TRINITY_DN77041_c1_g1	30.23	34.79	47.89	0	0	0	9.48	3.49E-07	Predicted Protein
78	TRINITY_DN35222_c0_g1	15.26	38.41	80.21	0	0	0	9.45	1.96E-05	Predicted Protein
79	TRINITY_DN2391_c0_g1	78.72	104.14	158.87	0.79	0	0	9.44	7.23E-05	Predicted Protein
80	TRINITY_DN2516_c0_g1	458.63	323.93	253.11	0.02	0.63	0.07	9.43	0.000307	Predicted Protein
81	TRINITY_DN46511_c0_g1	72.21	154.98	205.77	1.64	0	0	9.42	0.000319	Predicted Protein

82	TRINITY_DN36625_c1_g2	89.44	109.84	109.25	0.31	0	0	9.42	1.83E-05	Calcium-binding protein KIC (KCBP-interacting calcium-binding protein)
83	TRINITY_DN7685_c0_g1	221.59	64.74	65.95	0	0.41	0	9.41	0.000547	Predicted Protein
84	TRINITY_DN9211_c0_g1	31.99	33.43	40.13	0	0	0	9.40	3.09E-07	UDP-glycosyltransferase 86A1, EC 2.4.1.-
85	TRINITY_DN3577_c0_g1	300.57	101.41	106.24	0.11	0.13	0	9.40	0.000377	Predicted Protein
86	TRINITY_DN3536_c0_g1	22.14	46.38	39.74	0	0	0	9.37	5.78E-07	Predicted Protein
87	TRINITY_DN5723_c0_g1	126.54	95.72	114.61	0.01	0.19	0	9.35	1.33E-05	Predicted Protein
88	TRINITY_DN1537_c0_g1	31.3	25.7	47.69	0	0	0	9.35	1.16E-06	Predicted Protein
89	TRINITY_DN4694_c0_g2	26.98	40.75	35.09	0	0	0	9.34	2.77E-07	Predicted Protein
90	TRINITY_DN2595_c0_g1	43.67	16.56	51.04	0	0	0	9.34	1.85E-05	Predicted Protein
91	TRINITY_DN3685_c0_g1	352.21	44.47	22.53	0	0.16	0	9.33	0.004358	Predicted Protein
92	TRINITY_DN4195_c0_g1	47	27.15	28.37	0	0	0	9.31	3.65E-06	Predicted Protein
93	TRINITY_DN2611_c0_g1	90.71	128.82	181.06	0.08	0.13	0	9.30	8.52E-06	Predicted Protein
94	TRINITY_DN2751_c0_g1	77.66	76.97	116.69	0.04	0	0.02	9.28	1.45E-06	Predicted Protein
95	TRINITY_DN71914_c0_g1	20.85	31.78	49.56	0	0	0	9.27	1.06E-06	Predicted Protein
96	TRINITY_DN115569_c0_g1	20.27	35.02	43.43	0	0	0	9.24	6.82E-07	Predicted Protein
97	TRINITY_DN2702_c0_g1	68.05	69.26	96.15	0.03	0	0.03	9.23	8.23E-07	Predicted Protein
98	TRINITY_DN3092_c0_g1	568.39	135.64	138.06	0.14	0.35	0	9.23	0.005382	Glucan endo-1,3-beta-glucosidase, acidic isoform, EC 3.2.1.39 ((1->3)-beta-glucan endohydrolase, (1->3)-beta-glucanase) (Beta-1,3-endoglucanase)
99	TRINITY_DN2152_c1_g1	21.54	25.27	51.61	0	0	0	9.20	1.98E-06	Predicted Protein
100	TRINITY_DN3685_c0_g2	199.1	149.86	136.23	0.01	0.58	0	9.19	0.000104	Copia protein (Gag-int-pol protein) [Cleaved into: Copia VLP protein; Copia protease, EC 3.4.23.-]

STable 7b. Top 100 downregulated genes from nickel susceptible samples compared to the control in *Pinus banksiana*

Rank	Gene ID	Sus 1	Sus 2	Sus 3	Water 1	Water 2	Water 3	logFC	Adj. P. Value	UniProt Description
0	TRINITY_DN432_c0_g1	0	0	0	77.54	17.58	69.88	-12.147	8.42E-05	Predicted Protein
1	TRINITY_DN2314_c0_g1	0	0	0	40.88	14.56	52.04	-11.582	2.29E-05	Predicted Protein
2	TRINITY_DN4176_c0_g1	0	0.14	0.04	61.56	18.42	66.16	-11.488	5.99E-05	Chalcone synthase, EC 2.3.1.74 (Naringenin-chalcone synthase)
3	TRINITY_DN24626_c0_g1	0	0.04	0.03	21.48	21.87	17.99	-10.913	2.30E-07	Predicted Protein
4	TRINITY_DN26931_c0_g1	0	0	0.55	65.61	45.82	36.39	-10.864	2.13E-05	Probable aquaporin PIP2-8 (Plasma membrane intrinsic protein 2-8, AtPIP2;8) (Plasma membrane intrinsic protein 3b, PIP3b)
5	TRINITY_DN4059_c0_g1	0	0	0	20.09	12.1	19.58	-10.661	1.53E-06	Predicted Protein
6	TRINITY_DN4890_c0_g1	0	0	0	15.59	12.05	25.46	-10.643	1.24E-06	Predicted Protein
7	TRINITY_DN53932_c0_g1	0	0.04	0	17.81	11.58	17.09	-10.514	1.10E-06	Predicted Protein
8	TRINITY_DN2202_c0_g1	0	0	0	12.61	15.48	16.45	-10.433	1.05E-07	Predicted Protein
9	TRINITY_DN30654_c0_g1	0	0	0	14.69	11.78	14.4	-10.336	4.72E-07	Predicted Protein
10	TRINITY_DN20386_c0_g2	0	0	0	27.65	4.28	16.45	-10.308	0.000156	Predicted Protein
11	TRINITY_DN1934_c0_g1	0	0	0	16.23	6.2	17.34	-10.203	1.25E-05	Predicted Protein
12	TRINITY_DN5585_c0_g1	0	0.34	0.59	81.26	16.83	119.24	-10.081	0.002538	Predicted Protein
13	TRINITY_DN69830_c0_g4	0	0.04	0	10.13	7.29	18.59	-10.047	2.81E-06	Predicted Protein
14	TRINITY_DN40558_c0_g1	0.08	0.1	0	36.31	14.48	19.64	-10.006	2.74E-05	Predicted Protein
15	TRINITY_DN6996_c0_g5	0	0	0	12.87	8.76	10.4	-9.985	1.17E-06	Predicted Protein
16	TRINITY_DN216_c0_g1	0.1	0.12	0.05	38.41	25.04	25.45	-9.863	3.90E-06	Fatty acyl-CoA reductase 2, chloroplastic, AtFAR2, EC 1.2.1.84 (Fatty acid reductase 2) (Male sterility protein 2)
17	TRINITY_DN293_c0_g1	0.2	0.93	0.54	83.3	131.42	164.86	-9.758	1.23E-05	Delta-selinene-like synthase, chloroplastic, PsTPS-Sell, EC 4.2.3.76
18	TRINITY_DN293_c0_g1	0.2	0.93	0.54	83.3	131.42	164.86	-9.758	1.23E-05	Alpha-humulene synthase, EC 4.2.3.104 (Terpene synthase TPS-Hum, PgTPS-Hum)

19	TRINITY_DN293_c0_g1	0.2	0.93	0.54	83.3	131.42	164.86	-9.758	1.23E-05	Delta-selinene synthase, EC 4.2.3.71, EC 4.2.3.76 (Agfdsel1)
20	TRINITY_DN522_c0_g3	0	0	0	8.24	4.71	17.93	-9.728	1.28E-05	Predicted Protein
21	TRINITY_DN37470_c0_g1	0	0	0	13.75	5.47	8.44	-9.722	9.79E-06	Predicted Protein
22	TRINITY_DN59077_c1_g1	0	0	0.09	11.37	9.17	20.15	-9.717	3.35E-06	Predicted Protein
23	TRINITY_DN2880_c0_g2	0	0	0	19.16	1.84	13.12	-9.650	0.000464	Predicted Protein
24	TRINITY_DN185135_c0_g1	0	0	0	10.52	6.31	8.09	-9.618	2.17E-06	Predicted Protein
25	TRINITY_DN1400_c0_g1	0	0.21	0.12	24.93	11.67	26.83	-9.607	2.19E-05	Subtilisin-like protease SBT5.6, EC 3.4.21.- (Subtilase subfamily 5 member 6, AtSBT5.6)
26	TRINITY_DN39137_c0_g1	0	0	0	9.95	4.07	10.82	-9.534	1.07E-05	Predicted Protein
27	TRINITY_DN159567_c0_g1	0	0	0.09	11.89	6.31	15.47	-9.457	9.34E-06	WAT1-related protein At5g07050
28	TRINITY_DN3390_c0_g1	0	0	0	9.96	3.94	7.77	-9.369	1.00E-05	Predicted Protein
29	TRINITY_DN85728_c0_g1	0	0.18	0.12	16.24	13.3	22.79	-9.354	4.12E-06	Transcription repressor MYB5 (AtM2) (Myb-related protein 5, AtMYB5)
30	TRINITY_DN85728_c0_g1	0	0.18	0.12	16.24	13.3	22.79	-9.354	4.12E-06	Transcription factor MYB123 (Myb-related protein 123, AcMYB123)
31	TRINITY_DN1643_c0_g1	0	0.13	0.23	29.06	12.13	17.23	-9.340	3.95E-05	Predicted Protein
32	TRINITY_DN7878_c0_g1	0.05	1.23	2.45	124.44	78.86	175.53	-9.336	0.000362	Predicted Protein
33	TRINITY_DN50988_c0_g1	0	0	0	8.96	3.64	8.45	-9.315	9.97E-06	Predicted Protein
34	TRINITY_DN3730_c0_g1	0.16	0.15	0.66	67.3	33.24	49.71	-9.309	0.000253	Cytochrome P450 720B2, EC 1.14.-.- (Cytochrome P450 CYPB)
35	TRINITY_DN15988_c0_g1	0	0	0	23.84	1.19	6.84	-9.277	0.001286	Predicted Protein
36	TRINITY_DN43851_c0_g1	0	0.04	0.05	9.06	4.69	18.41	-9.264	2.80E-05	Predicted Protein
37	TRINITY_DN20386_c0_g1	0	0	0	7.77	6	5.13	-9.220	1.67E-06	Predicted Protein
38	TRINITY_DN4520_c0_g1	0	0	0	9.57	4	5.78	-9.219	9.27E-06	Predicted Protein
39	TRINITY_DN17540_c0_g1	0	0	0	10.32	6.62	3.33	-9.217	1.66E-05	Predicted Protein
40	TRINITY_DN1550_c0_g1	0	0	0.51	18.5	9.11	17.44	-9.206	4.81E-05	Predicted Protein
41	TRINITY_DN69950_c0_g1	0	0	0	10.17	0.94	19.9	-9.205	0.001196	Predicted Protein

42	TRINITY_DN51950_c1_g1	0	0	0	6.24	5.15	7.26	-9.197	8.15E-07	Predicted Protein
43	TRINITY_DN175470_c0_g2	0	0	0	7.48	3.57	7.41	-9.145	6.05E-06	Predicted Protein
44	TRINITY_DN53758_c0_g2	0	0	0	4.11	6.36	7.87	-9.094	4.59E-07	Predicted Protein
45	TRINITY_DN1111_c0_g2	0.13	0.17	0.05	20.51	9.79	21.28	-9.072	3.18E-05	Homeobox-leucine zipper protein ATHB-5 (HD-ZIP protein ATHB-5) (Homeodomain transcription factor ATHB-5)
46	TRINITY_DN15910_c0_g1	0.09	0.58	0.31	49.33	33.41	37.21	-9.064	7.06E-05	Predicted Protein
47	TRINITY_DN63981_c0_g2	0	0	0	4.48	4.77	7.31	-8.985	7.10E-07	Predicted Protein
48	TRINITY_DN2085_c0_g1	0.18	1.05	0.47	100.49	52.63	54.79	-8.980	0.00067	Predicted Protein
49	TRINITY_DN8317_c0_g1	0	0.1	0	10.49	5.21	7.51	-8.970	1.16E-05	Predicted Protein
50	TRINITY_DN3595_c0_g1	0	0.29	0	11.84	5.86	13.89	-8.968	3.57E-05	Predicted Protein
51	TRINITY_DN6754_c0_g1	0	0	0	7.86	2.64	6.3	-8.968	1.92E-05	Predicted Protein
52	TRINITY_DN160749_c0_g1	0	0	0	8.48	2.5	5.97	-8.964	2.76E-05	Non-specific phospholipase C2, EC 3.1.-.-
53	TRINITY_DN1979_c0_g1	0.57	0.08	0.34	41.18	32.34	46.42	-8.945	4.76E-05	Predicted Protein
54	TRINITY_DN12418_c0_g1	0	1.01	0.33	36.43	22.5	33.82	-8.932	0.000147	Predicted Protein
55	TRINITY_DN4000_c0_g1	0	0	0	1.62	6.17	16.32	-8.913	0.000102	Predicted Protein
56	TRINITY_DN13770_c0_g1	0	0	0	5.02	3.18	7.71	-8.897	4.28E-06	Predicted Protein
57	TRINITY_DN1915_c0_g1	0	0	0.15	18.08	2.16	12.65	-8.891	0.000628	Predicted Protein
58	TRINITY_DN15569_c0_g1	0	0	0.11	8.75	4.05	9.5	-8.877	1.44E-05	Predicted Protein
59	TRINITY_DN124747_c0_g1	0	0.08	0	6.55	5.23	10.42	-8.869	4.75E-06	Predicted Protein
60	TRINITY_DN26605_c0_g2	0	0	0	2.45	6.9	7.85	-8.847	3.02E-06	Predicted Protein
61	TRINITY_DN61873_c0_g2	0.02	0.04	0.02	5.37	3.82	5	-8.811	1.64E-06	Receptor protein-tyrosine kinase CEPR1, EC 2.7.10.1 (Protein C-TERMINALLY ENCODED PEPTIDE RECEPTOR 1) (Protein XYLEM INTERMIXED WITH PHLOEM 1)
62	TRINITY_DN5372_c0_g1	0	0	0	7.25	1.67	7.18	-8.799	6.89E-05	Predicted Protein
63	TRINITY_DN301_c0_g2	0.35	0.05	0.21	29.17	6.67	30.94	-8.786	0.000674	Phenylcoumaran benzylic ether reductase PT1, PCBER-Pt1, EC 1.23.1.- (PtPCBER)

64	TRINITY_DN301_c0_g2	0.35	0.05	0.21	29.17	6.67	30.94	-8.786	0.000674	Phenylcoumaran benzylic ether reductase IRL1, EC 1.23.1.- (Isoflavone reductase-like 1, GbIRL1, IFR-like protein 1)
65	TRINITY_DN4725_c0_g2	0	0	0	3.29	9.45	3.54	-8.771	2.59E-06	Predicted Protein
66	TRINITY_DN15841_c0_g1	0	0	0	5.23	2.71	6.29	-8.759	6.22E-06	Predicted Protein
67	TRINITY_DN26605_c0_g1	0.15	0	0	6.61	7.11	10.35	-8.756	4.57E-06	Predicted Protein
68	TRINITY_DN1891_c0_g3	0	0	0	6.76	3.67	3.42	-8.747	7.22E-06	Predicted Protein
69	TRINITY_DN7784_c1_g1	0	0	0	8.87	2.18	3.94	-8.746	5.15E-05	Predicted Protein
70	TRINITY_DN7900_c0_g1	0	0	0	7.34	1.22	8.27	-8.738	0.000192	Predicted Protein
71	TRINITY_DN6386_c0_g2	0	0	0	4.88	3.66	4.48	-8.696	1.48E-06	Predicted Protein
72	TRINITY_DN7751_c0_g1	0	0	0	5.77	2.52	5.12	-8.689	8.66E-06	Predicted Protein
73	TRINITY_DN8038_c0_g1	0.27	0.53	4.04	122.65	81.13	105.38	-8.674	9.35E-05	Probable aquaporin PIP2-8 (Plasma membrane intrinsic protein 2-8, AtPIP2;8) (Plasma membrane intrinsic protein 3b, PIP3b)
74	TRINITY_DN113586_c0_g1	0	0.28	0	7.25	5.74	13.28	-8.669	2.30E-05	Predicted Protein
75	TRINITY_DN223175_c1_g1	0	0.45	0.56	29.73	13.33	28.61	-8.668	0.000278	Predicted Protein
76	TRINITY_DN71967_c0_g1	0	0	0	6.52	2.32	4.44	-8.657	1.67E-05	Predicted Protein
77	TRINITY_DN1126_c0_g1	0.11	0.07	0.24	20.81	18.8	10.98	-8.639	1.09E-05	L-type lectin-domain containing receptor kinase VIII.2, LecRK-VIII.2, EC 2.7.11.1
78	TRINITY_DN2994_c2_g1	0	0	0	8.78	0.9	7.01	-8.625	0.000459	Predicted Protein
79	TRINITY_DN260469_c0_g1	0	0	0	3.25	5	4.44	-8.596	4.44E-07	Predicted Protein
80	TRINITY_DN87537_c1_g2	0	0	0	4.36	1.76	7.92	-8.588	3.14E-05	Predicted Protein
81	TRINITY_DN44526_c0_g2	0	0.06	0	8.45	2.63	7.68	-8.572	5.53E-05	Predicted Protein
82	TRINITY_DN6254_c0_g1	0	0	0	5.43	7.86	1.5	-8.569	5.12E-05	Predicted Protein
83	TRINITY_DN20922_c0_g1	0	0	0	3.92	4.6	3.6	-8.568	7.25E-07	Predicted Protein
84	TRINITY_DN63391_c0_g1	0	0	0	6.17	1.74	5.13	-8.567	3.66E-05	Predicted Protein
85	TRINITY_DN3876_c1_g1	0.11	2.05	10.32	196.47	82.44	230.37	-8.555	0.000706	Predicted Protein
86	TRINITY_DN5658_c0_g1	0	0	0	6.27	2.86	3.03	-8.548	1.20E-05	Predicted Protein

87	TRINITY_DN284_c1_g1	0	0	0	8.44	0.52	10.01	-8.538	0.001541	Predicted Protein
88	TRINITY_DN1072_c0_g1	0.79	0.89	2.32	198.16	56.5	130.8	-8.520	0.00083	Predicted Protein
89	TRINITY_DN1317_c0_g1	0	1.04	1.03	39	15.69	47.16	-8.502	0.002024	Predicted Protein
90	TRINITY_DN97404_c0_g1	0	0	0.32	14.2	4.15	7.22	-8.495	0.00015	Protein STRICTOSIDINE SYNTHASE-LIKE 6, AtSSL6
91	TRINITY_DN97404_c0_g1	0	0	0.32	14.2	4.15	7.22	-8.495	0.00015	Protein STRICTOSIDINE SYNTHASE-LIKE 4, AtSSL4
92	TRINITY_DN9994_c0_g1	0	0	0	6.51	0.97	6.62	-8.472	0.000233	Predicted Protein
93	TRINITY_DN109736_c3_g1	0	0	0	3.66	3.29	4.16	-8.457	1.06E-06	Predicted Protein
94	TRINITY_DN2927_c0_g1	0	0	0	4.26	2.75	4.05	-8.449	2.78E-06	Predicted Protein
95	TRINITY_DN5062_c0_g2	0	0.31	0	10.4	7.97	3.99	-8.449	5.98E-05	Predicted Protein
96	TRINITY_DN123612_c0_g1	0	0	0	7.64	0.87	5.84	-8.445	0.000374	Predicted Protein
97	TRINITY_DN4800_c1_g2	0	0	0	4.88	2.4	3.84	-8.443	6.54E-06	Predicted Protein
98	TRINITY_DN98979_c0_g4	0	0	0	3.3	4.07	3.81	-8.443	5.94E-07	Probable galactinol--sucrose galactosyltransferase 6, EC 2.4.1.82 (Protein DARK INDUCIBLE 10) (Raffinose synthase 6)
99	TRINITY_DN13295_c0_g1	0	0	0	4.44	4.08	2.63	-8.442	2.86E-06	Predicted Protein
100	TRINITY_DN20766_c0_g1	0	0.04	0.5	10.17	5.57	10.32	-8.427	5.82E-05	Subtilisin-like protease SBT1.7, EC 3.4.21.- (Cucumisin-like serine protease) (Subtilase subfamily 1 member 7, AtSBT1.7) (Subtilisin-like serine protease 1, At-SLP1)

STable 12a. Top 50 upregulated genes from copper resistant samples compared to copper susceptible samples in *Pinus banksiana*

Rank	Gene ID	Res 1	Res 2	Res 3	Sus 1	Sus 2	Sus 3	logFC	Adj. P. Value	UniProt Description
0	TRINITY_DN35689_c0_g1	12.05	7.41	11.07	0	0	0	9.21	0.00002	Predicted Protein
1	TRINITY_DN10618_c0_g1	17.42	2.72	9.6	0	0	0	8.82	0.00181	Predicted Protein
2	TRINITY_DN91621_c0_g2	13.93	4.82	5.68	0	0	0	8.78	0.00025	Predicted Protein
3	TRINITY_DN199894_c0_g2	9.44	9.02	1.99	0	0	0	8.45	0.00117	Predicted Protein
4	TRINITY_DN28042_c0_g3	4.91	8.95	2.74	0	0	0	8.26	0.00022	Cytochrome P450 750A1, EC 1.14.-.- (Cytochrome P450 CYPC)
5	TRINITY_DN7900_c0_g1	6	6.27	3.22	0	0	0	8.25	0.00007	Predicted Protein
6	TRINITY_DN2617_c0_g1	8.29	4.5	3.27	0	0	0	8.24	0.00017	Predicted Protein
7	TRINITY_DN20922_c0_g1	3.17	6.13	4.05	0	0	0	8.02	0.00004	Predicted Protein
8	TRINITY_DN236262_c0_g1	11.08	1.85	3.41	0	0	0	7.96	0.00197	Predicted Protein
9	TRINITY_DN95006_c0_g1	6.22	4.28	1.99	0	0	0	7.87	0.00033	Predicted Protein
10	TRINITY_DN219929_c1_g1	2.74	4.62	4.69	0	0	0	7.86	0.00003	Predicted Protein
11	TRINITY_DN4529_c0_g1	3	7.73	1.66	0	0	0	7.73	0.00069	1,8-cineole synthase, chloroplastic, EC 4.2.3.108 (Terpene synthase TPS-Cin, PgTPS-Cin)
12	TRINITY_DN13781_c0_g3	16.16	15.27	4.31	0	0	1.35	7.73	0.00318	Predicted Protein
13	TRINITY_DN216_c0_g1	58.07	22.76	12.46	0.07	0.49	0.97	7.72	0.00440	Fatty acyl-CoA reductase 2, chloroplastic, AtFAR2, EC 1.2.1.84 (Fatty acid reductase 2) (Male sterility protein 2)
14	TRINITY_DN9994_c0_g1	8.13	1.94	2.38	0	0	0	7.67	0.00114	Predicted Protein
15	TRINITY_DN5226_c2_g1	3.74	2.06	5.32	0	0	0	7.66	0.00014	Predicted Protein
16	TRINITY_DN57458_c1_g1	2.43	3.07	4.49	0	0	0	7.58	0.00004	Predicted Protein
17	TRINITY_DN3869_c0_g1	3.23	4.31	2.12	0	0	0	7.58	0.00009	Predicted Protein
18	TRINITY_DN47098_c0_g1	7.77	2.08	1.81	0	0	0	7.58	0.00131	Predicted Protein
19	TRINITY_DN19214_c1_g2	3.44	3.21	2.82	0	0	0	7.57	0.00004	Predicted Protein
20	TRINITY_DN40558_c0_g2	1.22	7.95	3.16	0	0	0	7.57	0.00127	Predicted Protein
21	TRINITY_DN18490_c0_g1	2.06	7.43	1.88	0	0	0	7.57	0.00066	Predicted Protein
22	TRINITY_DN9649_c1_g3	0.84	8.97	3.91	0	0	0	7.54	0.00382	Predicted Protein
23	TRINITY_DN148688_c0_g2	6.51	3.72	1.03	0	0	0	7.54	0.00203	Predicted Protein

24	TRINITY_DN100_c0_g2	7.29	15.7	4.96	0	0.41	0.08	7.53	0.00072	Predicted Protein
25	TRINITY_DN178176_c0_g1	3.36	4.4	1.77	0	0	0	7.53	0.00017	Predicted Protein
26	TRINITY_DN3659_c0_g1	8.49	2.81	0.93	0	0	0	7.50	0.00393	Predicted Protein
27	TRINITY_DN10188_c2_g1	2.92	2.4	3.97	0	0	0	7.49	0.00005	Predicted Protein
28	TRINITY_DN12221_c2_g1	6.18	0.9	5.2	0	0	0	7.47	0.00372	Predicted Protein
29	TRINITY_DN20798_c1_g1	1.28	5.26	3.85	0	0	0	7.47	0.00044	Predicted Protein
30	TRINITY_DN18848_c2_g1	1.01	9.32	2.52	0	0	0	7.47	0.00293	Predicted Protein
31	TRINITY_DN16610_c0_g1	1.37	5.49	3.34	0	0	0	7.46	0.00038	Predicted Protein
32	TRINITY_DN22750_c0_g1	4.64	1.9	2.79	0	0	0	7.45	0.00023	Predicted Protein
33	TRINITY_DN21758_c0_g1	5.12	3.05	1.37	0	0	0	7.44	0.00060	Predicted Protein
34	TRINITY_DN191914_c0_g1	1.21	2.46	9.54	0	0	0	7.44	0.00172	Predicted Protein
35	TRINITY_DN61037_c1_g1	4.43	3.34	1.34	0	0	0	7.41	0.00048	Predicted Protein
36	TRINITY_DN51306_c0_g1	32.05	61.43	35.69	0.19	0.97	7.2	7.39	0.00007	Predicted Protein
37	TRINITY_DN107831_c0_g1	3.04	2.65	2.56	0	0	0	7.38	0.00005	Predicted Protein
38	TRINITY_DN94182_c0_g3	4.2	4.9	0.81	0	0	0	7.36	0.00247	Predicted Protein
39	TRINITY_DN6981_c0_g1	5.02	1.85	2.01	0	0	0	7.34	0.00043	Predicted Protein
40	TRINITY_DN11710_c0_g2	150.88	92.2	20.39	1.25	0.47	3.43	7.33	0.00128	Predicted Protein
41	TRINITY_DN45928_c0_g1	2.12	1.09	8.85	0	0	0	7.27	0.00239	Predicted Protein
42	TRINITY_DN18761_c1_g1	11.47	2.81	7.04	0	0.78	0	7.27	0.00242	Predicted Protein
43	TRINITY_DN2127_c0_g1	124.49	62.29	28.73	1.17	0.35	5.16	7.23	0.00034	Early light-induced protein 1, chloroplastic
44	TRINITY_DN267012_c0_g1	2.7	3.15	1.72	0	0	0	7.23	0.00011	Predicted Protein
45	TRINITY_DN6038_c8_g1	4.83	1.74	1.73	0	0	0	7.22	0.00056	Predicted Protein
46	TRINITY_DN25814_c0_g1	1.52	1.55	7.34	0	0	0	7.21	0.00101	Predicted Protein
47	TRINITY_DN1258_c1_g1	8.13	6.28	5.36	0	0	0.94	7.20	0.00047	Predicted Protein
48	TRINITY_DN107808_c1_g2	5.12	5.07	3.74	0.03	0.02	0.29	7.19	0.00019	Predicted Protein
49	TRINITY_DN18729_c0_g1	1.71	4.11	1.89	0	0	0	7.19	0.00018	Predicted Protein
50	TRINITY_DN870_c0_g2	1.27	3.87	2.91	0	0	0	7.18	0.00024	UDP-glycosyltransferase 75C1, Abscisic acid beta-glucosyltransferase, Indole-3-acetate beta-glucosyltransferase, SlUGT75C1, EC 2.4.1.121, EC 2.4.1.263

STable 12b. Top 50 downregulated genes from copper resistant samples compared to copper susceptible samples in *Pinus banksiana*

Rank	Gene ID	Res 1	Res 2	Res 3	Sus 1	Sus 2	Sus 3	logFC	Adj. P. Value	UniProt Description
0	TRINITY_DN3519_c0_g1	0	0	0	191.35	54.37	115.22	-11.34	0.00021	Predicted Protein
1	TRINITY_DN43547_c0_g1	0	0	0	162.58	38.33	61.13	-10.81	0.00035	Predicted Protein
2	TRINITY_DN2824_c0_g1	0	0.03	0	90.93	154.91	84.36	-10.53	0.00000	Polygalacturonase, PG, EC 3.2.1.15 (Pectinase)
3	TRINITY_DN2824_c0_g1	0	0.03	0	90.93	154.91	84.36	-10.53	0.00000	Probable polygalacturonase At1g80170, PG, EC 3.2.1.15 (Pectinase At1g80170)
4	TRINITY_DN1315_c0_g1	0.43	0.06	0.31	763.2	1448.5	490.5	-10.28	0.00001	Beta-glucosidase 12, EC 3.2.1.21
5	TRINITY_DN1315_c0_g1	0.43	0.06	0.31	763.2	1448.5	490.5	-10.28	0.00001	Furcatin hydrolase, FH, EC 3.2.1.161
6	TRINITY_DN1315_c0_g1	0.43	0.06	0.31	763.2	1448.5	490.5	-10.28	0.00001	Non-cyanogenic beta-glucosidase, EC 3.2.1.21
7	TRINITY_DN1315_c0_g1	0.43	0.06	0.31	763.2	1448.5	490.5	-10.28	0.00001	Beta-glucosidase 27, Os8bglu27, EC 3.2.1.21
8	TRINITY_DN1315_c0_g1	0.43	0.06	0.31	763.2	1448.5	490.5	-10.28	0.00001	Beta-glucosidase 11, Os4bglu11, EC 3.2.1.21
9	TRINITY_DN1315_c0_g1	0.43	0.06	0.31	763.2	1448.5	490.5	-10.28	0.00001	Beta-glucosidase 24, Os6bglu24, EC 3.2.1.21
10	TRINITY_DN1315_c0_g1	0.43	0.06	0.31	763.2	1448.5	490.5	-10.28	0.00001	Beta-glucosidase 13, Os4bglu13, EC 3.2.1.21
11	TRINITY_DN67935_c0_g1	0	0	0	16.39	97.3	73.99	-10.13	0.00080	Predicted Protein
12	TRINITY_DN702_c0_g1	0	0.03	0	59.4	116.45	27.95	-9.93	0.00006	Cytochrome P450 71AU50, EC 1.14.-.-
13	TRINITY_DN702_c0_g1	0	0.03	0	59.4	116.45	27.95	-9.93	0.00006	Cytochrome P450 750A1, EC 1.14.-.- (Cytochrome P450 CYPC)
14	TRINITY_DN2358_c0_g1	0	0	0	81.45	89.01	7.38	-9.91	0.00287	Predicted Protein
15	TRINITY_DN31159_c0_g1	0	0	0	32.73	41.22	41.42	-9.83	0.00001	Predicted Protein
16	TRINITY_DN157611_c0_g2	0	0	0	22.19	59.12	26.75	-9.60	0.00002	Predicted Protein
17	TRINITY_DN10725_c0_g1	0	0	0	29.76	70.11	14.01	-9.55	0.00010	Predicted Protein
18	TRINITY_DN30360_c0_g2	0	0	0	98.39	13.66	18.36	-9.53	0.00190	Predicted Protein
19	TRINITY_DN251401_c0_g1	0	0	0	93.47	11.8	22.49	-9.52	0.00209	Predicted Protein
20	TRINITY_DN27632_c0_g2	0	0	0	8.22	77.05	47.39	-9.45	0.00238	Predicted Protein
21	TRINITY_DN10160_c0_g1	0	0	0	14.16	73.48	23.65	-9.41	0.00024	Predicted Protein
22	TRINITY_DN1453_c1_g4	0	0	0	36.74	50.95	10.28	-9.37	0.00016	Predicted Protein

23	TRINITY_DN57079_c0_g1	6.63	0	0	223.25	327.76	184.27	-9.36	0.00049	Predicted Protein
24	TRINITY_DN3979_c0_g1	0.05	0.01	0	52.76	91.37	16.98	-9.28	0.00028	Predicted Protein
25	TRINITY_DN4524_c0_g3	0	0	5.98	113.8	426.21	83.05	-9.21	0.00327	Predicted Protein
26	TRINITY_DN34759_c0_g1	6.79	0	0	322.78	155.49	180.5	-9.18	0.00153	Predicted Protein
27	TRINITY_DN73957_c1_g1	0	0	0	11.64	28.85	41.17	-9.11	0.00023	Predicted Protein
28	TRINITY_DN75419_c0_g1	0.25	0	0	62.72	75.65	55.6	-9.08	0.00003	Predicted Protein
29	TRINITY_DN9012_c0_g1	0	0	0	22.31	72.56	6.41	-9.07	0.00112	Predicted Protein
30	TRINITY_DN1628_c0_g1	7.75	0.43	0	1238.41	1180.01	590.75	-9.07	0.00011	Trypsin inhibitor [Cleaved into: Trypsin inhibitor chain A; Trypsin inhibitor chain B]
31	TRINITY_DN3979_c1_g1	0	0	0	47.13	42.56	4.42	-9.05	0.00236	Predicted Protein
32	TRINITY_DN157611_c0_g3	0	0	0	17.21	32.42	19.18	-9.03	0.00001	Predicted Protein
33	TRINITY_DN15815_c1_g1	0	0	0	6.21	49.45	40.59	-9.03	0.00232	Predicted Protein
34	TRINITY_DN95424_c0_g1	0	0	0	11.51	54.25	15.08	-8.96	0.00022	Predicted Protein
35	TRINITY_DN7685_c0_g1	0.35	0.17	0.18	509.79	347.25	228.34	-8.94	0.00001	Predicted Protein
36	TRINITY_DN1456_c0_g1	1.37	0	1.34	512.91	233.93	218.11	-8.92	0.00030	Predicted Protein
37	TRINITY_DN71807_c0_g2	0	0	0	22.55	16.31	22.17	-8.92	0.00003	Predicted Protein
38	TRINITY_DN4477_c1_g1	0.88	0	0	81.97	139.91	53.7	-8.90	0.00024	Predicted Protein
39	TRINITY_DN7520_c2_g1	0	0	0	9.41	27.2	33.69	-8.88	0.00027	Predicted Protein
40	TRINITY_DN4184_c0_g1	0.18	0	0	46.12	92.42	26.45	-8.83	0.00016	Predicted Protein
41	TRINITY_DN7066_c0_g1	0	0	0	20.01	31.33	9.88	-8.80	0.00004	Predicted Protein
42	TRINITY_DN933_c0_g1	1.8	0	0.74	315.27	351.67	163.92	-8.78	0.00017	Predicted Protein
43	TRINITY_DN1728_c0_g1	0	0	0	11.2	40.87	13.71	-8.77	0.00010	Predicted Protein
44	TRINITY_DN58476_c0_g1	0	0	0.69	19.97	131.68	83.6	-8.71	0.00446	Predicted Protein
45	TRINITY_DN106984_c0_g1	0	0	0	13.93	11.45	34.39	-8.69	0.00029	Predicted Protein
46	TRINITY_DN16651_c1_g1	0	0	0	5.99	54.4	17.47	-8.68	0.00142	Predicted Protein
47	TRINITY_DN94859_c1_g2	0	0	0	15.4	19.32	16.7	-8.67	0.00001	Predicted Protein
48	TRINITY_DN53823_c0_g1	0	0	0	24.5	12.76	14.3	-8.66	0.00005	Predicted Protein
49	TRINITY_DN2764_c0_g1	0.03	0	0	27.4	33.19	14.81	-8.65	0.00002	WRKY transcription factor 6 (WRKY DNA-binding protein 6, AtWRKY6)
50	TRINITY_DN3685_c0_g1	0.54	0.06	0	173.37	95.47	98.32	-8.63	0.00025	Predicted Protein

STable 13a. Top 25 upregulated genes from copper susceptible samples compared to water controls in *Pinus banksiana*

Rank	Gene ID	Sus 1	Sus 2	Sus 3	Water 1	Water 2	Water 3	logFC	Adj. P. Value	UniProt Description
0	TRINITY_DN2786_c0_g1	670.58	354.91	364.1	0	0	0	13.15	8.45E-06	Predicted Protein
1	TRINITY_DN1628_c0_g1	1238.41	1180.01	590.75	0	0.32	0	12.80	2.48E-05	Trypsin inhibitor [Cleaved into: Trypsin inhibitor chain A; Trypsin inhibitor chain B]
2	TRINITY_DN258556_c0_g1	248.22	356.86	541.07	0	0	0	12.77	1.88E-05	Predicted Protein
3	TRINITY_DN1368_c0_g1	1712.84	2189.53	1629.49	0	1.3	0.07	12.73	2.67E-06	Predicted Protein
4	TRINITY_DN5716_c0_g1	2481.86	3248.79	5881.21	0	7.03	0.41	12.53	6.37E-04	Predicted Protein
5	TRINITY_DN2832_c0_g1	358.6	494.32	122.28	0	0	0	12.49	3.11E-05	Predicted Protein
6	TRINITY_DN5391_c1_g1	496.98	221.21	166.02	0	0	0	12.43	3.94E-05	Predicted Protein
7	TRINITY_DN57079_c0_g1	223.25	327.76	184.27	0	0	0	12.22	1.57E-07	Predicted Protein
8	TRINITY_DN5965_c1_g1	799.48	842.36	692.63	0.33	0	0	12.12	2.95E-06	Predicted Protein
9	TRINITY_DN50999_c1_g1	333.04	156.25	133.24	0	0	0	11.95	1.73E-05	Predicted Protein
10	TRINITY_DN55243_c0_g1	115.54	286.47	226.14	0	0	0	11.88	1.05E-05	Predicted Protein
11	TRINITY_DN1520_c0_g1	1020.58	623.65	1427.83	0.02	0.65	0	11.86	1.18E-03	Trypsin inhibitor [Cleaved into: Trypsin inhibitor chain A; Trypsin inhibitor chain B]
12	TRINITY_DN5795_c0_g1	851.63	854.34	325.97	0	0.84	0	11.83	2.09E-04	Predicted Protein
13	TRINITY_DN7061_c1_g1	194.74	291.48	98.46	0	0	0	11.82	2.94E-06	Predicted Protein
14	TRINITY_DN8563_c1_g1	131.04	322.9	115.04	0	0	0	11.71	4.77E-06	Predicted Protein
15	TRINITY_DN4524_c0_g3	113.8	426.21	83.05	0	0	0	11.63	9.67E-05	Predicted Protein
16	TRINITY_DN257933_c1_g1	201.53	169.25	77.24	0	0	0	11.48	4.34E-06	Predicted Protein
17	TRINITY_DN3536_c0_g1	122.8	169.34	90.42	0	0	0	11.28	3.13E-07	Predicted Protein
18	TRINITY_DN237688_c0_g1	211.18	103.61	72.51	0	0	0	11.25	1.84E-05	Predicted Protein
19	TRINITY_DN7685_c0_g1	509.79	347.25	228.34	0	0.41	0	11.24	6.78E-05	Predicted Protein
20	TRINITY_DN14732_c0_g1	372.88	97.02	31.35	0	0	0	11.18	1.92E-03	Predicted Protein
21	TRINITY_DN12750_c0_g1	166.37	64.69	116.96	0	0	0	11.11	3.61E-05	Predicted Protein
22	TRINITY_DN2463_c0_g1	818.33	234.67	289.22	0	0.04	0.11	11.02	2.24E-03	Predicted Protein
23	TRINITY_DN3069_c0_g1	313.54	458.61	155.11	0	0.37	0	10.98	6.68E-05	Predicted Protein
24	TRINITY_DN2221_c0_g1	664.03	226.26	181.23	0	0.68	0	10.90	1.96E-03	Predicted Protein

25	TRINITY_DN3092_c0_g1	661.05	923.49	459.73	0.14	0.35	0	10.88	6.47E-06	Glucan endo-1,3-beta-glucosidase, acidic isoform, EC 3.2.1.39 ((1->3)-beta-glucan endohydrolase, (1->3)-beta-glucanase) (Beta-1,3-endoglucanase)
26	TRINITY_DN4477_c1_g1	81.97	139.91	53.7	0	0	0	10.74	1.70E-06	Predicted Protein
27	TRINITY_DN1315_c0_g1	763.2	1448.5	490.5	0.14	1.09	0	10.71	7.58E-05	Beta-glucosidase 12, EC 3.2.1.21
28	TRINITY_DN1315_c0_g1	763.2	1448.5	490.5	0.14	1.09	0	10.71	7.58E-05	Furcatin hydrolase, FH, EC 3.2.1.161
29	TRINITY_DN1315_c0_g1	763.2	1448.5	490.5	0.14	1.09	0	10.71	7.58E-05	Non-cyanogenic beta-glucosidase, EC 3.2.1.21
30	TRINITY_DN1315_c0_g1	763.2	1448.5	490.5	0.14	1.09	0	10.71	7.58E-05	Beta-glucosidase 27, Os8bglu27, EC 3.2.1.21
31	TRINITY_DN1315_c0_g1	763.2	1448.5	490.5	0.14	1.09	0	10.71	7.58E-05	Beta-glucosidase 11, Os4bglu11, EC 3.2.1.21
32	TRINITY_DN1315_c0_g1	763.2	1448.5	490.5	0.14	1.09	0	10.71	7.58E-05	Beta-glucosidase 24, Os6bglu24, EC 3.2.1.21
33	TRINITY_DN1315_c0_g1	763.2	1448.5	490.5	0.14	1.09	0	10.71	7.58E-05	Beta-glucosidase 13, Os4bglu13, EC 3.2.1.21
34	TRINITY_DN3685_c0_g2	458.68	319.42	270.94	0.01	0.58	0	10.68	4.23E-05	Copia protein (Gag-int-pol protein) [Cleaved into: Copia VLP protein; Copia protease, EC 3.4.23.-]
35	TRINITY_DN89721_c0_g1	78.43	118.71	57.37	0	0	0	10.67	6.77E-07	Predicted Protein
36	TRINITY_DN2391_c0_g1	858.87	316.78	250.41	0.79	0	0	10.66	2.47E-03	Predicted Protein
37	TRINITY_DN129489_c0_g1	108.85	67.2	66.28	0	0	0	10.65	2.71E-06	Predicted Protein
38	TRINITY_DN705_c0_g1	396.92	327.8	168.62	0	0.2	0.08	10.61	5.98E-05	Aldehyde oxidase GLOX, EC 1.2.3.1 (Glyoxal oxidase, VpGLOX)
39	TRINITY_DN6211_c0_g1	84.27	82.59	60.21	0	0	0	10.56	4.71E-07	Predicted Protein
40	TRINITY_DN77041_c1_g1	119.39	88.54	34.89	0	0	0	10.55	1.71E-05	Predicted Protein
41	TRINITY_DN2914_c0_g1	125.88	118.78	89.54	0	0.03	0	10.53	1.15E-06	Protein TIFY 10b, OsTIFY10b (Jasmonate ZIM domain-containing protein 7, OsJAZ7) (OsJAZ6)

42	TRINITY_DN2914_c0_g1	125.88	118.78	89.54	0	0.03	0	10.53	1.15E-06	Protein TIFY 3B (Jasmonate ZIM domain-containing protein 12)
43	TRINITY_DN34759_c0_g1	322.78	155.49	180.5	0	0.56	0	10.40	2.41E-04	Predicted Protein
44	TRINITY_DN6089_c0_g1	198.66	247.89	178.38	0	0.52	0	10.38	1.19E-05	Predicted Protein
45	TRINITY_DN4195_c0_g1	66.81	67.79	59.62	0	0	0	10.34	5.60E-07	Predicted Protein
46	TRINITY_DN1537_c0_g1	83.24	55.67	49.47	0	0	0	10.29	2.21E-06	Predicted Protein
47	TRINITY_DN9955_c0_g1	73.8	59.93	51.33	0	0	0	10.27	9.89E-07	Predicted Protein
48	TRINITY_DN40097_c0_g1	364.94	781.26	1375.23	0	3.39	0.69	10.26	1.28E-03	Predicted Protein
49	TRINITY_DN4694_c0_g2	103.71	56.82	31.28	0	0	0	10.22	1.99E-05	Predicted Protein
50	TRINITY_DN141140_c2_g1	355.97	220.27	133.34	0	1.24	0	10.22	3.52E-04	Predicted Protein